Investigating the non-cell autonomous role of astrocytic HSPB1 in Alzheimer's Disease

Sung, Katie

Awarding institution:
King's College London

Investigating the non-cell autonomous role of astrocytic HSPB1 in Alzheimer's Disease

Katherine Sung

Thesis submitted in the fulfilment of the degree of Doctor of Philosophy

Basic and Clinical Neuroscience

Institute of Psychiatry, Psychology and Neuroscience

King's College London

April 2022

Declaration

I hereby declare all work presented in this thesis is my own, except for the following:

Primary mouse astrocyte culture experiments:

- Fangjia Yang performed all data collection and analysis and prepared the figure of primary mouse astrocytes treated with cytokines TNFα and IL1α (Figure 4.1, Page 148)

IL-6 ELISA data of organotypic brain slice culture media:

- Media harvested from organotypic brain slice cultures treated with cytokines TNFα and IL1α was collected and analysed by Caoimhe Goldrick (Figure 4.15, Page 178) and the figure was adapted by Katherine Sung for this thesis

Preliminary data on the secretion of human HSPB1 in the slice media of slices transduced with GFAP-HSPB1-AAV:

- Slices transduced and western blot run by Fangjia Yang (Figure 6.1, Page 234)

Primary mouse neurons were kindly prepared by Dr Maria Jimenez Sanchez and the preparation and characterisation of TgCM media was kindly performed by Dr Beatriz Gomez Perez-Nievas

Tau-AAV transduced organotypic brain slice culture characterisation:

- Due to time constraints related to the COVID-19 shut-down of laboratories, characterisation experiments for the tau-AAV transduced organotypic brain slices was done in collaboration with Dr Diana Flores Dominguez and Emily Groves (Chapter 4, Section 4.4.4)
- Slice preparation was performed by Katherine Sung, virus transduction was performed by Emily Groves and imaging was performed by Dr Diana Flores Dominguez
- Sarkosyl extraction of tau and western blot analysis presented in this thesis was performed by Katherine Sung
- All figures relating to the characterisation of tau-AAV slices produced for this thesis by Katherine Sung

Katherine Sung
April 2022

Abstract

Alzheimer's disease is a progressive neurodegenerative disease which is primarily associated with the accumulation of amyloid-β (Aβ) and tau to form extracellular Aβ plaques and intracellular neurofibrillary tangles (NFT). Recently there has been increasing focus on other pathological changes associated with AD, such as neuroinflammation which, along with the accumulation of tau, most strongly correlates with cognitive decline. One major player in neuroinflammation is astrocytes. In AD, reactive astrocytes accumulate around amyloid plaques. Molecular chaperones play an essential role in maintaining protein homeostasis and preventing protein aggregation by binding to misfolded proteins. One family of these chaperones are the small heat shock proteins (sHSPs). In addition to classical chaperone functions, sHSPs have also been implicated in other functions including cytoskeleton stabilization, anti-apoptotic and anti-inflammatory functions. Evidence suggests that sHSPs are upregulated in reactive astrocytes in neurodegenerative diseases, including AD, however their exact role has yet to be determined. Further to this, a number of studies have suggested that overexpressing astrocytic sHSPs in animal models of neurodegenerative disease may be protective in a non-cell autonomous manner. Therefore, the hypothesis for this thesis is that the upregulation of the ubiquitously expressed and stress-induced sHSP HSPB1, specifically in the astrocytes, is neuroprotective against AD-relevant pathology through a non-cell autonomous mechanism.

To explore this hypothesis, the localisation and expression of HSPB1 was first characterized in human AD temporal cortex of different Braak stages by immunofluorescent analysis. In order to study the non-cell autonomous function of astrocytic HSPB1, organotypic brain slice culture models were used to replicate some of the pathological traits seen in AD, through treatment with cytokines known to induce reactive astrocytes in neurodegenerative disease and also with physiologically relevant levels of Aβ oligomers. A disease relevant tau pathology model was then set-up by transducing both primary mouse neurons and brain slices with tau adeno-associated virus (AAV) constructs. Finally,

the potentially protective functions of HSPB1 were explored using recombinant HSPB1 treatment and by overexpression of astrocytic HSPB1 in the slices through AAVs.

Human data confirmed that HSPB1 is localised within reactive astrocytes in the AD brain and also showed that there were more HSPB1 positive reactive astrocytes in close proximity to amyloid plaques. Further to this, immunofluorescent analysis revealed that the majority of amyloid plaques found in the most severe AD cases were also HSPB1 positive, suggesting that HSPB1 is being extracellularly released in response to AD pathology. In those slices treated with cytokines, reactive astrocytes were induced and HSPB1 was found to co-localise with reactive astrocytes, reflecting what was seen in the human AD brain. Transduction with a pro-aggregatory mutant tau-AAV construct resulted in the accumulation of hyperphosphorylated tau in both the primary neurons and slice cultures. Interestingly, the accumulation of tau inclusions in the primary neurons was reduced in those neurons treated with recombinant HSPB1, highlighting the potentially protective chaperone function of extracellular HSPB1. Further studies will be necessary to conclude whether astrocytic HSPB1 can also reduce tau pathology in brain slices.

All in all, the organotypic brain slice cultures proved to be a good model for replicating some of the relevant AD pathological traits seen in the human disease, however further work is required to gain a deeper understanding behind the mechanisms by which HSPB1 may be protective in response to AD pathology. Overall this work contributes to current knowledge around the astrocytic sHSP response in AD.

Acknowledgments

Firstly I would like to thank my primary supervisor, Dr Maria Jimenez Sanchez. It's truly been an invaluable experience working in your lab and learning from you! Thank you for your scientific guidance and endless knowledge over the past 3 years. Thank you also to Professor Wendy Noble for all your friendly advice and encouragement, and for sharing my passion for LFC (up the reds!). Additional thanks go to George and Chen at the KCL WCIC imaging facility for all your help and knowledge about everything microscopes.

Thank you to Team Tau for always being there to lend a helping hand: Fangjia, Paula, Louisa, Saskia, Chen and honorary member Sarah for taking me under her wing when I first joined. Special mentions go to my fellow Lost Scientists, Matt and Emily. Thanks for always being up for a much needed pub trip and for sharing in the many trials and tribulations of the slices cultures.

Thank you to my family: my parents and my brother Mark. Thank you mother and father for providing much needed sanctuary away from PhD life and ensuring I am ALWAYS well fed, with the many many many meals out, and endless supplies of Maoams and nut bars. This PhD would never have been possible if you hadn't worked so hard to ensure that we had the best life possible and the opportunities to pursue whatever we wanted ("Immigrants, we get the job done"). And thank you to Mark, always on point to cheer me up with your witty one-liners or sarcastic comments, providing a completely different take on the world and keeping me well and truly grounded (SCOUSE).

Thank you to the London B group: John, Harry, Holly and Mike. I literally would not have made it through COVID-19 without you all. Thank you for providing much needed relief (and alcohol!) from

this whole process, being the best cheerleaders ever, and for accepting the products of all my stress baking without complaint! Can't wait to celebrate together! "All I need is Six."

Thank you to Matty, for putting up with my rantings and ravings and many an emotional breakdown. For encouraging me and supporting me (mainly in the form of chocolate, sweets and desks), and for dragging me, kicking and screaming, across the finish line. I genuinely could not have done this without you (or the penguin).

And finally, I'd like to dedicate this thesis to my cousin David, whose kindness, passion and strength inspired me to finish this degree, no matter how close I came to giving up. In my eyes, you will always be the first PhD in the family.

Table of Contents

List of figures

List of tables

Publications

Sung, K., and Jimenez-Sanchez, M., (2020), Autophagy in Astrocytes and its Implications in Neurodegeneration, *Journal of Molecular Biology*, 432(8): 2605-2621

Abbreviations

AAV	adeno-associated virus
ABL1	ABL proto-oncogene 1 non-receptor tyrosine kinase
ACD	Alpha-crystallin domain
acLDL	Acetylated low-density lipoprotein
AD	Alzheimer's disease
ADP	Adenosine diphosphate
AICD	amyloid precursor protein intracellular domain
ALDH1L1	Aldehyde dehydrogenase 1 family member L1
ALS	Amyotrophic lateral sclerosis
APLP1	Amyloid precursor-like proteins 1
APLP2	Amyloid precursor-like proteins 2
APOE	Apolipoprotein E
APP	Amyloid precursor protein
ARPE19	Adult human retinal pigment epithelial cells
ATP	Adenosine 5'-triphosphate
Aβ	Amyloid beta
BACE1	beta-site cleaving enzyme 1
BIN1	Bridging Integrator 1
BNE	BrainNet Europe protocol (of Braak staging)
C1q	Component 1 subcomponent q
CA1	Hippocampal Cornu Ammonis
CAII	Carbonic anhydrase 2
CASS4	Cas Scaffold Protein Family Member 4
CBD	Corticobasal degeneration
Cdk5	Cyclin-dependent kinase-5
CMT	Charcot-Marie-Tooth disease
CNS	Central nervous system
CSF	Cerebrospinal fluid
CSF1R	Colony-stimulating factor 1 receptor
C-terminal	Carboxy-terminal
CTF	Carboxyl-terminal fragments
CTFβ	C-terminal bound amyloid precursor protein

DAPI	4’ 6-diamidino-2-phenylindole
DEGS	Differentially expressed genes
DS	Down Syndrome
EAE	Experimental autoimmune encephalomyelitis
EGFP	Enhanced green fluorescent protein
ELISA	Enzyme-linked immunosorbent assay
EOAD	Early-onset Alzheimer’s disease
ER	Endoplasmic reticulum
F	Female
FFPE	formalin-fixed paraffin embedded
FTDP-17	Frontotemporal dementia and parkinsonism linked to chromosome 17
FTLD	Frontotemporal lobar degeneration
FTLD-tau	Frontotemporal dementia tauopathies
FUS	Fused in sarcoma protein
GFAP	Glial fibrillary acidic protein
GSK	Glycogen synthase kinase
GWAS	Genome-wide associated studies
HCHWA-D	Human hereditary cerebral haemorrhage with amyloidosis of the Dutch type
HD	Huntington’s disease
HEK293T	Human embryonic kidney 293T
HSP	Heat-shock protein
htt	Huntingtin
IL1α	Interleukin 1 alpha
IL-1β	Interleukin-1 beta
IL-6	Interleukin-6
iNOS	Inducible nitric oxide synthase
iPSC	Induced pluripotent stem cell-derived
ITGB1	Integrin Subunit Beta 1
kb	kilobase
kDa	Kilodalton
KO	Knock-out
LCN2	Lipocalin 2
LOAD	Late-onset Alzheimer’s disease
LPS	Lipopolysaccharides

LSS	Low speed supernatant
LTP	Long-term potentiation
M	Male
MAP	Microtubule-associated protein
MAP2	Microtubule-associated protein 2
MAPK	Microtubule affinity-regulating kinase
MAPT	Microtubule-associated protein tau
MCI	Mild cognitive impairment
MMSE	Mini-Mental Status Examination
MS	Multiple Sclerosis
MTBD	microtubule binding domain
N	N-terminal domains
NAPDH	Nicotinamide adenine dinucleotide phosphate
N-APP	N-terminal bound amyloid precursor protein
NBD	Nucleotide binding domain
NfL	Neurofilament light chain
NFT	Neurofibrillary tau tangles
NMR	Nuclear magnetic resonance
NO	Nitrogen oxide
Nrf2	Nuclear factor-erythroid factor 2-related factor 2
p3	3 peptide
PBD	Peptide-binding domain
PD	Parkinson’s disease
PET	Positron emission tomography
PHF	Paired helical filaments
PiB	Pittsburgh Compound B
PKA	Cyclic adenosine monophosphate-dependent protein kinase A
PMD	Post-mortem delay
PP2A	Protein phosphatase 2A
PSEN1	Presenilin 1
PSEN2	Presenilin 2
PSP	Progressive supranuclear palsy
R	Microtubule-binding repeat domain
rAAV	recombinant adeno-associated virus

RNA	Ribonucleic acid
ROS	Reactive Oxygen Species
RPE	Retinal pigment epithelial
sAPPα	Soluble amyloid precursor protein alpha
sAPPβ	Soluble amyloid precursor protein beta
Sarkosyl	N-lauryl-sarcosine
sHSP	Small heat-shock protein
SI	Sarkosyl insoluble
SORL1	Sortilin Related Receptor 1
STAT3	Signal transducer and activator of transcription 3
TDP	TAR DNA binding protein 43
TEFB	Transcription factor EB
Tg	Transgenic
TgCM	Transgenic conditioned media
TGFB	Transforming growth factor beta
TLR	Toll-like receptors
TNF	Tumour necrosis factor
TNFα	Tumour necrosing factor alpha
TPR	Tetratricopeptide repeat
TREM2	Triggering receptor expressed on myeloid cells 2
TUNEL	TdT-mediated dUTP-biotin nick end labelling
VEGF	Vascular endothelial growth factor
VG	Viral genomes
WGL	Whole-genome linkage
WPRE	Woodchuck Hepatitis Virus (WHP) Posttranscriptional Regulatory Element
WT	Wild-type
WtCM	Wild-type conditioned media

Chapter 1: Introduction

1.1 Alzheimer's Disease

1.1.1 Historical perspective

Alzheimer's disease (AD) was first described by German clinical psychiatrist and neuropathologist Alios Alzheimer in 1906 (Stelzmann et al., 1995). Alzheimer first met 51 year old Auguste Deter at a mental asylum in Frankfurt, where she presented with progressive change in personality, rapidly worsening memory, and overall cognitive decline up until her eventual death 5 years later (Hippius and Neundorfer, 2003). Alzheimer's initial post-mortem pathological analysis of Auguste's brain highlighted "numerous miliary foci" of extracellular structures and intracellular fibril bundles which are more commonly known today as the classical hallmarks of disease, the extracellular amyloid-β plaques and neurofibrillary tau tangles (NFT) (Cipriani and Dolciotti, 2011). Over 100 years later, significant advancements have been made in regards to the genetic basis and molecular biology of the disease, however much is still unknown and a suitable treatment or cure has yet to be found.

1.1.2 Prevalence and diagnosis

AD is the most common form of dementia with an enormous global and economic impact. The numbers of those affected are set to triple from 50 million in 2018 to 152 million by 2050 and the current cost of the condition is around a trillion US dollars a year, forecast to double by 2030 (Patterson 2018). In the UK alone, there were an estimated 900,000 people living with dementia in 2019, leading to the total cost of care being £34.37 billion, and the number of those diagnosed is expected to sharply increase to over 1.6 million by 2040, mainly due to an accelerated ageing population (Wittenberg et al., 2019).

The diagnostic criteria for AD divides the clinical onset into three general phases: preclinical, mild cognitive impairment (MCI) and AD dementia, with each period of disease falling in the range of decades (Hane et al., 2017). AD begins with a long asymptomatic preclinical stage and it is assumed that if a patient reaches preclinical stage, they are highly likely to develop AD if they live long enough (Jack et al., 2012). The preclinical phase is characterised by general cerebral amyloidosis at a level which is not yet detectable using currently available techniques and normal performance on cognitive functional tests such as the Mini-Mental Status Examination (MMSE) (Hane et al., 2017). The MCI phase of AD is characterized by a noticeable reduction in cognitive function although only to such a minor extent and so the patients are still able to remain an autonomous member of society. They or a family member will become aware of clinical symptoms including a decline in memory, attention, language and/or executive function which worsen over time, however there is still no laboratory test which officially confirms the diagnosis of MCI (Albert et al., 2011). The final AD dementia stage is diagnosed in the clinical setting using a thorough patient history and cognitive tests such as MMSE, where a diagnosis must confirm the impairment in at least two defined categories which include: the ability to remember new information, general reasoning, visuospatial ability, language function or changes in personality or behaviour (McKhann et al., 2011).

1.1.3 Genetics of AD

The main biological risk factor for AD is age (Carr et al., 1997), and 65 years is used to determine whether a patient is categorised as having either early-onset (EOAD) or late-onset AD (LOAD; (Cacace et al., 2016)). Less than 10% of all AD patients are diagnosed with the rare autosomal EOAD and can become symptomatic from anywhere between 30 and 65 years of age (Wimo et al., 2015). LOAD is the most common form of AD, making up to 95% of AD cases (Kamboh 2018), and occurs sporadically due to a combination of genetic and environmental risk factors (Khanahmadi et al., 2015). In addition to the typical memory impairment, EOAD patients also suffer from further focal

cortical symptoms such as, visual impairment, apraxia and aphasia, whereas LOAD patients mainly present with memory impairment (Cacace et al, 2016).

Early Onset Alzheimer's disease (EOAD)

Large and detailed monogenic studies helped in the identification of high-penetrant mutations in three EOAD genes, coding for the amyloid precursor protein (APP), and presenilin 1 and 2 (PSEN1 and PSEN2). Mutations in these genes all lead to an increased aggregation of neurotoxic amyloid species (Tanz and Bertrami, 2005).

The first gene associated with inherited EOAD was identified through the exploration of Down Syndrome (DS), caused by triplicate copies of chromosome 21 and where patients are shown to develop similar amyloid and tau pathology as seen in AD patients (Wisniewski et al., 1985). Whole-genome linkage (WGL) studies in AD patients confirmed a genetic deficit found on chromosome 21q and further to this the APP gene was also mapped to the very same chromosome (George-Hyslop et al., 1987; Goldgaber et al., 1987). APP was later conclusively linked to AD familial pathogenesis thanks to the extended segregation studies into another amyloid based disease, human hereditary cerebral haemorrhage with amyloidosis of the Dutch type (HCHWA-D) (Broeckhoven et al, 1990; Goate et al., 1991). In addition to this, it was confirmed that a duplication of this APP gene was also sufficient to cause EOAD (Rovelet-Lecrux et al., 2006; Sleegers et al., 2006). This overexpression of APP has also been replicated in various mouse models of AD, which reflect a similar age-dependent increase in extracellular Amyloid-β (Aβ) plus other neuropathological and behavioural changes seen in the human disease (Elder et al., 2010).

Aβ is the result of the cleavage of APP by two aspartyl proteases, β- and γ-secretases (Haass et al., 2012). It has been found that mutations within the Aβ region of APP cause the increase in overall levels and aggregation of Aβ which leads to EOAD, whilst mutations near to β- and γ-secretases sites can alter the $A\beta_{40}$/ $A\beta_{42}$ ratio (Chartier-Harlin et al., 1991; Citron et al., 1992; Irvine et al., 2008; Scheuner et al., 1996). Conversely, a mutation in APP linked to an Icelandic population has been shown to actually reduce the overall production of Aβ and therefore protects against the cognitive decline normally found in late-onset AD (Jonsson et al., 2012).

The other genes best associated with EOAD are PSEN1 located on chromosome 14 and PSEN2 found on chromosome 1 (Levy-Lahad et al., 1995; Sherrington et al., 1995). The presenilins are serpentine proteins and catalytic subunits of the γ-secretases complex, responsible for cleavage of the Aβ C-terminus (De Strooper and Annaert, 2010; Bentahir et al., 2006). Inherited mutations in PSEN1 and PSEN2 increase the $A\beta_{42}$/ $A\beta_{40}$ ratio which leads to a particularly aggressive and early form of AD (Kumar-Singh et al., 2006), and this increase in $A\beta_{42}$ relative to $A\beta_{40}$ levels has also been replicated in presenilin mouse models of AD (Jankowsky et al., 2004). The mutations found in three different EOAD associated genes all seem to result in a similar change in the balance of the different Aβ products. This strongly suggests the involvement of Aβ in a final common pathway of AD pathogenesis (Masters et al., 2015).

Late Onset Alzheimer's disease (LOAD)

Genome-wide linkage studies and follow-up association studies into LOAD families identified the apolipoprotein E (APOE) gene, found on chromosome 19, as the greatest risk factor for developing AD (Pericak-Vance et al., 1991; Saunders et al., 1993; Strittmatter et al., 1993). APOE is a secreted glycoprotein that binds and catabolises cholesterol and phospholipids (Jones et al., 2011) and is

primarily produced by astrocytes and microglia in the brain (Huang et al., 2004). APOE has three common isoforms ε2, ε3 and ε4, which differ by only two amino acid residues resulting in differing abilities in lipid binding, receptor affinities as well as stability and clearance (Serrano-Pozo et al., 2021). Having one APOE ε4 allele increases the risk of developing AD by a factor of three and having two alleles further increases this risk up to 12-fold (Rebeck et al., 1993; Farrer et al., 1997), whereas carrying an APOE ε2 allele is proven to be the strongest protective genetic factor against sporadic AD by reducing risk by at least 40% (Corder et al., 1994; Reiman et al., 2020). Further to predicting the risk of developing AD, different APOE alleles also determine the age of onset of cognitive impairment, as APOE ε4 carriers experience earlier cognitive decline compared to APOE ε2 genotypes who present with a later onset (Serrano-Pozo et al., 2015).

One of the first studies linking APOE to AD pathology observed APOE immunoreactivity within the hallmarks of the disease, Aβ plaques and NFT (Namba et al., 1991). Since then, there have been a number of studies clearly demonstrating a direct interaction between APOE and the Aβ peptide (Serrano-Pozo et al., 2021) and the effects of different APOE isoforms on influencing tau pathology (Zhao et al., 2018; Shi et al., 2017). Further to this, in a number of *in vivo* mouse models of disease, it has been demonstrated that there is an isoform-dependent reduction in Aβ plaque load and an onset of Aβ build-up (Masters et al., 2015), supporting the notion that APOE is in fact a strong risk factor for AD pathogenesis.

The continued discovery of novel LOAD affecting loci is indispensable in further understanding AD aetiology. Genome-wide associated studies (GWAS) have successfully identified polymorphisms in or near genes involved in biological processes such as endocytosis, immune response, inflammation and tau pathology such as BIN1, CD33, SORL1, TREM2 and CASS4 (Karch and Goate, 2015; Lambert et al., 2013). Of particular note are those genes involved in the immune response such as CD33,

expressed on myeloid cells and microglia (Griciuc et al., 2013; Malik et al., 2013), and TREM2, expressed on microglia stimulating phagocytosis and suppressing inflammation (Rohn 2013). This is an addition to those lesser known genes CASS4 and FERMT2, involved in cytoskeletal function and tau processing (Karch and Goate, 2015; Shulman et al., 2014; Pluskota et al., 2011; Kirsch et al., 1999). These genetic discoveries highlight the importance of inflammation and tau processing in AD pathology. Although GWAS has been invaluable in identifying novel genetic associations of AD, this has led only to a minimal explanation of the disease heritability. More recently focus has shifted towards the system-wide interactions which define the disease state, through the exploration of pathway and network driven models with the help of transcriptomic and proteomic analysis. These studies have not only confirmed the association of previously identified genes such as APP, APOE and TGFB but have also highlighted novel genes such as ABL1 and ITGB1 and previously underexplored pathways such as the brain "glutamate-glutamate cycle" pathway (Li et al., 2019; Li et al., 2018; Patel et al., 2019). This new data will not only aid in our understanding of the disease but also add vital insight into potential therapeutic targets.

1.1.4 Neuropathology of AD

AD is defined by a specific neuropathological profile of the classical hallmarks of disease: hyperphosphorylated tau to form intracellular NFT and extracellular Aβ to form diffuse or neuritic plaques (*Figure 1.1*) (Stelzmann et al., 1995; Jack et al., 2018). However, there is currently an increased focus on the contribution of other cellular processes to disease progression, such as synaptic and neuronal loss and neuroinflammation (Henstridge et al., 2019). Recently improved biomarker and CSF monitoring capabilities allows the tracking and defining of each stage of neuropathological development in more detail (*Figure 1.2)* (Vermunt et al., 2019; Long and Holtzman, 2019). Firstly there's early deposition of Aβ in the cortex, detected by Pittsburgh Compound B (PiB) imaging and cerebrospinal fluid (CSF) levels of $A\beta_{42}$ (Morris et al., 2009; Bateman

et al., 2012) which simultaneously occurs alongside neuroinflammatory changes, such as microgliosis which can be confirmed using PK11195 positron emission tomography (PET) imaging (Jack and Holtzman, 2013). Following this, there is an accumulation and spread of tau pathology from the temporal lobes to the neocortex, measured through PET imaging and identified through the increased in phosphorylated tau (Vos et al., 2013; Fagan et al., 2014). Synapse loss and dysfunction and eventual neurodegeneration results from the continuous build-up of tau (see Chapter 1, Section 1.1) and can be monitored using imaging analysis of cortical and hippocampal volume and more recently through examination of neurofilament light chain (NfL) CSF levels (Gordon et al., 2018; Bridel et al., 2019). The onset and eventual cognitive decline is seen to most strongly correlate with the accumulation of neuroinflammation (see Chapter 1, Section1.5) (in the form of reactive astrocytes) and tau phosphorylation (Ingelsson et al., 2004; Perez-Nievas et al., 2013) (see Chapter 1, Section 1.5).

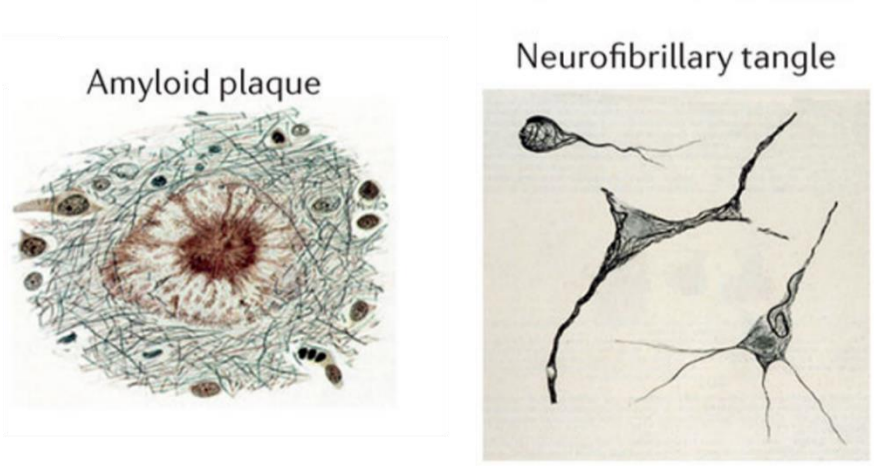

Figure 1.1: Aβ plaque and NFT found throughout the AD brain.

Images taken from Spielmeyer's classic textbook 'Histopathologie des Nervensystems', plaque and tangles stained using Bielschowsky silver staining method, figure adapted from Masters et al., 2015

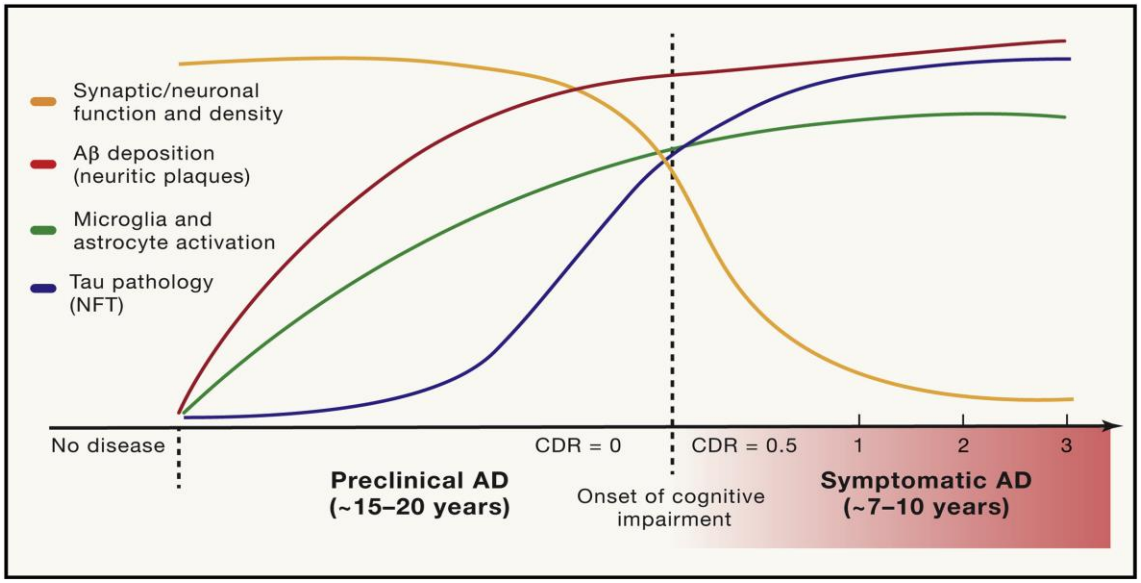

Figure 1.2: Graph outlining the timing of all the major pathological events which occur throughout AD in relation to the clinical progression.

The preclinical AD phase is characterised by the onset of amyloid deposition along with neuroinflammatory changes including microglia activation. Next, NFT pathology spreads from the temporal lobes into the neocortex, accumulating alongside synaptic dysfunction and loss. Onset and progression of cognitive decline correlates with the accumulation of tau pathology and hippocampal volume loss. Figure adapted from Long and Holtzman, 2019

1.2 Amyloid-β and amyloid-β pathology

1.2.1 Amyloid precursor protein (APP) processing

The amyloid precursor protein (APP) belongs to a family of mammalian proteins which also include amyloid precursor-like proteins 1 and 2 (APLP1 and APLP2) (De Strooper and Annaert, 2000). All proteins are single-pass type 1 integral transmembrane proteins with large extracellular domains and short intracellular domains and the family of proteins are processed similarly to APP (Kang, 1987; O'Brien and Wong, 2011).

APP can be processed in a number of ways, broadly split into the non-amyloidogenic and amyloidogenic pathways which result in the generation of the Aβ peptide (*Figure 1.3*). During the non-amyloidogenic pathway, APP is first proteolyzed on the cell membrane by α-secretase to produce a soluble APPα (sAPPα) peptide which is extracellularly released. These resulting products may then be involved in processes such as growth regulation and neuroprotection. Otherwise, sAPPα may go on to be further cleaved by γ-secretase in the cytoplasm resulting in two further peptides, the APP intracellular domain (AICD) and a 3 kilodalton (kDa) peptide (p3) (De Strooper and Annaert, 2000; Guo etal., 2021). This AICD produced, as a result of initial cleavage by α-secretase, can then be rapidly degraded either by the endosomal/lysosomal pathway or insulin degrading enzyme (Vingtdeux et al., 2007; Edbauer et al., 2002).

The main contributors to the amyloidogenic pathway are the β- and γ-secretases. The β-secretase involved is the β-site cleaving enzyme 1 (BACE1) and cleaves the N-terminus of the Aβ peptide whilst the γ-secretase cleaves the C-terminal end (De Strooper and Annaert, 2000). When APP is first cleaved by BACE1, soluble APPβ peptide (sAPPβ) is released and transported to the extracellular

space. This can then be further processed to form N-APP which may further contribute to AD pathophysiology due to its ability to initiate apoptosis and neuronal death (Nikolaev et al., 2009). After initial cleavage by β-secretase, the remaining C-terminal bound APP fragments (CTFβ) can be cleaved by γ-secretase in the endosome to generate Aβ peptides varying in length from 34 to 50 amino acid residues (Kummer and Heneka, 2014). About 90% of the Aβ fragments are the relatively stable $A\beta_{40}$ and whilst the longer $A\beta_{42}$ form is less abundantly available than the $A\beta_{40}$ derivative, it is more prone to oligomerisation (Irvine et al., 2008). In healthy younger brains the balance between production and clearance of the Aβ peptides such as the pro-aggregatory hydrophobic $A\beta_{42}$ are maintained, but in AD brains these peptides progress into toxic oligomers and fibrils leading to a wide range of pathological features such as reduced synaptic activity and eventual synaptic loss (Long and Holtzman, 2019).

In addition to the well-established APP cleavage pathways, newer δ- η- and meprin pathways have also been discovered and shown to result in additional N-terminal fragments (Muller et al., 2017). In the case of the η-pathway, the higher molecular mass carboxyl-terminal fragments (CTF) are generated by the combined cleavage of η-secretase with either α-secretase or β-secretase. These have then been found to be enriched in dystrophic neurites in both AD animal models and human AD brains and seen to attenuate normal neuronal activity highlighting the functional relevance of this APP processing pathway and a potential new avenue for therapeutic strategies (Willem et al., 2015).

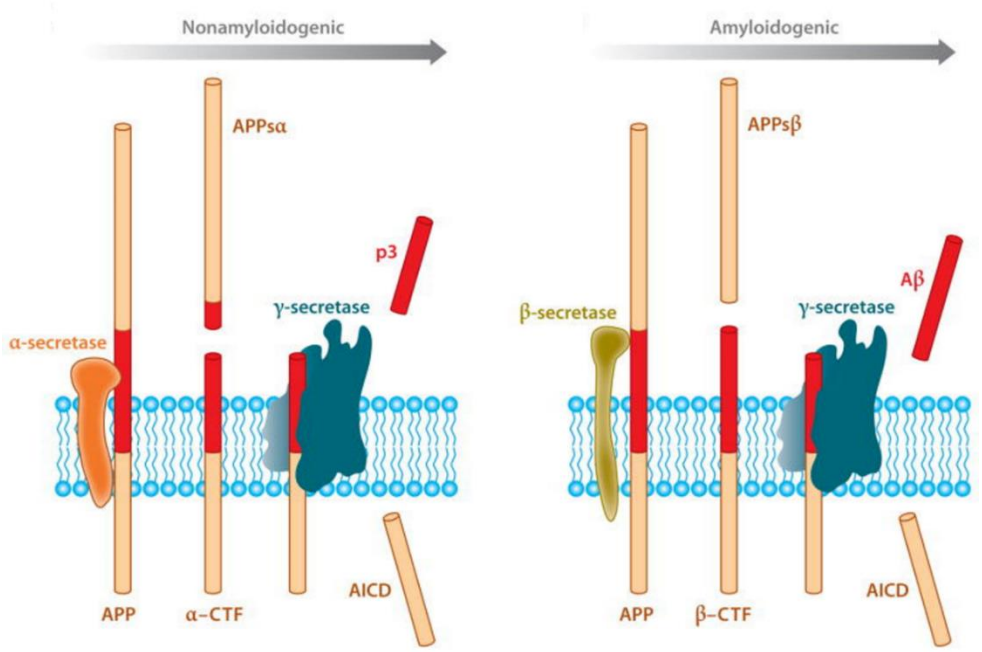

Figure 1.3: Non-amyloidogenic and amyloidogenic pathways of APP processing.

APP processing can occur either via the non-amyloidogenic or amyloidogenic pathway. Red region highlights the transmembrane region of APP. In the non-amyloidogenic pathway, APP is cleaved firstly by α-secretase and then by γ-secretase, resulting in the sAPPα and AICD. In the amyloidogenic pathway, APP is processed firstly by BACE1 and then by γ-secretase resulting in the formation of the sAPPβ and the AICD. Figure adapted from De Strooper and Annaert, 2000

1.2.1.1 Amyloid-β species

A range of soluble Aβ species have now been identified with different Aβ species forming as a result of Aβ self-aggregation (Walsh and Selkoe, 2020). The different soluble species include monomers and oligomers, discovered and investigated mainly using synthetic peptides acquired through cell culture and mouse models as well as extracts taken from the human brain (McDonald et al., 2015; Brinkmalm et al., 2019; Sehlin et al., 2012).

There is increasing evidence that the smaller oligomeric forms of Aβ may be the most toxic form, rather than the insoluble plaques. In a study involving elderly and AD patients, both groups

presented a high plaque burden, however, the AD patients had a higher ratio of soluble oligomer Aβ to plaque compared to their elderly counterparts (Esparza et al., 2012). It has also been shown in a number of studies that, when extracting Aβ from human AD brains, the majority of the extracted Aβ is of higher molecular weight and actually non-toxic (Yang et al., 2017; Hong et al., 2018; Shankar et al., 2008). However, once these larger oligomers were broken down into lower molecular weight oligomers or when only the small diffusible portion of Aβ was isolated and collected, these fractions were then able to impair long-term potentiation (LTP) and cause neurotoxicity, proving to be the synaptotoxic species in the brain (Yang et al., 2017; Hong et al., 2018; Shankar et al., 2008). In fact, it has been suggested that the insoluble senile plaques are likely to sequester high molecular weight oligomers, acting as a reservoir to prevent further Aβ degradation into smaller toxic oligomers (Koffie et al., 2009; Yang et al., 2017).

1.2.1.2 Amyloid-β plaques

The main constituent of Aβ plaques is the Aβ peptide (Masters et al., 1985) formed by the cleavage of the APP by β-secretase followed by γ-secretase (Haass et al., 2012). The Aβ peptides are susceptible to aggregate into higher order β-sheet oligomers and fibrils, ultimately resulting in the formation of an extracellular insoluble amyloid plaque that define AD neuropathology (Long and Holtzman, 2019). Aβ plaques can be morphologically classified as either diffuse or dense-core plaques, based on absence or presence of conformational β-sheet staining using Congo Red and Thioflavin-S (Serrano-Pozo et al., 2011). Plaques can also be further defined as neuritic meaning they are associated with nearby dystrophic neurons and are surrounded by activated glial cells (Wippold et al., 2008). Diffuse plaques are Congo Red and Thioflavin-S negative and non-neuritic as they are not associated with other pathological features such as glial accumulation or synapse loss. They are commonly found in those cognitively intact older patients (Serrano-Pozo et al., 2011; Masliah et al., 1990). Dense-core plaques, also known as neuritic plaques and consist of a compact core which

stains positive using Congo Red and Thioflavin-S which is are typically surrounded by dystrophic neurons, activated glial cells such as astrocytes and microglia and synaptic loss (Knowles et al., 1999; Urbanc et al., 2002; Vehmas et al., 2003).

As originally described by Braak and Braak, there are three distinguishable stages in the gradual development of cortical amyloid deposition (Braak and Braak, 1997) as summarised below (*Figure 1.4*):

- Stage A – plaque deposition initially occurs in the basal neocortex region, mainly in those unmyelinated areas such as the perirhinal and entorhinal fields
- Stage B – accumulation of amyloid plaques spread to adjacent neocortical areas and hippocampal regions such as the subiculum and CA1
- Stage C – eventual build-up of amyloid across all areas of the cortex, including the more myelin dense neocortical regions

It was once assumed that the staging of amyloid accumulation correlated with AD disease severity, however this has now been shown to be largely mistaken with the exception for the most severe disease stage (Boluda et al., 2014).

Building on the Braak staging of amyloid deposition, Thal phases further describes the accumulation of Aβ in the cerebellum and brainstem nuclei (Thal et al., 2002), and is used to assist with the neuropathological scoring of disease severity (*Figure 1.4*):

- Phase 1 – characterised exclusively by Aβ deposits in the neocortex
- Phase 2 – Aβ appears in the entorhinal region, the CA1 region of the hippocampus and the insular cortex
- Phase 3 – occurrence of Aβ in the diencephalic nuclei and the striatum

- Phase 4 – Aβ deposits spread to additional distinct brainstem nuclei
- Phase 5 – Aβ spreads to the remaining regions of the brainstem and to the molecular layer of the cerebellum

Thal staging assists in diagnosis through the implementation of a more sensitive staining method (Thal et al., 2002) and has been adopted by the NIA-AA and BrainNet Europe (Montine et al., 2016, Alafuzoff et al., 2009). During the neuropathological diagnosis of AD, Thal phases 1-4 can be confirmed by the presence of amyloid deposition in the medial temporal lobe (Thal et al., 2006) and it has been found that neurologically normal patients can also appear to be phase 1-3 (DeTure et al., 2019).

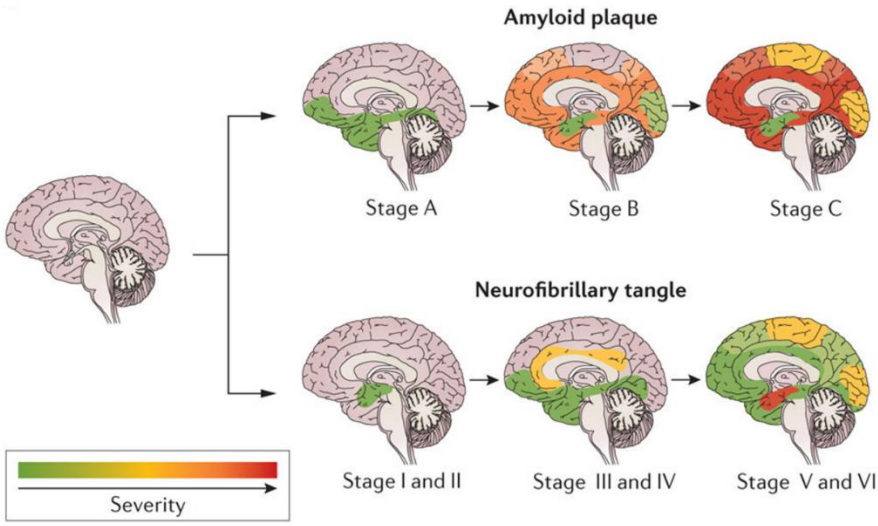

Figure 1.4: Spread of amyloid plaque pathology and NFT tangle pathology across the AD brain.

Schematic showing the characteristic pathologic spread and increasing burden of protein accumulation in AD. Amyloid deposition precedes NFT build-up, originating in the frontal and temporal lobes, eventually spreading to the hippocampus and limbic system (top row). NFT accumulation begins in the medial temporal lobes, then spreads into the hippocampus and into other areas of the neocortex (bottom row). Figure adapted from Masters et al., 2015

1.3 Tau

1.3.1 Tau structure and function

Tau is a member of the microtubule-associated protein (MAP) family, originally identified as a heat stable protein with an essential role in microtubule assembly and cytoskeletal stability (Weingarten et al., 1975). Tau is found in a number of animal species, including *Caenorhabditis elegans*, *Drosophila*, rodents, monkeys and humans. In humans, these tau proteins are mainly found in neurons, although non-neuronal cells, such as glial cells in pathological conditions, have also been seen to contain trace amounts (Buée et al., 2000). Within the neurons, tau is predominantly found highly phosphorylated and located in the axons where it promotes microtubule stabilisation and polymerisation (Hanger et al., 2009).

Human tau is encoded by the microtubule-associated protein tau (MAPT) gene which contains 16 exons located over 100 kilobases (kb) on chromosome 17q21 (Neve et al., 1986; Goedert et al., 1988). MAPT is alternatively spliced at exons 2, 3 and 10 to form six major isoforms between 352 and 441 amino acids long (Goedert et al., 1989). Exons 2 and 3 encode for N-terminal domains (N) and exon 10 encodes for the carboxy-terminal (C-terminal) microtubule-binding repeat domain (R) and so each of the tau variants differ due to the absence or presence of 1 or 2N in addition to either 3 or 4R (*Figure 1.5*) (Goedert and Jakes, 1990). Each of these different isoforms are likely to link to specific physiological roles as they are differentially expressed. In early development, only one short tau variant is expressed in the brain whereas all six isoforms are present in the mature brain. Further to this, in healthy adult brains the ratio of 3R to 4R is approximately 1:1 but this ratio has seen to change in different diseases (Schweers et al., 1994; Buée et al., 2000; Kosik et al., 1989). It is also important to note that the proportions of tau isoforms differs from species to species, with adult

mouse brain express the three isoforms of 4R (Kosik et al., 1989) whilst murine 3R tau is expressed in only the neurons of new-born mice (Llorens-Martin et al., 2012).

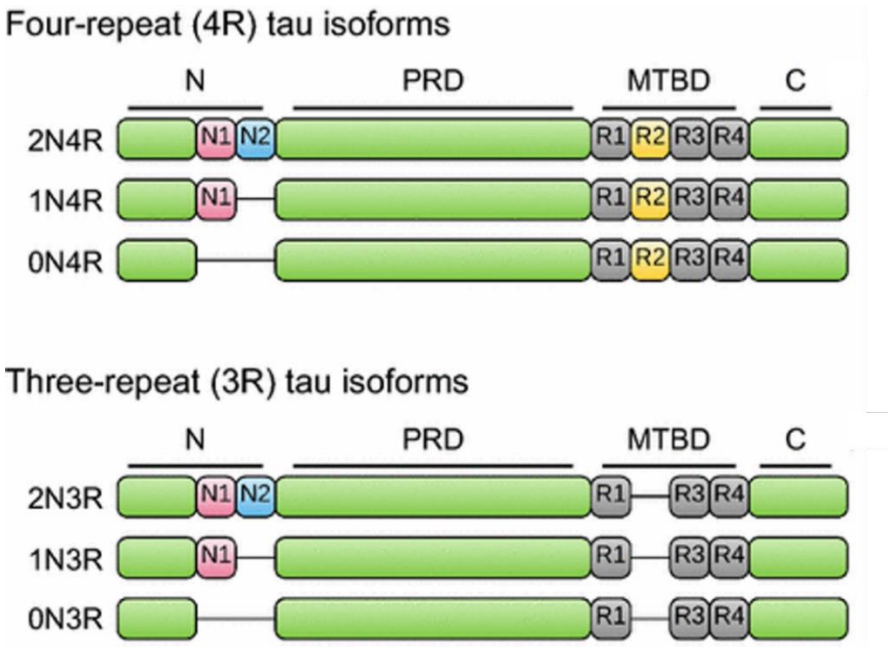

Figure 1.5: Different tau isoforms and corresponding MAPT domains which are alternatively spliced in the human central nervous system (CNS).

Exons 2 and 3 in the N-terminal region are either excluded (0N) or differentially included leading to 1N (exon 2) or 2N (exon 2 and 3) tau isoforms. Alternative splices in the microtubule binding region (MTBD) results in either 3R or 4R tau isoforms. Figure adapted from Guo et al., 2017

The tau molecule can be divided into four major domains as follows. Firstly, there is the N-terminal domain containing the two distinct alternatively spliced N-terminal regions. Next is the proline-rich domain. Thirdly, there is the microtubule binding domain containing the four repeat motifs and flanking regions which allows tau to bind and stabilise microtubules, and finally the C-terminal tail of tau (Guo et al., 2017; Mandelkow and Mandelkow, 2012; Mukrasch et al., 2009). Tau is a natively unfolded protein with a highly flexible structure which allows for the intramolecular interactions

between its differently charged C- and N-terminus domains (Jeganathan et al., 2008; Mukrasch et al., 2009; Jeganathan et al., 2006).

The N-terminal domain projects away from the microtubule surface and so does not bind to microtubules directly however it does have a vital role in regulating microtubule dynamics by interacting with the cell membrane and other cytoskeleton proteins such a neurofilament proteins, whilst influencing the spacing between microtubules and other cellular components (Chen et al., 1992; Brandt et al., 1995; Hirokawa et al., 1988). The exact function of the different N-terminal inserts is unknown, however they have been implicated in determining the distribution and localisation of tau (Liu and Goatz, 2013; Paholikova et al., 2015; Gauthier-Kemper et al., 2011; Liu et al., 2016). The proline-rich domain provide recognition sites enabling the interactions with the Src-homology-3 containing proteins including the Src family of kinases which act as important signal intermediaries regulating a variety of cellular processes including cell growth and survival (Parsons et al., 2004; Morris et al., 2011; Guo et al., 2017). This region has also been implicated in important roles in nuclear function, as it functions as a DNA interacting site (Qi et al., 2015), and it is also involved in the regulation of microtubule assembly and actin binding, supporting the function of the proline-rich domain in maintaining the neuronal cytoskeleton (Eidenmüller et al., 2001; He et al., 2009). The microtubule binding domain of the tau protein is responsible for mediating the interaction between tau and the microtubules (Pîrşcoveanu et al., 2017; Buée et al., 2000; Drechsel et al., 1992; Sillen et al., 2007). Further to this, the microtubule binding domain has been shown to bind ribonucleic acid (RNA) and also associate with lipid membranes (Brady et al., 1995; Thurston et al., 1996; Kampers et al., 1996; Georgieva et al., 2014). Finally, the C-terminal tau tail has not been fully established although studies suggest it may be involved in influencing the interaction of other domains with other proteins (Connell et al., 2001).

1.3.2 Tau Phosphorylation

Tau is able to undergo a range of post-translational modifications, including acetylation, glycosylation, nitration, ubiquitination, truncation, and phosphorylation (Marcelli et al., 2018). The most commonly described modification is tau phosphorylation. Tau contains 85 different phosphorylation sites which include 45 serine, 35 threonine and 5 tyrosine residues (Hanger et al., 2009). The different tau phosphorylation states are dependent on the balance of specific kinases and phosphatases. The tau kinases can be categorised as proline-directed serine/threonine-protein kinases such as glycogen synthase kinase (GSK) and cyclin-dependent kinase-5 (Cdk5), non-proline-directed serine/threonine-protein kinases such as microtubule affinity-regulating kinases (MAPKs) and cAMP-dependent protein kinase A (PKA) and thirdly, protein kinases specific for tyrosine residues such as Src and Fyn (Martin et al., 2011). Protein phosphatases counterbalance the physiological impact of kinases. Protein phosphatase 2A (PP2A) has been shown to regulate the phosphorylation of tau and PP2A activity is markedly reduced in the AD brain, possibly contributing to the increase tau pathology seen in the disease (Gong et al., 2000; Liu et al., 2005). A further phosphatase, PP5 has also been implicated in tau phosphorylation and its activity is also reduced by about 20% in the neocortex of AD brains (Liu et al., 2005).

The role of tau phosphorylation has been implicated in tau self-aggregation. Tau is generally a soluble protein that appears unfolded in its native form, however under certain conditions, once tau become detached from microtubules, it is able to aggregate to form higher order aggregated tau oligomers and eventually paired helical filaments (PHF) in AD (von Bergen et al., 2000; Mandelkow et al., 2007). It has been found that both tau phosphorylation in the proline-rich regions flanking the microtubule domain and phosphorylation in the C-terminal both trigger and promote tau self-aggregation (Eidenmüller et al., 2001; Liu et al., 2007).

It has also been demonstrated that tau phosphorylation may exacerbate neurodegeneration via other mechanisms besides microtubule destabilisation and self-aggregation. Studies have shown that the mislocalisation of tau from axons and the subsequent accumulation of hyperphosphorylated tau within the dendritic spines impairs synaptic function (Hoover et al., 2010). Further to this, phosphorylated tau has been proven to modulate activation of kinases GSK3 and Cdk5 within synaptic terminals, disrupting synaptic transmission (Moreno et al., 2016). The phosphorylation of tau has also been seen to block its normal biological fucntion by protecting tau from degradation by the proteosome system and by impeding tau interaction with the cytoplasmic membrane and DNA, therefore causing an obstruction to a range of subsequent signalling pathways (Dickey et al., 2007; Hanger et al., 2009).

1.3.3 Tau seeding and propagation

Prion-like protein propagation is a phenomenon where proteins aggregate and spread across the brain via intracellular transmission between neighbouring cells (Fraser 2014). The prion-like properties of tau were initially described in the P301S tauopathy model in which overexpression of human tau is restricted to the entorhinal cortex in young mice but as the mice ages, tau progresses along an anatomically connected network of neurons via a trans-synaptic mechanism, with eventual tau pathology propagating to the dente gyrus and CA1 regions of the hippocampus (de Calignon et al., 2012; Liu et al., 2012; Calafate et al., 2015). Successive studies have similarly shown that when injecting brain extracts taken from the P301 mouse into mouse models overexpressing either human or mouse tau, there is again an aggregation of tau not only at the site of injection but also in synaptically connected distal regions, reiterating the fact that the pattern of spread is determined by connectivity and not proximity (Clavaguera et al., 2009; Ahmed et al., 2014). This phenomenon has also been reproduced using patient-derived tau from human brain extracts (Robert et al., 2021). This allows researchers to recapitulate distinct disease specific tau, containing the human specific

isoforms into a number of rodent models, including wild-type (WT) mice, transgenic (Tg) mouse models of Aβ and mice encoding a humanized MAPT sequence (Guo et al., 2016; He et al., 2017; He et al., 2020).

The conformation of tau species seems to be critical in determining tau spread as certain structures seem to encourage tau aggregation and propagation more than others. In AD brains, C-terminally truncated tau is found abundantly in the synaptic terminals and this tau cleavage may facilitate tau secretion and therefore propagate disease (Sokolow et al., 2014). In the SHSY5Y cell model, the 24kDa C-terminal fragmented tau proved to be more susceptible to aggregation and also propagated more readily compared to the full-length tau through increased frequency of cell binding (Matsumoto et al., 2015). Taken together, these studies highlight just some of the literature which supports the prion-like notion of tau pathology and could suggest an explanation of how tau aggregation may spread to more widespread brain regions during AD and thus aggravating the neurodegenerative process (Goedert et al., 2017).

1.3.4 Neurofibrillary tau tangles

Neurofibrillary tau tangles (NFT) are comprised of the microtubule-associate protein tau which has been phosphorylated and subsequently assembled into PHF, (Grundke-Iqbal et al., 1986)). NFT are pathological but are not necessarily associated with cell death, and neurons containing NFT are able to survive for decades, suggesting a potentially protective role of NFT (Morsh et al., 1999; Spires-Jones et al., 2009). The spread of NFT follows a spatiotemporal progression across six distinct stages, known as Braak stages I - VI (Braak and Braak, 1991; Braak and Braak, 1995). Braak staging is used to assess the severity of AD and is summarised as follows (*Figure 1.4*):

- Stages I – II, also referred to as the transentorhinal stages, are characterised by the mild presence of NFT mostly in the transentorhinal region and hippocampal CA1 region and corresponds to the least severe AD cases
- Stages III – IV, also referred to as the limbic stages, sees the spread of NFT to the thalamus, the amygdala, the hippocampal CA4 region and the basal ganglia
- Stages V – VI, also referred to as the isocortical stages, where the remainder of the hippocampal formation is affected and there is significant accumulation of NFT in the isocortical regions, with the exception to the motor cortex, eventually resulting in mass atrophy to the temporal and frontal cortices. This corresponds to the most severe stage of AD

1.3.5 Tauopathies

Tauopathies are a group of sporadic or familial neurodegenerative diseases characterised histopathologically by the filamentous accumulation of hyperphosphorylated tau in neurons or glial cells or both (Chung et al., 2021; Arendt et al., 2016). Tauopathies are further classified into two groups, primary and secondary tauopathies, with primary tauopathies defined as being dependent on tau as a major contributing factor whereas secondary tauopathies are defined by the substantial aggregation of another protein considered the primary driver of disease progression (Kovacs 2016, Williams 2006). The most common secondary tauopathy is AD (Chung et al., 2021).

As the anatomical and cellular pattern of the tau pathology within these primary tauopathies is generally involving the frontotemporal lobes of the brain, primary tauopathies are also sub-grouped under the umbrella term of frontotemporal lobar degeneration (FTLD). This encompasses a number of diseases characterised by the destruction of the frontal and temporal lobes (Seltman and Matthews, 2012; Mackenzie, 2010). FTLD patients can be further categorised according to the

misfolded intracellular protein found in the brain into FTLD-TDP representing a build-up of TDP-43, FTLD-FUS representing the build-up of the fused in sarcoma protein (FUS) or FTLD-tau (Mackenzie et al., 2010). The group of FTLD-tau diseases included Picks disease, progressive supranuclear palsy, corticobasal degeneration and FTD with microtubule-associated tau (MAPT) gene and globular glial tauopathy (Arendt et al., 2016).

1.3.5.1 MAPT mutations

The first mutation discovered in the MAPT gene was the P301L mutation, associated with frontotemporal dementia tauopathies (FTLD-tau) and which leads to tau dysfunction and neuronal death (Chung et al., 2021; Hutton et al., 1998; Poorkaj et al., 1998). A number of MAPT mutations have now been located and have shown to mostly cause frontotemporal dementias but are also involved in Parkinson's disease, Dementia with Lewy bodies and Amyotrophic lateral sclerosis (ALS) (Ghetti et al., 2014). MAPT mutations can cause tau pathology by enhancing tau aggregation or by increasing the levels of tau phosphorylation and by altering the ratio of 3R to 4R isoforms (Alonso et al., 2004; Chung et al., 2021). In those diseases with a higher proportion of 4R tau, this mutation can influence the microtubule binding capabilities of tau as 4R tau isoforms are more inclined to bind to microtubules (Lu and Kosik, 2001). Besides microtubule function, the influence of disease specific MAPT mutations has not been fully established.

1.4 Interactions between tau and amyloid-β

The current disease hypothesis of AD postulates that Aβ, in the form of either plaques or the soluble oligomeric form, is responsible for initiating the pathological cascade which in turn causes tau misfolding and spread throughout the cortex, ultimately leading to neurodegeneration and cognitive

decline (Busche and Hyman, 2020). This hypothesis has been supported by both human genetic associations and through various experimental models of disease. Those patients who carry mutations in Aβ related genes, such as APP and PSEN1/2 accumulate amyloid earlier in the disease and are associated with a much earlier age of onset but a comparable rate of progression of clinical symptoms compared to those who suffer from sporadic AD (Ryan et al., 2016). In the 3xTg-AD mouse model which develops both Aβ and tau pathology, the presence of plaques precedes the development of plaques and treatment with an Aβ antibody reduced early-disease stage tau pathology (Oddo et al., 2003). In two transgenic mouse models overexpressing APP, the APP/Swe and the APPPS1 mouse, the presence of endogenous mouse tau was found in the CSF at the time point when each of the mouse models showed substantial Aβ pathology (Maia et al., 2013). Moreover, treating these mice with a BACE1 inhibitor targeting Aβ pathology also prevented further age-related accumulation of this murine tau (Schelle et al., 2017).

Recently, this theory has come under scrutiny as a number of clinical trials involving therapeutics focussed purely on reducing Aβ pathology, which proved to be curative in mice, have failed to significantly improve clinical symptoms or slow disease progression (Busche and Hyman, 2020). There is now increasing evidence indicating that the interplay between amyloid and tau may be much more complex than originally theorised. For example, mouse studies now suggest that amyloid-β is able to influence and enhance tau pathology throughout the disease, even at the later stages and not just at the beginning (Bennett et al., 2017; Busche et al., 2019). Further to this, there have been a number of mechanistic lessons learnt from various models of AD which support a more synergic, rather than causative relationship between these two proteins. Cross breeding mouse models overexpressing tau with mouse models overexpressing APP has resulted in enhanced pathological phenotypes compared to parental lines, as demonstrated by the crossing of the APPPSW1 models with the P301L tauopathy mouse (Bennett et al., 2017). The resulting cross

demonstrated accelerated formation of phosphorylated tau along with increased tau tangles and increasing number of reactive astrocytes and activated microglia (Bennett et al., 2017). More interestingly, by crossing various different mouse models overexpressing APP with tau mouse models overexpressing the human mutant 4R tau, it was determined that it was the soluble form of Aβ which was associated with more aggressive phosphor-tau propagation into the hippocampal regions and not the intracellular Aβ aggregates (Gomes et al., 2019).

1.5 Neuroinflammation

One of the strongest correlates of cognitive decline in AD is the accumulation of neuroinflammation (Ingelsson et al., 2004; Perez-Nievas et al., 2013). Neuroinflammation is generally defined by the production of a combination of pro-inflammatory cytokines such as IL-6 and tumour necrosis factor (TNF), chemokines, small molecules such as nitrogen oxide (NO) and reactive oxygen species (ROS), by the innate immune cells of the central nervous system, those of which included microglial and astrocytes (DiSabato et al., 2016). The release of pro-inflammatory cytokine IL-1β simultaneously activated pathways found in both pre- and post-synaptic activation which resulted in eventual synapse loss (Mishra et al., 2012). The release of TNF recruits caspase-8 which in turn activates TNF receptor 1 and initiates apoptosis and cell death in neurons (Micheau and Tschopp, 2003). And finally microglia recruited during inflammation can mediate synaptic loss through excessive synapse pruning (Hong et al., 2016). This data highlights some of the literature which supports the detrimental effects of neuroinflammation in driving disease progression through promoting synaptic dysfunction, and exacerbating neuronal death.

1.5.1 Microglia

Microglia are innate immune cells which derive from the myeloid lineage within the CNS, and arise by haematopoiesis, the formation of blood cell components, in early embryonic development (Leng and Edison, 2021). Microglia have essential functions throughout the whole of one's lifespan, from development through maturation and eventual senescence of the CNS and has important roles in synaptic pruning, neuronal apoptosis, the maintenance of synaptic plasticity and immune surveillance (Salter and Stevens, 2017; Ousman and Kubes., 2012; Paolicelli et al., 2011). Microglial receptors are able to detect abnormal proteins such as pathogens and cell debris, which induce a microglial response(Leng and Edison, 2021). This leads to microglial internalisation and degradation of pathogenic species in addition to increasing microglial expression of chemokine receptors and interferons which also contribute to the neuroinflammatory process (Solé-Domènech et al., 2016; Bajetto et al., 2002; Owens et al., 2014).

1.5.2 Microglia in AD

The proportion of activated microglia strongly correlate with presence of amyloid and tau neuropathology and the rate of cognitive decline in AD (Felsky et al., 2019). Although microglial activation is heavily associated with disease pathology, it is still unclear as to whether this phenomenon is protective or harmful in AD.

Variants in the triggering receptor expressed on the TREM2 gene have been found to increase the risk of AD by 2-4 times, comparable to those patients who have one copy of APOE ε4, the most common risk factor for the disease (Gratuze 2018). TREM2 is highly expressed on microglia and is involved in promoting microglial phagocytosis and survival whilst modulating inflammatory signalling. Interestingly, TREM2 has also been shown to bind and support phagocytosis of soluble Aβ (Gratuze et al., 2018; Shi and Holtzman, 2018). Further to this, TREM2 knock-out (KO) mice have

been shown to have exacerbated build-up of amyloid due to a reduction in phagocytic clearance of Aβ (Parhizkar et al., 2019). Conversely, pharmacological depletion of the colony-stimulating factor 1 receptor (CSF1R), essential for microglial survival, led to the elimination of microglia in a mouse model of AD and impaired plaque development in the parenchymal space (Spangenberg et al., 2019).

The data surrounding microglia interaction with tau pathology suggest a more detrimental role of microglia in disease. The depletion of TREM2 has been shown to mitigate neuroinflammation and astrocyte reactivity and protects from tau related neuronal loss in various mouse models of tauopathy (Sayed et al., 2018; Leyns et al., 2017). Further to this, microglia are able to internalize tau both *in vitro* and *in vivo* (Bolós et al., 2016), and by attenuating microglia it is possible to suppress tau propagation via the inhibition of microglia secretion of tau oligomer containing exosomes (Asai et al., 2015).

1.5.3 Astrocytes

In the human brain, glial cells constitute about 50% of all cell types, with different brain regions exhibiting unique groups of glial cells (Azevedo et al., 2009; Herculano-Houzel, 2014). Approximately 20% of these glial cells are made up of specialised cells called astrocytes (Pelvig et al., 2008). The full function of astrocytes is relatively unknown, however, they have generally been accepted as "housekeeping cells", promoting neuronal health and survival. Their role includes surveying and maintaining the extracellular area, involvement in cell-to-cell communication through gap junctions and signalling (through the reliance on intracellular levels of calcium), the regulation of blood flow and circulation, the maintenance of the blood brain barrier (BBB) and the development and upkeep of synaptic function and neurotransmission (Allen and Eroglu, 2017; Verkhratsky et al., 2015).

As astrocytes are heavily involved in the homeostasis of the CNS it is hardly a surprise that they are also widely implicated in neurodegeneration. Astrocytes respond to injury by undergoing a morphological and functional transformation into reactive astrocytes. Under different pathological situations, astrocytes change their morphology, gene expression and function in accordance to the form and severity of the insult. The resulting change in astrocytic activity is complex and not well understood and can cause a toxic gain or loss of function with the potential to impact surrounding cell types (Sofroniew and Vinters, 2010). This process has been defined as reactive astrogliosis and those astrocytes observed in pathological conditions are referred to as reactive astrocytes (Escartin et al., 2021). The overall impact of reactive astrocytes on different diseases is complex and differs from disease to disease and the exact role reactive astrocytes is yet to be fully determined. For example, in the APP/Swe mouse models of AD, inhibiting transcriptional factor STAT3 and therefore preventing astrogliosis led to a reduction in in amyloid-β levels and strongly ameliorated spatial learning and memory decline (Reichenbach et al., 2019), however, deleting two genes which encode filament proteins required for astrocyte activation in the same transgenic mouse model of AD resulted in an increase in amyloid plaque load (Kraft et al., 2013). Furthermore, the activation of the aforementioned STAT3 pathways was detrimental in AD (Reichenbach et al., 2019), but has proved protective against other neurodegenerative injuries by promoting synaptic plasticity after motor neuron injury (Tyzack et al., 2014) and initiating scar formation after spinal cord injury (Herrmann et al., 2008).

Adding to this complexity, it is difficult to distinguish the contribution of reactive astrocytes from the contribution of the other main contributor to the immune responses in the brain, the microglia (Heneka et al., 2014). Both reactive astrocytes and microglia activation are a central feature in neurodegeneration and communication between the two types of glial cells occurs through signal release from astrocytes onto microglia and vice versa (Haim et al., 2015). These astrocytic signals can

promote both the anti- and pro-inflammatory properties of microglia (Farina et al., 2007; Jha et al., 2019). Conversely, harmful reactive astrocytes are induced by inflammatory microglia (Liddelow et al., 2017). Although it remains unclear to what extent reactive astrocytes are protective or damaging during disease progression, there is a substantial body of evidence implicating the importance of reactive astrocytes in neurodegeneration.

1.5.4 Astrocytes in Alzheimer's disease and other tauopathies

In AD, the accumulation of reactive astrocytes, along with tau phosphorylation, very strongly correlates with cognitive decline (Ingelsson et al., 2004; Perez-Nievas et al., 2013). In human brains, these reactive astrocytes are seen to accumulate around amyloid plaques (Itagaki et al., 1989; Wisniewski and Wegiel, 1991). Astrocytes can mediate the uptake and degradation of Aß as well as the secretion of Aß-degrading proteases, and therefore mediate a reduction in the overall amyloid pathology (Leissring, 2016; Ries and Sastre, 2016). In addition, astrocytes are the main source of APOE, the greatest genetic risk factor in late-onset AD (Corder et al., 1993; Saunders et al., 1993; Strittmatter et al., 1993), which is required to enable the aforementioned Aß uptake and degradation (Koistinaho et al., 2004; Deane et al., 2008; Li et al., 2012).

Conversely, transcriptomic studies have shown that astrocytes in AD mice develop a proinflammatory phenotype and reduced expression of neuroprotective genes (Orre et al., 2014). In single-cell transcriptome analysis of human AD brains, astrocytes were shown to preferentially express genes which are associated with a response to neurodegeneration, such as clusterin (Mathys et al., 2019) and C3 (Liddelow et al., 2017; Grubman et al., 2019). In addition to this, astrocytes are also able to incite their own neurotoxic effects when exposed to AD-relevant proteins due to astrocytic loss of calcium regulation or glutamatergic function (González-Reyes et al., 2017; Scimemi

et al., 2013; Ye et al., 2015). This is in line with the recent suggestion of an "A1" subtype of reactive astrocytes attributed to AD and other neurodegenerative diseases. These are found to lose the ability to promote neuron and synaptic protection (Liddelow et al., 2017), in addition to perhaps mediating some of the harmful phenotypes exerted by Aß in neuronal health and synaptic function, as reported extensively in the literature (Abeti et al., 2011; Garwood et al., 2011; Jana and Pahan, 2010; Iram et al., 2016). However, strategies to combat astrocyte reactivity by depleting GFAP and vimentin in a transgenic mouse model of AD showed contradictory results (Kraft et al., 2013; Kamphuis et al., 2015). More recently, modulation of astrocyte reactivity through the STA3 pathway, support a deleterious role of astrocytes in AD (Ceyzériat et al., 2018).

As well as associating with amyloid plaques, astrocytes are also seen to accumulate with NFT, and the burden of these reactive glia correlates with the burden of tau pathology in human AD brains (Serrano-Pozo et al., 2011). Whilst tau accumulates preferentially in neurons in AD, a recent study found the presence of astrocytes with 3R tau inclusions in the hilus regions of the dentate gyrus in AD cases, which was further exacerbated by the presence of hyperphosphorylated tau (Richetin et al., 2020). Most other tauopathies are characterized by tau pathology both in neurons and glial cells, including oligodendrocytes and astrocytes. Reactive astrocytes are commonly found in these diseases and correlate with degeneration, suggesting that they may play a role in these diseases (Kahlson and Colodner, 2015).

1.5.5 Non-cell autonomous role of astrocytes in neurodegeneration

There has been an increasingly influx of evidence to suggest that AD disease is not restricted to the neurons, and interactions with other immunological mechanisms, such as neuroinflammation and

the crucial players microglia and astrocytes, plays an important role in driving the pathogenic process (Heneka et al., 2015). One example of this has been demonstrated by exploring the role astrocytes in maintaining the homeostatic balance of oxidative stress. In normal physiological conditions, astrocytes are seen to produce antioxidants in order to protect neurons, which are particularly vulnerable to hydrogen peroxide toxicity (Desagher et al., 1996). However, it has been found that the Aβ peptide can modify the glucose metabolism and cause NAPDH related oxidative stress in astrocytes. This in turn causes the astrocytic release of hydrogen peroxide and glutathione, resulting in neuronal glutathione depletion, impaired neuronal viability and eventual neuronal death (Abramov et al., 2004; Allaman et al., 2010). It has been argued that perhaps small amounts of ROS may provide beneficial neuroprotective functions through ROS induction of anti-oxidant systems and trophic factors (Chun and Lee, 2018), however, overproduction of ROS can in turn trigger inducible nitric oxide synthase (iNOS) expression and thus cause nitrosative stress and eventual death in neurons (Akama and van Eldik, 2000; Bagheri et al., 2017).

In recent years there has been increased focus on the implication of the non-cell autonomous role of astrocytes in neurodegenerative diseases. To explore this, a number of studies have been implemented to examine this interaction in ALS. It has been demonstrated in a rat model of the disease that when the TDP-43 mutation is restricted to astrocytes, this is able to cause a non-cell autonomous progressive loss of motor neurons, leading to ALS-like paralysis in the animal (Tong et al., 2013). This non-cell autonomous interaction has also been replicated when using a mouse model of ALS which mimics the endogenous expression of mutant TDP-43 found in disease. The excising of the TDP-43 mutation in the motor neurons only caused a delay in the onset of motor symptoms and subsequent motor neuron death but still resulted in degeneration of the axons and astrogliosis, highlighting the impact of both the neuron-neuron and astrocyte-neuron interactions in the disease (Ditsworth et al., 2017). Recent studies found that induced pluripotent stem cell-derived (iPSC) astrocytes from ALS patients carrying the C9orf72 mutation exhibited reduced secretion of

antioxidant proteins which in turn led to a toxic increase in oxidative stress in motor neurons generated from human embryonic stem cells (Birger et al., 2019). In contrast, healthy astrocytes can protect motor neurons in ALS. Co-culturing healthy iPSC-derived astrocytes with iPSC-derived motor neurons which have been exposed to TDP-43 aggregates seeded from post-mortem ALS spinal cord led to a significant reduction in these TDP-43 aggregates and apoptotic marker caspase-3 in the motor neuron (Smethurst et al., 2020).

To investigate the neuronal-astrocytic interplay in Huntington's disease (HD), a transgenic mouse model expressing a mutant form of the protein huntingtin (htt), specifically in the neurons, was crossed with a different transgenic mouse which expressed the mutant htt with 98 polyQ repeats specifically in the astrocytes. This led to a transgenic cross whose neurological symptoms became more severe and whose death occurred earlier than the mouse with mutant htt in the neurons only (Bradford et al., 2010), indicating the importance of glial dysfunction in exacerbating neuropathology in HD. Increasing the accumulation of mutant htt specifically in the astrocytes of another mouse model of Huntington's disease, the HD140Q knock-in mouse which expresses mutant htt ubiquitously but does not display neurodegeneration, led to an overall increase in endogenous mutant htt as well as a significant loss of neurons in the striatum of the mouse brain, highlighting how mutant htt can exacerbate neurodegeneration when htt is also present in the neuronal cells (Jing et al., 2021).

A new AD mouse containing toxin-triggered reactive astrocytes has the ability to manipulate the reactivity of astrocytes to become either mild or severe *in vivo* (Chun et al., 2020). When severe astrocytes are triggered in these mice, it results in hydrogen peroxide mediated neuronal loss as detected by neuronal markers NeuN and MAP2 in the CA1 regions and the cortex, along with significant presence of neuronal apoptosis as detected by chromatic condensation of nuclei. These

neurodegenerative changes were also accompanied by a significant increase in phosphorylated tau in the neurons of the CA1 region (Chun et al., 2020). Further to this, a transgenic mice which overexpress Nrf2, the master regulator of antioxidant and proteostasis genes (Kobayashi et al., 2016; Tebay et al., 2015), specifically in astrocytes (GFAP-Nrf2 mouse) was crossed with the P301S tauopathy mouse and the APPswe/PS1de9 (APP/PS1) mouse to explore whether the overexpression of astrocytic Nrf2 could alter the pathology progression in either transgenic cross (Jiwaji et al., 2022). In the P301S x GFAP-Nrf2 mouse, the levels of cortical neurodegeneration and phospho-tau accumulation were reduced compared to the P301S mouse, highlighting the non-cell autonomous neuroprotective effect of Nrf2-driven reactive astrocytes. Additionally, the AAP/PS1 x GFAP-Nrf2 mouse displayed a reduction in plaque density in the cortex and the hippocampus when compared to the APP/PS1 mouse due to enhanced clearance and autophagy mediated by the Nrf2-astrocytes (Jiwaji et al., 2022). Conversely, in a tauopathy mouse model, removing astrocytic APOE4, the strongest risk factor for AD (Saunders et al., 1993), at the onset of tau pathology markedly reduced tau accumulation and subsequent brain shrinkage and RNA sequencing analysis revealed gene expression changes in neurons, oligodendrocytes and microglia (Wang et al., 2021). Interestingly, the removal of astrocytic APOE4 reduced microglial synaptic pruning and phagocytosis of synaptic elements, reducing tau-associated synapse loss usually seen in this tau model (Wang et al., 2021),

The contribution of astrocytes to tau spreading highlights a much debated non-cell autonomous function of these glial cells in AD. In the human disease, the trans-synaptic tau propagation has been heavily implicated in disease spread (Braak and Tredici, 2018). However, it has also been confirmed that tau is also taken up by astrocytes and the primary source of tau within astrocytes is due to internalisation of the protein (Ferrer et al., 2018). Since then, a number of studies have underlined astrocytes as crucial participants in tau spread, in addition to neurons, with specific astrocytic phenotypes such as thorn-shaped astrocytes, heavily implicated in the role of hyperphosphorylated

tau propagation (Ferrer et al., 2018; Perea et al., 2019; Kovacs, 2020). Once the tau is internalised by astrocytes, and even before the astrocytes have released and enabled tau spread, this accumulation within the glial cells is enough to mediate a toxic non-cell autonomous reaction in neighbouring neurons. It was found that this accumulation of astrocytic tau may cause a reduction in gliotransmitter (e.g. ATP) availability, causing a reduction in synaptic vesicle release and expression of synaptic proteins and therefore synaptic dysfunction in nearby neurons (Piacentini et al., 2017). To further aggravate matters, exposure of these tau-containing astrocytes to Aβ oligomers may induce the excessive release of phosphorylated tau, via exosomes, indicating a potential mechanism behind how Aβ and tau interactions may exacerbate tau pathology (Chiarini et al., 2017).

The evidence for the role of astrocytes in preventing tau spread primarily comes from the exploration of the dysregulation of autophagy in the context of neurodegeneration with particular focus on transcription factor EB (TFEB) (Constanza and Spada, 2019). TEFB is the regulator of many lysosomal genes and under stress it initiates nuclear transcription of genes responsible for the upregulation of autophagosome formation, lysosomal biogenesis and lysosomal function (Sardiello et al., 2009). TFEB has been shown to be upregulated and activated in response to tau pathology in both humans and mouse models of tau, as well as in Aβ and combined Aβ and tau pathology experimental models of disease (Song et al., 2020; Martini-Stoica et al., 2018). Both the endogenous increase in astrocytic TFEB expression and induced TFEB expression in astrocytes, led to enhanced autophagy and lysosomal activity, and so a reduction in protein accumulation and aggregation and tau spread. This resulted in an overall neuroprotective response as demonstrated by improved synaptic and cognitive function (Song et al., 2020; Martini-Stoica et al., 2018; Xiao et al., 2014).

1.6 Molecular Chaperones

The protein quality control system is required to maintain protein homeostasis by ensuring the correct folding and assisting in degradation when needed, and one major player within this system are the molecular chaperones (Brehme et al., 2014). The broad function of the molecular chaperones includes interacting with, stabilising or assisting another protein in obtaining its functionally active conformation, without being present in the final structure (Harti and Hayer-Hartl, 2009). Molecular chaperones are also referred to as heat-shock proteins (HSP) as they were first described to be upregulated in response to heat stress (Ritossa 1962). These heat shock proteins are usually classified into different families depending on their molecular weight as follows: HSP40, HSP60, HSP70, HSP90, HSP100 and small HSP (sHSPs) (Hartl et al., 2011), however they have also been classified according to functional families which corresponded to the following nine chaperone families: HSP90, HSP70, HSP60, HSP40, Prefoldin, sHSPs, TPR-domain containing, organelle specific chaperone of the ER and organelle specific chaperones of the mitochondria (Brehme et al., 2014; Hartl and Hayer-Hartl, 2002; Kleizen and Braakman, 2004; Tatsuta et al., 2004). The different families of HSP co-exist and interact within the cell to forming cooperative networks and pathways to support protein homeostasis (Hartl et al., 2011). Out of all the HSP families, this thesis will only briefly describe the structure and function of those HSP most relevant for this PhD project, HSP70, HSP40, HSP90 and the sHSPs (see Chapter 1, Section 1.7).

1.6.1 The HSP70 family

The constitutively expressed HC70, and stress-inducible form HSP70, is the most well studied molecular chaperone which has vital roles in proteostasis control (Chaari 2019) and increased levels of HSP70 have shown to prevent toxic protein aggregation in a model of neurodegeneration (Auluck et al., 2002). HSP70 is made up of two functional domains, the conserved N-terminal ATPase, also

known as the nucleotide binding domain (NBD) and the C-terminal peptide-binding domain (PBD), consisting of a β-sheet sandwich subdomain and a α-helical lid domain (Ciechanover et al., 1980; Zhu et al., 1996). The β-sheet sandwich of the PBD recognises the hydrophobic amino acids within proteins (Rudiger et al., 1997) whilst the NBD controls whether the chaperone is in an open ATP-bound state with low-substrate affinity or a closed ADP-bound state with high substrate affinity (Mayer and Bukau, 2005). The hydrolysis of ATP to ADP is modulated by HSP40 (also known as DNAJ) and other nucleotide-exchange factors, which leads to lid closure and stable peptide binding (Xu et al., 2018; Kampinga and Craig, 2010). In order to open the lid and release the substrate, a nucleotide-exchange factor binds to the ATPase domain on HSP70, catalysing ADP back to ATP (Hartl et al., 2011). Although HSP40 functions as a co-chaperone to HSP70, it has also been seen to bind directly to protein and act as its own independent chaperone (Kampinga and Craig, 2010; Chaari, 2019).

1.6.2 The HSP90 family

HSP90 is the most abundant HSP found in the cell and is localised in both the cytosol and the ER (Hoter et al., 2018). HSP90 acts downstream of the HSP70 system, playing a key role in the structure maturation and regulation of protein conformation of signal-transduction molecules such as kinases (McClellan et al., 2007; Hoter et al., 2018). HSP90 functions as a dimer of subunits which are assembled by the highly conserved C-terminal domain or dimerization domain, containing the major binding sites, which aid in interactions with other co-chaperones (Pearl and Prodromou, 2006; Richer and Buchner, 2006). The highly conserved N-domain is responsible for the hydrolysis of ATP and is joined to the C-terminal domain by a middle M domain (Shiau et al., 2006). HSP90 has been implicated in the stabilization and activation of a number of proteins which are involved in processes such as cell signalling and transcription (Picard, 2002; Voisine et al., 2010)

1.6.3 The role of molecular chaperones in AD

It has been shown that in the post-mortem cortical brain tissues from AD cases, there is a significant increase in HSP70 compared to age-matched controls (Perez et al., 1991). Further to this, HSP70 was found within amyloid plaques and neurofibrillary tangles (Hamos et al., 1991). Meanwhile, in the hippocampal regions of the AD brain, it was established that there was a reverse correlation between the appearance of HSPs and phosphorylated tau within the neurons, where neurons strongly stained with HSP70 or HSP90 did not stain for phospho-tau (Dou et al., 2003). It was also found that gene expression across all families of the chaperone proteins was repressed in the AD brain compared to healthy controls (Brehme et al., 2014).

In response to amyloid-β, expression of HSP70 and the sHSP CRYAB is upregulated in *C. elegans* as a protective response against Aβ accumulation (Fonte et al., 2002). HPS70 was also upregulated in neuronal cultures in response to intracellularly expressed $A\beta_{42,}$ and viral overexpression of HSP70 led to a reduction in neuronal apoptosis (Magrané et al., 2004). *In vitro*¸ HSP70 and HSP90 blocked Aβ self-aggregation by binding specifically to the oligomeric form, redirecting away from self-assembly and forming soluble circular oligomers instead (Evans et al., 2006). Furthermore, it was confirmed that treatment with a combination of HSP70, HSP40 and HSP90 altered the structures of both oligomers and fibrils which did not occur when each chaperone was added individually (Evans et al., 2006). HSPs have also been studied in relation to the other pathological AD protein, tau. A number of studies, have determined that HSPs including HSP90, HSP70 and the sHSPs, are able to recognise hyperphosphorylated tau and aid in its recycling (Luo et al., 2007; Dou et al., 2003; Karagöz et al., 2014; Du and Yan, 2010). In the brain of a tauopathy mouse model, which expressed 4Rm V337M mutant form of tau normally associated with frontotemporal dementia and parkinsonism linked to chromosome 17 (FTDP-17) (Tanemura et al., 2002) there was a significant decrease in the expression levels of HSP90, and cellular models determined that increasing levels of HSP70 and HSP90 increased

tau solubility and promoted the binding of tau to microtubules, in turn reducing the levels of phosphorylated and insoluble tau all through direct chaperone-tau interactions (Dou et al., 2003).

1.7 Small Heat Shock Proteins (sHSPs)

1.7.1 Structure of small heat shock proteins

One sub-family of these heat shock proteins are the small heat shock proteins (sHSPs) which are characterised by their small 12 to 43 kDa size and the presence of the conserved α-crystallin domain (ACD) (Golenhofen and Bartelt-Kirbach, 2016). *Table 1.1* shows the nomenclature used for the 10 members of this family found to date (Kampinga et al., 2009).

Family name	Alternative name	Tissue location	Function
HSPB1	HSP27 (human) HSP25 (mouse)	Ubiquitous with high levels in the heart, and muscle	Chaperone, stabilisation of cytoskeleton, anti-apoptotic, anti-inflammatory
HSPB2	MKBP	Heart and skeletal and smooth muscle	Chaperones DMPK gene (kinase), myofibrillar integrity, anti-apoptotic
HSPB3	HSPL27	Heart, brain, skeletal and smooth muscle	Target-protein dependent chaperone, myofibrillar integrity
HSPB4	αA-crystallin	High expression in the eye lens, skeletal muscle, liver, spleen, low levels in adipose tissue	Chaperone, genomic stability, eye lens
HSPB5	αB-crystallin	Ubiquitous, high expression in eye lens, heart and muscle	Chaperone, stabilisation of cytoskeleton, cell cycle, eye lens, regulating muscle differentiation, anti-apoptotic
HSPB6	HSP20	Ubiquitous, high expression in muscle	Smooth muscle, cardioprotective, chaperone, anti-apoptotic
HSPB7	cvHSP	Heart and skeletal muscle, low levels in adipose tissue	Chaperone, maintaining myofibrillar integrity
HSPB8	HSP22 HSP11	Ubiquitous	Chaperone, induction of autophagy
HSPB9	CT51	Testis	Linked to cancer and testis antigen
HSPB10	ODF1 ODFP	Testis	Elastic cytoskeleton structure

Table 1.1 Nomenclature, location and function of human sHSPs.

Adapted from Boncoraglio et al., 2012; Golenhofen and Bartelt-Kirbach, 2016; Kampinga et al., 2009 and Bakthisaran et al., 2015

The structure of the sHSPs and the dynamic nature of the different domains (*Figure 1.6*) are imperative in determining whether a client protein is able to bind and whether the sHSP can perform its chaperone function (Webster et al., 2019). The ACD is composed of antiparallel β-strands which can interact with these same β-strands in other sHSPs, allowing for the formation of dimers and oligomers (Kim 1998). Either side of the ACD are the N- and C-terminal regions which are more variable between sHSP families (Golenhofen and Bartelt-Kirbach, 2016) and these regions contain various phosphorylation sites, essential for allowing the dynamic exchange of subunits required by the sHSPs to carry out their chaperone functions (Hochberg and Benesch, 2014).The relatively disordered nature of the N- and C-terminals, compared to the conserved nature of the ACD, allows for the flexibility required for the sHSPs to interact with the client protein and other sHSPs (Jehle et al., 2011; Stromer et al., 2004; Carver et al., 2017).

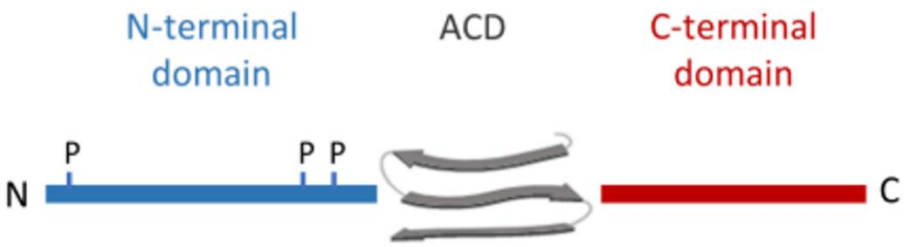

Figure 1.6: General structure of the small heat shock protein (sHSP), conserved across all the different families.

ACD = α-crystallin domain made up of antiparallel β-strands, P = phosphorylation sites, figure created by Katherine Sung

In order for sHSPs to interact with their client proteins, they utilise hydrophobic surfaces by which they attach to the hydrophobic surfaces on the client proteins which have been exposed due to misfolding or denaturation (Haslbeck et al., 2005; Jaya and Vierling, 2009; Sharma et al., 1997).

Exposure of these hydrophobic binding sites on the sHSPs could potentially cause instability in the sHSPs themselves and to overcome this, these hydrophobic regions are sequestered into large, dormant multimeric sHSP oligomers, ready to disperse into smaller oligomers when they need to become active (Santhanagopalan et al., 2018; Haslbeck et al., 2018; Basha et al., 2012). Many factors can influence the size of these structures and whilst HSPB1 and CRYAB can form homooligomers exceeding 20 subunits *in vitro*, other sHSPs tend to form smaller oligomers or dimers (Mymeikov et al., 2017). The formation of heterodimers and heterooligomers, formed under continuous subunit exchange between different sHSPs, have also been shown to regulate chaperone activity (Bova et al., 2000; Arrigo, 2013). Although the physiological relevance of these difference heteroliogmeric combinations is not fully known, there has been emerging evidence of a growing number of combinations, including HSPB1/HSPB5 (Aquilina et al., 2013) and HSPB8 with a number of different sHSPs including HSPB1 and HSPB5 (Sun et al, 2004).

sHSPs are also regulated by post-translational modifications, such as thiolation and the most well-studied phosphorylation, which may affect chaperone structure and mutimerization dynamics and therefore alter their ability to carry out chaperone functions (Nagaraj et al., 2003; Eaton et al., 2002; Ito et al., 2001; van den Ijssel et al., 1998; Hayes et al., 2009). It is generally reported that phosphorylation within the N-terminal regions of the sHSPs reduces the size of the oligomer although the opposite has been reported and the phosphorylation of CRYAB has been shown to form smaller but increasingly diverse globular assemblies (Shemetov et al., 2011; Ecroyd et al., 2007; Peschek et al., 2009)

1.7.2 Function of small heat shock protein

The sHSPs of interest for this PhD project are HSPB1 and HSPB5 and so the remainder of this chapter will primarily focus on these. These are the most well studied sHSPs, found to be ubiquitously expressed and along with HSPB8, are highly expressed in the human brain (Quraishe et al., 2008). Mutations in sHSPs can cause a number of pathological conditions due to the loss of function of sHSPs leading to a compromised ability in coping with stress, or the toxic gain of function resulting in increased misfolding or inadequate binding with cellular targets (Bakthisaran et al., 2015). Mutations include missense, frame shift, nonsense and elongation mutations and can occur along the entire length of the sHSPs, including within the C-terminal, N-terminal or β-strand regions (Benndorf et al., 2014). The exact molecular and cellular consequence of these sHSPs mutations are not fully understood but they are mostly implicated in muscle and motor neurone diseases (Laskowska et al., 2010). Most HSPB1 mutations are autosomal dominant and correlate with the development of a distal hereditary motor neuropathy, also known as Charcot-Marie-Tooth (CMT) disease characterised by muscle weakness as a result of motor and sensor neurons atrophy (Datskevich et al., 2012). Mutations in CRYAB are associated with the development of a number of congenital diseases including cataracts, myofibrillar myopathy and cardiomyopathy and some CRYAB mutations can cause multiple symptoms spreading across a number of different congenital diseases (Sacconi et al., 2012).

As part of their classical chaperone function, sHSPs are able to bind partially denatured proteins to prevent irreversible aggregation, but unlike other chaperones such as the HSP70 family, they are unable to re-fold these complexes back into their original shapes (Horwitz, 1992; Jakob et al., 1993; Haslbeck et al., 2005). Besides their classical chaperone function, sHSPs have also been implicated in other functions such as cytoskeleton stability, anti-inflammatory and anti-apoptotic functions

(Boncoraglio et al., 2012; Wettstein et al., 2012; van Noort et al., 2012; Garrido et al., 2001; Kamradt et al., 2002).

1.7.2.1 Anti-aggregation function of sHSPs

The sHSPs have been shown to interact and prevent the aggregation of the main pathological proteins of AD. CRYAB is able to interact with Aβ monomers in order to prevent any further neurotoxicity (Mannini et al., 2012). Intracellular CRYAB also binds misfolded oligomer species to form long-lasting Aβ complexes, preventing fibril elongation and thus protecting cells from the potential apoptosis associated with protein misfolding (Dehle et al., 2010; Shammas et al., 2011). Overexpression of CRYAB in N2a cells demonstrated its involvement in reducing the levels of phosphorylated tau and tau neurofilaments whilst also reducing GSK-3β, a tau kinase found aberrantly accumulated in NFT-containing neurons (Björkdahl et al., 2008).

In vitro, HSPB1 has been seen to interact with and sequester Aβ oligomers into larger, non-toxic aggregates, and neurons deficient for HSPB1 displayed increased sensitivity to Aβ toxicity as they were increasingly susceptible to neuronal death (Ojha et al., 2011). HSPB1 is also able to bind to tau in aggregation-induced conditions by interacting with tau oligomers and delaying the subsequent formation of toxic tau fibrils (Baughman et al., 2018). This function is mediated via the N-terminal region of HSPB1, the region vital to initiate the chaperone activity of HSPB1 (Baughman et al., 2020). Furthermore, HSPB1 can alter the conformation of pathological hyperphosphorylated tau and reduce levels of hyperphosphorylated tau through facilitating its degradation and dephosphorylation and providing a neuroprotective effect (Shimura et al., 2004). Linked to this, an increase in HSPB1 interaction specifically with hyperphosphorylated tau can reduce tau levels, however, binding of

phosphorylated HSPB1 to tau can lead to the accumulation of soluble tau intermediates (Abisambra et al., 2010).

1.7.2.2 Anti-inflammatory functions of sHSPs

These anti-inflammatory properties of sHSP have been explored in a number of studies. Exposure to extracellular sHSPs appears to activate macrophages during inflammatory stress, stimulating the release of anti-inflammatory cytokines and chemokines (Bhat and Sharma, 1999; De et al., 2000; van Noort et al., 2010; Banerjee et al., 2011). Over the years, there have a been a number of studies testing the potentially anti-inflammatory roles of CRYAB using various animal disease models in which neuroinflammation is seen to be a key pathological event. In models of experimental autoimmune encephalomyelitis (EAE), the disease model used to study multiple sclerosis (MS) in rodents, it has been found that administering CRYAB is able to suppress lipopolysaccharides (LPS) induced inflammation and markedly improves symptoms and outcome (Ousman et al., 2007; Guo et al., 2019). In addition to this, systemic administration of mice with recombinant CRYAB after a stroke saw a reduction in both stroke volume and inflammatory cytokines (Arac et al., 2011).

There have been fewer studies exploring the anti-inflammatory properties of HSPB1, however, given the structural homology between sHSPs, it is highly likely both sHSPs share some similar anti-inflammatory functions (van Noort et al., 2012). There has been increased focus on the protective role of HSPB1 after ischemic stroke, where levels of astrocytic HSPB1 are upregulated (Bartelt-Kirbach and Golenhofen, 2014). Injection of human-derived HSPB1 into a mouse after cerebral ischemia provided neuroprotection against inflammation-related neuronal death (Teramoto et al., 2013). Further to this, it has been demonstrated that HSPB1 can also modulate the immune response in atherosclerosis through modulating NF-κB activity in macrophages (Batulan et al., 2016).

1.7.2.3 sHSPs interactions with the cytoskeleton

Disruption of cytoskeleton assembly is one of the early effects of stress which can lead to eventual cell death (Singh et al., 2007). Studies on the lens cytoskeleton led to the discovery that sHSPs, namely CRYAB, could interact with both the intermediate filaments and their soluble subunits (Nicholl and Quinlan, 1994) and the importance of the physiological role of CRYAB-filament interactions was confirmed when it was found that mutations in CRYAB cause aggregation of these filaments in desmin related myopathies (Vicart et al., 1998). Since then, both CRYAB and HSPB1 have been shown to interact with these filaments and prevent their reorganisation, but they are unable to prevent filament collapse (Perng et al., 1999; Perng et al., 1999). Further to this, upon heat stress, CRYAB directly interacts with actin and regulates filament dynamics *in vivo,* protecting cells from stress-induced death (Singh et al., 2007), whilst HSPB1 binds to denatured actin monomers or short oligomers which have dissociated from the longer actin filaments as a result of heat stress and protects them from further aggregation (Pivovarova et al., 2007). Lastly, CRYAB can also associate with the tubulin subunits of microtubules to prevent aggregation *in vitro* (Arai and Atomi, 1997).

1.7.2.4 Anti-apoptotic functions of sHSPs

Apoptosis is a form of programmed cell death, regulated by a family of proteases called caspases which induce apoptosis and subsequent removal of damaged proteins (Li and Yuan, 2008). There are three main apoptotic pathways: the extrinsic, the intrinsic and the ER stress-related pathway. HSPB1 and CRYAB have demonstrated anti-apoptotic abilities, but with each different sHSP targeting and inhibiting different factors of the apoptosis pathways (Garrido et al., 2001; Kamradt et al., 2002). HSPB1 can exert anti-apoptotic effects via interactions with a number of apoptotic markers involved in any of the three main apoptotic pathways (Shan et al., 2021). Phosphorylated forms of HSPB1 are able to interact with Daxx in the extrinsic pathway, preventing the formation of Daxx-FAS and Daxx-ASK1, required for Daxx-mediated apoptosis (Charette and Landry, 2006). This phosphorylated form

of HSPB1 is also able the bind to ASK1 and inhibit the downstream extrinsic apoptosis pathway, thus mediating neuroprotection in response to ischemic injury in mice (Stetler et al., 2012). HSPB1 has the ability to further impact apoptosis through regulation of the intrinsic apoptosis pathway. In brief, the intrinsic pathway, also known as mitochondria-mediated apoptosis, can be induced by a number of external factors such as ROS, cytotoxicity and nutrient deprivation leading to the release of cytochrome c from the mitochondria into the cytosol, causing the activation of caspase-9, followed by activation of caspases-3, 6 and 7 leading to apoptosis (Singh et al., 2019; Shakeri et al., 2017; Shan et al., 2021). It has been reported that HSPB1 is able to protect against atherosclerosis in coronary heart disease and that this is due to HSPB1 suppression of the levels of ROS production which in turn reduces cytochrome c release from the mitochondria and therefore inhibits the endothelial apoptosis found in this disease (Tian et al., 2016; Zhang et al., 2017). HSPB1 has also been shown to bind directly to modulators of the intrinsic apoptotic pathways such as cytochrome c, preventing further activation of downstream caspases (Bruey et al., 2000) and caspase-3, inhibiting activation of this caspase and thus blocking subsequent apoptosis (Voss et al., 2007).

CRYAB has also been shown to associate with the intrinsic apoptotic pathway. CRYAB interaction with pro-apoptotic regulators Bax and Bcl-Xs in human lens and retinal cells and in rat myocardium cells prevented the translocation of these pro-apoptotic modulators from the cytosol into the mitochondria preserving mitochondrial integrity and preventing further cytochrome c release (Mao et al., 2004). Also, in the human lens and retinal cells, CRYAB has been shown to directly interacts with cytochrome c *in vitro* and *in vivo* and overexpression of CRYAB protected cytochrome c from oxidative inactivation (McGreal et al., 2012).

1.7.3 Small heat shock proteins in Alzheimer's disease and other tauopathies

The sHSPs have the ability to perform a number of potentially neuroprotective roles in the brain, such as the aforementioned chaperone-like function, anti-inflammatory and anti-apoptotic roles, all which may prove useful in neurodegenerative diseases such as AD. The function of sHSPs in AD however has not been fully determined, but the majority of studies indicate an increase in HSPB1 (Renkawek et al., 1994; Wilhelmus et al., 2006) specifically in reactive astrocytes during neurodegenerative disease. CRYAB has also been shown to increase in reactive astrocytes (Renkawek and Voorter, 1994; Shinohara et al., 1993) but also in other cell types such as neurons (Mao et al., 2001; Kato et al., 1992) and oligodendrocytes (Renkawek and Voorter, 1994; Shinohara et al., 1993; Iwaki et al., 1992), most recently supported by transcriptome analysis of AD brains (Mathys et al., 2019). Moreover, some studies have also shown an increase in both HSPB1 and CRYAB in relation to the two main pathological hallmarks of AD. In those reactive astrocytes close to Aβ plaques, an increase in CRYAB and HSPB1 expression has been shown (Renkawek and Voorter, 1994; Wilhelmus et al., 2006; Renkawek et al., 1994) whilst an increase in neuronal tau was found to drive the levels of astrocytic HSPB1 in an animal model of AD (Filipcik et al., 2015).

In other non-AD tauopathies with excessive glial pathology, (such as corticobasal degeneration (CBD) and FTLD-tau), the expression of both HSPB1 and CRYAB has been shown to increase specifically only in astrocytes, whilst being generally unchanged in neurons (López-González et al., 2014). A small proportion of both HSPB1 and CRYAB has also been seen to associate with tau in the form of astrocytic tau inclusions (Dabir et al., 2004; Wilhelmus et al., 2006).

A number of mouse models have been used to investigate the potential role of sHSPs within AD brain. In two different mouse models of AD, the Tg2576 transgenic mouse expressing AAP with

Swedish mutations (Hsiao et al., 1996) and the APPswe/PS1dE9 double transgenic mouse expressing both human and mouse APP (Jankowsky et al., 2004), plaques are apparent from 11-12 months of age, but more interestingly, HSPB1 was found in the penumbral area surrounding these plaques (Ojha et al., 2011), reflecting what is seen in the human AD brain (Wilhelmus et al., 2006), and emphasizing the use of these mouse models for studying sHSPs in the human disease. To this end, a mouse overexpressing human HSPB1 was crossed with the APPswe/PS1dE9 AD mouse to investigate the chaperone functions of HSPB1 against aggregation of amyloid-β (Tóth et al., 2013). Not only was plaque burden reduced in this double transgenic mouse, compared to the AD mouse model, but it was also established that spatial learning and long-term potentiation was also improved (Tóth et al., 2013). Overexpressing HSPB8 in the tauopathy rTg4510 mouse by bilateral injection of an adeno-associated virus (AAV) into the brain protected the mice from tau-mediated deficits in spatial learning and memory and rescued LTP deficits in the rTg4510 mice but did not alter the levels of phosphorylated tau (Ospina et al., 2022). On the contrary, crossing a mouse deficient in both HSPB2 and CRYAB with the Tg2576 mouse resulted in a cross with severely impaired locomotive function compared to each individual mouse models (Ojha et al., 2011).

1.7.4 Non-cell autonomous role of small heat shock proteins in neurodegenerative diseases

As previously mentioned, in recent years there has been growing interest in the non-cell autonomous role of astrocytes and its implication in neurodegenerative diseases such as ALS and Huntington's disease (HD) (Tong et al., 2013; Ditsworth et al., 2017; Bradford et al., 2010). More interestingly, it is through the use of HD animal models where the potential non-cell autonomous role of sHSPs in neuron-astrocyte communication during neurodegenerative diseases was first studied. Overexpression of astrocytic CRYAB in a mouse model of HD has been shown to be protective against the progression of disease, through the modulation of mutant htt levels and inclusion body formation, leading to improved motor and cognitive function (Oliveira et al., 2016). In

addition, it was demonstrated that by exclusively expressing the human heat shock protein DNAJB6, a potent suppressor of PolyQ aggregation, in *D. melanogaster* astrocytes, it is possible to delay progressive neuronal degradation and therefore prolong lifespan (Bason et al., 2019). Although the potentially protective role of astrocytic sHSP has been demonstrated in neurodegenerative disease such as ALS and HD, there is a distinct lack of studies exploring the non-cell autonomous effects of astrocytic sHSP on neurons in AD.

1.7.5 Secretion of sHSPs

Traditionally, the role of sHSPs has been confined to intracellular chaperone functions, however, emerging evidence has suggested a protective role for extracellular sHSPs in pathological conditions. The presence and role of extracellular sHSPs in disease has been highlighted in human patients with neuroinflammatory related diseases. MS patients have elevated levels of sHSPs in the serum (Ce et al., 2011) and sHSPs are increased in both the plasma and the CSF found in the CNS during cerebral ischemia (Hecker and McGarvey 2011). When looking more specifically at the presence of extracellular sHSPs in neurodegeneration, it was found that there was an increase in autoantibodies against CRYAB in the serum of both AD and Parkinson' disease (PD) patients (Papuć et al., 2016; Papuć et al., 2015). Further to this, a number of recent large-scale multilayer proteomic profiling studies have identified HSPB1 in the CSF of AD patients (Sathe et al., 2019; Bai et al., 2020; Bader et al., 2020).

1.7.6 Secretory mechanism of sHSP

On a molecular level, sHSPs lack the classical N-terminal signalling peptide required for sorting to the ER and subsequently through the ER-Golgi complex, leading to release by the classical secretory

pathway (Mambula et al., 2007). This is a feature also seen in other immune-modulators such as IL-α, and IL-β (Prudovsky et al., 2003). Therefore, there have been a number of other suggestions made as to how sHSPs are released. Initially it was assumed that sHSPs release was a consequence of cell death, when sHSPs are released either by passive or active secretion after necrosis, as seen after the induction of cell death in T-lymphocytes and HeLa cells (De Maio and Vazquez, 2013; Basu et al., 2000; Saito et al., 2005). However, studies have since demonstrated the release of sHSPs under normal physiological conditions and other possible mechanisms have been discussed, such as the exosomal or lysosomal pathways (Reddy et al., 2018; den Broek et al., 2021).

1.7.6.1 HSPB1

The exosomal pathway has been implicated in HSPB1 release, not only due to the confirmed physical interaction between HSPB1 and different components of the exosome, but also due to the presence of HSPB1 within the exosomes under physiological conditions (Reddy et al., 2018; den Broek et al., 2021). It is still subject to debate as to whether HSPB1 are localised to either the lumen or the membrane of the exosome. *Shi et al., 2018* found HSPB1 localised in the exosomal membrane where it was able to significantly stimulate NF-κB activation, supporting the anti-inflammatory role of this exosome-bound HSPB1. The ability of HSPB1 to interact with other cell surface receptors such as TLRs and oestrogen-receptor β, also supports its interaction with the surface membrane (Yusuf et al., 2009; Rayner et al., 2009). Contrary to this, *Clayton et al., 2005*, located HSPB1 within the exosome lumen and not at the surface membrane in B-cell exosomes (Clayton et al., 2005). In any case, a number of studies support the idea of exosomal release. Under normal steady state conditions, exosomes contain HSPB1 and under heat stress, both the quantity of exosomes and the levels of HSPB1 were both upregulated (Clayton et al., 2005). Inhibition of exosome synthesis in

human macrophages reduced the levels of HSPB1, and extracellular HSPB1 release is detected in the exosomes upon stimulation with Aβ in primary rat astrocytes (Nafar et al., 2016).

Another reported secretory pathway explaining sHSPs release is the autophagy-lysosome pathway. To investigate the mechanisms underlying atherosclerosis, macrophages were treated with oestrogen or acetylated low-density lipoprotein (acLDL), which increased HSPB1 secretion and its association with two different lysosomal markers LAMP1 and Lysotracker (Rayner et al., 2008). In addition to this, it was demonstrated that non-phosphorylated HSPB1 co-localised more with LAMP1 compared to its phosphorylated mutant forms, strongly indicating HSPB1 cellular release through secretory lysosomes where it interacts with Vascular endothelial growth factor (VEGF) and plays a role in maintaining the balance between physiological and pathological angiogenesis (Lee et al., 2012).

1.7.6.2 CRYAB

The secretion of CRYAB has more strongly been associated with exosomes than HSPB1. Immunogold labelling of CRYAB within isolated exosomes confirmed the presence of CRYAB within these exosomes (Sreekumar et al., 2010). CRYAB has been found to reside in detergent-resistant membrane domains which are essential for exosome biogenesis and inhibition of exosomes has been shown to significantly reduce the release of CRYAB, from retinal pigment epithelial (RPE) cells (Sreekumar et al., 2010).. Conversely, inhibition of CRYAB expression in adult human retinal pigment epithelial cells (ARPE19) resulted in the inhibition of exosome secretion, implying CRYAB also plays a role in exosome biogenesis (Gangalum et al., 2016). Additionally, unlike HSPB1, post-translational modifications can influence CRYAB secretion, with phosphorylation and the prevention of O-

GlcNAcylation of CRYAB significantly reducing CRYAB secretion via exosomes (Kore and Abraham, 2016).

1.7.7 Function of extracellular sHSP

1.7.7.1 HSPB1

The function of extracellular HSPB1 is relatively unknown however a variety of studies using *in vitro* and experimental disease models have reported the possible involvement of extracellular sHSPs in a number of functions, highlighting the potential therapeutic activity of these extracellular sHSPs (Reddy et al., 2018). Extracellular sHSPs are mainly able to act as soluble signalling molecules that bind to surface reactors on target cells such as CD40, CD36 and TLR, leading to the initiation of the inflammatory process (den Broek et al., 2021). The potential extracellular role of HSBP1 in modulating the immune response has been highlighted through its role in activating and modulating NF-κB activity in macrophages during disease, and thus causing an upregulation in both pro- and anti-inflammatory cytokines and growth factors such as VEGF (Salari et al., 2013; Batulan et al., 2016; Jin et al., 2014; Thuringer et al., 2013). In an experimental mouse model of EAE, treatment with intra-peritoneal injections of HSPB1 reduced paralysis through modulating inflammatory cytokines IL-2, IL-6 and IFNγ. Further to this, paralysis was found to return after treatment was halted, suggesting HSPB1 to be acting as a biological inhibitor whose potential therapeutic effects relies on HSBP1 levels being above a defined serological level (Kurnellas et al., 2012).

The potential role of protein interaction and the subsequent chaperone function of extracellular sHSPs has also been explored. It has been suggested that exposure to Aβ can trigger the exosomal release of astrocytic HSPB1 which then interacts with this extracellular Aβ (Nafar et al, 2016). This extracellular HSBP1 may then act as a chaperone protein to mediate the sequestration of toxic Aβ

oligomers into non-toxic Aβ aggregates (Ojha, 2011; Kudva, 1997) as a protective role against AD-related pathology.

Finally, treatment with HSPB1 peptides has also displayed potential anti-apoptotic function by inhibiting the development of cataracts in rats, through inhibiting protein insolubilisation and oxidative stress, thought to be instigated by the conserved crystallin domain shared across all sHSPs (Nahomi et al, 2015). On the whole, these observations strongly indicate the role of extracellular HSPB1 may include modulating inflammatory response, chaperone-activity and a role in preventing cell death.

1.7.7.2 CRYAB

The most well described function of extracellular CRYAB has been its role in promoting an anti-inflammatory response, demonstrated through investigation of a number of inflammatory diseases and conditions. In a rat model in which an inflammatory response is induced using sliver nitrate, cytokines TNFα and IL1α are released and NOS production is increased. However, when these animals are treated with intraperitoneal CRYAB, this cytokine and NOS production is inhibited (Masilamonia et al., 2005). In stroke patients there is evidence of an increase in CRYAB compared to health controls (Arac et al., 2011). Exogenous administration of therapeutic CRYAB in animal models of inflammatory diseases including stroke, MS and ischemia lead to a reduction in the immune response, via interaction with TLRs and not lymphocytes, and a reduction of inflammatory cytokines such as IL-6 (Rothbard et al., 2012). In support of CRYAB anti-inflammatory functions as a result of interaction with the innate immune system, CRYAB was also found to reduce levels of secondary damage after CNS trauma in a spinal cord injury model, leading to improved locomotor skills by modulating inflammatory response and reducing macrophage recruitment (Klopstein et al., 2012).

Extracellular CRYAB has also been seen to act on the major glial cells involved in neuroinflammation to promote neuroprotective function. A number of studies have demonstrated the induction of microglia by CRYAB via TLR2 along with the induction of a number of other anti-inflammatory mediators during MS (Bsibsi et al., 2013; Bsibsi et al., 2014). Further to this, in a mouse model of EAE, there is increased astrocytic release of CRYAB within exosomes which is seen to reduce microglia inflammation in a non-cell autonomous manner whilst also reducing astrocytic inflammation in an autonomous fashion (Guo et al., 2019). Finally, CRYAB also elucidated a protective neuroglial response in a model of tauopathy (Hampton et al., 2020). In the P301S tauopathy mouse model, CRYAB was intracerebrally infused into 8 week old mice leading to a rescue of neuronal loss in the outer cortical layers of the brain, presenting the first experimental evidence in the support of the neuroprotective role or CRYAB in a model of tau-related neurodegeneration.

In addition to its anti-inflammatory role, extracellular CRYAB has also protective chaperone activity. CRYAB has been shown to reduce oligomer $A\beta_{42}$ induced toxicity when added extracellularly via promoting the assembly of larger oligomer species, reducing the exposure of highly reactive hydrophobic surface receptors and reducing diffusional mobility. CRYAB was also effective after oligomer formation indicating the potential ability to also neutralise toxic oligomers after they have formed (Mannini et al., 2012).

Finally, extracellular CRYAB also possess anti-apoptotic and protein stabilisation properties. In cultured human lens epithelial cells, CRYAB was able to protect from protein aggregation and also displayed significant protection against oxidative stress induced and heat stress linked cell death (Christopher et al., 2014). And in addition to this, using a rat model of cataract development, CRYAB was shown to inhibit cataract linked cell apoptosis along with inhibition of oxidative stress, protein insolubilization and caspase activity in the lens (Nahomi et al., 2013).

1.8 Organotypic brain slice cultures

1.8.1 History and development

One of the earliest definitions of the term “organotypic” was used by Crain in 1951 to describe tissue which “largely retains its characteristic architecture, remains functional and if derived from undifferentiated material, it may develop in culture in a surprisingly normal way” (Crain 1966). The first example of an organotypic culture was demonstrated through studies on the development and differentiation of a chick embryo eye (Reinbold 1954). The first published organotypic brain tissue explored granule cells in the mouse cerebellum (Wolf 1970). A number of techniques were tested to help enable long-term survival of brain tissue and of these techniques, the roller-tube and the membrane interface techniques are the most widely implemented.

The best example of the roller-tube technique was optimised by Gähwiler, who attached 300-400µm thick brain slices to a glass coverslip and this coverslip was then placed inside a tube containing culture media. This tube was then constantly rotated in a humidified incubator at 37°C to ensure the slices are continuously oxygenated (Gahwiler, 1981; Gahwiler et al., 1997). Unfortunately, tissue cultured in this manner does not maintain a complete architecture and suffered the high risk of falling of the slide. These issues were later resolved with the introduction of the membrane interface technique, placing the tissue at the intersect between a consistently humidified atmosphere and a nutrient rich culture medium, provided via a semi-porous membrane (Stoppini et al., 1991). These tissues were able to sufficiently attach to the membrane whilst maintaining its cytoarchitecture. Therefore, this became the technique of choice for the majority of laboratories and will be the technique used throughout this thesis (*Figure 1.7*).

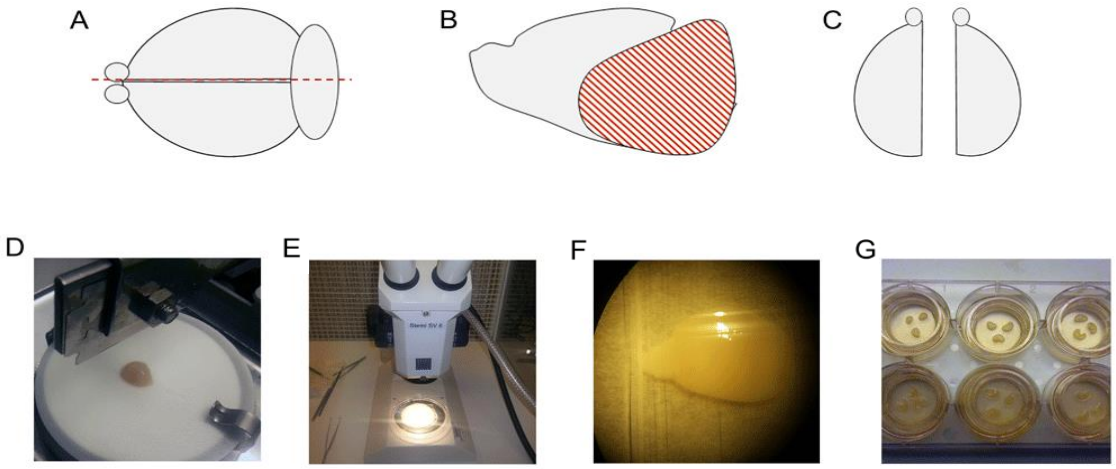

Figure 1.7 Schematic summarising the preparation of organotypic slice cultures

A) Brain bisected along the midline using a razor, B) The thalamus, brainstem and cerebellum are removed (red), C) The two hemi-brains are kept in oxygenated dissection buffer throughout the process, D) One hemi-brain is cut coronally at 350µm by McIlwain chopper, E) - F) Slices are carefully separated under a dissection microscope , G) Three slices are then placed onto Millipore membrane, held in a six well plate. Figure adapted from Croft and Noble, 2018;

1.8.2 Advantages of *ex vivo* organotypic brain slice cultures

Culture of cell lines and primary cells *in vitro* are the most widely used models to investigate the cellular and molecular biology of brain cells, including the survival, morphology and function of cell types such as neurons, astrocytes and microglia. However, such systems do not reflect the complete natural *in vivo* environment due to the lack of interactions with other cell types or an extracellular matrix (Humpel, 2015; AlaylioĞlu et al., 2020). Organotypic brain slice cultures are an integrated system, containing all physiologically relevant cell types that retain functional and anatomical connectivity (Croft and Noble, 2018; Bahr, 1995). These different neuronal and non-neuronal glial cells found in these slice cultures are representative of the proportions found *in vivo* (Staal et al., 2011; del Rio et al., 1991; Croft et al., 2019), particularly important for this PhD project as this

system will also allow for the study of the non-cell autonomous role astrocytes may have on neurons.

Organotypic brain slices also represent an *ex vivo* model capable of replicating the *in vivo* disease progression of neurodegenerative diseases such as AD, through an accelerated timeline whilst reducing the number of experimental animals required for a study (Croft and Noble, 2018). Multiple slices are prepared from one single animal, up to a maximum of 36 slices of a thickness of 350µm, to allow for the investigation of multiple experimental variables and disease-related changes over the same time period (Croft et al., 2017). Further to this, postnatal mice prior to weaning are used to prepare the organotypic slice cultures, which reduce expenditures on maintaining aged mice with potentially harsh phenotypes (Croft and Noble, 2018).

Finally, the organotypic slice culture system allows for the study of molecular and cellular processes which are usually inaccessible *in vivo* (Harwell and Coleman, 2016). In the absence of a blood brain barrier, the brain slice cultures can be manipulated through the addition of compounds or recombinant proteins directly into the culture medium (Croft et al., 2017) or transduced with recombinant adeno-associated viral (rAAV) system (Croft et al., 2019), which enables genetic manipulations. The slice cultures are also capable of performing other experiments which may not be viable in an *in vivo* system such as long-term live imaging or cell electrophysiology (Croft et al., 2019) .

Despite the aforementioned advantages of the organotypic brain slices cultures for the study of neurodegenerative disease, there are also a number of limitations. Firstly, although the slices have been shown to maintain cells associated with the vascular system (Hutter-Schmid et al., 2015), the model cannot replicate an intact blood-brain barrier, a feature essential for use of slices in the pre-

clinical setting for testing potential new drug candidates. Secondly, immediately after slice preparation, a layer of reactive astrocytes develops on the outer surface of the cultures as a response to injury (Benediktsson et al., 2005) which could interfere with analysis of the physiologically balanced environment one is trying to create. Similarly, the preparation of these slices also causes axonal damage and can results in the loss of target innervation. Although axonal damage can be somewhere ameliorated using nerve growth factors (Humpel 2015), the issues involving the glial scar and the axon damage can be resolved by waiting for two weeks before using the brain slices in any analysis to allow for astrocyte reactivity and the acute effects of axotomy to diminish. Finally, over time, the slice cultures can become flattened *in vivo*, as a means of macroscopic survival which can alter the overall anatomical structure and electrophysiological properties.

1.8.3 Modelling disease using organotypic brain slice cultures

Organotypic slice cultures have been used to study the underlying pathological mechanisms in AD, particularly through the use of acute, short-term slice cultures in electrophysiology based synaptic experiments (Fitzjohn et al., 2008), although it is important to note that the slices chosen for this PhD are exclusively the long-term slices. Slices have been used to explore one of the main pathological features of AD, the accumulation of Aβ peptides into extracellular plaques (Long and Holtzman, 2019). Recent attempts have focussed on culturing slice cultures from established transgenic mouse models of Aβ pathology with majority failing to achieve a robust pathology. Slices cultured from the TgCRND8 mouse did not produce plaque pathology even after 12 weeks *in vivo* and the addition of pharmacological manipulation (Harwell and Coleman, 2016), and slices cultured from the 3xTg-AD mouse model demonstrated an over-production of the pro-aggregatory $A\beta_{42}$ peptide but not amyloid deposition after 28 DIV (Croft et al., 2017). Conversely, brain slices cultured from adult APPSweDI mice have gone on to develop Thioflavin-S positive plaques which were also

surrounded by activated glia, replicating the human pathology in cultures which were only 2 weeks old (Humpel 2015).

There has also been a concerted effort in trying to replicate and understand the molecular mechanisms of tau phosphorylation and accumulation using organotypic brain slice cultures. Brain slice cultures have provided a tool to accelerate the development of tau pathology *ex vivo* when compared to their *in vivo* counterpart. Slices cultured from both the P301L and htau mice developed confirmational and phosphorylated tau after only 2 weeks *in vivo,* a process which would take at least 4 months and 6 months respectively (Lewis et al., 2000; Andorfer et al., 2003). Further to this, slices prepared from the 3xTg-AD mouse not only developed phosphorylated tau 12 times quicker than *in vivo*, but these slices also contributed to further our knowledge about tau release and its membrane redistribution, a factor that is recognised as an underlying pathological contribution to AD (Croft et al., 2017). In addition, slice cultures have also proved to be a useful platform to test and screen for tau antibodies with the potential long-term goal of implementing these antibodies into clinical trials (Gu et al., 2013; Croft et al., 2018). The main drawback of the slice cultures to study tau pathology is that they rely heavily on the overexpression of human tau, as seen in the *in vivo* rodent models, which does not fully recapitulate the human disease (Dawson et al., 2018), however they are still a useful tool in building on our current understanding of tau pathology in AD and other tauopathies.

As it is now understood that AD is not only defined by protein aggregation, other pathological features have also been explored using the organotypic brain slice cultures. As slices contain a whole host of CNS cells, they have proven to be valuable tools in investigating the complex role of inflammation in AD (Phillips et al., 2014; Tejera and Heneka, 2016). The role of both astrocytes and microglia in response to Aβ has been examined using organotypic slices. These cultures have

emphasized the importance of microglia in protecting against amyloid accumulation potentially through enhance phagocytosis (Fan and Tenner, 2004; Hellwig et al., 2015), whilst the intricacies of the astrocytic response to amyloid has also been observed (Xu et al., 1999). These studies have stressed the potential of using slice cultures to study neuroinflammation in disease, and more importantly, the sophisticated interaction between inflammatory glia and other cell types which occur in multifaceted diseases like AD.

Finally, brain slice cultures have also recently been used in conjunction with other technologies such as the rAAV system to efficiently transduce genes of interest into non-transgenic slice cultures in order to induce the previously challenging *ex vivo* protein inclusions found in AD or PD (Croft et al., 2019). This has eliminated the need to maintain a colony of transgenic mice from which to obtain postnatal pups for slice culture preparation. In addition to this, the AAV system can also be used to target specific cell types within the integrated slice culture system, with this expression shown to last up to many months (Croft et al., 2019). Known mutations in the human APP, presenilin or MAPT genes can now be delivered into the slice culture model via viral constructs to help further our understanding on how these mutations may cause AD pathology and to explore the interconnected physiological mechanisms related to brain function. Since it is possible to distinguish and manipulate different cell types within one complete, integrated system, it makes the organotypic slice cultures a good model for the study of the effects of the non-cell autonomous role of astrocytic sHSPs on other cellular elements, in a disease relevant network. Therefore, organotypic brain slice cultures have been selected as the model of choice for this PhD project.

1.9 Aims and objectives

The original hypothesis for this PhD project was that the upregulation of CRYAB and HSPB1 seen specifically in reactive astrocytes in AD would lead to the protection of neurons against AD pathology in a non-cell autonomous manner. In order to explore this hypothesis, three main objectives were addressed:

1. Investigate the cellular location and expression of CRYAB and HSPB1 in human post-mortem AD brain tissue

Recently, a number of single-cell transcriptomic studies have implicated sHSPs as being strongly associated with the pathological process of AD (Mathys et al., 2019; Grubman et al., 2019). Previous studies have also investigated the localisation and expression of CRYAB and HSPB1 in the human AD brain, however, these studies have reported sHSPs to be in a number of different cell types and the levels of sHSPs in relation to amyloid plaque pathology has not been fully characterised (Renkawek et al., 1994; Wilhelmus et al., 2006; Renkawek and Voorter, 1994; Shinohara et al., 1993). Therefore, the first aim of this thesis was to investigate the location and expression of CRYAB and HSPB1 in human brain sections of AD patients to determine their significance in relation to one of the main pathological features of the disease, the amyloid plaques.

2. Characterise the organotypic brain slice culture model for studying the non-cell autonomous role of HSPB1 in relation to AD pathology

In order to further study the role of HSPB1 in the response to AD-pathology, it was necessary to establish a model in which it is possible to monitor and manipulate HSPB1 in an environment which mimics the AD brain. To do this, the organotypic brain slice cultures were chosen as it is possible to represent all the relevant cellular components of the brain within a complete, anatomically and

functionally connected system (Staal et al., 2011; del Rio et al., 1991; Croft et al., 2019), which is necessary to explore the non-cell autonomous aspect of HSPB1 function. In order to replicate some of the pathological changes seen in AD, the slices were treated with cytokines known to be released by activated microglia during neurodegeneration (Liddelow, 2017; Leng and Edison, 2021) and physiologically relevant levels of Aβ oligomers (Perez-Nievas et al., 2021). Furthermore, slices were also transduced with AAVs in order to replicate tau pathology (Croft et al., 2019).

3. Determine whether HSPB1 is protective against AD-relevant pathologies by exploring its impact on cell toxicity, synaptotoxicity, neuroinflammation and tau accumulation in the organotypic slice model of tau pathology

Within this aim, the potential role of extracellular HSPB1 will be explored through treating the slice cultures with recombinant HSPB1 and investigating the impact this has in those slices treated with cytokines and transduced with tau-AAVs. In addition to this, astrocytic HSPB1 will be overexpressed specifically in the reactive astrocytes through the use of AAV constructs to determine whether HSPB1 is protective in a non-cell autonomous means.

Chapter 2: Materials and Methods

2.1 Animals

Pregnant CD1 wild-type (WT) mice at embryonic day 14 (E14) were purchased from Charles River. CD1 pups were then taken for the preparation of organotypic slice cultures at postnatal days 8-11. Tau knock-out (KO) and htau mice were obtained from the Jackson Laboratory. Tau KO mice (Tucker et al., 2001) are generated by targeted mutation through inserting an enhanced fluorescent green protein (EFGP) coding sequence into the first microtubule associated protein tau (MAPT) exon, disrupting tau expression. The Tau KO mouse is crossed with the 8c mouse (Duff et al., 2000) to generate the htau mouse (Andorfer et al., 2003). This htau mouse expresses all six isoforms of human MAPT (including 3R and 4R isoforms) but does not express endogenous mouse tau. A colony of htau breeding mice was established at King's College London (KCL). htau mice were bred with Tau KO mice to maintain the htau colony for future breeding. htau mice formed breeding pairs with unrelated htau mice to produce htau pups which were used for the preparation of slice cultures at 8-11 days postnatal. WT mouse on the same C657BL/6 background were also purchased from Charles River and were bred to produce pups to be used as age-matched slice culture controls. All housing and experimental procedures were carried out in compliance with the local ethical review panel of KCL under a UK Home Office project licence (P5E7F2A5E), held in accordance with the Animals Scientific Procedures Act 1986.

2.2 Genotyping

2.2.1 DNA extraction

DNA extraction and polymerase chain reaction (PCR) were carried out using reagents from, and according to the protocol in the REDExtract-N-Amp™ Tissue PCR Kit Protocol (Sigma-Aldrich). In

short, ear snips were taken from mice and incubated in a 125µl mixture of Extraction and Tissue Preparation solution for 10 minutes at room temperature. The DNA samples were then incubated at 95°C for 3 minutes before 100µl Neutralisation Solution B was added. Samples were thoroughly mixed using a vortex and stored at -20°C until use.

2.2.2 Polymerase chain reaction

PCR amplification of genomic DNA was performed using PCR reaction mix with total volume of 25µl per reaction, primarily made up of REDExtract-N-Amp™ PCR Reaction Mix (buffer, salts, dNTPs, Taq polymerase, REDTaq® dye, and JumpStart Taq antibody). Additional component of the PCR reaction mix includes 10µM final concentration of all primers, template DNA and nuclease-free water (Thermo Scientific Ltd., UK), details of which differ depending on the experiment (as seen in the *Table 2.1 and 2.2*). The PCR was then carried out on using the conditions specified in *Table 2.3*.

2.2.3 Electrophoresis of PCR products

A 1% w/v agarose gel was cast to resolve the resulting PCR products. Agarose (Sigma) was added to 1x TAE buffer (40mM Tris-base, 0.11% w/v Glacial acetic acid, 1mM EDTA) and heated in the microwave for about 1 minute until it had fully dissolved. The mixture was allowed to cool slightly before adding 1mg/ml ethidium bromide (Sigma) to allow for visualisation of the DNA bands. The gel mixture was then poured into a gel mould, combs added and left for 30 – 45 minutes until the gel had completely set. After, the gel was placed in an electrophoresis tank (BioRad), fully covered with 1x TAE, 20µl DNA sample was loaded alongside 5µl Quick-Load® 100 bp DNA Ladder (New England Biolabs) and ran for 45 minutes at 120V before being visualised and imaged using U:Genius UV Transilluminator [Syngene]. GAPDH was detected at around 350 bp and htau was detected at about 250bp.

Primers for htau identification		
Name	**5' – sequence – 3'**	**Expected MW**
htau forward	GTG TCT GCT GCT CCC TAG TCT GG	249
htau reverse	GCC AAA TGG TGC CCA CAC CTT CC	249
GAPDH forward	GGT GCTG AGT ATG TCG TGG AGT	369
GAPDH reverse	CCC ACT GCC TAC ATA CCA TGA	369

Table 2.1: Primers used for genotyping htau mice

htau PCR Reaction Mix (20µl)		
Reagent	**Volume (µl)**	**Final Concentration**
REDExtract-N-Amp™ PCR Reaction Mix	10	1x
Forward Primer	1	1µm
Reverse Primer	1	1µm
DNA extract	4	1:20
Nuclease-free water	2	-

Table 2.2: Components of the PCR reaction mix used in htau genotyping

htau PCR Cycling parameters (37 cycles)			
Step	**Temperature**	**Time**	**Cycles**
Initial Denaturation	94°C	3 mins	1
Denaturation	94°C	30 secs	35
Annealing	70°C	20 secs	
Extension	72°C	1 min	
Final Extension	72°C	10 min	1
Final Hold	4°C	Forever	

Table 2.3: PCR cycling parameters used for htau genotyping

2.3 Cell culture

2.3.1 Primary mouse cortical neuron cultures

2.3.1.1 Preparation of primary mouse cortical neuron cultures

All primary mouse neuron cultures were kindly prepared for me by Dr Maria Jimenez-Sanchez using the protocol summarised as follows. Embryos were extracted from pregnant CD1 mouse at E15 – 16, and the heads collected in HBSS (Thermo Fisher Scientific) on ice. Brains were removed from the skulls and cortices were separated from the cerebellum and the striatum, and meninges removed to prevent fibroblast contamination in the cultures. All cortices were collected together in HBSS and kept on ice. The HBSS was then removed and the cortices were trypsinised in a solution of 0.25% Trypsin (Gibco, 25200) in a 37°C water bath for 20 minutes, with the mixture inverted every 5 minutes. After 20 minutes, the trypsinisation solution was removed and the cortices were washed with HBSS three times. Any remaining HBSS was removed and replaced with Neurobasal (NB) media (NB media (Gibco™, 12349-015), 200mM B27 supplement, (Gibco™, 17504-044), GlutaMAX™ Supplement (Gibco™, 35050-061), 100mM Sodium pyruvate (Gibco™, 11360070), 100x Penicillin/Streptomycin (Gibco™, 15140122). Tissue was triturated and passed through a 70µm cell strainer (Falcon, 352340) then diluted in NB media at 6ml cell suspension per embryo. Neurons harvested from one brain were seeded in a 12-well plate, pre-coated with 10ug/ml Poly-D-lysine (PDL; Sigma-Aldrich, P7280). Neurons used for immunocytochemistry were cultured on sterile autoclaved coverslips. Neurons were seeded at a density of 2.5 x 10^6 cells/well.

2.3.1.2 Treatment of primary mouse cortical neurons

In order to model human tau pathology in the primary mouse cortical neurons, we used the recombinant adeno-associated virus (rAAV) system (Croft et al., 2019) in collaboration with Professor Todd Golde and Dr Cara Croft. The wild-type tau AAV (AAV2/TM8-WT-htau0N4R-EGFP),

the mutant tau AAV (AAV2/TM8-P301L/S320F-htau0N4R-EGFP) constructs (both in Opti-MEM media, Thermo Fisher Scientific) or EGFP control (pAAV[Exp]-CMV>EGFP:WPRE, VectorBuilder) where added directly to the NB media at 6 DIV at MOI: 100,000. At 12 or 15 DIV, NB media was collected for cell toxicity assays whilst neurons were collected or fixed for either immunoblotting or immunocytochemistry.

Alongside the transduction of primary neurons with tau-AAVs, the neurons were concurrently treated with recombinant human HSPB1 protein. 1, 10 and 50ng/ml HSPB1 was prepared in sterile and filtered 0.1% BSA/PBS solution from the original solution provided by the supplier (R&D systems, concentration of 0.342mg/ml in 25 mM HEPES, 100 mM NaCl and 1 mM DTT, pH 7.5, 0.2 µm filtered). HSPB1 was then added straight to the NB media at 6, 8 and 10 DIV. The untreated control neurons for these experiments were treated with comparable volumes of sterile filtered 0.1% BSA/PBS in the exact same way. At either 12 or 15 DIV, NB media was collected for cell toxicity assays whilst neurons were harvested either for immunoblotting or immunocytochemistry.

2.3.1.3 Preparation of cell lysates for western blot

NB media was collected, centrifuged at 1,000 rpm for 5 min to eliminate cell debris and stored at -20°C for cell toxicity assay. Neurons were briefly washed with DPBS (Gibco™, 14190144) and then 100µl 1x laemmli buffer (Tris-HCl pH 6.8, 20% SDS, 0.05% β-mercaptoethanol, Glycerol, Bromophenol blue, H20, diluted with PBS) was added to each well. Cells were vigorously scraped from the surface of the well, collected and boiled at 95°C for 15 minutes before loading for western blotting.

2.4. Organotypic brain slice cultures

2.4.1 Preparation of organotypic brain slice cultures

Organotypic slice cultures were prepared according to *Croft and Noble, 2018*. Brain slices were prepared from CD1 WT, C657BL/6 WT and htau pups at 8-11 days postnatal. Animals were decapitated with accordance to the UK Animals in Scientific Procedures Act (1986). The brain was then removed from the skull and bisected along the midline using a scalpel. Both hemisects were kept in continuously oxygenated ice-cold sterile filtered (0.2µm) dissection buffer pH 7.4 (124 mM NaCl, 3 mM KCl, 1.2 5mM KH2PO4, 8.2 mM MgSO47H20, 2.65 mM CaCl2, 3.5 mM NaHCO3, 1.99 mM Ascorbic Acid, 10 mM Glucose, 0.02 ATP, ultrapure H20) throughout the preparation procedure. Under the dissection microscope, the thalamus, brainstem and cerebellum were removed to leave the cortex and hippocampus attached by connecting regions. The hemi-brain was then placed on moistened filter paper (Fisher Scientific Ltd, 1001-055) and sectioned into 350µm coronal slices using the McIlwain chopper. Once cut, the brain slices were then separated using a hippocampal dissection tool. At first, 18 slices were consecutively taken per hemi-brain and moved to 0.4µm pore membrane inserts (Millipore, 10412511), 3 slices per insert. However, it was soon established that the first and last three slices per hemi-brain did not yield a viable volume of protein after culture and so were excluded from the preparation. This resulted in an eventual total of 12 slices taken per hemi-brain. These inserts were contained in 6-well plates, with each well containing 1ml of prewarmed sterile filtered (0.2µm) culture media pH 7.1 (19.3 mM NaCl, 5 mM NaHCO3, 2.7 mM CaCl22H20, 2.5 mM MgSO47H20, 0.5 mM Ascorbic Acid, 1.8g BME in 200 ml culture media, 40 mM Glucose, 1 M HEPES, 1% (v/v) Glutamax, 0.5% (v/v) Penicillin/Streptomycin, 0.033% Insulin, 25% (v/v) heat inactivated horse serum, ultrapure H20). The slice cultures were then kept in a sterilised incubator at 37°C for 14 DIV – 28 DIV. The culture media was changed to fresh prewarmed culture media three hours after the initial slice preparation and then every 2 to 3 days.

Slice cultures appeared white and swollen immediately after preparation and over the next few days they would continue to swell before returning to their original size, eventually becoming transparent by 2 weeks *in vitro*, if they were healthy and viable. If slices became white and crusty in appearance after the initial 2-week incubation period, this would signify cell death and these slices would not be used for any further experimental procedure.

2.4.2 Treatment of organotypic brain slice cultures

Organotypic slices prepared from WT CD1 pups were treated at 21 DIV with 30ng/ml recombinant mouse TNFα (0.3 µl from 100 µg/ml TNFα stock, R&D Biosystems, 410-MT) and 3ng/ml IL1α (0.6 µl from 5 µg/ml IL1α stock, Sigma) in 1ml of either fresh, prewarmed culture media or fresh prewarmed NB media. 1ml of media containing the treatment was added to the well, outside of the insert, and 50µl of media containing the treatment was added directly on top of the slices, inside the insert. Slices were left in treated media for 24 hours. After treatment, slices were harvested to be used for immunofluorescence or western blotting and NB media was collected to be used in cell toxicity assays.

Organotypic slices prepared from WT CD1 pups were also treated at 21 DIV with physiologically relevant levels of amyloid-β (Aβ) oligomers. In collaboration with Dr Beatriz Gomez Perez-Nievas, primary mouse neurons were cultured from the Tg2576 mouse which expresses human APP with the Swedish mutation (Hsiao et al., 1996). These neurons secrete concentrations of Aβ40 and Aβ42 at a physiologically relevant ratio of 1:10 into the media. This media is known as Tg conditioned media (TgCM). Wild type neurons are also cultured from littermates and this culture media is collect as a control (WtCM). Slices are first pre-treated in NB media for 24 hours. This media is then discarded and slices are then treated with TgCM diluted in NB media to get a final concentration 2nM Aβ40/0.2nM Aβ42. Equivalent volumes of WtCM were used to treat control slices. After treatment, slices were collected for western blotting and the media was collected for cell toxicity assays.

In order to model human tau pathology in the WT CD1 slices, we used the aforementioned tau-AAVs (C. P.-D.-L.-L. Croft C. 2019). The wild-type (AAV2/TM8-WT-htau0N4R-EGFP) or mutant tau (AAV2/TM8-P301L/S320F-htau0N4R-EGFP)) rAAV constructs were added directly into the culture media, 3 hours after initial slice culture preparation on 0 DIV. Final titres varied from $2x10^{10}$ – $2x10^{11}$ viral genomes (VG) per well containing 3 organotypic brain slices (see *Table 2.4*). Slices were then either fixed for immunofluorescence or harvested for the sarkosyl extraction of tau after 28 DIV.

rAAVs were also used to overexpress human HSBP1 specifically in astrocytes. Constructs were produced and purchased from VectorBuilder and included an AAV targeting astrocytes, also known as GFAP-AAV (pAAV[Exp]-GFAP(short)>TagBFP2:WPRE) and a construct targeting HSPB1 specifically in astrocytes, also known as GFAP-HSPB1-AAV (pAAV[Exp]-GFAP(short)>hHSPB1[NM_001540.5](ns):P2A:TagBFP2:WPRE), all provided in PBS buffer (see *Table 2.5*). The GFAP-AAV was expressed under the GFAP promoter, tagged with blue fluorescent protein (BFP), and included the regulatory element WPRE. The GFAP-HSPB1-AAV was also expressed under the GFAP promoter, tagged with BFP and included both the regulatory element WPRE and inserted P2A linker. All were applied as stated above, directly into the culture media on 0 DIV at $2x10^{10}$ VG/well. Slices were then either fixed for immunofluorescence analysis or harvested for sarkosyl extraction of tau after 28 DIV.

Slices were also treated with the recombinant human HSPB1 protein. After 14 DIV, each time the culture media was changed (every 2-3 days), 50ng/ml HSPB1 was added to the fresh culture media, up until the slices were harvested. The untreated control slices for these experiments were treated with 50µl sterile filtered 0.1% BSA/PBS in the exact same way. Slices were then harvested for sarkosyl extraction of tau after a total of 28 DIV.

AAV	Catalogue #	Original Viral Titre (VG/ml)	Final Viral Titre (VG/ml)	Volume added (µl per ml)
pAAV[Exp]-GFAP(short)>h**HSPB1**[NM_001540.5](ns):P2A:TagBFP2:WPRE	VB210211-1047trt	19 x 10^{11}	2 x 10^{10}	10.47 µl
pAAV[Exp]-**GFAP**(short)>TagBFP2:WPRE	VB210218-1066qmw	18.20 x 10^{11}	2 x 10^{10}	10.99 µl

Table 2.4: Concentrations used for the transduction of organotypic brain slices cultures with either GFAP-AAV or GFAP-HSPB1-AAV

Virus concentration:	**1x**			**2x**		**5x**		**10x**	
	Original Titre (VG/ml)	**Final Titre (VG/well)**	**Vol added (µl/ml)**	**Final titre (VG/well)**	**Vol added (µl/ml)**	**Final titre (VG/well)**	**Vol added (µl/ml)**	**Final titre (VG/well)**	**Vol added (µl/ml)**
Wild type tau AAV2/TM8-WT-htau0N4R-EGFP	4x10^{12}	2x10^{10}	5	4x10^{10}	10	1x10^{11}	25	2x10^{11}	50
Mutant tau AAV2/TM8-P301L/S320F-htau0N4R-EGFP	2x10^{12}	2x10^{10}	10	4x10^{10}	20	1x10^{11}	50	2x10^{11}	100

Table 2.5: Concentrations used for the transduction of organotypic brain slice cultures with either WT-tau AAV or P301L/S320F tau AAV

2.4.3 Preparation of organotypic brain slice lysates for western blot

Slice lysates were prepared according to the protocol adapted from (Croft et al., 2017). Slices were first washed in ice-cold PBS three times for five minutes each, to remove any slice culture media. Slices were then scraped off the membrane and placed in an Eppendorf tube with extra strong (2x) lysis buffer (10 mM Tris-HCl (pH 7.5), 0.5% (w/v) Sodium dodecyl sulphate (SDS), 20 mM Sodium deoxycholate, 1% (v/v) Triton X-100, 75 mM Sodium chloride, 10 mM EDTA, 2 mM Sodium orthovanadate, 1.25 mM Sodium fluoride, 1x Protease inhibitor cocktail solution taken from 25x inhibitor tablet by Roche). This was then left on ice for thirty minutes, ensuring the solution was vortexed at least every ten minutes. Samples were then spun in a desktop centrifuge at 13,000rpm for 20 minutes at 4°C, the supernatant collected and stored at -20°C until needed.

2.5. Biochemical analysis

2.5.1 Sarkosyl extraction of tau

Sarkosyl extraction of tau was also performed using the organotypic brain slices cultures in order to analyse the tau pathology induced by the transduction with tau-AAVs. The sarkosyl extraction of tau was performed according to (Greenberg and Davies, 1990). Once slices were ready to be harvested, they were briefly washed in ice-cold PBS and kept on ice. Slices were then pooled from 3-4 inserts per hemi-brain and weighed to determine the relative volumes of homogenisation buffer to use. Slices were then homogenised in homogenisation buffer (50 mM TBS pH 7.4, 10 % Sucrose, 2 mM EGTA, 1x Phosphatase inhibitor cocktail solution taken from 10x inhibitor tablet by Roche, 1x Protease inhibitor cocktail solution taken from 25x inhibitor tablet by Roche) using a handheld homogeniser or by vigorously pipetting up and down at 100mg/mL. The homogenate was then centrifuged at maximum speed on a desktop centrifuge (12,000 – 14,000g) for 20 minutes at 4°C. An

aliquot of the resulting low speed supernatant (LSS) was taken for storage at -20°C for future use in western blot. This LSS contains a mixture of sarkosyl soluble and sarkosyl insoluble tau. The pellet was also stored at -20°C. The remaining volume of LSS was measured and collected into a Beckman ultracentrifuge tube where sarkosyl (20% solution, Sigma) was added to give a final concentration of 1%. This solution of LSS and sarkosyl was then shaken for 30 minutes at room temperature before being spun in an ultracentrifuge at 1000,000g for 1 hour at room temperature (21°C). The resulting high-speed supernatant (HSS) was then collected and stored at -20°C for future use in western blot. The HSS contains the sarkosyl soluble tau. The pellet was washed by adding 1% sarkosyl and spinning at 100,000g for 10 minutes. This pellet contains the sarkosyl insoluble tau. All the tau containing fractions (e.g. LSS, HSS etc) were mixed and resuspended in 2x samples buffer (National diagnostics), before use in western blots.

2.5.2 SDS-polyacrylamide gel electrophoresis (SDS-PAGE) and immunoblotting

2.5.2.1 SDS-PAGE

For gel electrophoresis, 10-12% poly-acrylamide gels were made and cast in BioRad 1.5mm glass plates and casting stands (running gel: H20, 30% acrylamide mix, 1.5 M Tris pH 8.8, 20% SDS, 20% APS, TEMED, stacking gel: H20, 30% acrylamide mix, 1 M Tris pH 6.8, 20% SDS, 20% APS, TEMED). Before running, samples were prepared in equal volumes of 2x laemmli buffer, heated in a heat block at 95°C for 10 mins and spun in a desktop centrifuge at 10,000g for 20 seconds. Once all samples and protein ladder (Protein molecular weight marker Precision Plus Protein™ All-Blue Standard, BioRad Laboratories Inc., USA) had been loaded, the gels were inserted into Mini-PROTEAN® Tetra Vertical Electrophoresis Cell (BioRad) and were electrophoresed at 120V using BioRad power pack 200 in 1x running buffer (10x transfer buffer, 20% SDS, H20), until the proteins had reached the bottom of the gel.

2.5.2.2 Immunoblotting

Proteins were then transferred to PVDF 0.45µm pore membranes (Millipore) in 1x transfer buffer (Tris-base, 10 M HCl, H20, Methanol) at 100V for 1 hour at approximately 4°C, using an ice pack. Membranes were then blocked in blocking solution (Odyssey® Blocking buffer) for 1 hour at room temperature before incubating in primary antibody overnight (*Table 2.6*). Membranes were then washed with washing buffer (50 mM TBS + 1% Tween), three times for 10 minutes on the shaker, before incubating in secondary antibody (*Table* 4) in the dark for 4 hours at room temperature. Membranes were then scanned using Odyssey® Infra-red Imaging system (Li-Cor Biosciences) at 680 and 800nm wavelength to detect the probed proteins.

Antibody	Specificity	Species	Source	Concentration
CP27	Amino acids 130-150 of human tau (phosphorylated and non-phosphorylated)	Mouse monoclonal	Kind gift from P. Davies	1:100
CRYAB	Anti-Alpha β crystallin	Mouse monoclonal	Abcam, ab13496	1:1000
GFAP	Glial fibrillary acidic protein	Rabbit polyclonal	Dako, N1506	1:1000
HSPB1	Recombinant human HSP27	Rabbit polyclonal	Enzo, ADI-SPA-803-F	1:1000
HSPB1	Recombinant mouse HSP25	Rabbit polyclonal	Enzo, ADI-SPA-801-F	1:1000
HSPB8	Anti-small heat shock protein HspBb/Hsp22	Rabbit polyclonal	Cell signalling, 30595	1:1000
IBA-1	Ionized calcium binding adaptor molecule 1 (Iba1) is a microglia/macrophage-specific calcium-binding protein	Rabbit polyclonal	Wako, 019-19741	1:500
LCN2	Detect mouse Lipocalin-2/NGAL	Goat polyclonal	R&D biosystems, AF1857	1:500
PHF-1	Tau phosphorylated at ser 396 and 404	Mouse monoclonal	Kind gift from P. Davies	1:1000
PSD95	Postsynaptic Density protein 95	Rabbit monoclonal	Cell Signalling, 3450	1:1000

Serpin A3N	Detects mouse myeloma cell line NS0-derived recombinant mouse Serpin A3N	Goat polyclonal	R&D biosystems, AF4709	1:500
SYP	Amino acids 221-313 on human synaptophysin	Mouse monoclonal	Santa Cruz, sc-17750	1:1000
Total Tau	C-terminal part of human tau protein expressed in E. coli; aa. 243-441, contains the four repeated sequences involved in microtubule binding (MTB)	Rabbit polyclonal	Dako, A0024	1:1000
B-Actin	Loading control	Mouse monoclonal	Abcam, ab8224	1:1000

Table 2.6: List of primary antibodies used for western blotting in this thesis

Antibody	Catalogue number	Host species	Concentration
IRDye® 680RD Donkey anti-Mouse IgG Secondary Antibody	926-68072	Donkey	1:10,000
IRDye® 680RD Goat anti-Mouse IgG Secondary Antibody	926-68070	Goat	1:10,000
IRDye® 680RD Donkey anti-Rabbit IgG Secondary Antibody	926-68073	Donkey	1:10,000
IRDye® 680RD Goat anti-Rabbit IgG Secondary Antibody	926-68071	Goat	1:10,000
IRDye® 800CW Donkey anti-Mouse IgG	926-32212	Donkey	1:10,000
IRDye® 800CW Goat anti-Mouse IgG	926-32210	Goat	1:10,000
IRDye® 800CW Goat anti-Rabbit IgG Secondary Antibody	926-32211	Goat	1:10,000
IRDye® 800CW Donkey anti-Rabbit IgG Secondary Antibody	926-32213	Donkey	1:10,000

Table 2.7: List of secondary antibodies used for western blotting in this thesis

2.6. Cell death assays

2.6.1 Lactate dehydrogenase assay

Cell death was determined by how much lactate dehydrogenase (LDH) was released from the slice cultures into the slice media. This was measured according to the manufacturer's protocol (Promega, CytoTox 96® Non-Radioactive Cytotoxicity Assay). To minimize the interference of the culture media components with the assay reagents, slices were pre-treated in NB media for 24 hours before performing the LDH assay. 50µl of either NB media or slice lysate (previously lysed in extra strong lysis buffer) was loaded in triplicate into a 96-well plate. 50µl CytoTox 96® Reagent was added to each sample and incubated in the dark at room temperature. After 30 minutes, 50µl Stop Solution was added to each well and the absorbance signal was measured immediately at 490nm using a Wallac 1420 Victor3™ plate reader (PerkinElmer, USA). The LDH levels in the media were measured relative to the total LDH levels detected in the slice lysates.

2.7. Human brain tissue immunohistochemistry

2.7.1 Immunohistochemical staining

Formalin-fixed paraffin embedded (FFPE) human brain tissue sections were provided by the London Neurodegenerative Disease Brain Bank (*Table 2.8*). 7µm temporal cortex and cerebellum sections were taken from patients across Braak stages 2, 4 and 6 and those patients with a diagnosed MAPT mutation (frontotemporal dementia with parkinsonism linked to chromosome 17 (FTDP-17) owing to the tau intron 10 + 16 mutation) (five patients per diagnostic group, 12 sections per patient). These sections were then analysed using immunohistochemistry (IHC) to determine the cellular location of sHSP in human diseased brain.

Firstly, the wax was melted by placing sections on a 95°C heat block for 25 minutes. Next, sections were dewaxed by placing in xylene (Sigma) for 5 minutes before rinsing off and being placed in fresh xylene for a further 5 minutes. Sections were then rehydrated in 99% followed by 70% ethanol (in water), for 5 minutes each, before being rinsed in ultra-pure water for 5 minutes. Antigen retrieval was then carried out by placing sections in citrate buffer (0.01 M of Sodium citrate, pH 6) and microwaving on medium-high power for 6 minutes followed by microwaving twice on low power for 5 minutes. Sections were then cooled by adding ultra-pure water until covered and left to stand for 5 minutes. Next sections were rinsed in 1x TBS (Tris Base, NaCL, H20 800ml, pH 7.4) for 5 minutes whilst a hydrophobic wax boarder was applied around the sections using PAP pen (Sigma). Samples were then blocked in 300µl blocking buffer (1:100 normal goat serum (Sigma-Aldrich) in 1x TBS) for 1 hour at room temperature. Primary antibodies (*Table 2.9*) were prepared in 250µl blocking buffer and sections were incubated overnight at 4°C.

The next day, sections were washed in 1x TBS three times for 5 minutes each. The following steps were performed with the intention of protecting sections from the light as much as possible. Sections were incubated in 250µl secondary antibodies (*Table 2.10*) for 1 hour at room temperature. They were then washed twice with 1x TBS for 5 minutes each, before applying freshly prepared and double-filtered Sudan Black (Sigma 0.3 g in 100 mL of 70% ethanol) for 10 minutes until the sections turned dark. Sections were washed for a final three times in 1x TBS for 10 minutes each before being mounted using Fluoromount-G™ Mounting Medium with DAPI (Invitrogen™), sealed with nail varnish and stored in the dark at 4°C.

Case ID	Sex	Age	PMD	Pathological diagnosis
BBN_20012	F	86	45	Alzheimer type changes (ageing), BNE stage II, control
BBN_9958	F	84	53	Alzheimer changes, Braak II, consistent with patient's age
BBN_9926	F	84	35	Alzheimer changes Braak II consistent with normal aging
BBN002.33764	M	73	49	Early Alzheimer-type changes BNE stage I-II control
BBN002.30882	M	77	28.5	Mild to moderate amyloid angiopathy, capillary subtype
BBN_9908	F	82	20	Alzheimer's disease modified Braak IV with amyloid angiopathy
BBN_18793	M	81	51	Alzheimer's disease, BNE stage IV
BBN002.29410	M	84	86	Alzheimer's disease (modified Braak (BNE) stage IV) with moderate amyloid angiopathy
BBN002.28694	F	86	55.5	Alzheimer's disease (modified Braak (BNE) stage IV) with mild amyloid angiopathy
BBN_20124	F	81	20	Alzheimer's disease (Braak stage VI). Vascular disease
BBN002.26278	M	75	59	Alzheimer's Disease (modified Braak (BNE) stage V, Thal phase 5 with moderate-severe amyloid angiopathy

BBN002.29634	M	72	41	Alzheimer's disease (modified Braak/BNE stage VI) with extensive and capillary amyloid angiopathy and significant cerebrovascular pathology
BBN_24235	F	79	63	Alzheimer's disease BNE stage VI
BBN_9980	F	83	58	Alzheimer's disease Braak stage VI
BBN002.32597	F	85	12	Alzheimer's disease, BNE stage VI
BBN_15278	M	71	5	Frontotemporal degeneration (Tau Mutation - 10+16)
BBN_15269	M	67	35	Frontotemporal degeneration (Tau Mutation - 10+16)
BBN_15268	F	58	31	Frontotemporal degeneration (Tau Mutation - 10+16)
BBN_15266	F	75	100+	Frontotemporal degeneration MND inclusion
BBN_15265	F	63	22	Frontotemporal degeneration (Tau Mutation - 10+16)

Table 2.8: Case details of post-mortem human brain tissue used for immunohistochemical analysis for this thesis

Table shows Case ID, sex (M = male, F = female), Age (in years), post-mortem delay (PMD in hours) and pathological diagnosis (BNE staging) for cases from which temporal cortex FFPE sections were obtained

Antibody	Specificity	Species	Source	Concentration
6E10	This antibody is reactive to amino acid residue 1-16 of beta amyloid	Mouse monoclonal	Biolegend, 803002	1:200
ALDH1L1	Aldehyde Dehydrogenase 1 Family, Member L1	Mouse monoclonal	Antibodies online, ABIN1304519	1:200
AT8	Targets PHF-tau (Ser202/Thr205)a	Mouse monoclonal	ThermoFisher, MN1020	1:200
CAII	Anti-human Carbonic anhydrase 2/CA2 aa 200-300 (C terminal)	Rabbit monoclonal	Abcam, ab124687	1:100
CRYAB	Anti-Alpha β crystallin	Mouse monoclonal	Abcam, ab13496	1:200
CRYAB	Anti-Alpha β crystallin	Rabbit monoclonal	Cell Signalling, 45844	1:200
GFAP	Glial fibrillary acidic protein	Rabbit polyclonal	Dako, N1506	1:500
GFAP	Glial fibrillary acidic protein	Chicken polyclonal	Abcam, ab4674	1:500

HSP27	Recombinant human HSP27	Rabbit polyclonal	Enzo, ADI-SPA-803-F	1:200
IBA-1	Ionized calcium binding adaptor molecule 1 (Iba1) is a microglia/macrophage-specific calcium-binding protein	Rabbit polyclonal	Wako, 019-19741	1:200
MAP2	Microtubule associated protein 2	Mouse monoclonal	Sigma-Aldrich, 05-346	1:500
MAP2	Microtubule associated protein 2	Chicken polyclonal	GeneTex, GTX82661	1:500

Table 2.9: List of primary antibodies used for immunohistochemical analysis of human brain tissue sections

Antibody	Catalogue number	Host species	Concentration
Goat anti-mouse Alexa Fluor 568	A11004	Goat	1:250
Goat anti-mouse Alexa Fluor 488	A21121	Goat	1:250
Goat anti-rabbit Alexa Fluor 568	A11011	Goat	1:250
Goat anti-rabbit Alexa Fluor 488	A11034	Goat	1:250
Goat anti-chicken Alexa Fluor 647	A21449	Goat	1:250

Table 2.10: List of secondary antibodies used in immunohistochemical analysis of human brain tissue sections

2.7.2 Imaging of human brain immunohistochemistry

All images used for qualitative analysis were taken on the Zeiss AxioImager Z1 microscope using the AxioVision software (Zeiss). The correct filter sets were applied and the 10x, 20x and 40x objective lenses were used. Images were stored as .ZVI files. All parameters including exposure time, laser power, camera set-up and calibration were kept constant when capturing images.

All images used for quantitative analysis were taken on the Nikon Eclipse Ti Inverted Spinning Disk Confocal microscope, using Yokogawa CSU-1 disk head and Andor iXon EMCCD camera and Nikon Elements software (Nikon Instruments, UK). Laser wavelengths used included 405nm, 488nm, 561nm, 640nm. All parameters including exposure time, laser power, and objective (oil 40x) were kept constant when capturing images. Z-stacks were collected that covered a depth dependent on the size of the amyloid plaque in the field of view and stored as .ND2 files. A minimum of ten images per patient were taken for each of the different staining conditions.

2.8. Immunocytochemistry

2.8.1 Immunocytochemical staining

Neurons were then briefly washed in PBS before being incubated in 4% PFA (in 7.5% Sucrose/PBS) for 10 minutes. Cells were washed three times in PBS before being incubated in 50mM ammonium chloride for 5 minutes. After another 3x PBS wash, cells were incubated in 0.1% Triton X-100 (Sigma) in PBS for 5 minutes. After a further 3 washes in PBS, the neurons were incubated in 10% normal goat serum in PBS for 30 minutes at room temperature, gently rocking on the rocker. The relevant primary antibodies were then applied in blocking solution (*Table 2.11*) and the neurons were left at 4°C overnight in the dark. The next day, the neurons were washed three times with PBS before being incubated in the appropriate secondary antibodies (*Table 2.12*) at 4°C overnight in the dark. On the third day, the neurons were washed 3 times before being mounted in Fluoromount-G™ Mounting Medium, with DAPI and stored at 4°C in the dark.

Antibody	Specificity	Species	Source	Concentration
MAP2	Microtubule associated protein 2	Chicken polyclonal	GeneTex, GTX82661	1:500
MC1	Conformational change around residues 5-15 and 312-322 of tau	Mouse monoclonal	Kind gift from P. Davies	1:100

Table 2.11: List of primary antibodies used for immunocytochemistry analysis in this thesis

Antibody	Catalogue number	Host species	Concentration
Goat anti-chicken Alexa Fluor 647	A21449	Goat	1:1000
Goat anti-mouse Alexa Fluor 594	A11005	Goat	1:1000

Table 2.12: List of secondary antibodies used for immunocytochemistry analysis in this thesis

2.8.2 Imaging of immunocytochemical staining

All images were taken on the Zeiss AxioImager Z1 microscope using the AxioVision software (Zeiss). The correct filter sets and 10x, 20x and 40x objective lenses were used and the images were stored as .ZVI files. All parameters including exposure time, laser power, camera set-up and calibration were kept constant when capturing images. Any quantitative counts were performed whilst on the microscope, blinding the slides and looking directly down the eye piece at 20x or 40x objective.

2.9. Immunofluorescent staining of organotypic brain slice cultures

2.9.1 Immunohistochemical staining

Immunofluorescent (IF) staining was performed on organotypic slices according to an adapted version of the protocol by *Gogolla et. al., 2006*. The protocol was adapted as part of the optimisation process to enable the visualisation of the small heat shock proteins (sHSP) in the slice cultures. The adapted protocol was as follows. Firstly, slice culture medium was removed from both beneath and inside the insert using an aspirator and then washed briefly with cold PBS. Slices were then fixed by an overnight 4°C incubation in cooled 4% Paraformaldehyde (4% (w/v) PFA in 50 mM PBS), followed by an overnight incubation in cooled 20% methanol in 50 mM PBS. Slices were then washed in PBS before an overnight incubation in permeabilization solution (1% (v/v) Triton X-100 in 50 mM PBS). The permeabilization solution was then removed and slices were incubated overnight in a blocking solution (20% (w/v) BSA in 50 mM PBS). To reduce the volume of antibody needed, slices were then cut out of the surrounding insert membrane and each individual slice was then placed in its own individual well in a 24 or 48-well plate, ensuring the top side of the membrane always remained facing upwards. Slices were then incubated inside a wet chamber, overnight at 4°C, in primary antibody (5% (w/v) BSA in 50 mM PBS) according to the concentrations in *Table 2.13*. Slices were

next washed three times in washing solution (5% (w/v) BSA in 50 mM PBS) by carefully removing and replacing washing solution using a pipette, ensuring the slice did not become damaged or dried out. Slices were then incubated overnight in the complementary secondary fluorophore-couple antibody in the dark, at 4°C (see *Table 2.14*). Slices were washed as previously stated, and either mounted in Fluoromount-G™ Mounting Medium, with DAPI (Invitrogen™) or firstly incubated in Hoechst 33258 for 5 minutes at room temperature in the dark before being mounted in Fluoroshield Mounting Medium (Abcam, ab104135). Coverslips were then sealed with nail varnish and stored in the dark at 4°C.

Antibody	Specificity	Species	Source	Concentration
Anti-β-Tubulin III	Tubulin β 3 class III (TUBB3) also known as β-Tubulin III, is encoded by the gene mapped to human chromosome 16q24.3	Mouse monoclonal	Sigma-Aldrich, T8578	1:200
AT8	Targets PHF-tau (Ser202/Thr205)a	Mouse monoclonal	ThermoFisher, MN1020	1:200
CRYAB	Anti-Alpha β crystallin	Mouse monoclonal	Abcam, ab13496	1:100
GFAP	Glial fibrillary acidic protein	Rabbit polyclonal	Dako, N1506	1:200
GFAP	Glial fibrillary acidic protein	Chicken polyclonal	Abcam, ab4674	1:200
HSPB1	Recombinant mouse HSP25	Rabbit polyclonal	Enzo, ADI-SPA-801-F	1:200
HSPB1	Recombinant human HSP27	Rabbit polyclonal	Enzo, ADI-SPA-803-F	1:200
IBA-1	Ionized calcium binding adaptor molecule 1 (Iba1) is a microglia/macrophage-specific calcium-binding protein	Rabbit polyclonal	Wako, 019-19741	1:200
MAP2	Microtubule associated protein 2	Mouse monoclonal	Sigma-Aldrich, 05-346	1:200

MAP2	Microtubule associated protein 2	Chicken polyclonal	GeneTex, GTX82661	1:200
S100B	Anti- human S100 beta aa 50 to the C-terminus, astrocyte marker	Rabbit monoclonal	Abcam, ab52642	1:200
Total Tau	C-terminal part of human tau protein expressed in E. coli; aa. 243-441, contains the four repeated sequences involved in microtubule binding (MTB)	Rabbit polyclonal	Dako, A0024	1:200

Table 2.13: List of primary antibodies used in immunofluorescence analysis of organotypic brain slice cultures in this study

Antibody	Catalogue number	Host species	Concentration
Goat anti-mouse Alexa Fluor 568	A11004	Goat	1:500
Goat anti-mouse Alexa Fluor 488	A21121	Goat	1:500
Goat anti-rabbit Alexa Fluor 568	A11011	Goat	1:500
Goat anti-rabbit Alexa Fluor 488	A11034	Goat	1:500
Goat anti-chicken Alexa Fluor 647	A21449	Goat	1:500

Table 2.14: List of secondary antibodies used in immunofluorescence analysis of organotypic slice cultures in this thesis

2.9.2 Imaging of immunofluorescent staining of organotypic brain slice cultures

Images were taken on the Nikon Eclipse Ti Inverted Spinning Disk Confocal microscope, using Yokogawa CSU-1 disk head and Andor iXon EMCCD camera and Nikon Elements software (Nikon Instruments, UK). Laser wavelengths used included 405nm, 488nm, 561nm, 640nm. Images were also captured using Nikon Upright Ni-E with A1R confocal microscope and 2x Multi-alkali PMT & 2x GAsSP PMTs imaging system on Nikon Elements software (Nikon Instruments, UK). Laser wavelengths utilised on this system were 405nm, 488nm, 561nm, 640nm. All parameters including exposure time and laser power were kept constant when capturing images.

2.10 Statistical analysis

In general, for the human tissue qualitative analysis, at least 3 cases per Braak stage were used for each experiment and at least 3 sections from each case were used. For quantification of human tissue data, 5 cases of Braak VI severity were used and at least 20 images were taken per case. For

organotypic brain slice culture experiments, at least 3 slices were taken as technical replicates per pup. At least 3 pups were used for statistical analysis. Three technical repeats were taken per preparation of neuronal cultures and three biological repeats were used for statistical analysis.

All statistical analysis was carried out using GraphPad Prism 9.3 software (La Jolla, USA). Data was first tested for normality using D'agostino and Pearson. When comparing two unrelated groups, data was analysed using parametric unpaired t-test, whilst the paired t-test was used when comparing two related groups. When comparing more than two unrelated groups, the ordinary one-way ANOVA with Tukey's multiple comparison test was used. Differences were considered significant when $P<0.05$. Data are expressed as mean +/- standard error of the mean (SEM) unless stated.

Chapter 3: Characterization of the cellular localisation and expression of small heat shock proteins in the Alzheimer's disease brain

3.1 Introduction

Alzheimer's disease is characterised by the accumulation of hyperphosphorylated tau to form intracellular neurofibrillary tangles (NFT) and extracellular plaques of amyloid-β (Aβ) (Alzheimer et al., 1995). It was once assumed that amyloid accumulation correlated with disease severity, however this is now only seen in the most severe stage of disease (Boluda et al., 2014). It is now known that tau is a better correlate of cognitive decline in AD compared to Aβ (Giannakopoulos et al., 2003; Brier et al., 2016)

Braak staging is used to assess the severity of AD according to the spatiotemporal progression of NFT across six distinct stages (Braak and Braak, 1991; Braak and Braak, 1995). These six stages have been described in Chapter 1, Section 1.3 (*Figure 1.4*), but in brief, Stage I-II is characterised by NFT in the entorhinal and hippocampal CA1 region, Stage III-IV occurs when the NFT spreads to the thalamus and hippocampal region CA4 and finally Stage V-VI is defined by NFT spread to the rest of the hippocampus and the neocortex.

Previous studies have confirmed the presence of sHSPs within both diseased and healthy brains using immunohistochemical analysis (see summary *Tables 4.1 and 4.2*). In the healthy brain, CRYAB has primarily been associated with oligodendrocytes (Shinohara et al., 1993; Wilhelmus et al., 2006). In the AD brain, CRYAB has been localised to a number of different cell types. Firstly CRYAB has been found to be located in oligodendrocytes (Renkawek and Voorter, 1994; Shinohara, 1993; Iwaki, 1992). CRYAB is also found in reactive astrocytes proximal to the amyloid plaques (Renkawek and

Voorter, 1994; Shinohara et al., 1993; Iwaki et al., 1992; Wilhelmus et al., 2006). In addition to this, CRYAB has been found in the neurons in AD and the presence of CRYAB within the neurons have been shown to correlate with those brain regions associated with most severe neuronal loss (Iwaki et al., 1992; Mao et al., 2001). With regards to HSPB1 expression in AD, HSPB1 has been seen in reactive astrocytes across the brain but HSPB1 has also been found to co-localise with microglia (Wilhelmus et al., 2006) and occasionally in the neurons (Renkawek and Voorter, 1994). HSPB1 has also been assoicaited with reactive astrocytes near to amyloid plaques but this was based purely on morphology analysis of the astrocytes, and no dual immunofluorescence was used to confirm these HSPB1 positive cells were actually reactive astrocytes (Renkawek et al., 1994; Wilhelmus et al., 2006).

sHSPs have also been found to be expressed in a number of tauopathies where localisation has been more fully characterised compared to the AD brain (López-González et al., 2014; Dabir et al., 2004). CRYAB is robustly upregulated in astrocytes in a number of tauopathy disorders which involve significant glial contribution such as corticobasal degeneration, progressive supranuclear palsy (PSP) and FTD17 (López-González et al., 2014; Dabir et al., 2004). The expression of HSPB1 is also been localised to the astrocytes, and although the levels of HSPB1 are not as dramatically increased in these tauopathy brains compared to CRYAB, it was confirmed that all HSPB1 positive cells were also GFAP positive (López-González et al., 2014; Dabir et al., 2004).

CRYAB			
Control brains	**AD brains**	**Methodology**	**Reference**
	In the cortex: – In GFAP positive astrocytes – Found in astrocytes near to plaques In the hippocampus: – More CRYAB positive astrocytes compared to cortex – Co-localised with microglia – Very few CRYAB positive neurons – High expression in oligodendrocytes	– Mid-frontal, temporal and parietal cortex and hippocampus – Stained subsequent sections – GFAP staining to determine astrocytes – Ferritin and HLA-DR with LN3 staining for microglia – Oligodendrocytes determined by morphology only	*Renkawek et al., 1994*
– CRYAB positive oligodendrocytes	– CRYAB positive reactive astrocytes near plaques (*data not shown*) – CYRAB positive microglia near to plaques (*data not shown*)	– Occipital cortex and hippocampus – Stained subsequent sections	*Wilhelmus et al., 2006*
– CRYAB positive oligodendrocytes	– CRYAB positive reactive astrocytes – High expression found in oligodendrocytes but no different to levels found in control brains	– Temporal and frontal cortex	*Shinohara et al., 1993*
	– CRYAB positive neurons in layers 3 and 4 of cerebral cortex – CRYAB positive neurons correlated with areas of more severe neuronal loss	– Frontal gyrus, temporal gyrus, entorhinal gyrus and lingual gyrus	*Mao et al., 2001*
	– Low levels of CRYAB positive reactive astrocytes – High CRYAB expression in oligodendrocytes – Very few CRYAB positive neurons	– Neocortex and hippocampus – Stained subsequent sections	*Iwaki et al., 1992*

Table 3.1: Summary of previous immunohistochemical analysis exploring the localisation of CRYAB in the control and AD brain (Renkawek et al., 1994, Wilhelmus et al., 2006, Shinohara et al., 1993, Mao et al., 2001, Iwaki et al., 1992)

HSPB1			
Control brains	**AD brains**	**Methodology**	**Reference**
– HSPB1 found in astrocytes only – More HSPB1 positive astrocytes in the hippocampus	– High expression in reactive astrocytes – Often found in astrocyte around plaques – In hippocampus, occasionally found in neurons and NFT	– Frontal and temporal cortex and hippocampus – Stained subsequent sections – Astrocytes determined by morphology only	*Renkawek et al., 1994*
– Mainly found in leptomeningeal and parenchymal vessels – Few HSPB1 positive astrocytes and microglia	– HSPB1 positive reactive astrocytes near plaques (*data not shown*) – HSPB1 positive microglia near to plaques (*data not shown*) – HSPB1 co-localised with Aβ in 15% or cortical plaques and 35% hippocampal plaques	– Occipital cortex and hippocampus – Stained subsequent sections	*Wilhelmus et al., 2006*

Table 3.2: Summary of previous immunohistochemical analysis exploring the localisation of HSPB1 in the control and AD brain (Renkawek et al., 1994, Wilhelmus et al., 2006)

3.2 Aims

The primary objective of the studies presented in this chapter was to characterise the expression of the sHSPs HSPB1 and CRYAB in Alzheimer's disease, using post-mortem human brain tissue of the temporal cortex brain region. Previous studies have reported CRYAB and HSPB1 to be located in different cells within AD (Renkawek and Voorter, 1994; Shinohara et al., 1993; Iwaki et al., 1992; Mao et al., 2001; Wilhelmus et al., 2006), and other studies have used serially stained sections to confirm the presence of HSPB1 within astrocytes, rather than carrying out dual immunofluorescence staining using the same tissue section, and so no formal co-localisation analysis was performed (Renkawek and Voorter, 1994; Renkawek et al., 1994; Wilhelmus et al., 2006). Further to this, although an association between sHSPs and amyloid-β has been made in the AD brain (Renkawek and Voorter, 1994; Renkawek et al., 1994; Wilhelmus et al., 2006), there has yet to be quantitative analysis of the association of astrocytic sHSPs in relation to these amyloid plaques.

Therefore, the specific aims for this chapter were to:

1. Characterise the location and expression of CRYAB across different Braak stages in human AD brain tissue using immunohistochemical analysis
2. Characterise the location and expression of HSPB1 in relation to amyloid-β pathology, within different Braak stages of human AD brain tissue using immunohistochemical analysis

3.3 Methods

The materials and methods for this chapter have been described in full in Chapter 2, Section 7. Formalin-fixed paraffin embedded (FFPE) post-mortem tissue brain sections were acquired from the London Neurodegenerative Disease Brain bank. To summarise, FFPE sections 7 µm thick were taken from Braak II (n=5), Braak IV (n=5), Braak VI (n=5) and MAPT mutation cases (n=5) (*Table 3.3*). Sections underwent immunofluorescence using antibodies against sHSPs CRYAB and HSPB1, neuronal markers, astrocytic markers, microglial markers, oligodendrocyte markers and pathological markers against tau and amyloid-β. DAPI (4',6-diamidino-2-phenylindole) was used to stain neuronal nuclei. Images taken for qualitative analysis were obtained on the Zeiss AxioImager Z1 microscope using the AxioVision software (Zeiss) whilst images used for quantitative analysis were taken on the Nikon Eclipse Ti Inverted Spinning Disk Confocal microscope, using Yokogawa CSU-1 disk head and Andor iXon EMCCD camera and Nikon Elements software (Nikon Instruments, UK).

Case ID	Sex	Age	PMD	Pathological diagnosis
BBN_20012	F	86	45	Alzheimer type changes (ageing), BNE stage II, control
BBN_9958	F	84	53	Alzheimer changes, Braak II, consistent with patient's age
BBN_9926	F	84	35	Alzheimer changes Braak II consistent with normal aging
BBN002.33764	M	73	49	Early Alzheimer-type changes BNE stage I-II control
BBN002.30882	M	77	28.5	Mild to moderate amyloid angiopathy, capillary subtype
BBN_9908	F	82	20	Alzheimer's disease modified Braak IV with amyloid angiopathy
BBN_18793	M	81	51	Alzheimer's disease, BNE stage IV
BBN002.29410	M	84	86	Alzheimer's disease (modified Braak (BNE) stage IV) with moderate amyloid angiopathy
BBN002.28694	F	86	55.5	Alzheimer's disease (modified Braak (BNE) stage IV) with mild amyloid angiopathy
BBN_20124	F	81	20	Alzheimer's disease (Braak stage VI). Vascular disease
BBN002.26278	M	75	59	Alzheimer's Disease (modified Braak (BNE) stage V, Thal phase 5 with moderate-severe amyloid angiopathy
BBN002.29634	M	72	41	Alzheimer's disease (modified Braak/BNE stage VI) with extensive and capillary amyloid angiopathy and significant cerebrovascular pathology
BBN_24235	F	79	63	Alzheimer's disease BNE stage VI
BBN_9980	F	83	58	Alzheimer's disease Braak stage VI
BBN002.32597	F	85	12	Alzheimer's disease, BNE stage VI
BBN_15278	M	71	5	Frontotemporal degeneration (Tau Mutation - 10+16)
BBN_15269	M	67	35	Frontotemporal degeneration (Tau Mutation - 10+16)
BBN_15268	F	58	31	Frontotemporal degeneration (Tau Mutation - 10+16)
BBN_15266	F	75	100+	Frontotemporal degeneration MND inclusion
BBN_15265	F	63	22	Frontotemporal degeneration (Tau Mutation - 10+16)

Table 3.3: Case details of post-mortem human brain tissue used for immunohistochemical analysis in Chapter 3 of this thesis.

Table shows Case ID, sex (M = male, F = female), Age (in years), post-mortem delay (PMD in hours) and pathological diagnosis for cases from which temporal cortex FFPE sections were obtained, BNE = Brain Net Europe protocol of Braak staging

Figure 2.73.4 Results

3.4.1 CRYAB and HSPB1 antibody validation

CRYAB

Two different commercially available CRYAB antibodies, which have previously been used in human tissue, including the AD brain (López-González et al., 2014; Yang et al., 2022; Björkdahl et al., 2008) were used in the following experiments. They included a polyclonal CRYAB antibody in rabbit, produced by immunizing animals with a synthetic peptide corresponding to residues surrounding Glu165 of the human CRYAB protein (Cell signalling) and a mouse monoclonal antibody [1B6.1-3G4] against the full length native protein (purified) corresponding to cow CRYAB. To confirm the specificity of these antibodies for the use in this PhD project, western blot analysis was performed using lysates of human control brain, WT mouse brain and primary mouse astrocytes. When immunoblotting with anti-CRYAB (Cell signalling), a CRYAB band was detected around the predicted 22kDa size in the human control brain tissue but not in the primary mouse lysates, indicating this antibody detected the human CRYAB protein but not the mouse CRYAB protein (*Figure 3.1A*). When immunoblotting with anti-CRYAB (Abcam), a strong CRYAB specific band appeared at around 22kDa in both the human and mouse tissue, implying that this antibody detected both mouse and human CRYAB (*Figure 3.1B*). Faint bands at around 37kDa were also detected indicating that the CRYAB (Abacm) antibody may not be completely specific for CRYAB or it could be detecting a modified form of CRYAB (Nagaraj et al., 2003; Ito et al., 2001). To further ensure that the CRYAB antibodies were specifically detecting CRYAB in the human brain, dual immunofluorescence was performed simultaneously using both antibodies in a section taken from a Braak VI case (n=1). The dual immunofluorescence showed a subcellular localisation of CRYAB in the perinuclear region, which is detected by these two antibodies and the staining patterns completely overlap (*Figure 3.1C*). A similar pattern of CRYAB staining around the nucleus is also seen in mild Braak II cases, and in MAPT mutation cases *(Figure 3.3)*, suggesting this subcellular pattern is also observed in healthy controls

and does not change with disease severity. Dual immunofluorescence using only the AlexaFluor mouse 488 and AlexaFluor rabbit 568 secondary antibodies was also carried out to ensure the secondary antibodies were not detecting any specific staining which may interfere with immunohistochemical characterisation of the human brain tissue. The images revealed that no specific staining was detected by either of the AlexaFluor secondary antibodies (*Figure 3.1D).* The results of the western blotting analysis, the immunofluorescence and the use of these CRYAB antibodies in previous literature strongly suggest that the CRYAB antibodies were specifically detecting the human CRYAB in the human brain.

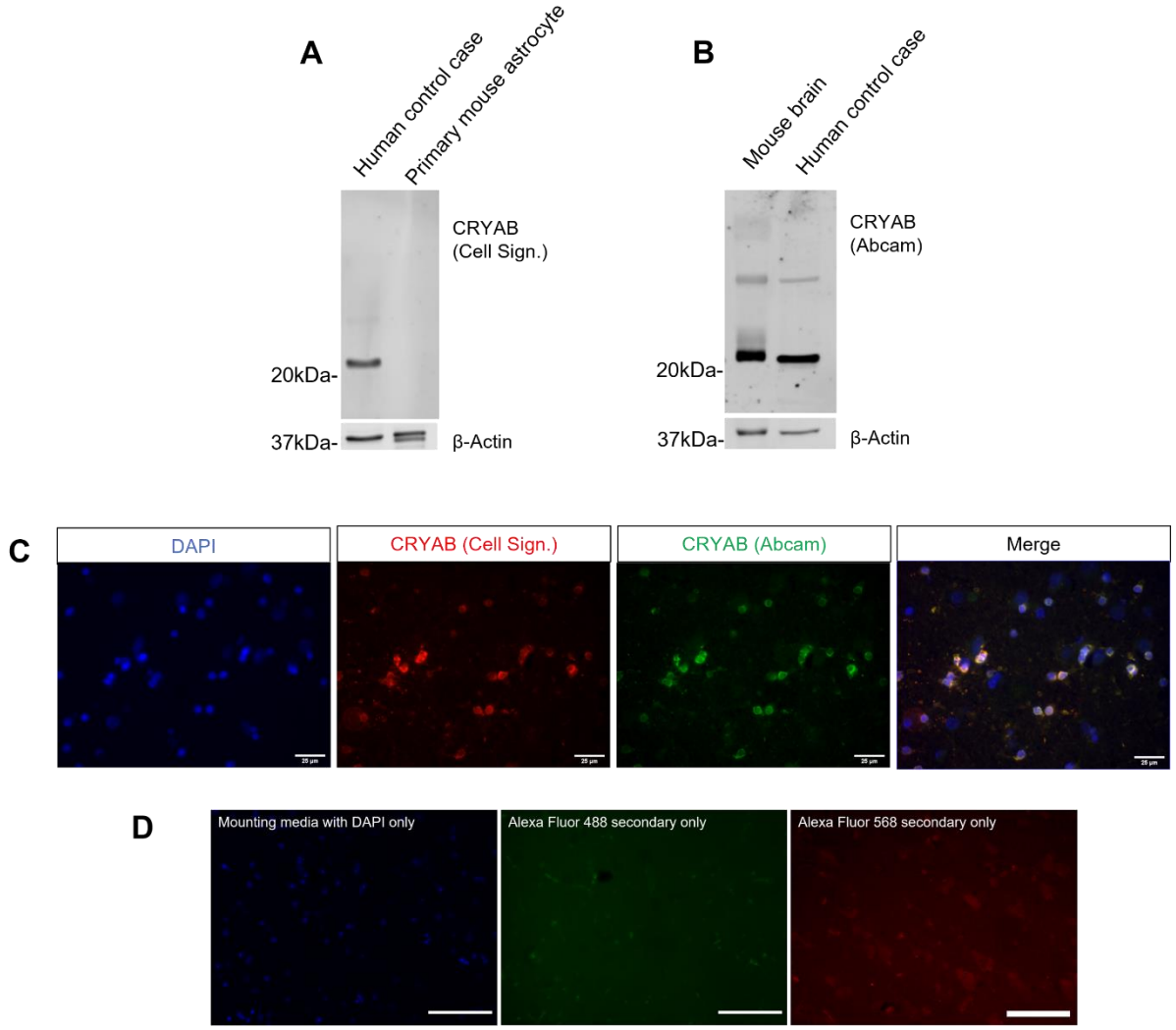

Figure 3.1: Specificity of the anti-CRYAB antibodies.

A) Western blot of human control brain lysates and primary mouse astrocyte lysates with antibodies against CRYAB (Cell signalling) and loading control β-Actin, n=1, B) Western blotting of CD1 control mouse brain lysate and control human brain lysate with antibodies against for CRYAB (Abcam) and loading control β-Actin, n=1,C) Dual immunofluorescent staining of Braak VI AD cases using antibodies against CRYAB, n=1, scale bar = 25µm, D) Representative image of dual immunofluorescence using Goat-anti mouse AlexaFluor secondary antibody 488 and goat-anti-rabbit AlexaFluor secondary antibody 568 and mounted with mounting media with DAPI, n=1, scale bar = 100µm. Secondary only immunofluorescence was also carried out using anti-mouse rabbit AlexaFluor secondary antibody 488 and anti-rabbit rabbit AlexaFluor secondary antibody 569, data not shown, but image looks representative to figure 3.2D.

HSPB1

Commercially available antibodies were also used to target HSPB1 in human brain tissue to determine the localisation and expression of this sHSP in relation to other cellular markers. Two different antibodies for HSBP1 were used, one polyclonal antibody raised in rabbit against recombinant mouse HSP25 (mouse HSPB1, Enzo 801-F) and one polyclonal antibody raised in rabbit against recombinant human HSP27 (human HSPB1, Enzo 803-F). Both antibodies have been used previously in the mouse brain (Afshar et al., 2017; Liebl et al., 2015) and the human AD brain (Wilhelmus et al., 2006; Braak and Tredici, 2017). The antibodies were initially validated by immunoblot of lysates from human control brain, WT mouse brains and primary mouse astrocytes. When using the mouse anti-HSPB1 antibody, a strong specific band at the expected weight of 25kDa appeared in the primary mouse astrocyte and brain lysates whereas only non-specific bands were detected in the human brain control tissue, suggesting a specificity for mouse HSPB1 (*Figure 3.2A*). When immunoblotting with the human HSPB1 antibody, there were no bands found in the mouse astrocyte or mouse brain lysates however there was a strong specific band at the expected weight of 25kDa in the human control brain lysate (*Figure 3.2B*). This data, along with the extensive list of published studies using these same antibodies, including one study also exploring HSPB1 in the human AD brain (Wilhelmus 2006), suggest that these antibodies are suitable to use for the human brain characterisation in this thesis.

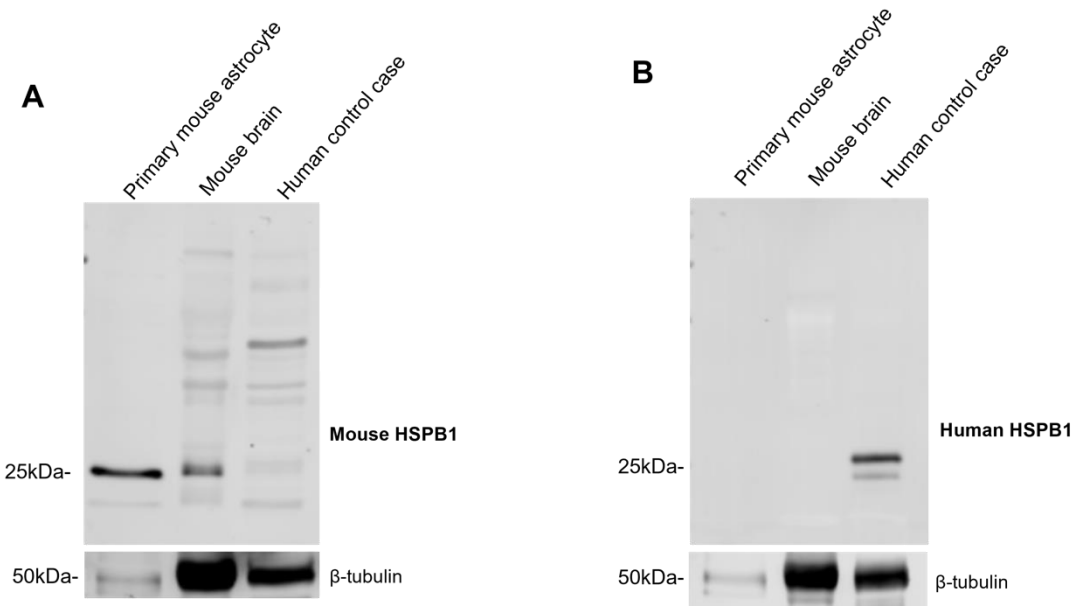

Figure 3.2: Specificity of the anti-HSPB1 antibodies

A) Western blot of primary mouse astrocyte lysates, control CD1 mouse brain lysates and human control brain lysates with antibodies against mouse HSPB1 (Enzo, 800-F) and loading control β-Actin, n=1, B)) Western blot of primary mouse astrocyte lysates, control CD1 mouse brain lysates and human control brain lysates with antibodies against human HSPB1 (Enzo, 803-F) and loading control β-Actin, n=1

3.4.2 CRYAB mostly co-localises with an oligodendrocyte marker in AD brain

As previously published studies seem to indicate that CRYAB expression is associated with astrocytes in AD (Renkawek and Voorter, 1994; Shinohara et al., 1993), brain tissue sections from Braak II (n=3), IV (n=3) and VI cases (n=3) were initially stained with an antibody against CRYAB and total astrocyte marker ALDH1L1. ALDH1L1 is a marker for aldehyde dehydrogenase 1 family member L1 and is used as an ubiquitous astrocyte marker (Serrano-Pozo et al., 2013). A case with frontotemporal dementia with parkinsonism linked to chromosome 17 (FTDP-17) owing to the tau intron 10 + 16 mutation, known to causes FTD-tau (Hutton et al., 1998) was used as a positive control as CRYAB has been shown to be strongly upregulated in reactive astrocytes in FTD-17 cases (Dabir et al., 2004). Immunofluorescence was carried out on three cases per Braak stage. Qualitative analysis revealed that the number and the intensity of CRYAB positive cells was increased in the more severe AD cases, whilst the number of ALDH1L1 positive astrocytes did not change with disease severity (*Figure 3.3*). There was no co-localisation between CRYAB positive cells and ALDH1L1 cells in any of the Braak II-VI cases (*Figure 3.3*). In the FTD-Tau case, there was some co-localisation between the CRYAB positive and ALDH1L1 positive cells (*Figure 3.3, arrowheads*), but the majority of CRYAB positive cells were not ALDH1L1 positive. This result suggests that some of the CRYAB positive cells could be co-localising with one specific subset of astrocyte, however, the majority of CRYAB positive cells are not astrocytes.

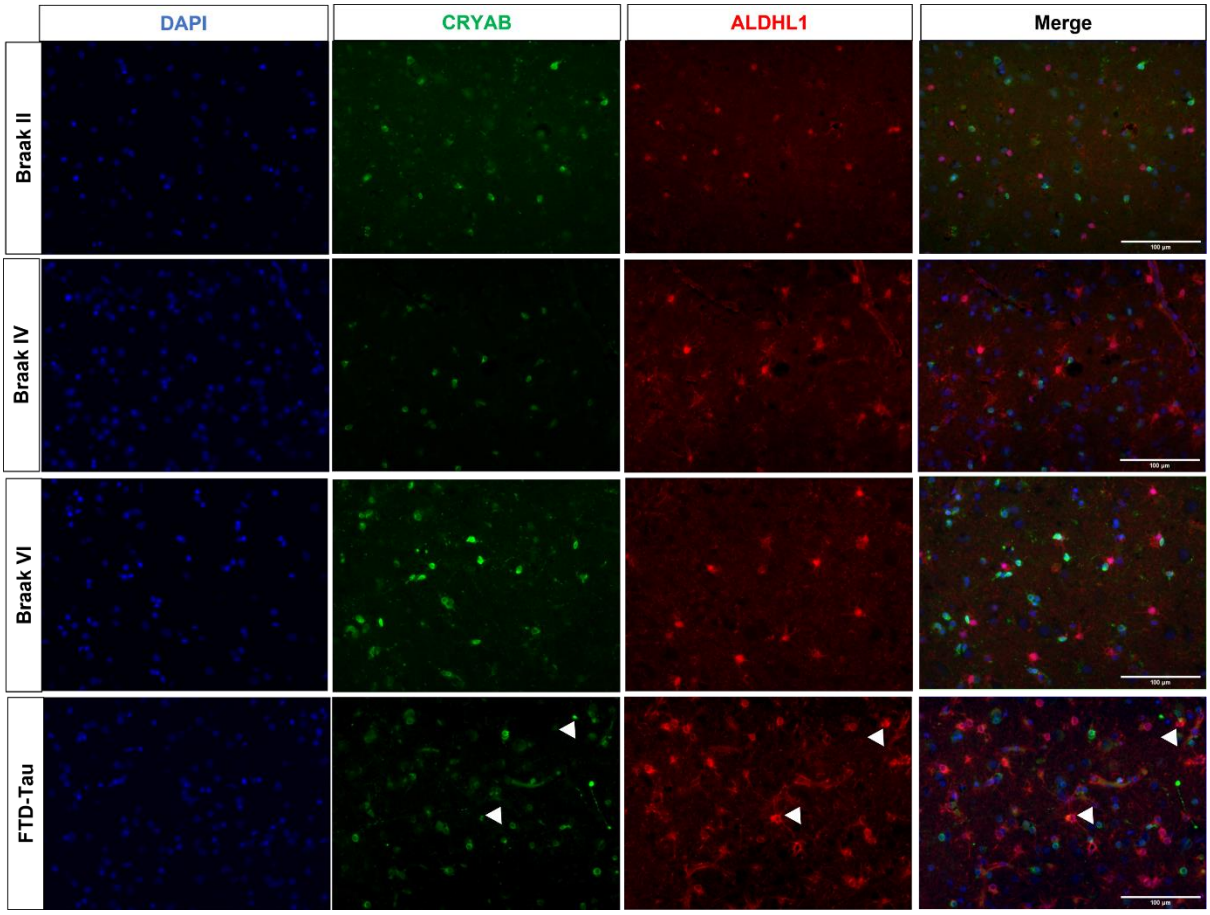

Figure 3.3: Immunofluorescent analysis of temporal cortex sections taken from Braak II, IV and VI cases, and FTD-17 case, using antibodies against CRYAB and total astrocytes (ALDHL1).

Representative image of three cases per Braak stage (total n=12), arrowhead indicates co-localisation between CRYAB and ALDH1L1 positive cells, images taken on Zeiss AxioImager Z1 microscope, scale bar = 100µm

Following this, CRYAB expression was investigated to determine whether localisation was restricted to reactive astrocytes within the AD brain. Brain tissue sections from Braak stage II, IV and VI AD cases were stained with antibodies raised against CRYAB, reactive astrocyte marker GFAP and amyloid-β marker 6E10. GFAP is a marker of glial fibrillary acidic protein, the major protein constituent of astrocyte intermediate filaments (Eng et al., 1971), and the 6E10 antibody is reactive to amino acid residue 1-16 of amyloid-β and APP and it also detects abnormally processed isoforms and precursor amyloid species (Pirttilä et al., 1994). Immunofluorescent staining was performed on three cases per Braak stage. In Braak II cases, the number of amyloid-β plaques was generally very low, whereas amyloid plaque pathology was identified in Braak IV and Braak VI cases, as seen by 6E10 immunofluorescence (*Figure 3.*4). The amyloid plaques in Braak VI cases were detected much more frequently that in Braak IV cases and the intensity of plaque staining was also increased (*Figure 3.4*). Further to this, GFAP positive reactive astrocytes were found surrounding these plaques as seen in the literature (Renkawek and Voorter, 1994; Wilhelmus et al., 2006), and there were more GFAP positive reactive astrocytes surrounding amyloid plaques in the Braak VI cases when compared to the Braak IV cases (*Figure 3.4, arrowheads*). Qualitative analysis of CRYAB immunofluorescence determined that CRYAB positive cells did not co-localise with GFAP positive reactive astrocytes in any of the Braak stage cases (*Figure 3.4*). These results indicate that CRYAB does not co-localise with GFAP positive reactive astrocytes in the AD brain and this is unaffected by AD severity.

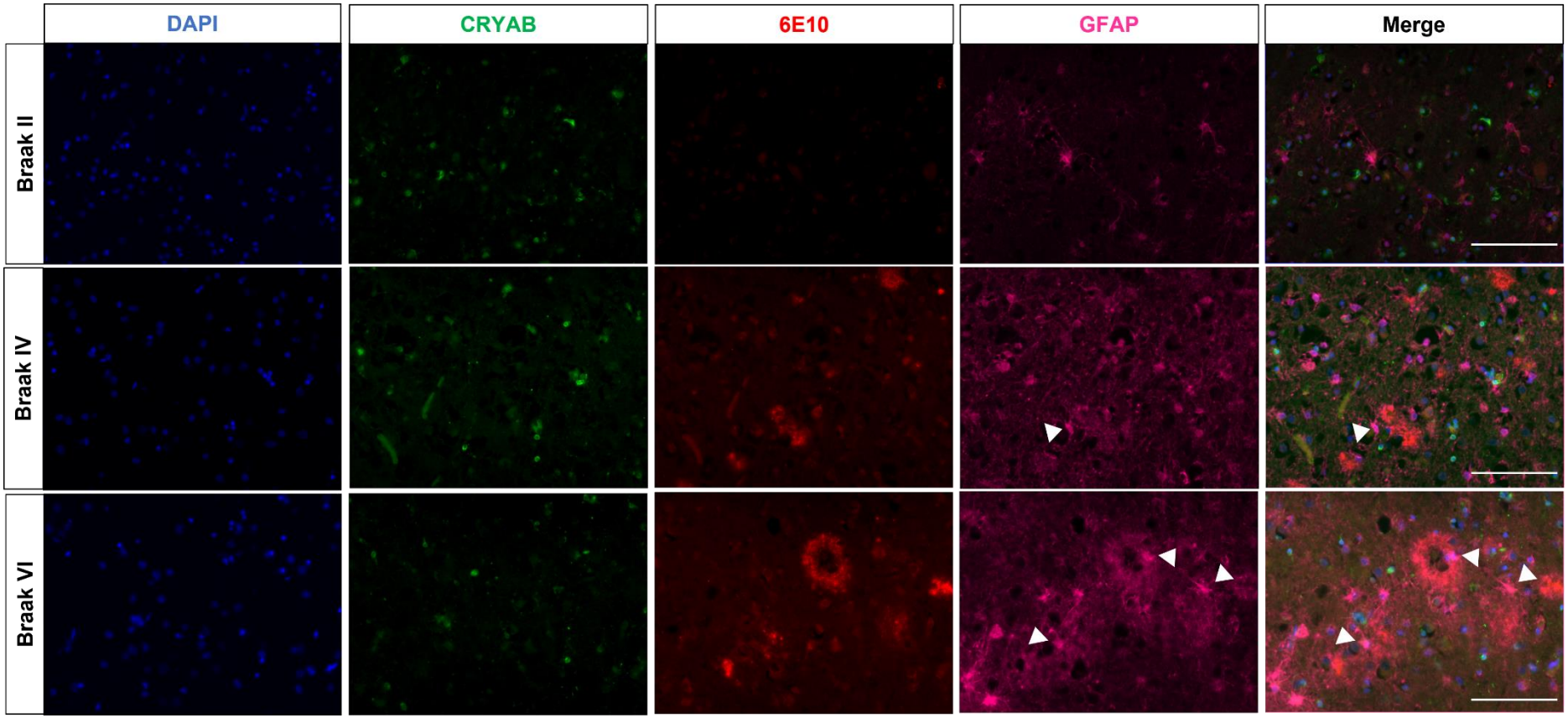

Figure 3.4: Immunofluorescent analysis of temporal cortex sections taken from Braak II, IV and VI cases using antibodies against CRYAB, amyloid-β (6E10) and reactive astrocytes (GFAP).

Representative images of three cases per Braak stage (total n=9), arrowhead indicates GFAP positive cells localising around amyloid plaques, images taken on Zeiss AxioImager Z1 microscope, scale bar = 100µm

Most previous studies have reported very low levels of CRYAB associated with neurons (Iwaki et al., 1992; Renkawek and Voorter, 1994), however, one study did report a number of CRYAB positive neurons in the cerebral cortex of AD (Mao et al., 2001) and so to further investigate the localisation of CRYAB, human brain sections from Braak II-VI cases were stained with an antibody against CRYAB, together with an antibody raised against microtubule-associated protein 2 (MAP2). MAP2 is a microtubule-associated protein which interacts with microtubules to maintain the structure of dendrites (Caceres et al., 1984). Immunostaining was performed in three different cases per Braak stage. MAP2 stained neuronal bodies and neuronal projections (*Figure 3.5*), however, no co-localization was observed between MAP2 and CRYAB, in any of the Braak stages (*Figure 3.5*). The data indicates that CRYAB is not expressed in neurons, neither in severe, moderate or mild AD cases.

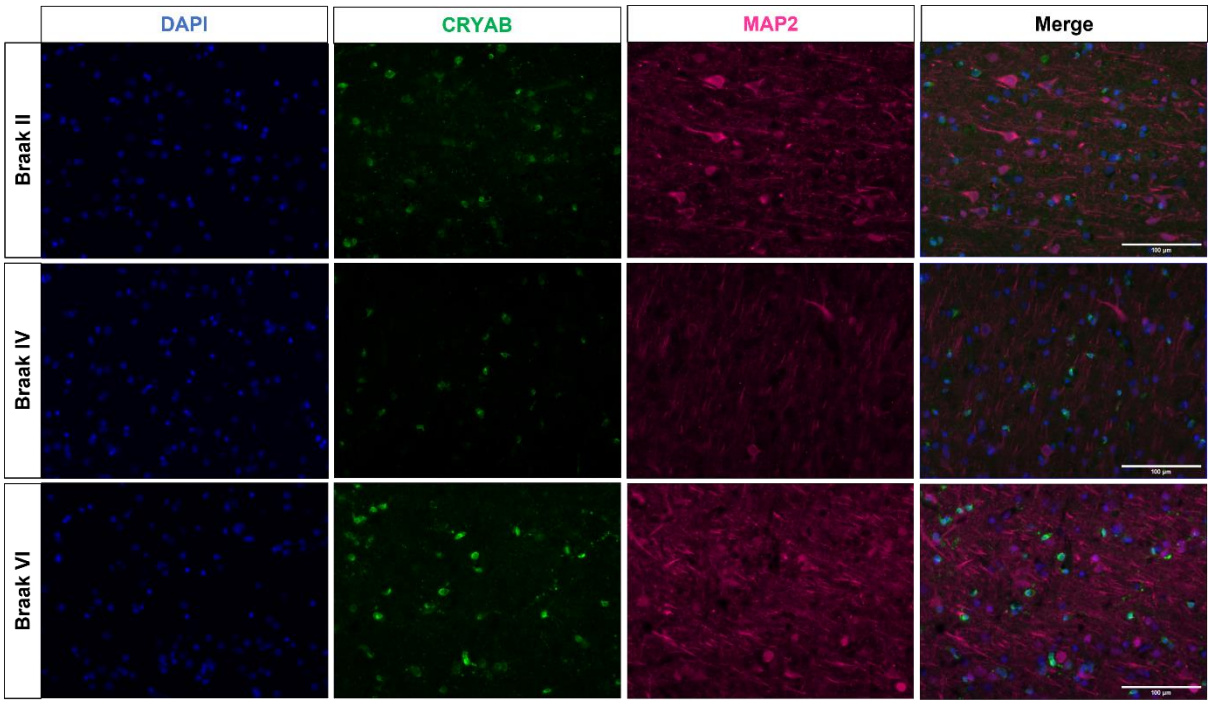

Figure 3.5: Immunofluorescent analysis of temporal cortex sections taken from Braak II, IV and VI cases using antibodies against CRYAB and neurons (MAP2).

Representative images of three cases per Braak stage (total n=9), images taken on Zeiss AxioImager Z1 microscope, scale bar = 100µm

It has been shown that CRYAB is located in oligodendrocytes in control and in AD brains (Renkawek and Voorter, 1994; Shinohara et al., 1993; Iwaki et al., 1992). Further immunofluorescence was carried out using sections from Braak II, IV and VI cases, three cases per Braak stage, with antibodies against oligodendrocytes, reactive astrocytes (GFAP) and CRYAB. The anti-carbonic anhydrase II antibody (CAII) was used to stain for oligodendrocytes as it detects all stages of oligodendrocyte lineage and also detects adult oligodendrocytes (Baumann and Pham-Dinh, 2001). Qualitative analysis determined that there were more CAII positive oligodendrocytes in the least severe AD Braak II cases, compared to the number of CAII positive oligodendrocytes in the most severe Braak VI cases (*Figure 3.6*). Immunofluorescence also indicated that the majority of CRYAB positive cells co-localised with CAII positive oligodendrocytes (*Figure 3.6*). There was a small subset of CRYAB positive cells which did not co-localise with either CAII-positive oligodendrocytes or GFAP-positive reactive astrocytes (*Figure 3.6, arrowheads*), however, all CAII cells looked to be CRYAB positive. These results suggest that the majority of CRYAB positive cells are oligodendrocytes but further work is required to determine which cell type the other CRYAB positive cells are co-localising with.

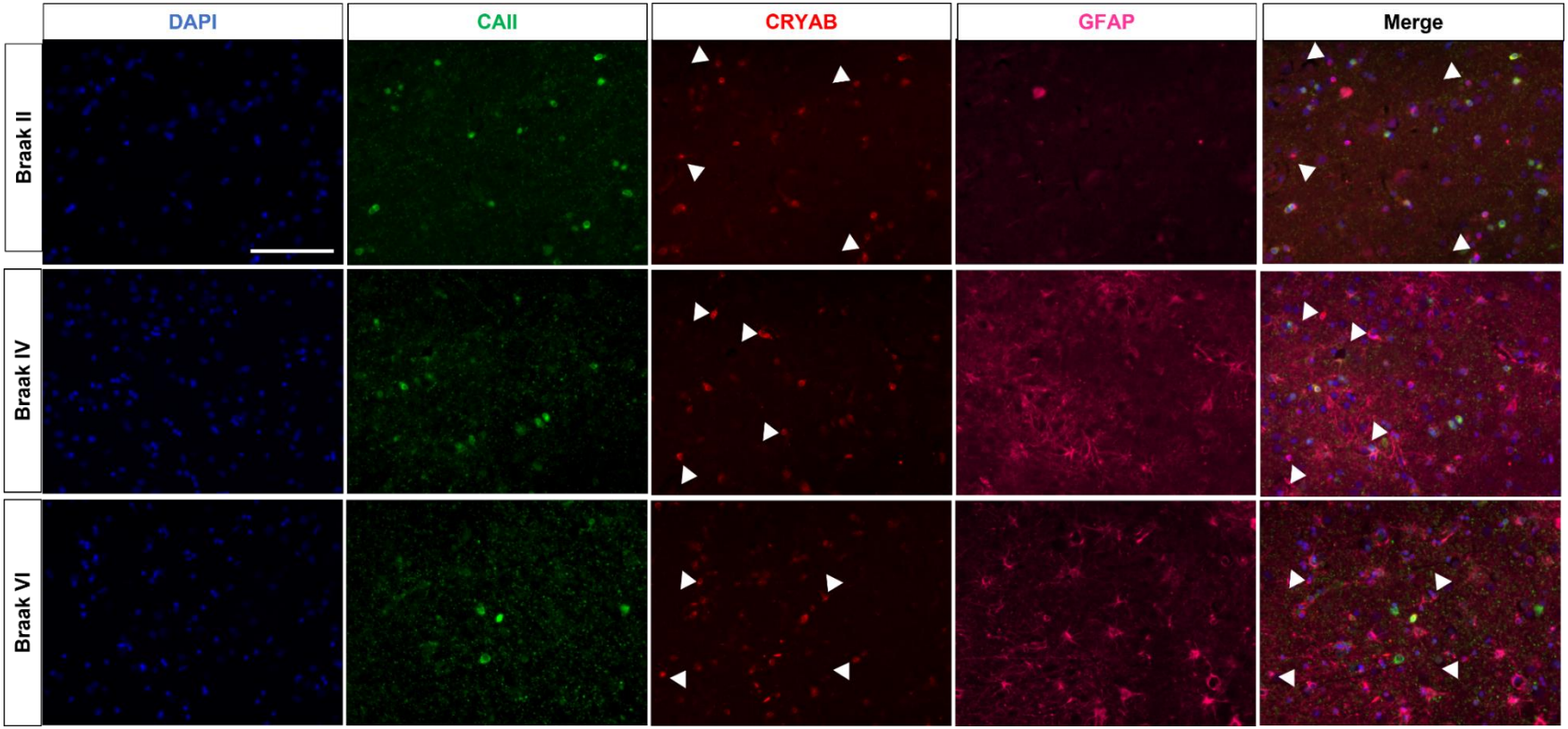

Figure 3.6: Immunofluorescent analysis of temporal cortex sections taken from Braak II, IV and VI cases using antibodies against CRYAB, oligodendrocytes (CAII) and reactive astrocytes (GFAP).

Representative images of three cases per Braak stages (total n=9). Arrowhead indicates CRYAB positive cells which did not co-localise with either CAII or GFAP staining, images taken on Zeiss AxioImager Z1 microscope, scale bar = 100µm

Literature has shown CRYAB to co-localise with microglia markers found near to amyloid plaques (Renkawek and Voorter, 1994; Wilhelmus et al., 2006). To determine whether the subset of CRYAB-positive CAII-negative cells that we observed were microglia, brain sections from 2 Braak VI cases were stained with CRYAB and microglial marker IBA-1. IBA-1 detects the calcium binding protein associated with membrane ruffling and phagocytosis of activated microglia (Jurga et al., 2020). Preliminary analysis suggest that CRYAB does not co-localise with IBA-1 positive microglia (*Figure 3.7*). However, it must be stressed that due to time constraints, full optimisation of the staining protocol with both the CRYAB and IBA-1 antibodies across all Braak stages was not carried out. Further optimisation is required in order to conclude whether CRYAB does in fact co-localise with microglia or not.

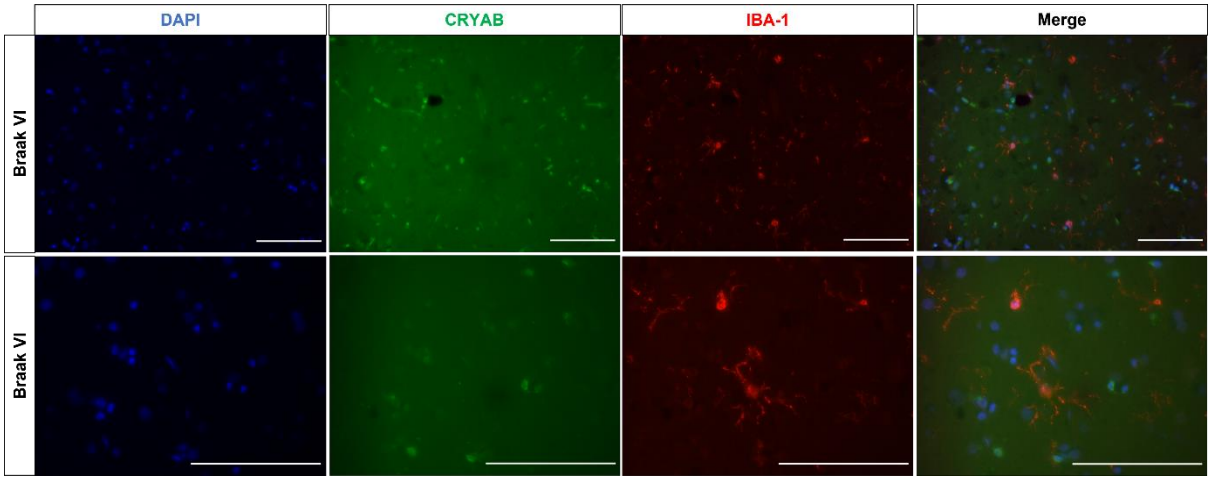

Figure 3.7: Immunofluorescent analysis of temporal cortex sections taken from Braak VI cases using antibodies against CRYAB and microglia (IBA-1)

Representative images of preliminary analysis of 2 Braak VI cases (total n=2), images taken on Zeiss AxioImager Z1 microscope, scale bar = 100µm

3.4.3 HSPB1 is expressed in reactive astrocytes in AD

As previously published studies strongly suggest an association between HSPB1 and reactive astrocytes in AD (Renkawek et al., 1994; Wilhelmus et al., 2006), immunofluorescence was performed on temporal cortex brain tissue sections from Braak II (n=3), IV (n=3) and VI cases (n=3). A case with FTDP-17 owing to the tau intron 10 + 16 mutation known to causes FTD-tau (Hutton et al., 1998) was used as a positive control as HSPB1 has been shown to co-localises with reactive astrocytes in FTD-17 cases (López-González et al., 2014). Brain sections were stained using a marker for HSPB1, reactive astrocytes (GFAP) and amyloid-β (6E10). The number and intensity of amyloid-β plaques increased with disease severity. HSPB1 positive cells and GFAP positive reactive astrocytes also increased with AD severity (*Figure 3.8*). In addition to this, the number of GFAP positive astrocytes surrounding amyloid plaques increased as the disease severity increase (*Figure 3.8*). In the mild Braak II cases, the majority of the GFAP positive astrocytes were also HSPB1 positive (*Figure 3.8, asterisk*), however there was the occasional HSPB1 positive cell that was not GFAP positive *(Figure 3.8*, arrowhead). In the moderate and severe Braak IV-VI cases, all the HSPB1 positive cells co-localised with GFAP positive reactive astrocytes, as reported in the literature (Renkawek et al., 1994; Wilhelmus et al., 2006). In the FTD-Tau samples there was no amyloid-β, as detected by 6E10 and HSPB1 co-localised with all GFAP positive reactive astrocytes (*Figure 3.8, asterisk*). These results support the notion that HSPB1 is upregulated in astrocytes during AD, as described in recent transcriptomic studies (Grubman et al., 2019; Smith et al., 2022; Mathys et al., 2019).

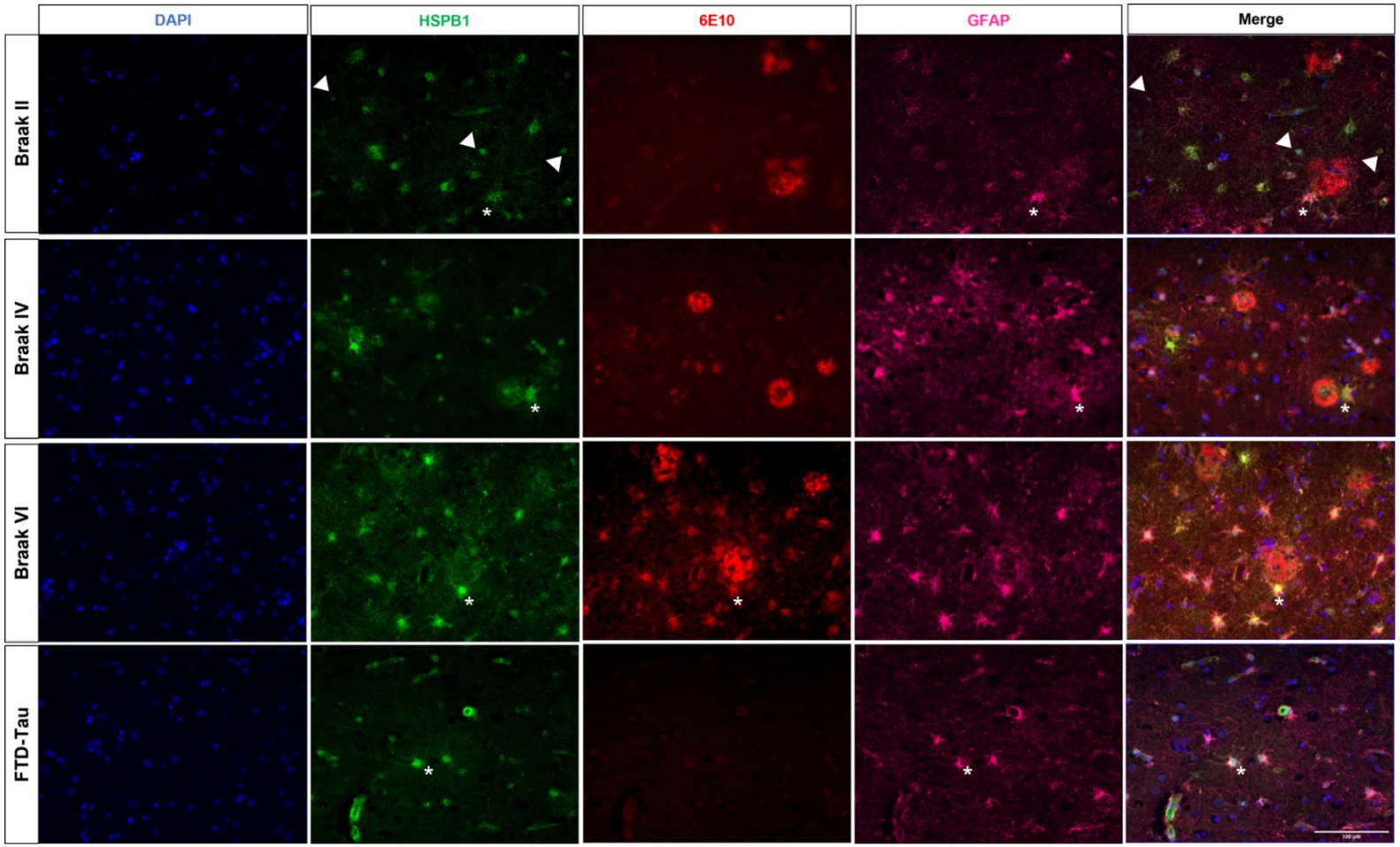

Figure 3.8: Immunofluorescent analysis of temporal cortex sections taken from Braak II, IV and VI cases and FTD-17 cases using antibodies against HSPB1, amyloid-β (6E10) and reactive astrocytes (GFAP).

Representative images of three cases per Braak stage (total n=12), asterisk indicate HSPB1 staining co-localising with GFAP positive staining, arrowhead indicates HSPB1 positive cells which are not positive for GFAP staining, images taken on Zeiss AxioImager Z1 microscope, scale bar = 100µm

As some positive HSPB1 positive cells did not co-localised with GFAP positive astrocytes, further immunostaining was performed using sections across all three severity groups of AD with antibodies against HSPB1 and neuronal marker MAP2, using three cases per Braak stage. The MAP2 staining confirmed the presence of both neuronal bodies and neuronal projections across all severities of AD but there was no co-localisation between either of these MAP2 positive structures and HSPB1 in any of the AD cases (*Figure 3.9).* Further investigation is required to determine the cell type of those HSPB1 positive cells in the mild AD cases which were not localised in the GFAP positive astrocytes.

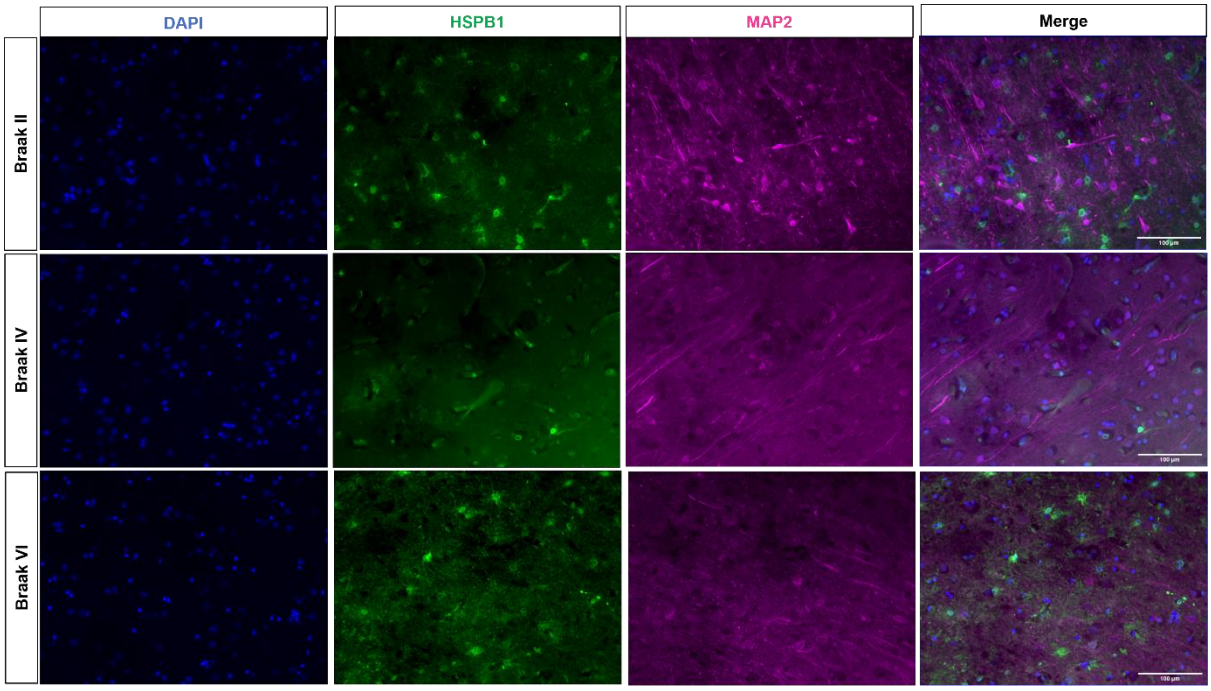

Figure 3.9: Immunofluorescent analysis of temporal cortex sections taken from Braak II, IV and VI cases using antibodies against HSPB1 and neurons (MAP2).

Representative images of three cases per Braak stage (total n=9), images taken on Zeiss AxioImager Z1 microscope, scale bar = 100µm

3.4.4 HSPB1 expression increases in those reactive astrocytes in close proximity to amyloid plaques

It has been shown that reactive astrocytes in close proximity to amyloid plaques express higher levels of reactive astrocyte markers such as GFAP (Itagaki et al., 1989; Perez-Nievas and Serrano-Pozo, 2018; Serrano-Pozo et al., 2011), therefore analysis was carried out to determine whether levels of HSPB1 correlate with this increased reactivity in astrocytes in AD.

To explore this interaction between HSPB1 and the reactive astrocytes associated with amyloid plaques, brain sections were analysed from five Braak VI AD cases as these most severe AD cases exhibited the most severe plaque pathology and the highest incidence of HSPB1- positive GFAP-positive reactive astrocytes. Sections were stained with antibodies against HSPB1, reactive astrocytes (GFAP) and amyloidβ (6E10) and images were taken proximal to (within a 50µm radius of the plaque edge) and distal to (50µm radius away from the plaque edge) amyloid plaque, using the Nikon Eclipse Ti Inverted Spinning Disk Confocal microscope. At least 10 images were taken distal and 10 images taken proximal to amyloid plaques for each case. The categories of proximal and distal to the plaques have been used previously to explore amyloid plaques in AD (Serrano-Pozo et al., 2016; Serrano-Pozo et al., 2011). The measurements proximal and distal to amyloid plaques was defined in previous studies which found that a 50µm radius was sufficient to avoid repeated counting of the same astrocytes in areas where there is a high density of plaques (Serrano-Pozo et al., 2010). Using these images proximal and distal to the amyloid plaques, manual counts were carried out to determine the proportion of GFAP positive astrocytes which were also HSPB1 positive, both proximal and distal to the amyloid plaques. Across all five Braak VI cases, there was an increase in the number of reactive astrocytes that were also positive for HSPB1 in close proximity to the amyloid plaques, when compared to the number of HSPB1 positive reactive astrocytes distal to the amyloid plaques (*Figure 3.10B)*. GFAP and HSPB1 expression was also assessed using ImageJ

software, showing an increase in the overall intensity of both GFAP and HSPB1 levels closer to the amyloid plaques (*Figure 3.10C*). Further to this, during the quantification of HSBP1 positive reactive astrocytes proximal to the amyloid plaques, it was noted that the plaques used in these images also contained HSPB1 positive staining. Quantification across all five Braak VI cases revealed that 86.38% of 6E10 positive plaques were also positive for HSPB1 (*Figure 3.10D*).

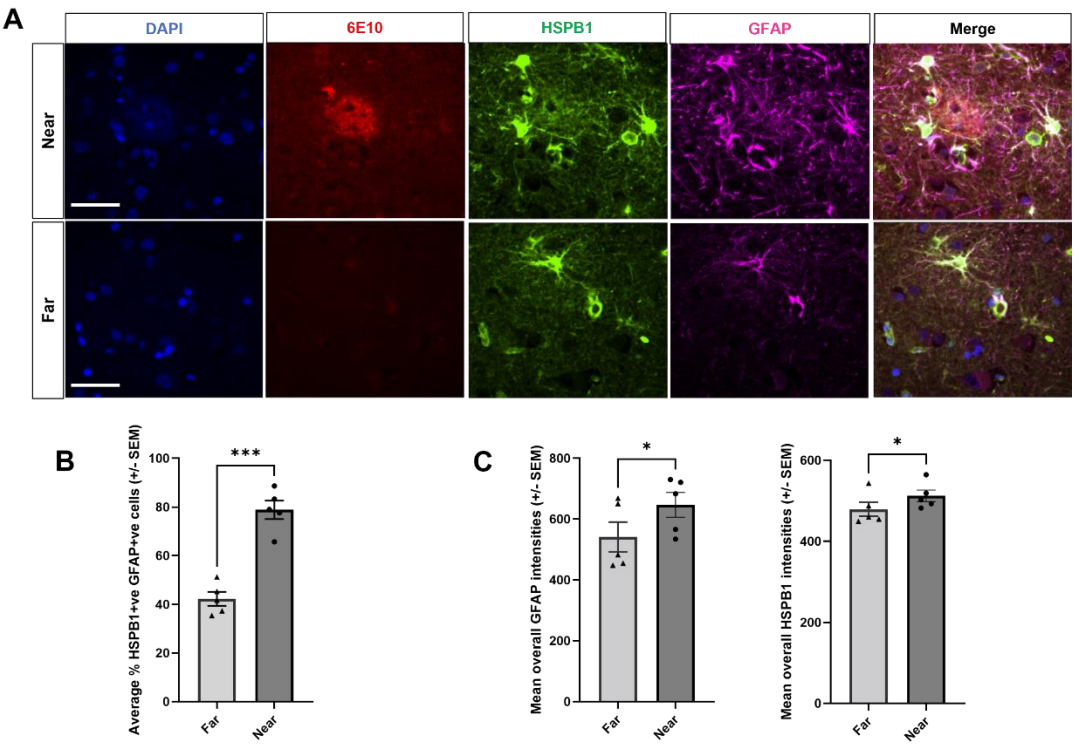

D

Case ID	Total # plaques	% HSPB1 positive plaques
BBN002.32597	13	94.87
BBN002.26278	14	100
BBN002.32597	24	64.69
BBN_9980	15	92
BBN_24235	18	80.34
Average		**86.38**

Figure 3.10: HSPB1 expression in reactive astrocytes proximal and distal to amyloid plaques in the temporal cortex of Braak VI AD cases.

*A) Immunofluorescence analysis temporal cortex sections taken from Braak VI cases using antibodies against amyloid-β (6E10), HSPB1 and reactive astrocytes (GFAP) proximal (within a 50µm radius of the plaque edge) and distal to (50µm radius away from the plaque edge) amyloid plaques, 20 cases per Braak stage were stained (total n=100), imaged using Nikon Eclipse Ti Inverted Spinning Disk Confocal microscope, scale bar = 50µm B) Graph shows proportion of HSPB1 positive reactive astrocytes proximal to the amyloid plaques. MEAN +/- SEM from Braak 6 cases (n=5), paired t-test, ***P=0.0007. C) Graphs show overall GFAP and HSPB1 expression proximal to the amyloid plaques. MEAN +/- SEM taken from Braak 6 cases (n=5), paired t-test, *P<0.05, D) Table showing the number of plaques in each of the "proximal to amyloid plaque" images across all 5 Braak VI stage patients, and the number of those plaques which were positive for HSPB1 staining, represented as a percentage of total plaques*

3.5 Discussion

The main aim of this chapter was to determine the localisation and expression of CRYAB and HSPB1 in the human diseased brain. To do this, immunofluorescence analysis was performed on AD brain tissue sections taken from Braak II, IV and VI cases, using antibodies against our sHSPs of interest in combination with antibodies against other cellular markers for neurons and glial cells. The main findings from this chapter are as follows: 1) The majority of CRYAB positive cells, but not all CRYAB positive cells, co-localise with CAII positive oligodendrocytes in mild, moderate and severe AD cases, 2) HSPB1 expression seems to be restricted to reactive astrocytes only in the most severe Braak VI AD cases, whereas in mild AD cases, some HSPB1 also co-localises with another cell type, and 3) HSPB1 expression increases in those reactive astrocytes in close proximity to amyloid plaques in the most severe AD cases.

It is generally accepted that there is an increase in CRYAB expression in AD and tauopathy brains compared to controls (Renkawek and Voorter, 1994; Shinohara et al., 1993; Dabir et al., 2004). This is supported by western blotting analysis of brain lysates taken from AD cases, where CRYAB has been seen to be expressed at significantly higher levels in the frontal and temporal regions, compared to age-matched controls (Renkawek and Voorter 1994; Shinohara et al., 1993; Björkdahl et al., 2008). However, the results in the parietal lobes of the brain are less certain with only a trending increase or no significant differences reported in the levels of CRYAB in this region in AD brain compared to control (Shinohara et al., 1993; Wilhelmus et al., 2006). These regional differences in CRYAB expression in the AD brain support the idea that the upregulation of CRYAB is potentially the result of exposure to abnormal proteins Aβ and NFT as those areas associated with significantly increased CRYAB levels are regions generally most severely affected by AD pathology (Braak and Braak, 1997). This is corroborated by the study which found that CRYAB levels in the

lysates from the medial temporal cortex of the AD brain correlated with the levels of phosphorylated tau and NFT (Björkdahl et al., 2008). Although western blot analysis of brain lysates was not performed as part of this characterisation, qualitative analysis of CRYAB staining did confirm an increase in CRYAB positive cells and CRYAB staining intensity in sections from more severe Braak VI cases compared to mild Braak II cases, supporting the idea that CRYAB is increased in the AD brain.

The cellular localisation of CRYAB has been explored previously in a number of studies. CRYAB expression seems to be restricted to a specific subset of reactive astrocytes such as proliferating astrocytes (Renkawek and Voorter 1994; Shinohara et al., 1993; López-González et al., 2014) or those astrocytes (and microglia) associated specifically with amyloid plaques (Renkawek and Voorter, 1994; Wilhelmus et al. 2006). In tauopathies where there is a high levels of glial reactivity, a higher proportion of tau-associated astrocytes express CRYAB compared to non-tau associated astrocytes (López-González et al., 2014). Some CRYAB positive astrocytes such as hypertrophic astrocytes have also been seen to be more brain region specific as they are more frequently detected in the hippocampus rather than the neocortex (Shinohara et al., 1993; Renkawek, et al 1994). This could account for the apparent lack of CRYAB positive reactive astrocytes found in our study, as the focus was limited to the temporal cortex region only and no specific staining was performed for different astrocytic populations. Similar to our findings, CRYAB has not been found to be expressed in neurons in either control or less severe AD although this data was not shown in the publications (Renkawek, et al 1994; Iwaki et al., 1992). While in the most severe AD cases (Braak IV – VI) and other tauopathies, CRYAB expression was found in ballooned type neuron (Mao et al., 2001, López-González et al., 2014), which based on morphology alone, we could not identify in our tissue sections. Using CAII staining in the human tissue sections, the number of oligodendrocytes seemed to decrease as the severity of AD increased, supported by the literature that suggests that the increasingly severe white matter changes detected in AD are associated with dysfunctional

oligodendrocytes and the precursors required for remyelination (Nasrabady et al., 2018). We show that the majority of our CRYAB positive cells are also positive for the oligodendrocyte marker CAII. This is supported by a number of other studies which also implicate CRYAB positive oligodendrocyte cells in the AD brain (López-González et al., 2014). Furthermore, recently published transcriptomic analysis of AD brains support the upregulation of CRYAB in oligodendrocytes (Mathys et al., 2019). Although the majority of CRYAB positive cells were found to co-localise with CAII positive oligodendrocytes, not all CRYAB positive cells were also CAII positive, a trait that was seen in cases across all different AD severities, suggesting CRYAB to be localised in another cell type, an idea further confirmed through recent cell-specific transcriptome studies (Grubman et al., 2019). Overall, further exploration of CRYAB in the AD brain is required to confirm the cellular subtypes in which CRYAB is localised.

In order to confirm the location of CRYAB in the human brain tissue, the immunofluorescence analysis could be expanded to include more specific markers for oligodendrocytes to firstly confirm whether CRYAB is co-localising with oligodendrocytes and then to confirm which specific oligodendrocyte phenotype CRYAB is co-localising with (Baumann and Pham-Dinh, 2001). CAII is primarily used as a pan-oligodendrocyte marker and so other markers such as Nestin which can differentiate between proliferating progenitor oligodendrocytes and differentiated oligodendrocytes could also be utilised in these characterisation experiments (Gallo and Armstrong 1995). Additionally, markers for more specific astrocytic and neuronal phenotypes could also be employed, such as a marker for astrocyte proliferation (Escartin et al., 2021) and a marker for dystrophic neurons (Sharoar et al., 2021) to be used alongside CRYAB in more regions of the brain, such as the hippocampus. Co-localisation with microglial should also be further explored as few studies observed CRYAB localisation in microglia, particularly near to the amyloid plaques (Renkawek and Voorter, 1994; Wilhelmus et al., 2006). Furthermore, a more sensitive approach to explore the

localisation of CRYAB such as in situ hybridisation (ISH) in combination with immunohistochemistry (IHC) (Grabinski et al., 2015) could also be recommended.

The next main aim of this chapter was to investigate the expression of HSPB1 in human AD brains. Similar to what has been described for CRYAB, western blotting analysis of HSPB1 in AD brain found a significant increase in HSPB1 levels in the frontal cortex of AD brain compared to control (Renkawek et al., 1994; Björkdahl et al., 2008) and this increase was even more pronounced when comparing the hippocampal region between AD and age-matched controls (Renkawek et al., 1994). In terms of the cellular location of HSPB1, it is generally agreed that HSPB1 is found in reactive astrocytes in AD and these HSPB1 positive reactive astrocytes are more frequently found near to amyloid plaques, although this was not explored using co-localisation analysis (Renkawek et al., 1994; Wilhelmus et al., 2006). The results presented in this chapter confirm the co-localisation of HSPB1 with GFAP positive reactive astrocytes across all Braak severity groups and it is also shown that the number of HSPB1 positive astrocytes was increased in the most severe Braak VI cases. These results are supported by recent transcriptome studies which not only found that HSPB1 is specifically upregulated in astrocytes during AD (Grubman et al., 2019; Smith et al., 2022; Lau et al., 2020), but it was also found that there is an upregulation of HSPB1 in late-stage AD pathology cases compared to cases with early-stage AD pathology (Mathys et al., 2019). It is interesting to note here that although the majority of HSPB1 positive staining co-localised with reactive astrocytes, there were few HSPB1 positive cells that did not co-localised with reactive astrocytes, mostly in the mild Braak II cases. It would be interesting to expand the investigation into these HSPB1 positive cells which did not co-localise with GFAP-positive reactive astrocytes in the mild AD cases as it has been shown before that not all HSPB1 positive cells are reactive astrocytes in mild AD cases (Renkawek et al., 1994). It has been suggested that HSBP1 may be co-localising with another astrocytic subtype, however, this was purely based on astrocyte morphology and no other astrocytic markers were used

(Renkawek et al., 1994). Further to this, HSPB1 has been shown to co-localise with other glial cells such as microglia (Wilhelmus et al., 2006). Additional immunofluorescence analysis could be carried out to stain for microglia using, for example the marker IBA-1, which detects the specific calcium binding protein involved with membrane ruffling and phagocytosis in activated microglia (Jurga et al., 2020), and other astrocytic markers such as the pan-astrocyte marker ALDH1L1 or proliferating astrocytic markers such as PCNA (Escartin et al., 2021).

To further explore the HSPB1 association with reactive astrocytes and AD pathology, quantitative analysis was performed to explore the levels of HSPB1 in those reactive astrocytes near to amyloid plaques, in comparison to those HSPB1 positive astrocytes far from these amyloid plaques. The results show that there is an increase in the levels of HSPB1 in reactive astrocytes proximal to amyloid plaques and further to this, it was found that around 86% of amyloid plaques in the Braak VI cases were also positive for HSPB1. The presence of HSPB1 staining within the amyloid plaques has been seen previously, although mainly reported in the hippocampus and the levels in the literature are much lower than described here (35% senile plaques were HSPB1 positive in *Wihelmus et al., 2006*), perhaps due to the different brain regions explored (Wilhelmus et al., 2006; Ojha et al., 2011). This increase in HSPB1 near to the amyloid plaques has also been replicated in two amyloid mouse models of disease, strongly suggesting that this release to be an active process, rather than a passive leakage due to cell death (Ojha et al., 2011).

To conclude, as there was no clear indication as to where CRYAB is expressed in the human AD brain tissue sections, it was decided that the rest of the thesis would primarily focus on the non-cell autonomous role of astrocytic HSPB1 in AD.

Chapter 4: Investigating the organotypic brain slice cultures as a model to study small heat shock proteins in Alzheimer's Disease

4.1 Introduction

In the previous chapter of this thesis, it was confirmed that HSPB1 is localised in reactive astrocytes in AD and the levels of HSPB1 increase in those reactive astrocyte in close proximately to amyloid plaques. In order to further investigate the potential function of this increased HSPB1 in AD, it is necessary to establish a model in which we are able to identify and monitor HSPB1, along with other cell types such as aforementioned astrocytes, in an environment which replicates some of the pathological changes seen during the human disease.

4.1.1 Organotypic brain slice cultures

Organotypic brain slice cultures allow for the study of the physiological levels of multiple anatomically and functionally connected cell types, such as neurons and glial cells, within one complete system (Staal et al., 2011; del Rio et al., 1991; Croft et al., 2019; Bahr, 1995). For this reason, these slices cultures were chosen for this PhD project as they allow for the investigation of the non-cell autonomous function of astrocytic sHSPs on neurons

4.1.2 Modelling tau pathology using organotypic brain slices cultures

The htau mouse was generated from crossing two existing mouse lines (Andorfer et al., 2003). The 8c mouse expresses all human tau isoforms without producing tau pathology (Duff et al., 2000), whilst the tau KO mouse is generated by disrupting exon one of tau through the insertion of the enhanced green fluorescent protein (EGFP) (Tucker 2001). The resulting htau cross expresses all six

isoforms of human tau but no endogenous mouse tau (Andorfer et al., 2003). These mice develop tau pathology reflective of the early stages of human AD, including tau accumulation in the cell bodies and neuronal dendrites from 3 months with hyperphosphorylated tau developing between 6 and 15 months of age. This pathology is restricted to the neocortex and hippocampus and there is no evidence of behavioural disturbance, further replicating what is found during the early stages of the human disease (Andorfer et al., 2003). Organotypic brain slice cultures prepared from these mice develop abnormal conformational, AD tangle-associated tau after two weeks *in vitro*, demonstrating a robust acceleration of the phenotype normally seen *in vivo* (Duff et al., 2002).

Slices prepared from other tau transgenic mice have been able to recapitulate mechanisms of tau phosphorylation and tau release, but they have yet to establish robust neurofibrillary tau inclusions (Duff et al., 2002; Messing et al., 2013; Croft et al., 2017). *Croft et al., 2019* have recently used the recombinant adeno-associated viruses (rAAVs) to express a variety of different combinations of MAPT mutations within the slices. A pro-aggregatory mutant tau construct was selected based on data from the human embryonic kidney 293T (HEK293T) cell tau seeing model, which was used to test the ability of a number of different MAPT mutations, associated with Parkinsonism linked to chromosome 17 (FTDP-17), to form inclusion. This study found that mutations in P301L and S320F (Rosso et al., 2002) induced significant aggregation (Strang et al., 2018). Moreover, the combination of P301L and S320F mutations demonstrated even more robust tau aggregation in the absence of exogenous tau fibrils (Strang et al., 2018) and so this combination of mutations was used to create a pro-aggregatory P301L/S320F tau AAV construct. Brain slices transduced with AAVs expressing WT tau developed high levels of tau phosphorylation, albeit at a much slower rate and there was no evidence of tau inclusions (Croft et al., 2019), whilst the P301L/S320F tau AAV construct resulted in the formation of Thioflavin-S positive, highly phosphorylated sarkosyl insoluble tau inclusions, with tau accumulation also found in the somatodendritic compartments at 28 DIV, as seen in the human

disease (Uchihara et al., 2001). Further to this, this system was also able to allow for testing of four GSK-3β inhibitors and their potential as tau targeting therapeutics (Croft et al., 2019).

4.1.3 Treating brain slices with cytokines TNFα and IL1α to replicate reactive astrocytes found in neurodegeneration

Activation of immune mediators is critical in the regulation of AD progression, and reactive astrogliosis along with activated microglia are now known to be pathological features of disease (Long and Holtzman, 2019). Neuroinflammation is the result of the release of pro-inflammatory cytokines, chemokines, and reactive oxygen species by immune response cells including microglia and astrocytes in response to insult or injury (Leng and Edison, 2021). The release of these neuroinflammatory factors can lead to synapse loss (Hong et al., 2016) and eventual neuronal cell death (Micheau et al., 2003). During neuroinflammation, the glial cells are also involved in microglia-astrocyte crosstalk. The proportion of activated microglia strongly correlates with the presence of amyloid and tau neuropathology and rate of cognitive decline, as seen in AD (Felsky et al., 2019), and this activated microglia have recently been shown to induce reactive astrocytes *in vivo* (Liddelow et al., 2017). The strongest inducers of these reactive astrocytes were the cytokines interleukin 1 alpha (IL1α), tumour necrosis factor alpha (TNFα) and complement component 1, subcomponent q (C1q). All three of these cytokines are highly expressed by microglia (Zhang et al., 2014). Data from Fangjia Yang in our laboratory has shown that when treating primary mouse astrocytes with two of these cytokines, TNFα and IL1α, the levels of reactive astrocyte markers LCN2 and Serpina3n, and pro-inflammatory cytokine IL-6 are increased (*Figure 4.1*).

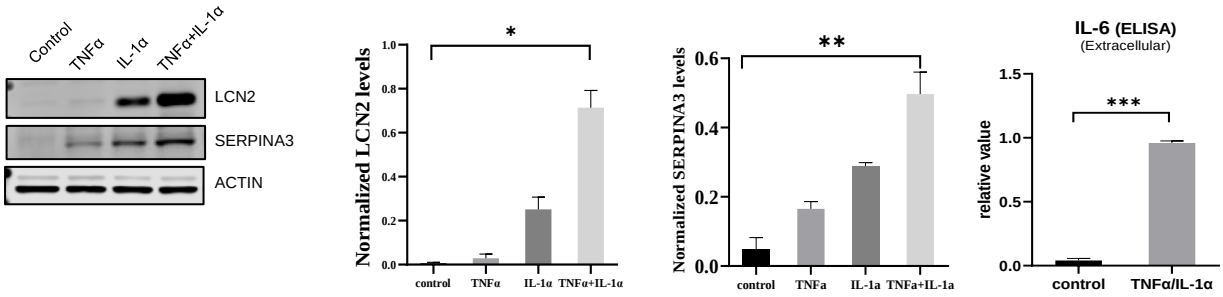

Figure 4.1: Data produced by Fangjia Yang in our laboratory showing immunoblotting analysis to detect reactive astrocyte markers LCN2 and Serpina3n and pro-inflammatory cytokine IL-6 by ELISA in primary mouse astrocytes treated with cytokines TNFα and IL1α for 24rs.

*a) Western blot of LCN2 and Serpina3n in cell lysates. ß-actin was used as the loading control,. b-c) Quantification of LCN2 (b) and Serpina3n (c). N=3 independent primary astrocyte cultures, error bars expressed as SD. *** p < 0.001, **** p < 0.0001. Unpaired one-way ANOVA, with Tukey's test. D) IL-6 level in media detecting by ELISA. N=3 independent primary astrocyte cultures, error bars expressed as SD. *** p < 0.001, t test*

4.1.4 Toxic effects of Aβ oligomers in AD

Different soluble species of amyloid-β (Aβ) are now known to exist in the human brain (McDonald et al., 2015; Brinkmalm et al., 2019; Sehlin et al., 2012; Walsh and Selkoe, 2020). Increasing evidence suggests that it is the oligomeric forms of Aβ which are the most toxic (Yang et al., 2017; Hong et al., 2018; Shankar et al., 2008) and that the insoluble amyloid plaques found in AD are actually protective by acting as a reservoir for larger oligomers to prevent degradation into smaller more toxic oligomers (Koffie et al., 2009; Yang et al., 2017)

The effects of Aβ on astrocytes has been explored using both cellular and animal models. Injecting $A\beta_{1-42}$ oligomers into the rat brain triggered upregulation of IL-1β and TNF-α in reactive astrocytes located in blood vessels, hippocampus and temporal cortex immediately after injection but also 72

hours post-injections and these astrocytes were also positively immunostained for NFκB (Carrero et al., 2012). Treating human astrocytes with recombinant $A\beta_{40}$ oligomers significantly reduced cell viability, increased reactive oxygen species and increased levels of TNFα, IL-6 and IL-1β (Braidy et al., 2019).

4.1.5 The production of Aβ oligomers

Tg2576 mice overexpress human APP (isoform 695) which contains the double Swedish mutation, under the control of the hamster prion protein promoter. These mice exhibit impaired learning and memory by 9 to 10 months, along with cortical and limbic amyloid plaques, reflecting what is seen in the human disease (Hsiao et al., 1996). To produce a treatment which mimicked the Aβ levels found in the human AD brain (Ingelsson et al., 2004), neurons were cultured from the Tg2576 mouse and the media was collected after 14 days in culture (Hudry et al., 2012). The Aβ found in this media is naturally secreted in a 10:1 ration of $A\beta_{40}$:$A\beta_{42}$. The concentration of $A\beta_{40}$ and $A\beta_{42}$ is determined by ELISA and this medium is then diluted to a final concentration of 2nM $A\beta_{40}$/0.2nM $A\beta_{42}$ and is referred to as the TgCM (Wu et al., 2010; DaRocha-Souto et al., 2012; Wu et al., 2012). Recently it was found that treating primary neurons with these physiological levels of Aβ resulted in an increase in LCN2 and the induction of astrocytic inflammatory signalling pathways as demonstrated through the increase in NFκB along with the increase in the release of inflammatory cytokines (Perez-Nievas et al., 2021).

4.2 Aims

The overarching aim for this chapter was to determine whether organotypic brain slice cultures can be used as a model to study sHSPs in the context of AD pathology. In order to investigate this, the specific aims for this chapter are as follows:

1. Determine the cellular localization of HSPB1 in mouse organotypic brain slice cultures, in relation to HSPB1 expression in the human brain
2. Characterize stimuli that increase astrocyte reactivity by mimicking an AD-like brain environment in mouse brain slices. To do this, organotypic brain slices will be treated with cytokines that are known to be released by activated microglia in AD brain, as well as physiologically relevant levels of Aβ oligomers
3. Investigate whether astrocyte reactivity in mouse organotypic slices leads to an increase in the levels of HSPB1
4. Characterize a disease relevant model to study tau pathology in organotypic brain slice cultures, using AAV constructs

4.3 Methods

The materials and methods for this chapter have been described in full in Chapter 2, Section 7. In brief, organotypic brain slice cultures were prepared from WT CD1 mouse pups according to the protocol in *Croft and Noble, 2018*, as detailed in Chapter 1 Section 3.1. To characterise HSPB1 and CRYAB in the slice cultures, slices were fixed after 14 DIV and immunofluorescent staining was performed, as detailed in Chapter 2, Section 9.1, and imaged using the Nikon Eclipse Ti Inverted Spinning Disk Confocal microscope as described in Chapter 2, Section 9.2.

For the TNFα and IL1α treatment of organotypic slices, WT CD1 slices were treated with both 30ng/ml recombinant mouse TNFα and 3ng/ml recombinant mouse IL1α at 21 DIV. After the 24 hour cytokine treatment, slices were either fixed for immunohistochemical analysis or lysed (Chapter 2, Section 3.3) to be separated on a 12% poly-acrylamide gel and further analysed by western blotting (Chapter 2, Section 4.2). The conditioned media was collected for LDH assays (Chapter 2, Section 5.1).

For Aβ oligomer treatment of organotypic brain slices, primary neuronal cultures were kindly prepared by Dr Maria Jimenez Sanchez from the Tg2576 mouse The characterisation of the conditioned media was kindly performed by Dr Beatriz Gomez Perez-Nievas. Slice cultures were first pre-treated in prewarmed neurobasal media containing B27 serum free supplement (NB) media for 24 hours at 21 DIV. This NB media was then discarded and slices were treated with TgCM diluted in NB media or equivalent volumes of WtCM for 24 hours (Chapter 2, Section 3.2). After the 24 hour treatment with the physiologically relevant levels of Aβ, slices were harvested and western blotting analysis was performed. The media was also collected for use in a cell toxicity assay.

In collaboration with Professor Todd Golde, the recombinant adeno-associated virus (rAAV) system was implemented to induce tau pathology in the WT CD1 slices (Croft et al., 2019). rAAVs were provided by C. Croft and T. Golde. These were packaged in capsid stereotype 8 and expressed an EGFP transgene under the control of the hybrid cytomegalovirus enhancer/chicken β-actin (hCBA) promoter. Slice cultures were either transduced with a rAAV construct expressing WT Tau (rAAV2/8-WT-htau-EGFP) or a mutant tau construct expressing two tau mutations that result in a more pro-aggregatory construct (rAAV2/8-P301L/S320F-htau-EGFP). rAAV constructs were added directly into the slice cultures media at 0 DIV, 3 hours after the initial slice preparation at a final titre of $2x10^{10}$ –

$2x10^{11}$ viral genomes (VG) per well. Slices were either fixed for immunofluorescence or harvested for sarkosly extraction of tau after 28 DIV.

4.4 Results

4.4.1 HSPB1 co-localises with GFAP positive reactive astrocytes in organotypic brain slice cultures

In order to explore the non-cell autonomous function of HSPB1 in AD, it was first necessary to confirm whether the organotypic brain slice cultures were a suitable model for the detection of different cell types within one complete system. To determine this, slice cultures underwent an optimised staining protocol adapted from *Gogolla et. al., 2006*. This optimised protocol has been described in full in Chapter 2, Section 9.1, but in brief, the protocol introduced extended incubation times for the slice fixation and permeabilization steps and an overnight incubation at 4 °C was required when applying both primary and secondary antibodies (Chapter 2, Section 9.1).

Immunofluorescence was performed on WT CD1 slices to detect a number of different cell types such as astrocytes, microglia, neurons and the sHSPs CRYAB and HSPB1. To locate neurons within the slices, immunofluorescence was performed using antibodies against MAP2 and Alpha-β Tubulin III (*Figure 4.2*). MAP2 is a microtubule-associated protein (Caceres et al., 1984) and Alpha-β Tubulin III protein expression is restricted to neurons and forms an integral component of microtubules (Sullivan 1986). Astrocytes were visualised in the slice cultures using GFAP and S100B (*Figure 4.2*). GFAP is a marker of glial fibrillary acidic protein (Eng et al., 1971) and S100B is a calcium binding protein mainly concentrated in astrocytes (Michetti et al., 2019). Microglia were also identified in the slice cultures using IBA-1 (*Figure 4.2*), the ionized calcium-binding adaptor molecule 1 staining for microglial, a macrophage-specific calcium binding protein involved with membrane ruffling and

phagocytosis in activated microglia (Jurga et al., 2020). Tau was imaged using a total tau antibody (Dako tau), which detects the C-terminal region containing 4R repeated sequence involved in microtubule binding in the human tau protein (Gibbons et al., 2018). Finally, both the sHSPs of interest, CRYAB and HSPB1 were also detected with the slice culture system (*Figure 4.2*).

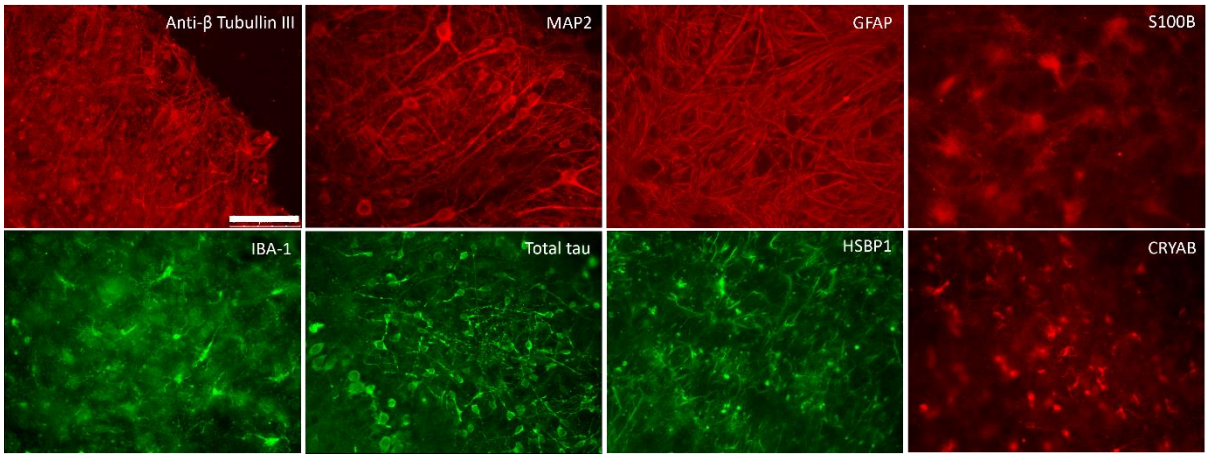

Figure 4.2: Immunofluorescence analysis of 21 DIV organotypic slice cultures with antibodies against neuronal markers (MAP2 and Anti-β Tubullin III), astrocytes (GFAP and S100B), microglia (IBA-1), tau (Dako Tau) and sHSPs CRYAB and HSPB1.

Immunofluorescence was carried out using optimised IF protocol adapted from Gogoll et al., 2006, representative images of n=3 slices, images were taken on Zeiss AxioImager Z1 microscope, scale bar = 75µm

As the human data presented in Chapter 3 of this thesis showed the localisation of HSPB1 within reactive astrocytes in the human AD brain, further dual immunofluorescence was carried out to explore the specific cellular localisation of HSPB1 in organotypic slice cultures. Immunofluorescent analysis of 21 DIV CD1 WT slices was carried out using antibodies against CRYAB and HSPB1 and reactive astrocytes (GFAP). As is reflected in our data in human brain, HSBP1 signal co-localised with GFAP indicating that HSPB1 is expressed in GFAP-positive astrocytes in the organotypic slice cultures

(159A). CRYAB did not co-localise with GFAP positive reactive astrocytes in the slice cultures, also reflecting what was shown in the human data presented in Chapter 3 (*Figure 4.3B).*

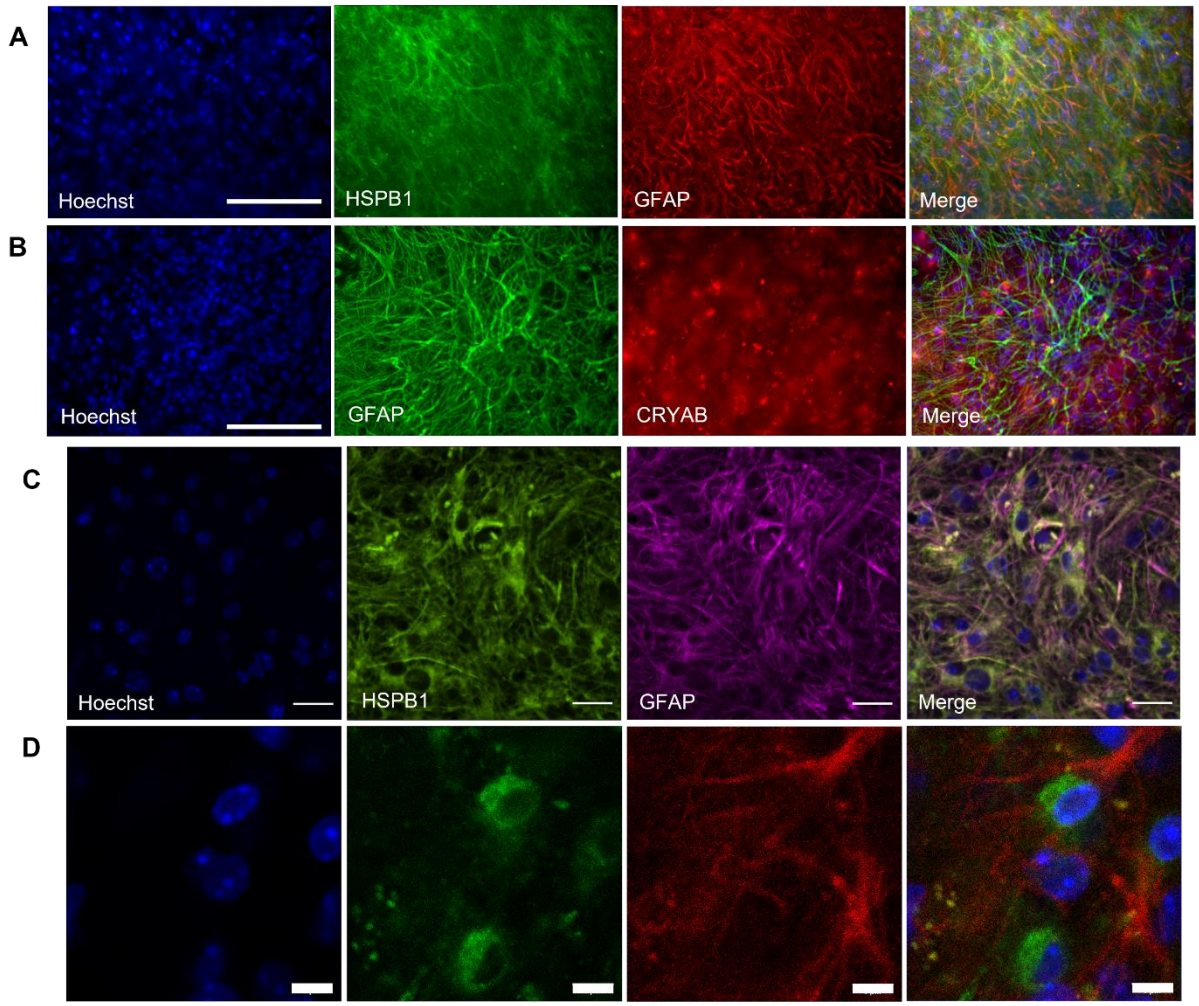

Figure 4.3: Immunofluorescent analysis of 21 DIV organotypic slice using antibodies against sHSP CRYAB and HSPB1 and reactive astrocytes (GFAP).

A) Representative image of three slices, images taken on Zeiss AxioImager Z1 microscope, scale bar = 75 µm, B) Representative image of three slices, images taken on Zeiss AxioImager Z1 microscope, scale bar = 75 µm, C) Higher magnification representative image of three slices, images taken Ti Inverted Spinning Disk Confocal microscope, scale bar = 30µm, D) Higher magnification of representative image of three slices, images taken Ti Inverted Spinning Disk Confocal microscope, scale bar = 6µm

4.4.2 TNFα and IL1α treatment of organotypic brain slice cultures induces reactive astrocytes, resulting in a trend towards an increase in HSPB1

It has been described by *Liddelow et al., 2017*, that in neurodegenerative diseases, astrocytes become reactive in response to LPS and IFN-γ and the release of cytokines TNFα and IL1α. Data generated by Fangjia Yang in the lab also found that treating primary mouse astrocytes with these same cytokines results in the increase in reactive astrocyte markers LCN2 and Serpina3n, in addition to an increase in the pro-inflammatory marker IL-6. To determine whether the levels of HSPB1 change when astrocytes become reactive in the organotypic brain slice cultures, WT CD1 slice cultures underwent a 24 hour TNFα and IL1α treatment at 21 DIV, after which slices were lysed for western blotting analysis.

As our data indicates that HSPB1 expression is restricted to astrocytes in both human brain and in organotypic brain slices, the levels of HSPB1 and reactive astrocyte markers (LCN2 and Serpina3n) were normalized to the levels of total astrocyte protein, detected with ALDH1L. Results indicate a trend towards an increase in LCN2 and HSPB1 (*Figure 4.4A and 4.4D*) in slices treated with TNFα and IL1α compared to the untreated controls. However, there were no differences in the levels of Serpina3n (*Figure 4.4B*) or in the levels of reactive astrocyte marker GFAP (*Figure 4.4C*)

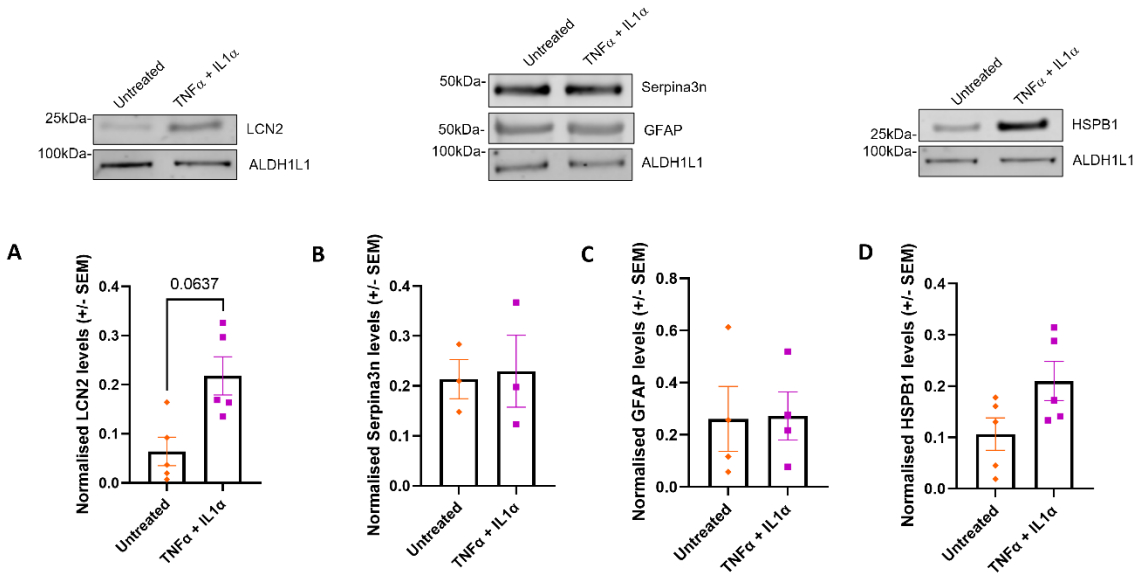

Figure 4.4: Levels of reactive astrocytes (LCN2, Serpina3n and GFAP) and HSPB1, normalised to total astrocyte protein (ALDH1L1) in 21 DIV organotypic brain slices treated for 24 hours with cytokines TNFα and IL1α

A) Representative western blot using antibodies against reactive astrocyte marker LCN2 and total astrocyte marker ALDH1L1, graph shows mean +/- SEM across 5 biological repeats, paired t-test. B) Representative western blot using antibodies against reactive astrocyte markers Serpina3n and GFAP and total astrocyte marker ALDH1L1, graph shows mean +/- SEM across 3 biological repeats paired t-test. C) Quantification of levels of GFAP normalised to ALDH1L1, graph shows mean +/- SEM across 4 biological repeats, paired t-test D) Representative western blot using antibodies for HSPB1 and total astrocyte marker ALDH1L1, graph shows mean +/- SEM across 5 biological repeats, paired t-test

As the levels of reactive astrocyte marker GFAP did not change with treatment when normalised to ALDH1L1, we also used GFAP as a loading control for total astrocyte protein. Reactive astrocyte markers LCN2 and Serpina3n and HSPB1 levels were normalised to GFAP levels during western blotting quantification. Analysis revealed a significant increase in both LCN2 and Serpina3n in the GFAP positive astrocytes in those slices treated with TNFα and IL1α, compared to the untreated slices (*Figure 4.5A and 4.5B*). Further to this, there was a trend towards an increase in HSPB1 levels in GFAP positive astrocytes in those slices treated with TNFα and IL1α compared to controls (*Figure*

4.5C). These results reflect what was shown in the human data presented in Chapter 3, where there was an increase in HSPB1 in those reactive astrocytes found specifically in AD cases near to amyloid plaques.

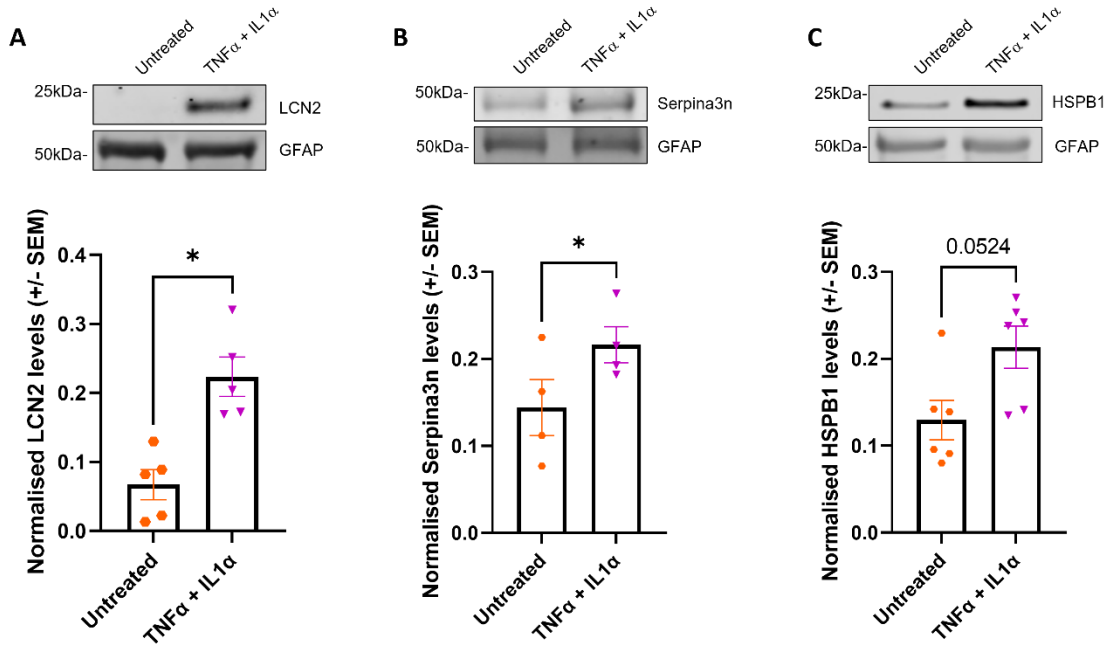

Figure 4.5: Levels of reactive astrocytes (LCN2 and Serpina3n) and HSPB1, normalised to GFAP levels, in 21 DIV organotypic brain slices treated for 24 hours with cytokines TNFα and IL1α.

*A) Representative western blot using antibodies against reactive astrocyte marker LCN2 and GFAP, graph shows mean +/- SEM across 5 biological repeats, paired t-test, *P<0.05, B) Representative western blot using antibodies against reactive astrocyte marker Serpina3n and GFAP, graph shows mean +/- SEM across 4 biological repeats, paired t-test, *P<0.05, C) Representative western blot using antibodies for HSPB1 and GFAP, graph shows mean +/- SEM across 6 biological repeats paired t-test*

As CRYAB is not observed in astrocytes, changes in CRYAB were determined by normalizing CRYAB protein levels to total protein levels using the loading control β-Actin. Treatment of organotypic brain slice cultures with TNFα and IL1α resulted in an increase in the level of reactive astrocyte marker LCN2 relative to β-Actin as a loading control, compared to untreated slices (*Figure 4.6A*), however, there were no significant changes in the levels of other reactive astrocyte markers Serpina3n or GFAP (*Figure 4.6B and 4.6C)*.

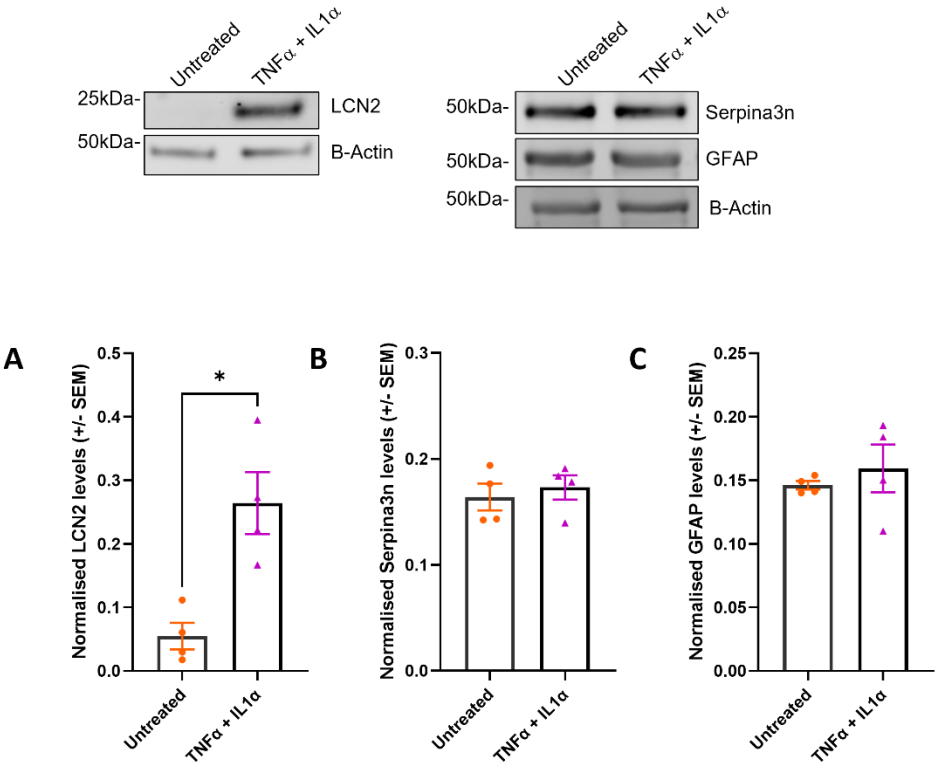

Figure 4.6: Levels of reactive astrocytes (LCN2, Serpina3n and GFAP) normalised to total protein (β-Actin) in 21 DIV organotypic brain slices treated for 24 hours with cytokines TNFα and IL1α.

*A) Representative western blot using antibodies against reactive astrocyte marker LCN2 and loading control β-Actin, graph shows mean +/- SEM across 4 biological repeats, paired t-test, *P<0.05, B) Representative western blot using antibodies against reactive astrocyte markers Serpina3n and GFAP and loading control β-Actin, graph shows mean +/- SEM across 5 biological repeats paired t-test, C) Graph shows mean +/- SEM across 5 biological repeats, paired t-test*

Western blot analysis showed a slight increase in the levels in HSPB1 in those slices treated with cytokines (*Figure 4.7A*). However, due to variability between different experimental repeats, the increase seen in *Figure 4.7A* rendered no significant differences in the levels of HSPB1 in those slices treated with cytokines, when compared to the untreated control slices (*Figure 4.7A*). Similarly, there was also no significant changes in the quantified levels of CRYAB in slices treated with TNFα and IL1α compared to untreated slices (*Figure 4.7A*).

Qualitative immunofluorescence image analysis showed that in both the untreated and cytokine treated slices, HSPB1 co-localised with GFAP positive astrocytes, mainly along the astrocytic processes (*Figure 4.7B*). CRYAB was found mainly around the nucleus and it did not co-localise with the GFAP positive astrocytic processes found in either the untreated or with TNFα and IL1α treated slices (*Figure 4.7C*). Quantification is required to confirm whether the increase in HSPB1 in the TNFα and IL1α treated slices is increased in reactive astrocytes, as suggested by western blotting analysis of the whole slice lysates.

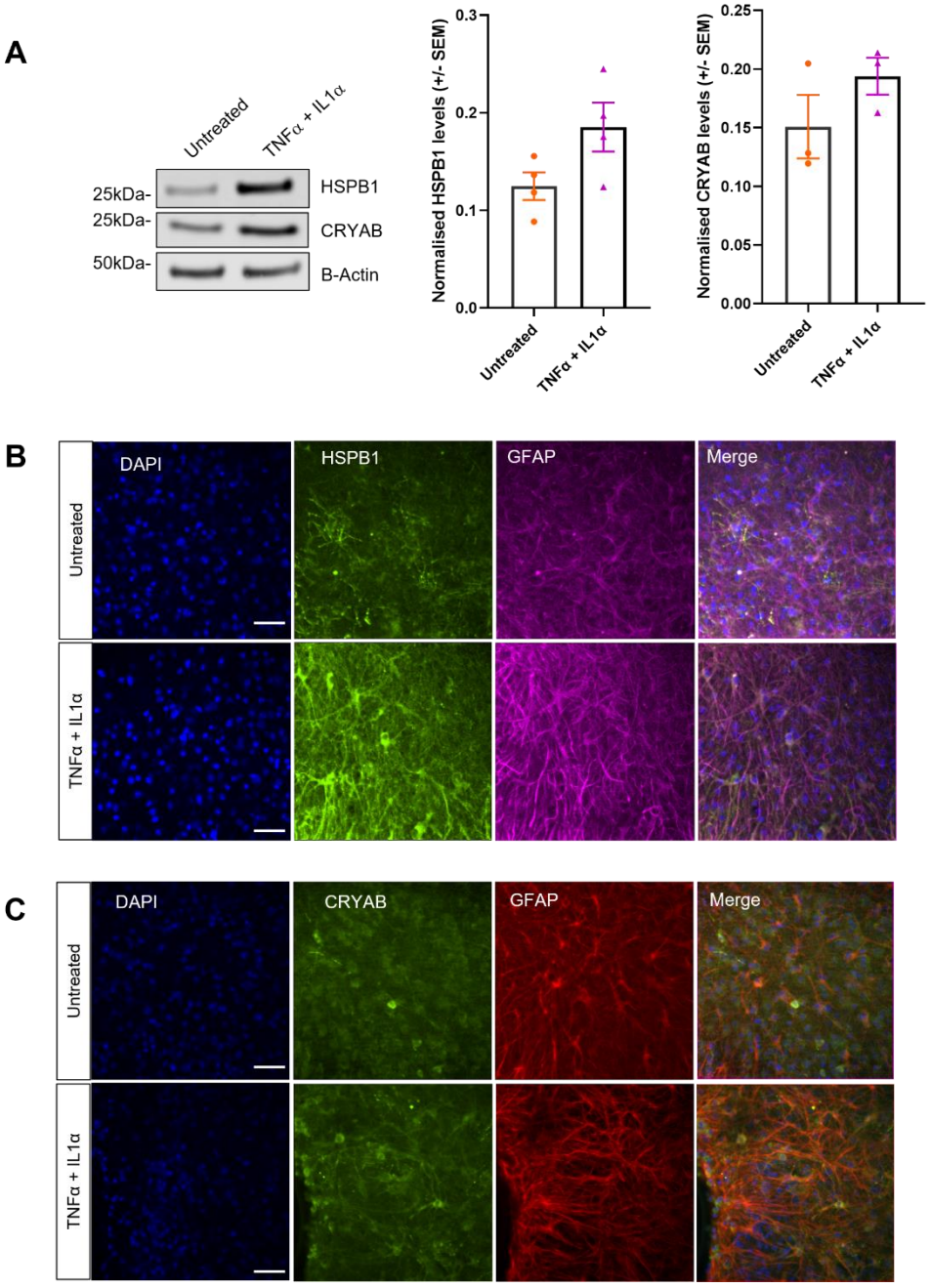

Figure 4.7: Levels of sHSPs HSPB1 and CRYAB, normalised to total protein (β-Actin) in 21 DIV organotypic brain slices treated for 24 hours with cytokines TNFα and IL1α.

A) Representative western blot using antibodies against reactive HSPB1, CRYAB and loading control β-Actin, graph shows mean +/- SEM across 4 biological repeats, paired t-test, B) Representative image of immunofluorescent analysis using antibodies against HSPB1 and reactive astrocytes (GFAP) in untreated slices and TNFα and IL1 treated slices, n=3, imaged on Nikon Eclipse Ti Inverted Spinning Disk Confocal microscope, scale bar = 50µm C) Representative image of immunofluorescent analysis of CRYAB and reactive astrocytes (GFAP) in untreated slices and TNFα and IL1 treated slices, n=3, imaged on Nikon Eclipse Ti Inverted Spinning Disk Confocal microscope, scale bar = 50µm

4.4.3 Treating organotypic slice cultures with physiologically relevant levels of Aβ oligomers does not alter the levels of HSPB1

Further treatments were performed using AD-relevant pathology, to investigate whether this would induce reactive astrocytes and whether this in turn would impact sHSPs levels within the slice cultures. In collaboration with Dr Beatriz Gomez Perez-Nievas, culture media was obtained and characterised from Tg2576 primary neurons. These neurons secreted at a physiologically relevant ratio of $A\beta_{40}$ and $A\beta_{42}$ into the media, known as TgCM. Wild-type neurons are also cultured from littermates and this media is collected as a control (WtCM). The slice cultures were then treated with 2nM Aβ40/0.2nM Aβ42 TgCM and equivalent volumes of WtCM at 21 DIV for 24 hours.

As was done with those slices treated with cytokines, the levels of protein in the slices treated with either TgCM or WtCM were first normalised the levels of GFAP by western blotting analysis. In those slices treated with TgCM, there was a trend towards an increase in the reactive astrocyte marker LCN2 compared to those slices treated with WtCM (*Figure 4.8A*). There were no significant differences in the levels of Serpina3n or HSPB1 between those slices treated with either WtCM or TgCM (*Figure 4.8B and 4.8C*),.

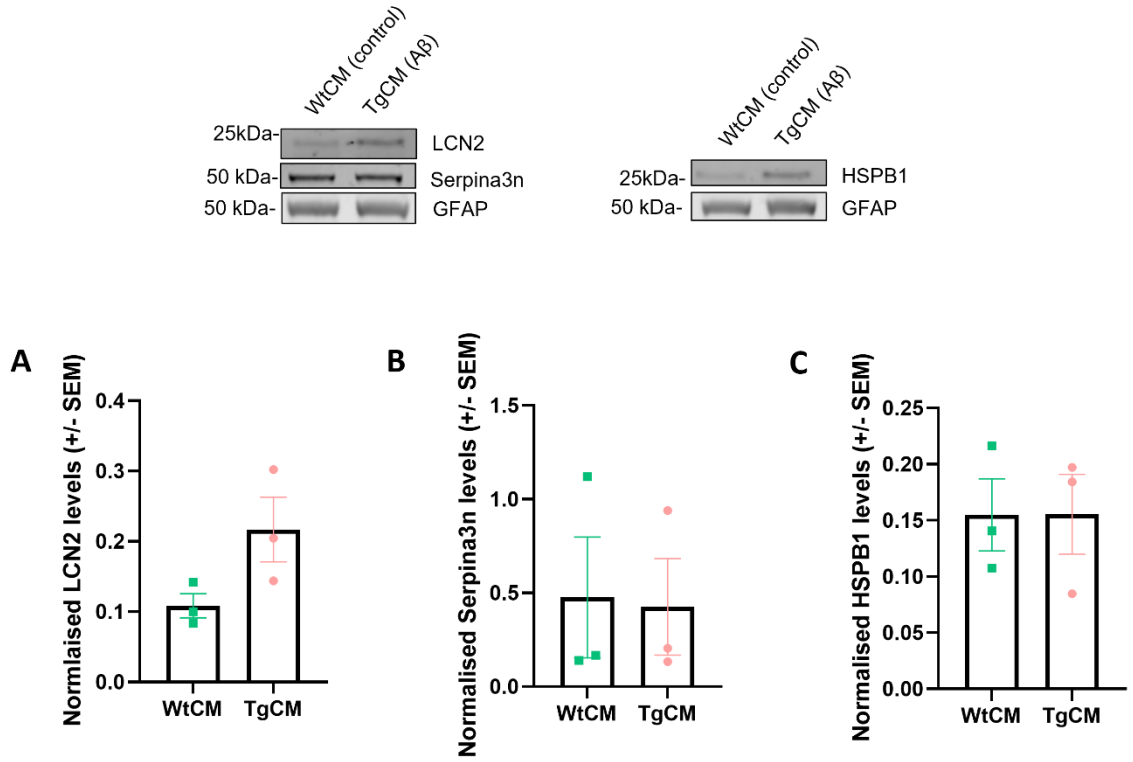

Figure 4.8: Levels of reactive astrocytes (LCN2 and Serpina3n) and HSPB1, normalised to GFAP levels in 21 DIV organotypic brain slices treated with wild-type conditioned media (WtCM) or Tg conditioned media (TgCM) for 24 hours.

Representative western blots showing antibodies against reactive astrocyte markers LCN2, Serpina3 and GFAP and HSPB1, A) Quantification of the levels of LCN2 normalised to GFAP, graph shows mean +/- SEM across 3 biological repeats, paired t-test B) Quantification of the levels of Serpina3n normalised to GFAP, graph shows mean +/- SEM across 3 biological repeats, paired t-test C) Quantification of the levels of HSPB1 normalised to GFAP, graph shows mean +/- SEM across 3 biological repeats, paired t-test

When normalising protein levels to the loading control β-Actin, western blot analysis indicated a similar trend towards an increase in LCN2 levels in those slices treated with TgCM compared to WtCM treated slices (*Figure 4.9A*). However, there was no significant difference in Serpina3n levels between WtCM and TgCM treated slices (*Figure 4.9B*). Further to this, there were no significant differences in the level of HSPB1 in those slices treated with WtCM and TgCM (*Figure 4.9D*),

however there did seemed to be a trend towards an increase in CRYAB in the TgCM treated slices (*Figure 4.9C*).

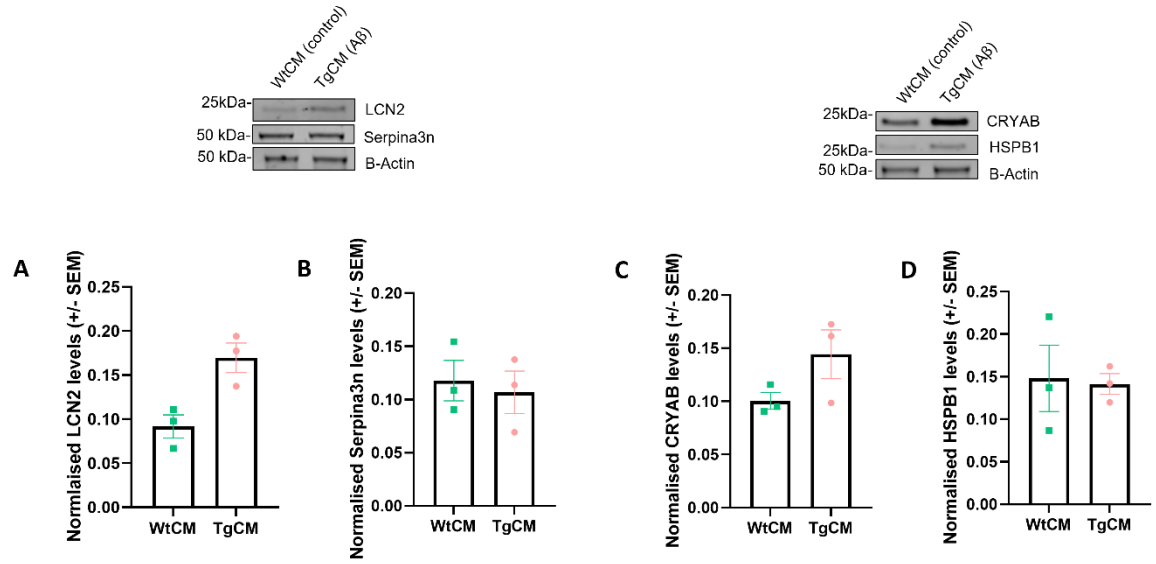

Figure 4.9: Levels of reactive astrocytes (LCN2 and Serpina3n) and sHSPs CRYAB and HSPB1, normalised to total protein (β-Actin), in 21 DIV organotypic brain slices treated for 24 hours with wild-type conditioned media (WtCM) or Tg conditioned media (TgCM).

Representative western blots showing antibodies against reactive astrocyte markers LCN2 and Serpina3 and sHSPs CRYAB and HSPB1, A) Quantification of the levels of LCN2 normalised to loading control β-Actin, graph shows mean +/- SEM across 3 biological repeats, paired t-test, B) Quantification of the levels of Serpina3n normalised to loading control β-Actin, graph shows mean +/- SEM across 3 biological repeats, paired t-test, C) Quantification of the levels of CRYAB normalised to loading control β-Actin, graph shows mean +/- SEM across 3 biological repeats, paired t-test D) Quantification of the levels of HSPB1 normalised to loading control β-Actin, graph shows mean +/- SEM across 3 biological repeats, paired t-test

4.4.4 Transduction of the organotypic brain slice cultures with mutant P301L/S320F-htau-EGFP AAV induces tau aggregation

Characterisation of organotypic brain slices prepared from htau mouse pups

To establish a model of tau pathology within the organotypic brain slice cultures, slices were initially prepared from the htau mouse model of AD (Andorfer et al., 2003; Duff et al., 2002). Slice cultures were prepared from the htau mice and age-matched C657BL/6 mice as controls and left in culture for up to 42 DIV. After 14DIV, slices were collected every 2 weeks for western blot and immunofluorescence analysis. Preliminary data showed an increase in total tau in those htau slices at 42 DIV compared to the age-matched C57BL/6 control mice (*Figure 4.10A*). Monitoring of the tau pathology across the ageing htau slices determined the presence of tau phosphorylated at Ser396/404, as detected by PHF-1, only after 42 DIV, but not at 28 DIV (*Figure 4.10B*). It was also shown that tau was detected within the htau slice cultures at 42 DIV, using an antibody against total tau (*Figure 4.10C*). As EGFP is inserted within exon 1 of the MAPT gene in these mice, mouse tau is not expressed and so the tau visualised by immunofluorescence represents human tau only. Preliminary observations suggested that the htau slice cultures were able to replicate some AD-relevant features of tau pathology, such as the presence of both human tau and phosphorylated tau, as detected by total tau immunofluorescence and PHF-1 by western blotting, respectively. Tau was found to accumulate in the cell bodies and age-related phosphorylated tau only occurred at a later stage, both reflective of what is seen in the early stages of human AD (Andofer et al., 2003). However, due to problems with the breeding of the mouse colony and additional time constraints due to COVID-19, it was decided a different model was required to replicate tau pathology in the organotypic brain slice cultures.

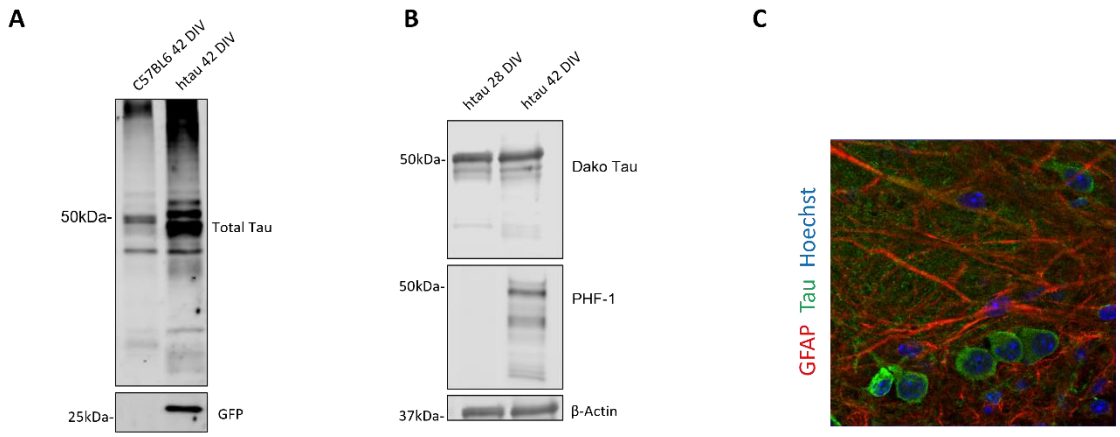

Figure 4.10: Preliminary data from the initial immunoblotting and immunofluorescent characterisation of tau pathology in 28 and 42 DIV organotypic brain slice cultures prepared from the htau mouse.

A) Representative blot using antibodies against total tau and GFP in 42 DIV C57BL/6 slices and 42 DIV htau slices, n=1, B) Representative blot using antibodies against total tau (Dakot Tau), tau phosphorylated at Ser396/404 (PHF-1) and loading control β-Actin in htau slices at 28 DIV and 42 DIV, n=1, C) Preliminary immunofluorescent analysis using antibody against total tau (Dako Tau), reactive astrocytes (GFAP) and nuclei (Hoechst) in 42 DIV htau slice, n=1 slice, imaged on Nikon Confocal Spinning Disk

Transduction of organotypic brain slice cultures using tau AAVs

In order to replicate tau pathology in the organotypic brain slice cultures, WT CD1 slices were transduced at 0 DIV with either WT tau (AAV2/TM8-WT-htau0N4R-EGFP) or mutant tau AAV (AAV2/TM8-P301L/S320F-htau0N4R-EGFP) constructs. A final titre of $1x10^{11}$ was added per well (each containing 3 slices) and slices were collected at 28 DIV for sarkosyl extraction of tau or immunofluorescent analysis. Sarkosyl extraction is a standard protocol used to determine the levels of insoluble tau in the brain (Greenberg and Davies, 1990). This protocol consists of sequential extraction in the ionic detergent N-lauryl-sarcosine (sarkosyl), which solubilizes the non-aggregated tau, while allowing the enrichment of aggregated hyperphosphorylated tau in the sarkosyl insoluble (SI) fractions (Ren and Sahara, 2013). In brief, slices were lysed, incubated with sarkosyl and then

subjected to differential centrifugation followed by western blot analysis of these fractions. Sarkosyl extraction of tau results in a number of fractions which included the low speed supernatant (LSS) fractions which contains both sarkosyl soluble and insoluble fractions, or total tau, and the sarkosyl insoluble tau fraction which consists of hyperphosphorylated tau which is biochemically comparable to NFT found in tauopathies (Li et al., 2015). Due to additional time constraints, the characterisation of tau AAVs in the organotypic brain slice cultures was done in collaboration with Dr Diana Flores Dominguez and Emily Groves.

Initial characterisation studies were performed in slices transduced with both WT tau and P301L/S320F tau AAVs at a recommended viral titre of $2x10^{10}$ VG/well, and slices were analysed at 14, 21 and 28 DIV. The experiments using this viral load concluded that transduction with this level of virus was too low to induce robust overall or phosphorylated tau pathology, even at the latest timepoint of 28 DIV. All sarkosyl extracted tau fractions were analysed by western blotting and there was no protein detected in the sarkosyl insoluble fractions in the slices treated with either WT tau or P301L/S320F tau at 28DIV (data not shown). Qualitative immunofluorescence analysis confirmed low levels of GFP-tagged tau in slices transduced with either WT tau or P301L/S320F tau at $2x10^{10}$ VG/well after 28 DIV (*Figure 4.11.*). Slices transduced with either tau-AAV at 5 times the initial titre $1x10^{11}$ after 28 DIV showed detectable levels of GFP-tagged tau (*Figure 4.11*) and so this was the titre that was subsequently used in the following experiments.

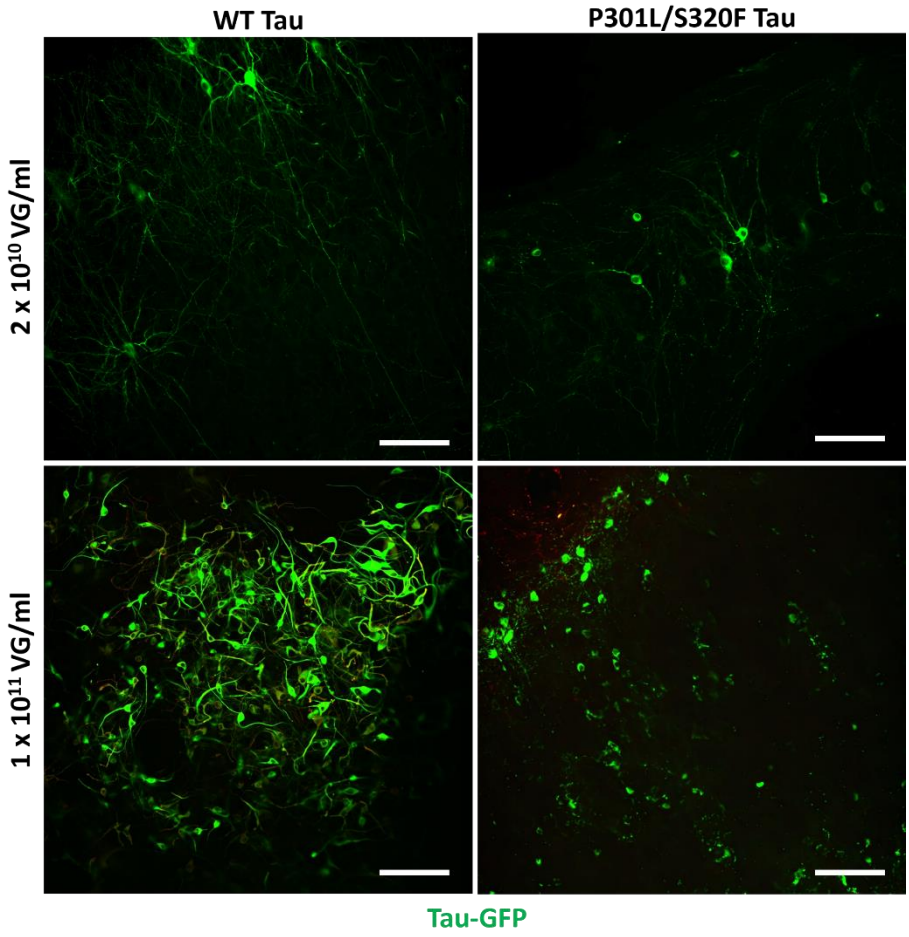

Figure 4.11: Preliminary immunofluorescent analysis GFP tagged tau pathology in slices transduced either WT Tau or P301L/S320F Tau AAVs at 2x10^10 (1x concentration) or 1x10^11 (5x concentration) viral genomes/ml on 0 DIV and collected at 28 DIV.

In collaboration with Dr Diana Flores Dominguez, slices (n=3) were fixed at 28 DIV and imaged on Nikon Confocal Spinning Disk, GFP-tau represents total tau levels, imaged on Nikon Confocal Spinning Disk, scale bar = 50µm

Follow-up studies found that there was more phosphorylated tau accumulation around the somatodendritic compartments, as detected by immunofluorescence with PHF1 antibody, at 35 DIV compared to 28 DIV (*Figure 4.12A*). However, when the sarkosyl extraction of tau fractions at 28 DIV and 35 DIV were analysed by western blotting, it was determined that accumulation of sarkosyl insoluble tau was lost after 28 DIV (*Figure 4.12B*), speculated as being due to an increase in cell death at 35 DIV, however this was not formally assessed. Therefore these characterisation studies confirmed the optimal conditions for slice tau-AAV transduction were: 1) viral titre of five times the original titre at $1x10^{11}$ and, 2) slices to be harvested at 28 DIV.

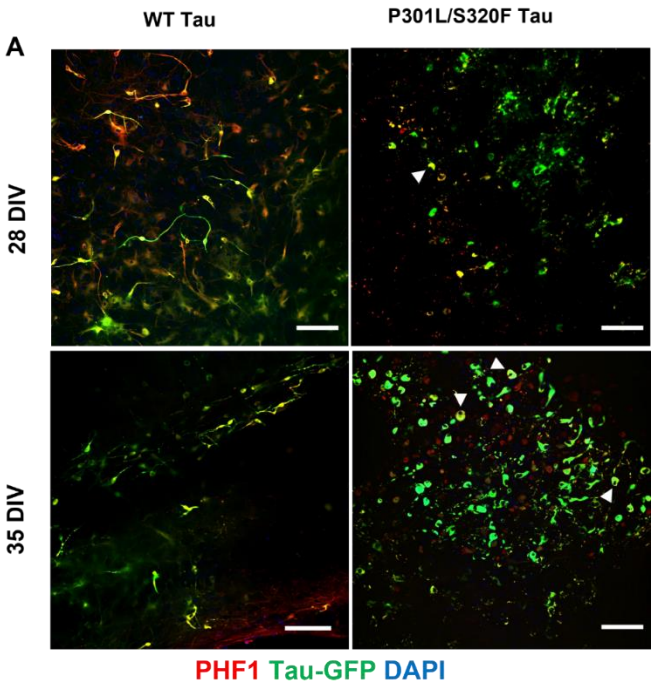

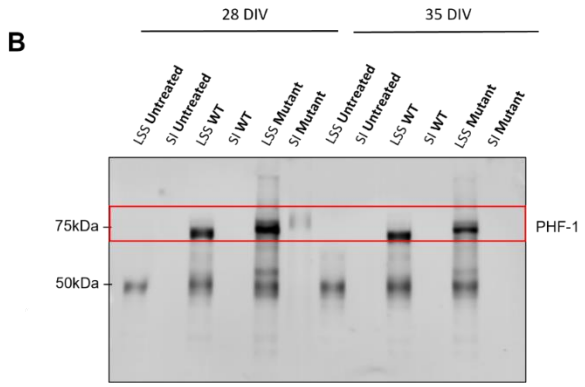

Figure 4.12: Initial immunofluorescent and immunoblotting characterisation experiments with organotypic brain slice cultures transduced with either WT Tau or P301L/S320F Tau at 1x10^11 viral genomes/ml on 0 DIV and collected at either 28 or 35 DIV.

A) In collaboration with Dr Diana Flores Dominguez, slices were fixed at 28 and 35 DIV and immunostained for phosphorylated tau at Ser396/404 (PHF-1), GFP-tau represents total tau levels, arrowhead highlight examples of phosphorylated tau accumulating in the somatodendritic compartments in those slices transduced with mutant P301L/S320F tau AAV, imaged on Nikon Confocal Spinning Disk, scale bar = 50µm, B) Sarkosyl insoluble tau fractions and the low-speed (soluble tau) supernatant (LSS) and sarkosyl insoluble tau pellets (SI) were analysed by western blotting for total tau and phosphorylated tau at Ser396/404 (PHF-1). The red box highlights the presence of hyperphosphorylated tau in the SI fraction of the mutant tau transduced only at 28 DIV and not at 35DIV, representative western blot shown of n=3

In slices transduced with both the WT tau and pro-aggregant mutant tau AAVs, the soluble total and phosphorylated tau are detected in the low speed supernatant fractions, as detected by the total tau antibody and PHF-1 (tau phosphorylated at Ser396/404) antibodies respectively (*Figure 4.13A*). When the levels of PHF-1 phosphorylated tau were quantified as a proportion of total tau, there was a significant increase in PHF-1 relative to total tau levels in the soluble fraction in those slices transduced with the mutant tau AAV compared to WT Tau transduced slices (*Figure 4.13B*).

Further to this, transduction with the double P301L/S320F tau mutation AAV resulted in the accumulation of sarkosyl insoluble hyperphosphorylated tau which was not present in the slices transduced with the WT tau construct (*Figure 4.13A*). When immunofluorescence was performed using an antibody against tau phosphorylated at Ser396/404 (PHF-1), WT tau expression resulted in the expression of GFP-tagged WT-tau and phosphorylated tau mainly in the axons of the neurons (*Figure 4.13C*), but in the mutant tau transduced slices, the accumulation of P301L/S320F GFP-tagged tau and phosphorylated tau (PHF-1) seemed to be restricted to the somatodendritic compartments of the neurons (*Figure 4.13C*).

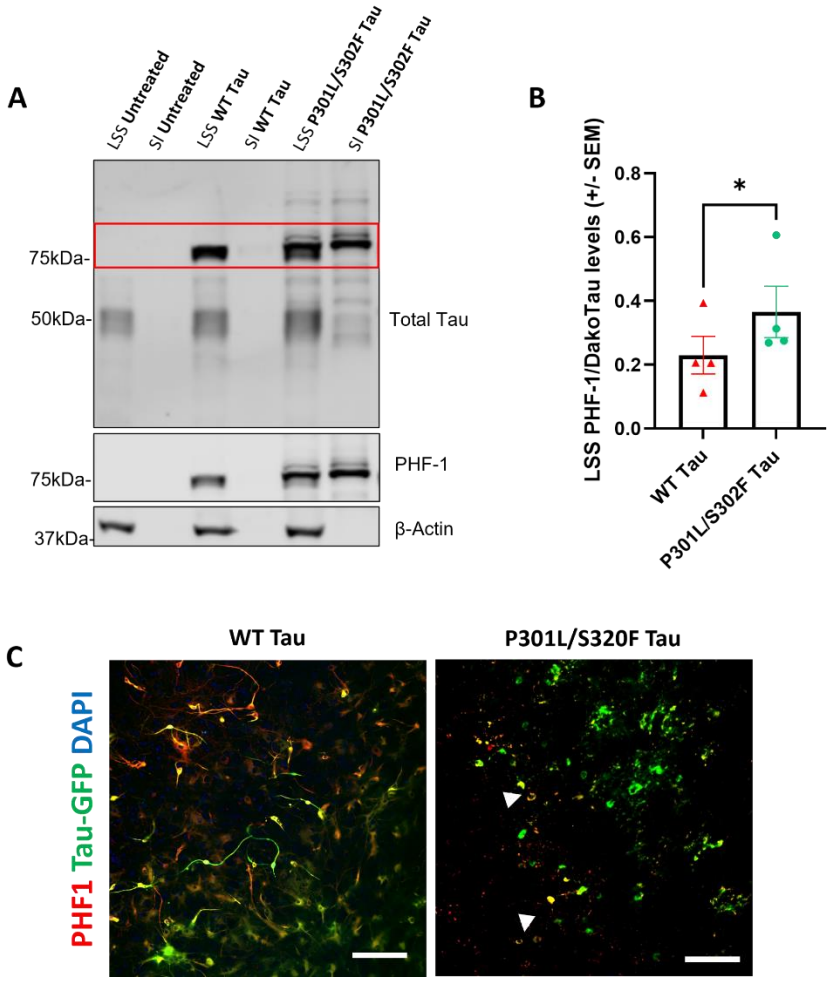

Figure 4.13: Immunofluorescent and immunoblotting characterisation of tau pathology in slices transduced with either WT Tau or P301L/S320F Tau AAVs at 1x10^11 viral genomes/ml on 0 DIV, collected and lysed at 28 DIV.

A) Sarkosyl insoluble tau fractions (SI) and soluble tau fractions in the low-speed supernatant (LSS) were analysed by western blotting and probed for total tau, phosphorylated tau at Ser396/404 (PHF-1) and a loading control (β-Actin). The red box highlights the bands that correspond to human tau tagged with GFP (around 75 KDa), while endogenous mouse tau can be detected at a molecular weight around 55 KDa. Representative western blot shown here of n=4. B) The levels of phosphorylated tau (PHF-1) in the LSS soluble fraction were quantified as a proportion of total tau. Graph shows mean +/- SEM of 4 animals, paired t-test (P>0.05). C) In collaboration with Dr Diana Flores Dominguez, slices were fixed at 28 DIV, for immunofluorescent analysis using a PHF- to detect tau phosphorylation at Ser396/404, GFP-tau represents total tau, arrowhead highlight the examples of phosphorylated tau accumulating in the somatodendritic compartments in those slices transduced with mutant tau AAV, imaged on Nikon Confocal Spinning Disk, scale bar = 50µm*

4.4.5 Treatment with cytokines TNFα and IL1α, Aβ oligomers or tau-AAVs does not cause cell toxicity in organotypic brain slices cultures

To rule out the possibility that changes to reactive astrocyte markers and sHSPs were due to cell toxicity as a consequence of treatments, the LDH assay was carried out to measure cell death. The LDH assay quantitatively measures lactate dehydrogenase (LDH), a stable cytosolic enzyme which is released upon cell death (Decker and Lohmann-Matthes, 1988). During the assay, the LDH released by the lysed cell converts a tetrazolium salt into a red formazan product. The amount of colour formed is directly proportional to the volume of released LDH and this is measured using visible wavelength absorbance data collected by a standard plate reader. The LDH assay was performed on the conditioned media collected from the slices after the 24 hours treatment with TNFα and IL1α or with Tg conditioned media treatment, or collected after the slices had been transduced with tau AAVs for 28 DIV. LDH assay was performed using neurobasal (NB) media rather than slice culture media as the phenol red in the slice culture media interferes with the absorbance reading of LDH. The LDH levels in the media were measured relative to the total LDH levels detected in the slice lysates.

No significant difference in cell death was observed between untreated slices and those slices treated with TNFα and IL1α for 24 hours (*Figure 4.14A*). LDH assays also confirmed that treatment with either Wt or Tg conditioned media for 24 hours was not toxic to the slice cultures (*Figure 4.14B*). Finally, data from one (two technical replicates) biological replicate shows there were no significant differences in cell toxicity in slices either transduced with the WT Tau or P301L/320F tau AAV constructs for 28 days (*Figure 4.14C*).

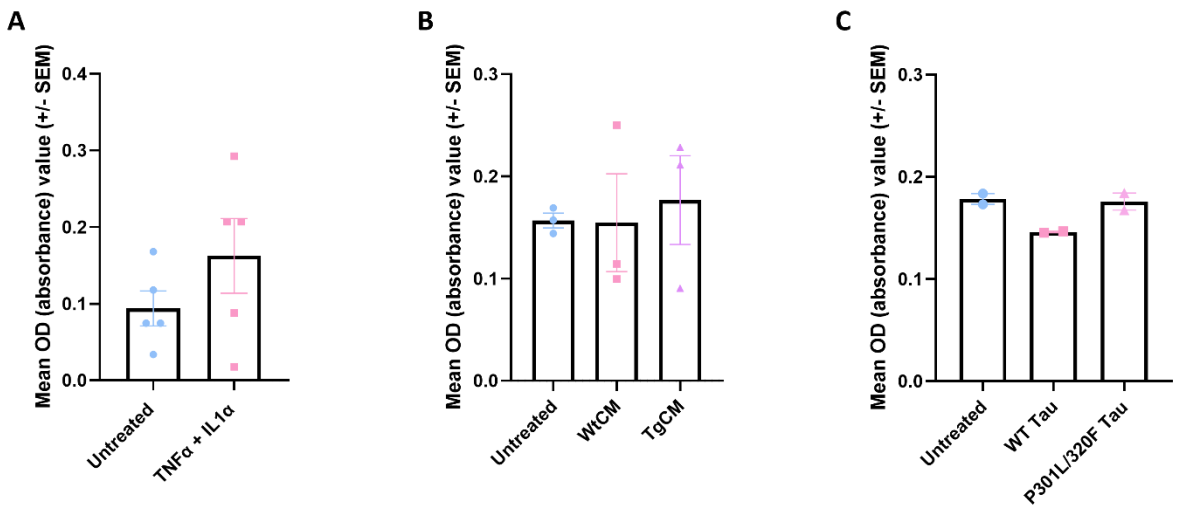

Figure 4.14: Cell toxicity measures in 21 DIV slices treated with cytokines TNFα and IL1α for 24 hours, 21 DIV slices treated with Ab oligomers for 24 hours or slices transduced with either WT tau or P301L/S320F tau at 1x10^11 viral genomes/ml on 0 DIV and collected at 28 DIV, all OD values in conditioned media were normalised to OD values in the slice lysates

A) LDH assay was performed in conditioned media and total protein lysates of untreated slices and slices treated with TNFα and IL1α for 24 hours, graph shows mean +/- SEM taken from 5 biological replicates. B) LDH assay was performed in conditioned media and total protein lysates of untreated slices and slices treated with either WT conditioned media (WtCM) or Aβ conditioned media (TgCM) for 24 hours, graph shows +/- SEM of 3 different biological repeats, C) LDH assay was performed in conditioned media and total protein lysates of untreated slices and slices transduced with either WT tau or P301L/S320F tau at 0 DIV and collected at 28 DIV, graph shows mean +/- SEM taken from 2 technical replicates (1 biological replicate)

4.5 Discussion

The central aim of this chapter was to determine whether organotypic brain slice cultures can be used as a tool to investigate sHSPs in the context of AD. To address this, slice cultures underwent 24 hour treatments with AD-relevant cytokines and physiologically relevant levels of Aβ oligomers in order to replicate the response seen in the human disease and explore the impact of these changes on the levels of the sHSPs CRYAB and HSPB1. Further to this, we used recombinant adeno-associated viruses (rAAV) to express disease variants of tau in organotypic brain slice cultures, using AAV constructs expressing either WT and P30L1/S320F tau, in order to replicate the aggregated tau seen in AD.

Upon examining the localisation of CRYAB and HSPB1 in the slice culture model, results indicated the co-localisation of HSBP1 with GFAP positive reactive astrocytes, reflecting what was concluded in the human data presented in Chapter 3 of this thesis. Further to this, the localisation of CRYAB was not associated with GFAP positive reactive astrocytes, also seen in the results outlined in Chapter 3, where the majority of CRYAB positive cells were co-localised with oligodendrocytes. Treating the organotypic brain slice cultures with cytokines TNFα and IL1α increased the levels of the reactive astrocyte markers LCN2 and Serpina3n and there was a trend towards an increase in the levels of HSPB1 within these astrocytes. Treatment of mouse brain slices with Aβ oligomers resulted in a trend towards an increase in reactive astrocyte maker LCN2 but did not significantly induce reactive astrocytes, and there were no significant changes in the levels of HSPB1 or CRYAB. Finally, transducing the slice cultures with the P30L1/S320F tau construct led to the production of hyperphosphorylated tau which was not present in the slices transduced with the WT tau AAV. Further to this, the phosphorylated tau found in the P30L1/S320F tau transduced slices was restricted to the somatodendritic compartments, replicating what has been found in the literature (Croft et al., 2019). Overall, these results together suggest that the organotypic brain slice cultures

are a good model for replicating some of the pathological changes seen in human AD and these slices could provide a useful toolkit for the study of sHSPs in the context of AD.

4.5.1 Characterisation of sHSPs in mouse organotypic brain slice cultures

Different studies have reported different localisation of CRYAB within the human brain, and in particular in AD brain (Renkawek and Voorter, 1994; Shinohara et al., 1993; Mao et al., 2001; Kato et al., 1992), reflecting the results presented in the human data found in Chapter 3, Section 3.4.2. of this thesis. It was concluded that the majority of CRYAB positive cells co-localised with the oligodendrocyte marker, CAII, however it was not confirmed what the remainder of the CRYAB positive cells were co-localising with. In the organotypic brain slice cultures, CRYAB was not seen to co-localise with any GFAP positive reactive astrocytes, replicating what was found in the human data and further investigation is required to confirm which cell type or types CRYAB is co-localising with in mouse brain slice cultures.

In contrast to this, in the human brain HSPB1 has conclusively been shown to increase in reactive astrocytes during AD (Renkawek et al., 1994; Wilhelmus et al., 2006). This was also corroborated in Chapter 3, Section 3.4.3 of this thesis, where there was clear co-localisation between HSPB1 and GFAP positive reactive astrocytes in brain tissue section taken from cases of varying AD severities. The results in this chapter indicate the same co-localisation of HSBP1 with GFAP positive reactive astrocytes within the organotypic brain slice cultures, reflecting what is seen in the human condition and therefore supporting the use of the slices as a potential physiologically relevant model to study HSPB1.

4.5.2 Using the organotypic brain slice cultures as a model to study sHSPs in the context of AD

In the study carried out by *Liddelow et al., 2017*, it was shown that the release of cytokines TNFα and IL1α from activated microglia was able to induce reactive astrocytes during neurodegeneration. Further to this, data from Fangjia Yang in the lab confirmed the increase in reactive astrocyte markers in primary mouse astrocyte cultures treated with TNFα and IL1α (*Figure 4.1*). It has also been found that of all the GFAP positive astrocytes found in the human AD brain, 60% of these reactive astrocytes mimic the same astrocyte phenotype which is induced by microglial cytokines TNFα and IL1α (Liddelow et al., 2017). The results in Chapter 3, Section 3.4.3 of this thesis confirmed there was an increase in HSPB1 in those reactive astrocytes found in the human AD brain. As the majority (60%) of these astrocytes have been found to react to TNFα and IL1α, it was assumed there would be an induction in reactive astrocytes and therefore an increase in HSPB1 in the slices culture model treated with the same TNFα and IL1α cytokine treatment.

To measure the levels of reactive astrocytes in treated slices, GFAP, LCN2 and Serpina3n were chosen. GFAP (Eng et al., 1971), is the most widely used marker of reactive astrocytes, however, it has now been advised that GFAP should not be completely relied upon as a determinant of reactive astrocytes (Escartin et al., 2021). In addition to GFAP, reactive astrocyte markers LCN2 and Serpina3n has been shown to increase in response to a diverse range of injury including ischemic stroke, representing a chronic injury involving cell death, and the complementary LPS-injection to mimic short-term inflammation which leaves the brain structure intact (Zamanian et al., 2012). LCN2, also seen to increase in response to other insults such as nerve injury (Gesase and Kiyama, 2007), was suggested as a marker of early reactive astrogliosis due to rapid downregulation of expression after initial astrocyte induction, whilst Serpina3n levels, also seen to be increased in ALS

(Fukada et al., 2007), remain elevated over a longer time course, representing a maker for more persistent reactive astrogliosis (Zamanian et al., 2012).

Slices treated with TNFα and IL1α did see an increase in reactive astrocyte marker LCN2. Preliminary data from Caoimhe Goldrick in our laboratory has also shown that in slices treated with the same TNFα and IL1α treatment there was an increase in pro-inflammatory marker IL-6 (*Figure 4.15*). IL-6 is a cytokine which is not only released by astrocytes but also by other glial cells and neurons (Kummer et al., 2021), but it has also been shown that astrocytes secrete IL-6 in response to repeated insult or systemic inflammation (Cunningham et al., 2019; Lopez-Rodriguez et al., 2021). When analysing the cytokine treated brain lysates, western blotting quantification of GFAP levels normalised to the total astrocyte marker ALDH1L1 revealed that the levels of GFAP did not change upon treatment, possibly due to the fact that GFAP does not uniquely detect reactive astrocytes but it also expressed by astrocytes under normal physiological conditions (Zamanian et al., 2012). For this reason, it was concluded that GFAP levels would be used as a second total astrocyte marker by which HSPB1 was normalised to in order to determine the change in HSPB1 across total astrocyte protein. Normalising to a total astrocyte marker seemed more relevant that normalising to loading control β-Actin as it has been confirmed in the literature (Wilhelmus et al., 2006) and in this thesis (Chapter 3, Section 3.4.4) that HSBP1 is primarily localised in reactive astrocytes in human AD. Upon normalising to GFAP levels, it was determined that there was an increase in reactive astrocytes, as measured using LCN2 and Serpina3n, and a trend towards an increase in HSPB1 in those slices treated with TNFα and IL1α. The immunofluorescence analysis determined that HSPB1 co-localised with GFAP positive astrocytes in both the untreated and the cytokine treated slices, further supporting the association between HSPB1 and reactive astrocytes as seen in the western blot analysis. However, further work is required to confirm the presence in reactive astrocytes in these slice cultures by performing dual immunofluorescence with another reactive astrocyte marker such as S100B and total astrocyte

marker ALDH1L1 (Escartin et al., 2021), and quantification of the immunofluorescence analysis is required to confirm the changes in HSPB1 levels seen by western blotting before it is concluded that HSPB1 localisation and expression in the slices cultures are replicating what is seen in human AD.

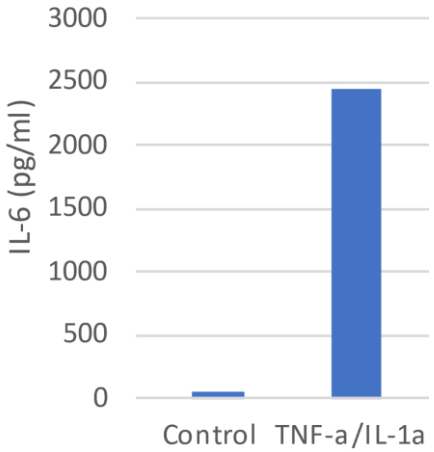

Figure 4.15: Preliminary IL-6 ELISA data produced by Caoimhe Goldrick in our laboratory using conditioned media collected from organotypic brain slice cultures treated at 21 DIV with TNFα and IL1α for 24 hours, (n=1)

There is a wealth of studies which support the notion that oligomeric Aβ, rather than insoluble amyloid plaques are toxic during AD (Yang et al., 2017; Hong et al., 2018; Shankar et al., 2008; Koffie et al., 2009). Moreover, Aβ oligomers have been shown to induce astrocytes to become reactive, either alone (Hu et al., 1998) or more recently, in combination with cytokines (LaRocca et al., 2021). Astrocytes have also been shown to produce and spread specific forms of oligomeric Aβ in the presence of APOE overexpression (Wang et al., 2019) and other specific oligomeric forms have been shown to specifically impact only astrocytes, which then go on to initiate damage in neurons (Narayan et al., 2014). In order to replicate these disease relevant changes in the organotypic slice cultures, Aβ was added to the slices at a final concentration of 2nM $A\beta_{40}$/0.2nM $A\beta_{42}$ in order to mimic levels seen in human AD, and incubated for 24 hours. In this instance, Aβ oligomer treatment

resulted in a trend towards an increase in reactive astrocyte marker LCN2 but did not alter the levels of reactive astrocyte marker Serpina3n. In addition to this, Aβ treatment led to a trend towards an increase in CRYAB but there were no changes in the levels of HSPB1.

Due to time constraints and technical difficulties, only three biological repeats were performed using the Aβ treatments in the slice cultures. This may explain why changes in reactive astrocyte markers were not observed with Aβ oligomer treatment as expected. Based on the variability seen in the slice experiments involving cytokine treatments, it would be necessary to carry out a least 6 replicates in an attempt to identify and replicate any potential biological response in the slices and reduce the variability highlighted by low numbers of replicates.

Another reason as to why the slice Aβ oligomer treatment did not induce reactive astrocytes could be due to the use of very low concentrations of 2nM $A\beta_{40}$/0.2nM $A\beta_{42}$. Although these concentrations were chosen to replicate physiological disease conditions, previous use of Aβ oligomers from cultured Tg2576 neurons and at similar concentrations, have predominantly been used in primary cell cultures (Hudry et al., 2012; Wu et al., 2010; Wu et al., 2012; DaRocha-Souto et al., 2012). Only one study has treated the larger more complex organotypic slice cultures with the same amounts of Tg2567 derived Aβ oligomers (Perez-Nievas et al., 2021). Although this study did not directly investigated the effect of Aβ oligomer treatments on astrocyte reactivity within the slices, it showed that the slices treated with TgCM replicated the tau mislocalisation at the synapse which was found in neurons treated with TgCM, implying that the same TgCM concentration and length of treatment used in the primary neurons could also elicit a similar effect in the slice culture systems (Perez-Nievas et al., 2021). Other studies have also induced a response in astrocytes through synthetic Aβ treatments at relatively high concentrations, however, these treatments may not reflect the physiological structure or levels present in the human disease, (Hu et al., 1998;

Muñoz et al., 2018; White et al., 2005; Diniz et al., 2017). Therefore it may prove advantageous to optimise the treatment protocols using the Aβ oligomers obtained from the Tg2576 mice by first extending treatment times to either 48 or 72 hours, in an attempt to elicit an astrocytic response whilst maintaining a physiologically relevant Aβ treatment concentrations.

It is also possible that the effect of Aβ was too small to detect using the western blotting techniques. More sensitive techniques for measuring changes such as an IL-6 enzyme-linked immunosorbent assay (ELISA), could be used to detect small changes in the pro-inflammatory response in response to Aβ treatments. In addition, western blot analysis was performed using the whole brain slice lysates rather than the astrocyte population alone, which may hinder astrocyte specific changes. Furthermore, to confirm whether the use of Aβ oligomers is a suitable tool to use in the slice cultures, it could have been valuable to confirm whether there were any changes in other glial cells within the slices as it has been shown that Aβ oligomers are a particularly strong activator of microglia (Reed-Geaghan et al., 2009). Extra optimisation is required to confirm the use of this as a means to study sHSPs in the context of Aβ pathology.

In order to replicate disease relevant tau pathology in the organotypic brain slice cultures, rAAV tau constructs were gifted from Professor Todd Golde and characterisation studies were carried out in collaboration with Dr Diana Flores Dominguez and Emily Groves (Croft et al., 2019). Transduction with both tau AAV constructs resulted in the phosphorylation of tau at Ser396/404, as detected by PHF-1 antibody, however there were notable differences in tau pathology in those slices transduced with the WT Tau constructs compared to P301L/S320F tau constructs, highlighting the opportunity this system provides for the replicating and analysing varying degrees of tau pathology with differing temporal progression. In those slices transduced with WT tau, there was phosphorylated tau present in the neuronal axons but there was no presence of tau inclusions, even at the latest time point at 28

DIV. In contrast, those slices transduced with P301L/S320F tau produced phosphorylated tau which was mainly driven to the somadendritic departments, in the same distribution that NFT are seen to accumulate in human AD (Uchihara et al., 2001). In addition, although the tau inclusions were not investigated further in this thesis, previous studies demonstrated by electron-microscopic ultrastructure analysis that the P301L/S320F tau inclusions resembled those mature neurofibrillary tangles found in AD (Croft et al., 2019; Grundke-Iqbal et al., 1986; Murray et al., 2014). Finally, western blot analysis confirmed the development of sarkosyl insoluble phosphorylated tau was unique to the P301L/S320F tau slices in the experiments presented in this chapter. Although this model utilises tau constructs reliant on a mutation not found in AD but instead is associated with the tauopathy FTD-17, it is the first slice model which has recapitulated tau inclusion pathology resembling the NFT in human AD, whilst also localising to the AD-relevant somadendritic region. In addition, the ability to induce varying degrees of tau pathology can be useful when replicating the different stages of human AD. All in all, the slices transduced with tau-AAVs provides a good model in which to study some of the pathological tau changes seen with AD.

Chapter 5: Does HSBP1 rescue AD-relevant pathology in the organotypic brain slice cultures?

5.1 Introduction

The purpose of this chapter was to build on previous work described in Chapter 4 of this thesis, to determine whether HSPB1 presents a non-cell autonomous pathway by which astrocytes may confer neuronal protection in the organotypic brain slice culture model of AD pathology.

5.1.1 Non-cell autonomous role of sHSPs in neurodegeneration

Recently there has been increasing interest in the non-cell autonomous role of astrocytic sHSPs in neurodegenerative diseases. Overexpression of astrocytic CRYAB been shown to be protective against the progression of disease in a mouse model of HD (Oliveira et al., 2016), whilst it was also demonstrated that expressing the human heat shock protein DNAJB6, in the astrocytes of a D. melanogaster model delays progressive neuronal degradation due to the suppression of PolyQ aggregation (Bason et al., 2019). Although the role of astrocytic sHSPs has been explored in other neurodegenerative diseases, there is a distinct lack of studies exploring this non-cell autonomous role of sHSPs in AD.

5.1.2 Extracellular sHSPs in disease

Emerging evidence has suggested a protective role for extracellular sHSPs in disease. Large-scale multilayer proteomic profiling studies have identified HSPB1 in the CSF of AD patients, where it was slightly increased compared to healthy individuals (Sathe et al., 2019; Bai et al., 2020; Bader et al., 2020), suggesting the secretion of sHSPs is increased in disease conditions.

5.1.3 Secretory mechanisms of extracellular sHSP

On a molecular level, sHSPs lack the classical N-terminal signalling peptide required for release by the classical secretory pathway (Mambula et al.,, 2007). The presence of HSPB1 has been confirmed within the exosome under normal physiological conditions (Reddy et al., 2018; den Broek et al., 2021), and more relevantly for this project, HSPB1 is released in exosomes from primary rat astrocytes after stimulation with Aβ (Nafar et al., 2016). Having said this, Fangjia Yang in our group detected HSPB1 in the conditioned media of primary mouse astrocytes and found HSPB1 was not present in extracellular vesicles. Instead, HSPB1 is in in the extracellular media as a free protein. To replicate this physiological free HSPB1, this project utilises a treatment with recombinant HSPB1 to investigate the potentially protective nature of this extracellular sHSP.

5.1.4 Function of extracellular chaperones

Chaperones play a vital role in the protein quality control system and their roles include involvement in protein folding, protein degradation and the regulation of protein aggregation and disaggregation (Wyatt et al., 2013). Most studies have focussed on the intracellular function of chaperones (Hartl et al., 2011), however, chaperones have also been found outside of the cell (Chaplot et al., 2020). The function of these extracellular chaperones may be altered due to the challenging conditions presented by the extracellular spaces, such as low ATP availability which may affect the interaction between chaperone and client protein (Gorman et al., 2007). For this reason, extracellular chaperones are found to bind to misfolded proteins to prevent aggregation, rather than refold them back into their native forms (Wyatt et al., 2013; Klaips et al., 2017). Secreted chaperones also deliver proteins to cell membrane receptors to encourage internalisation and subsequent lysosomal degradation (Yerbury et al., 2005).

5.1.5 Function of extracellular HSPB1

The role of extracellular HSPB1 is relatively unknown however a variety of studies using *in vitro* and experimental disease models have reported the involvement of sHSP in a number of functions, whilst highlighting the potential therapeutic activity of these extracellular sHSP (Reddy et al., 2018). Extracellular sHSPs have been seen to modulate inflammatory processes (den Broek et al., 2021). Moreover, in the experimental autoimmune encephalomyelitis (EAE) mouse model used to study the inflammatory disease multiple sclerosis in rodents, treatment with intra-peritoneal injections of HSPB1 reduced paralysis through the modulation of inflammatory cytokines IL-2, IL-6 and IFN-γ (Kurnellas et al., 2012). The protective chaperone function of HSPB1 has also been suggested, as exposure to Aβ can trigger the exosomal release of astrocytic HSPB1 which then goes on to interact with the extracellular Aβ (Nafar et al., 2016). This extracellular HSBP1 may then act as a chaperone protein to modulate the sequestration of toxic Aβ oligomers into non-toxic Aβ aggregates (Ojha et al., 2011; Kudva et al., 1997). Finally, extracellular HSPB1 has also displayed potential anti-apoptotic function. Intraperitoneal injection of HSPB1 peptides prevented protein aggregation and oxidative stress in a rat model of cataracts (Nahomi et al., 2015).

5.2 Aims

The previous chapter in this thesis established that 1) reactive astrocyte markers were induced in those slices treated with cytokines TNFα and IL1α, and 2) slices transduced with P301L/S320F tau-AAV resulted in the accumulation of sarkosyl insoluble hyperphosphorylated tau, in a similar distribution as to what is found in human AD. It was therefore concluded that the organotypic brain slice cultures provided a good model to study the function of sHSPs in the context of certain AD-pathologies.

Following on from this, the central aim for this chapter was to determine whether HSPB1 is protective against these induced AD-relevant pathologies by exploring its impact on cell toxicity, synaptotoxicity, neuroinflammation and tau accumulation in the organotypic slice model of tau pathology. To explore this primary objective, with a particular focus on the non-cell autonomous function of HSPB1, the specific aims for this chapter are as follows:

1) Investigate the role of extracellular HSPB1 in modulating neuroinflammation in the brain slices treated with cytokines TNFα and IL1α, by treating these slices with recombinant HSPB1 protein
2) Determine whether extracellular HSPB1 is capable of altering the accumulation of P301L/S320F tau in primary neurons and in brain slices
3) Explore the role of extracellular HSPB1 in protecting against neuronal cell death and synaptotoxicity in those slices treated with either cytokines or transduced with tau-AAVs
4) Determine whether astrocytic HSPB1 is protective against P301L/S320F tau pathology in a non-cell autonomous manner by overexpressing HSPB1 in astrocytes in slice cultures using AAV constructs

5.3 Methods

The materials and methods for this chapter have been described in full in Chapter 2 of this thesis. In brief, organotypic brain slice cultures were prepared from WT CD1 mouse pups according to the protocol in *Croft and Noble, 2018*, as detailed in Chapter 1 Section 3.1.

For cytokine treatment of the organotypic brain slice cultures (Chapter 2, Section 3.2), 21 DIV slices were treated with 30ng/ml recombinant mouse TNFα and 3ng/ml IL1α in 1ml pre-warmed culture media. Slices were incubated for 24 hours before the slices were collected for western blotting analysis and the media was collected for LDH assays. For the additional treatment of recombinant HSPB1 (Chapter 2, Section 3.2), 50ng/ml recombinant HSPB1 resuspended in filtered 0.1% BSA/PBS was added to the slice culture media along with the cytokine treatments at 21 DIV for 24 hours. The control slices for these experiments were treated with 50µl sterile filtered 0.1% BSA/PBS. Slices were then collected and lysed for western blot analysis and the media was collected for cell toxicity assays.

In order to replicate tau pathology in the slice cultures (Chapter 2, Section 3.2), slices were transduced at 0 DIV with either the wild-type (AAV2/TM8-WT-htau0N4R-EGFP) or mutant tau (AAV2/TM8-P301L/S320F-htau0N4R-EGFP) rAAV constructs at $1x10^{11}$ viral genomes (VG) per well containing 3 brain slices. At 28 DIV, slices were harvested and lysed for the sarkosyl extraction of tau (Chapter 2, Section 4.1). Tau fractions were then run on 10% % poly-acrylamide gel for western blotting analysis (Chapter 2, Section 4.2).

Constructs encoding the human HSPB1 under the human GFAP promoter (pAAV[Exp]-GFAP(short)>hHSPB1[NM_001540.5](ns):P2A:TagBFP2:WPRE) or the same constructs expressing

BFP2 only (pAAV[Exp]-GFAP(short)>TagBFP2:WPRE) were custom designed and packaged by VectorBuilder, all provided in PBS buffer. All were applied directly into the culture media on 0 DIV at $2x10^{10}$ VG/well. Slices were then either fixed for immunofluorescence analysis or harvested for the extraction of sarkosyl insoluble tau after 28 DIV.

For the treatment of recombinant human HSPB1 in slices transduced with tau-AAVs (Chapter 2, Section 3.2), after 14 DIV 50ng/ml recombinant HSPB1 was added to the slice culture media each time the media was changed (every 2-3 days), up until the slices were harvested at 28 DIV. The control slices for these experiments were treated with 50µl sterile filtered 0.1% BSA/PBS in the exact same way. Slices were then collected and lysed for analysis by western blotting or the lysates were used to extract sarkosyl insoluble tau.

All primary mouse neuron cultures were kindly prepared by Dr Maria Jimenez-Sanchez, from E15-16 wild type CD1 embryos (Chapter 2, Section 2.1). Neuron cultures were seeded in 12-well plates at a seeding density of 2.5×10^6 cells/well, with coverslips for immunofluorescence analysis and without for wester blotting. At 6 DIV, neurons were transduced with either the wild-type (AAV2/TM8-WT-htau0N4R-EGFP) or mutant tau (AAV2/TM8-P301L/S320F-htau0N4R-EGFP) rAAV constructs at MOI: 100,000. At 12 DIV, neurobasal (NB) media was collected for LDH assay and neuronal lysates were collected for western blots or fixed for immunocytochemistry.

Concurrent to the transduction with rAAV, neurons were also treated with recombinant human HSPB1 protein (Chapter 2, Section 2.1). HSPB1 was added straight into the NB media at 50ng/ml on 6, 8 and 10 DIV. The control neurons for these experiments were treated with comparable volumes of sterile filtered 0.1% BSA/PBS in the exact same way. At 12 DIV, NB was collected for cell toxicity assays whilst neurons were harvested either for immunoblotting or immunocytochemistry analysis.

5.4 Results

5.4.1 Recombinant HSPB1 treatment has no effect on neuronal and synaptic health in slices treated with cytokines TNFα and IL1α

The results presented in Chapter 4 of this thesis suggested the induction of reactive astrocytes in organotypic brain slice cultures treated with cytokines TNFα and IL1α, detected by the increase in reactive astrocyte marker LCN2. During neurodegeneration, increased secretion of cytokines TNFα and IL1α from activated microglia have been shown to induce reactive astrocytes (Liddelow et al., 2017), and in turn these reactive astrocytes are able to promote neurotoxicity (Liddelow et al., 2017; Stevens et al., 2007). To mimic the release of astrocytic HSPB1 seen in primary culture in our laboratory and in previous reports (Nafar et al., 2016), slice cultures were treated with recombinant human HSPB1 for 24 hours. Slice lysates were then analysed by western blotting to determine whether extracellular HSPB1 can protect from cell toxicity induced by pro-inflammatory cytokines (Liddelow et al., 2017).

The human recombinant protein was selected as opposed to the mouse HSPB1 protein as this project was primarily interested in the relevance of human HSPB1 within human disease. BLAST alignment of the mouse and human HSPB1 proteins found a 83% similarity and 90% positives between the two proteins and therefore the recombinant human HSPB1 seemed a suitable choice of treatment for the following experiments.

Slice cultures were first tested for cell toxicity using the LDH assay. The media from the slice cultures were collected for the assay and LDH levels were normalised to the total LDH measured in total protein lysates. Cytokine treatment was slightly toxic to the slice cultures, and HSPB1 treatment in both untreated and TNFα and IL1α treated slices slightly reduced cell toxicity, although these results were not statistically significant (*Figure 5.1A*). Next, to investigate programmed cell death in the

slices treated with the cytokines, the levels of caspase-3, an executioner caspase implicated in apoptosis, was measured. Slice lysates were probed with an antibody against caspase-3 antibody, which recognised the cleaved (active) form of this caspase. There was a slight increase in the levels of cleaved caspase-3 in those slices treated with TNFα and IL1α compared to the untreated slices, mirroring what was found by the LDH assay for cell toxicity. The treatment with recombinant HSPB1 did not alter the levels of apoptosis seen in either those untreated or TNFα and IL1α treated slices (*Figure 5.1B*).

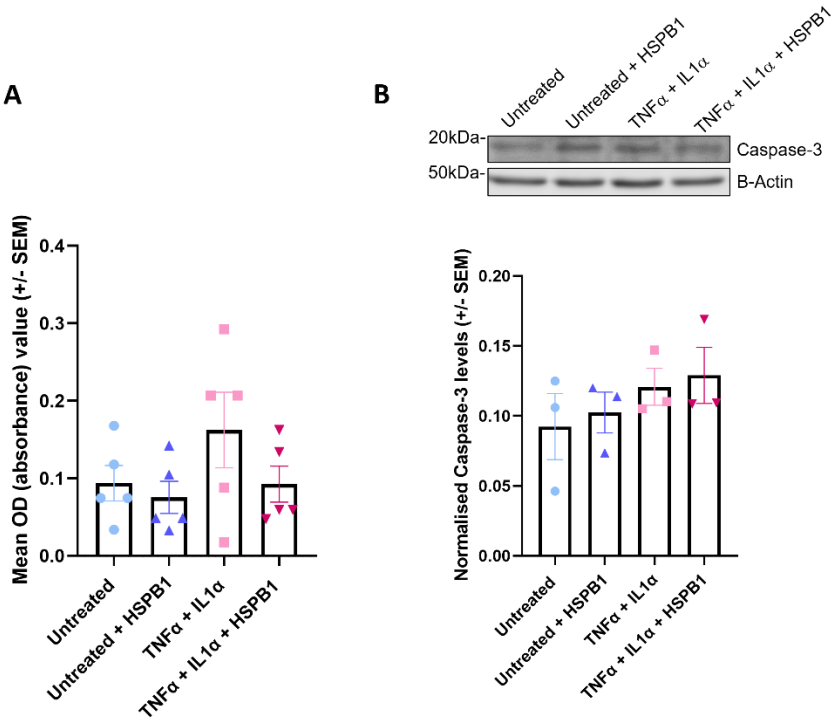

Figure 5.1: Cell toxicity measures in 21 DIV organotypic brain slices treated for 24 hours with cytokines TNFα and IL1α together with 50ng/ml recombinant human HSPB1 or BSA as a control.

A) LDH assay was performed in conditioned media and total protein lysates. OD values in conditioned media were normalised to OD values in the slice lysates, graph shows mean +/- SEM taken from 5 biological replicates, B) Western blot analysis of slice lysates using a marker for apoptosis (Caspase-3), levels of caspase-3 were normalised to loading control β-Actin, graph shows mean +/- SEM across 3 biological replicates.

Next, slice experiments were carried out to investigate whether TNFα and IL1α treatments were synaptotoxic to the slices and whether this toxicity could be rescued by extracellular HSPB1. Slices were treated with TNFα and IL1α and recombinant HSPB1 and were lysed for the quantification of synaptic proteins levels by western blotting. Synaptic proteins were analysed using antibodies against the postsynaptic protein PSD95 and the pre-synaptic protein synaptophysin. There were no significant differences in either pre or post-synaptic protein levels in those slices treated with TNFα and IL1α compared to untreated slices (*Figure 5.2*). Treatment with recombinant HSPB1 did not altered these levels of synaptic proteins in either the untreated or TNFα and IL1α treated groups (*Figure 5.2*).

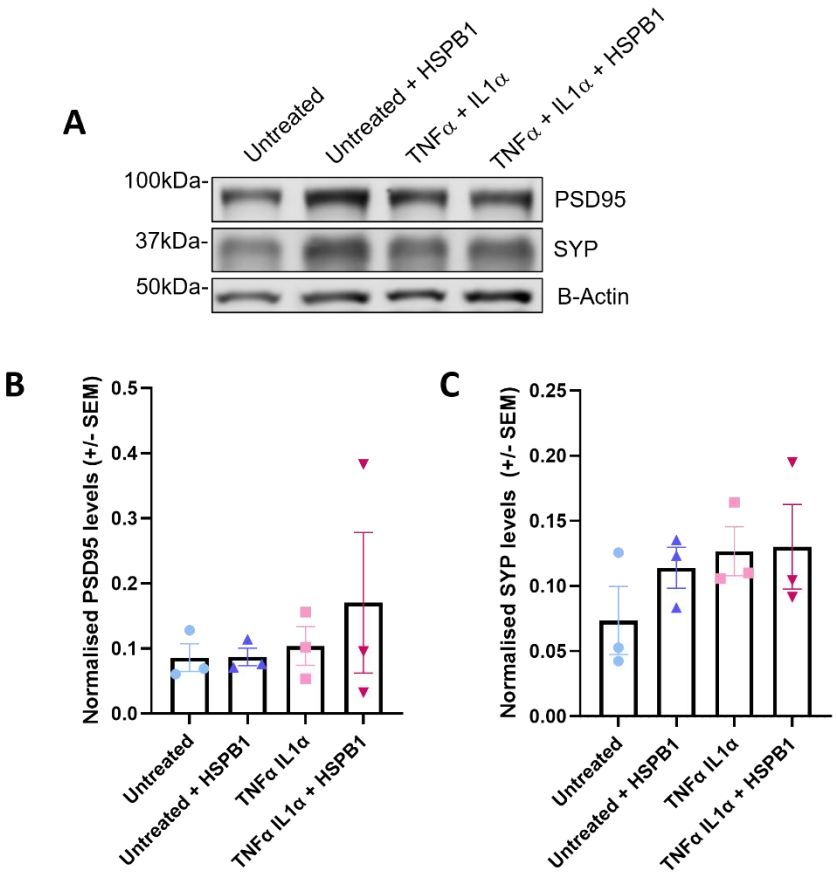

Figure 5.2: Levels of synaptic markers (PSD95 and synaptophysin) in 21 DIV organotypic brain slices treated for 24 hours with TNFα and IL1α together with 50ng/ml recombinant human HSPB1 or BSA as a control.

A) Representative western blot using antibodies against post-synaptic protein (PSD95), pre-synaptic protein (Synaptophysin), and loading control β-Actin. B) Western blot analysis of slice lysates with antibodies against post-synaptic marker PSD95 normalised to the loading control β-Actin, graph shows mean +/- SEM across 3 biological repeats. C) Western blot analysis of slice lysates with antibodies against pre-synaptic marker synaptophysin (SYP) normalised to the loading control β-Actin, graph shows mean +/- SEM across 3 biological repeats.

5.4.2 Treatment with recombinant HSPB1 did not alter the levels of reactive astrocytes induced in the slices by cytokines TNFα and IL1α

Evidence from the literature indicates that extracellular HSPB1 may have a role in modulating the inflammatory response (Salari et al., 2013; Batulan et al., 2016; Jin et al., 2014; Thuringer et al., 2013; Kurnellas et al., 2012). Therefore, the organotypic brain slices were treated with human recombinant HSPB1 to explore whether this could prevent the increase in reactive astrocyte markers induced in those slices treated with cytokines TNFα and IL1α, as described in Chapter 4, Section 4.4.2 of this thesis. Slices were simultaneously treated with TNFα and IL1α along with recombinant HSPB1 at either 10ng/ml or 50ng/ml. The controls for these experiments were treated with either 10 or 50µl sterile filtered 0.1% BSA/PBS to account for any potential effects from excess BSA levels.

Previous experiments involving slices treated with cytokines established that GFAP could be used as a loading control for total astrocyte protein, as the levels of GFAP do not seem to change with treatments, reflecting what is seen in total astrocyte levels detected using ALDH1L1 (Chapter 4, Section 4.4.2). For this reason, levels of reactive astrocyte markers LCN2 and Serpina3n were initially normalised to GFAP levels in western blotting analysis. As was seen in previous experiments (Chapter 4, Section 4.4.2), there was an increase in the levels reactive astrocyte marker LCN2 in those slices treated with TNFα and IL1α compared to controls. This may not have reached significance as seen before due to the relatively low numbers of replicates. Slice treatment with recombinant HSPB1 did not alter the levels of LCN2 in those slices treated with TNFα and IL1α (*Figure 5.3B*).

The levels of Serpina3n did not change in those slices treated with TNFα and IL1α compared to controls, again, reflecting what was seen previouls (Chapter 4, Section 4.4.2). Treatment with recombinant HSPB1 at 50ng/ml slightly reduced Serpina3n levels in the untreated slices whilst

recombinant HSPB1 treatment at both 10ng/ml and 50ng/ml reduced Serpina3n levels in those slices treated with cytokines, albeit not to a statistically significant level (*Figure 5.3C*).

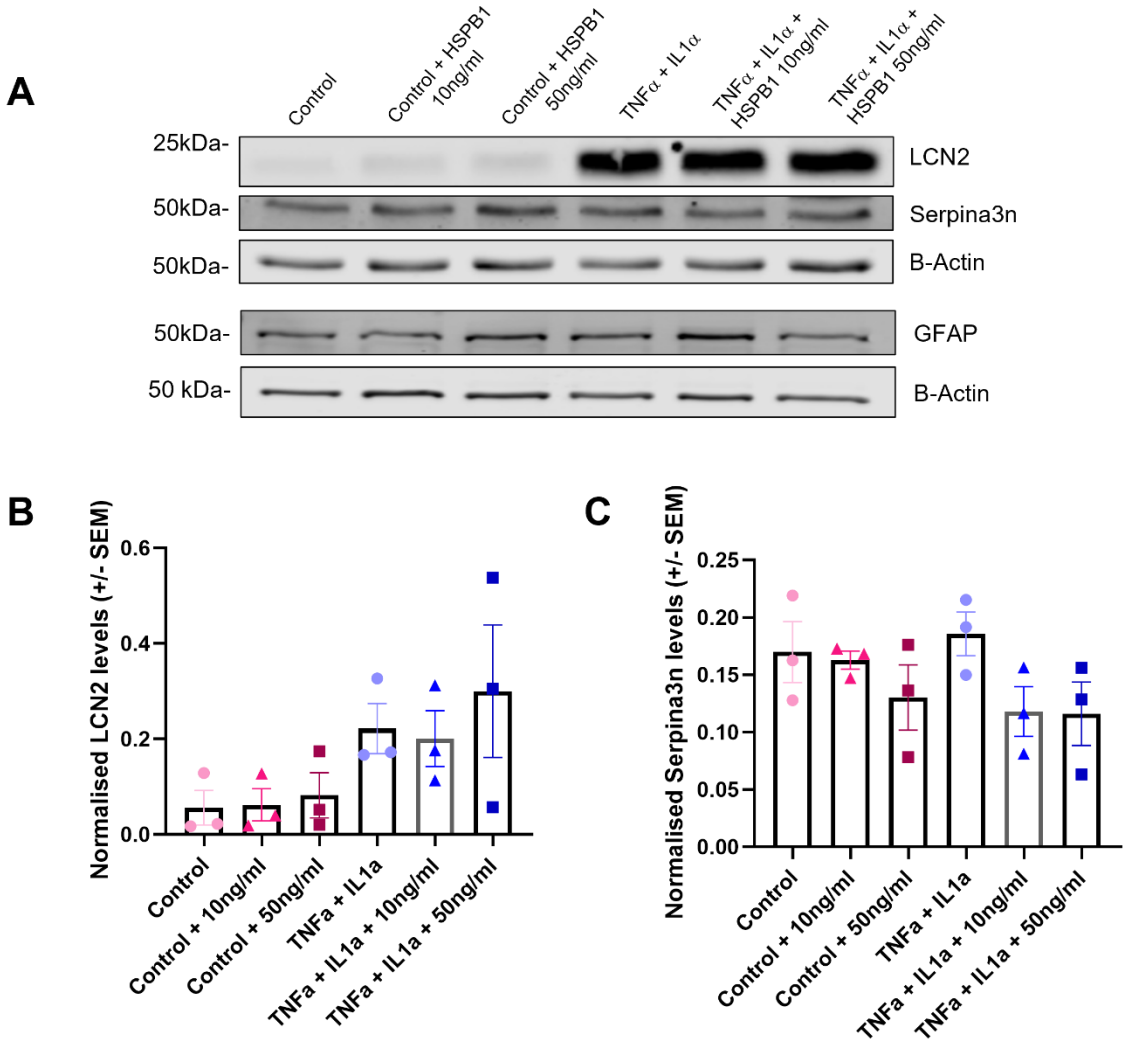

Figure 5.3: Changes in reactive astrocyte markers (LCN2 and Serpina3n) normalised to GFAP levels in 21 DIV organotypic brain slices treated with TNFα and IL1α together with recombinant human HSPB1 at 10 or 50ng/ml or BSA as a control.

A) Representative western blot using antibodies against reactive astrocytes markers LCN2, Serpina3n and GFAP and loading control β-Actin. B) Western blot analysis of slice lysates with antibodies against LCN2 normalised to GFAP levels, graph shows mean +/- SEM of 3 biological replicates. C) Western blot analysis of slice lysates with antibodies against Serpina3n normalised to GFAP levels, graph shows mean +/- SEM of 3 biological replicates

Replicating what was performed in Chapter 4 of this thesis, the levels of astrocytic proteins in slices treated with TNFα and IL1α plus recombinant HSPB1 were then normalised to the loading control β-Actin. As expected, GFAP levels did not change between those slices treated with TNFα and IL1α, supporting its use as an astrocytic loading control (*Figure 5.4A*). LCN2 levels reflected what was seen in the western blot analysis normalised to GFAP, a strong trend towards an increase in LCN2 levels in TNFα and IL1α treated slices that were largely unaffected by recombinant HSPB1 treatment (*Figure 5.4B*). Lastly, the levels of Serpina3n normalised to β-Actin closely reflected the levels of Serpina3n normalised to GFAP in those slices treated with TNFα and IL1α and recombinant HSPB1. However, the initial reduction in Serpina3n (seen when normalised to GFAP) levels caused by recombinant HSPB1 treatments in both cytokine and untreated control were less pronounced, supporting the use of a more specific astrocyte marker as a loading control in order to pick up more subtle, physiologically relevant changes (*Figure 5.4C*).

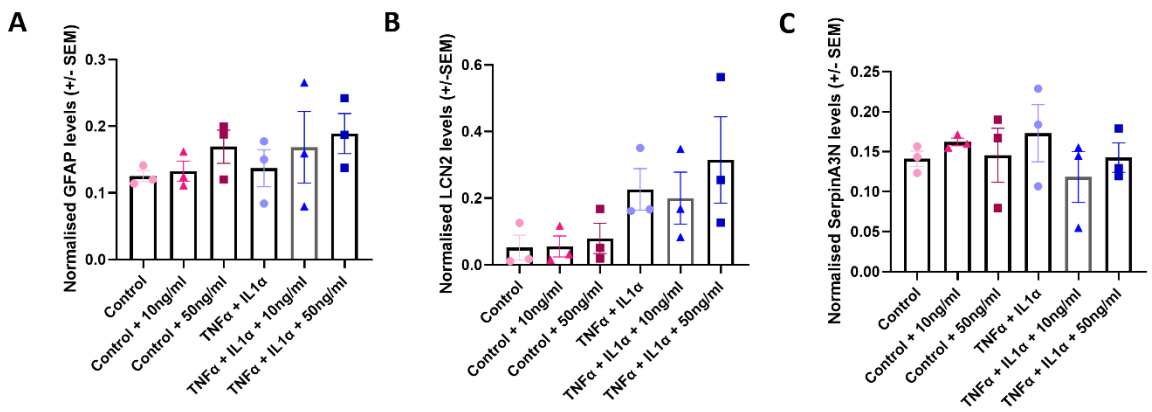

Figure 5.4: Changes in reactive astrocyte markers (GFAP, LCN2 and Serpina3n) normalised to total protein (β-Actin) in 21 DIV organotypic brain slices treated with TNFα and IL1α together with recombinant human HSPB1 at 10 or 50ng/ml or BSA as a control

A) Western blot analysis of slice lysates with antibodies against reactive astrocyte marker GFAP normalised to loading control β-Actin, graph shows mean +/- SEM of 3 biological replicates. B) Western blot analysis of slice lysates with antibodies against reactive astrocyte marker LCN2 normalised to loading control β-Actin, graph shows mean +/- SEM of 3 biological replicates. C) Western blot analysis of slice lysates with antibodies against reactive astrocyte marker Serpina3n normalised to loading control β-Actin, graph shows mean +/- SEM of 3 biological replicates

5.4.3 Recombinant HSPB1 treatment reduces the accumulation of P301L/S320F tau inclusions in primary mouse neurons

It has been shown in a number of *in vitro* studies that HSPB1 is able to bind to tau and reduce tau aggregation and fibril formation (Lin et al., 2020; Baughman et al., 2018; Abisambra et al., 2010; Freilich et al., 2018). Not only this, but HSPB1 is also capable of reducing tau levels in mice (Shimura et al., 2004; Abisambra et al., 2010). In order to investigate the potentially protective chaperone functions of extracellular HSPB1, recombinant HSPB1 treatment was investigated, firstly in primary neurons and then in the *ex vivo* organotypic brain slice culture model to determine whether HSPB1 was able to modulate the induced tau-AAV pathology.

Firstly, primary mouse neuronal cultures were also transduced with the tau-AAVs to determine whether this resulted in the induction of tau pathology similar to what was seen in the slices. Either the wild-type tau AAV (AAV2/TM8-WT-htau0N4R-EGFP) or the mutant tau AAV (AAV2/TM8-P301L/S320F-htau0N4R-EGFP) constructs were added to the media of the neurons at 6 DIV at a final concentration of MOI: 100,000. Neurons were then also treated with recombinant human HSPB1 at 50ng/ml at 6, 8 and 10 DIV. Neurons and media were then collected for characterisation using immunoblotting and immunofluorescent analysis.

Initial cell toxicity assays were performed to determine whether transduction with the P301L/S320F tau AAV is more toxic to the neurons than transduction with the WT Tau AAV. There were no significant differences in cell death in neurons transduced with WT tau AAV compared to those neurons transduced with the mutant tau AAV constructs (*Figure 5.5A*) Further LDH assays are necessary to determine whether transduction with either tau-AAV impacts neuronal toxicity when compared to the non-transduced neurons. Neuronal lysates were then analysed by western blotting

and probed for a marker of apoptosis, cleaved-caspase 3. This experiment was only performed in one biological replicate due to technical difficulties, however, there was no differences in the levels of caspase 3 cleavage in those neurons transduced with WT tau AAV compared to those neurons transduced with P301L/S320F tau AAV (*Figure 5.5B*).

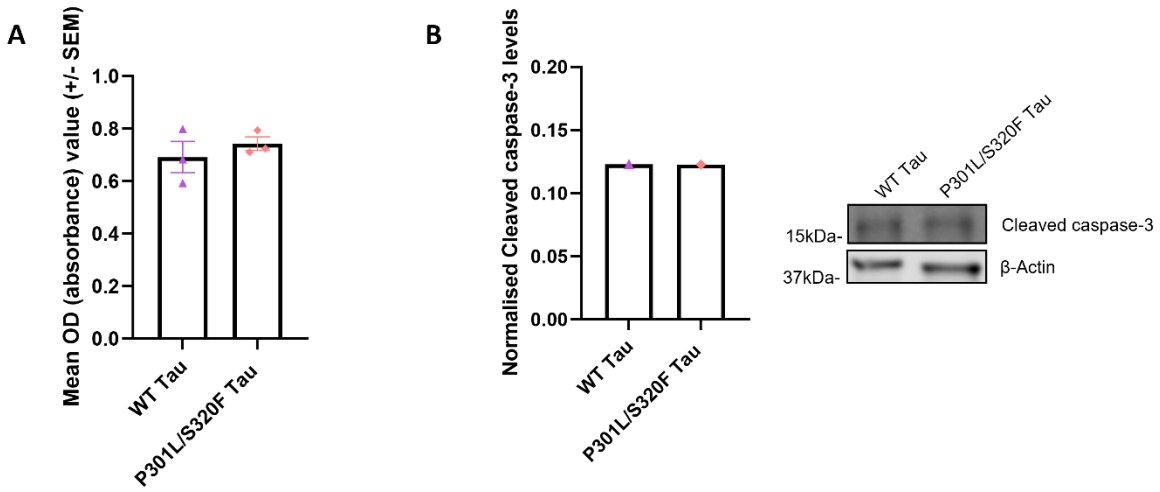

Figure 5.5: Cell toxicity assays in primary mouse neurons transduced at 6 DIV with either WT tau or P301L/S320F tau AAV constructs (MOI =100,000) and harvest at 12 DIV.

A) LDH assay was performed in conditioned media, graph shows mean +/- SEM taken from 3 biological replicates, B) Neuronal were lysed and analysed by western blotting using antibodies against apoptosis (cleaved caspase-3) and normalised to loading control β-Actin, graph shows 1 biological replicate

Immunofluorescence analysis was performed at 12 DIV with neurons transduced with either WT or P301L/S320F tau and immunolabelled with the MC1 antibody, which detects tau in an abnormal conformation (Jicha 1998). In those neurons transduced with the mutant tau AAV constructs, tau accumulated in MC1 positive tau structures which were not found in those neurons transduced with the WT tau AAVs (*Figure 5.6*). These structures congregate mainly in the soma of the neurons, as seen in the organotypic brain slice cultures transduced with the mutant tau constructs (*Figure 11, Chapter 4, Section 4.4.3*). Further to this, these MC1 positive tau structures were also found along the neuronal processes, in a dotty pattern, again, unique to those neurons transduced with P301L/S320F tau AAV constructs.

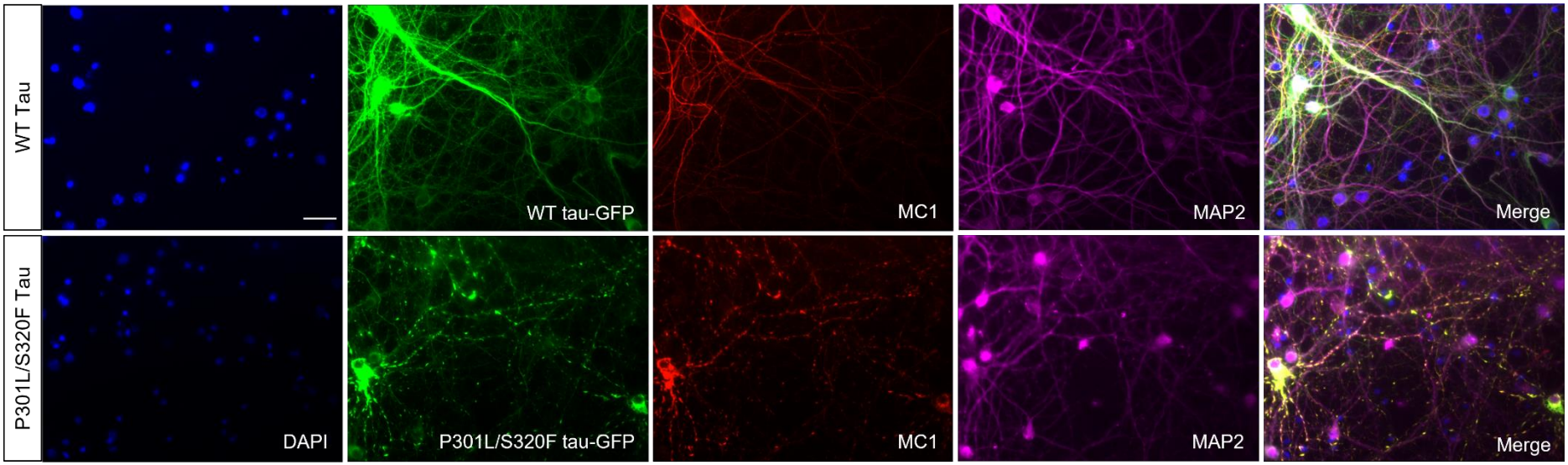

Figure 5.6: Immunofluorescent analysis of primary mouse neurons transduced at 6 DIV with either wild-type (WT) tau AAV or the P301L/S320F tau AAV constructs at MOI=100,000 and collected at 12 DIV with antibodies against tau in an abnormal conformation (MC1) and neurons (MAP2)

Representative image from 3 biological replicates. Images were taken on the Zeiss AxioImager Z1 microscope, scale bar = 25µm

Western blot analysis of neurons transduced with either WT tau or P301L/S320F tau AAVs was performed using antibodies against total tau (Dako tau) and phosphorylated tau at Ser396/404 (PHF-1). Phosphorylated tau was quantified as a proportion of total tau and showed a trend towards an increase in phosphorylated tau in those neurons transduced with the mutant tau AAV compared to neurons transduced with WT tau AAV (*Figure 5.7*). Both the immunofluorescence analysis and western blotting analysis of tau-AAV induced pathology in the primary neurons reflect the results of the characterisation of tau-AAV performed in the slice cultures found in Chapter 4 of this thesis (Chapter 4, Section 4.4.3).

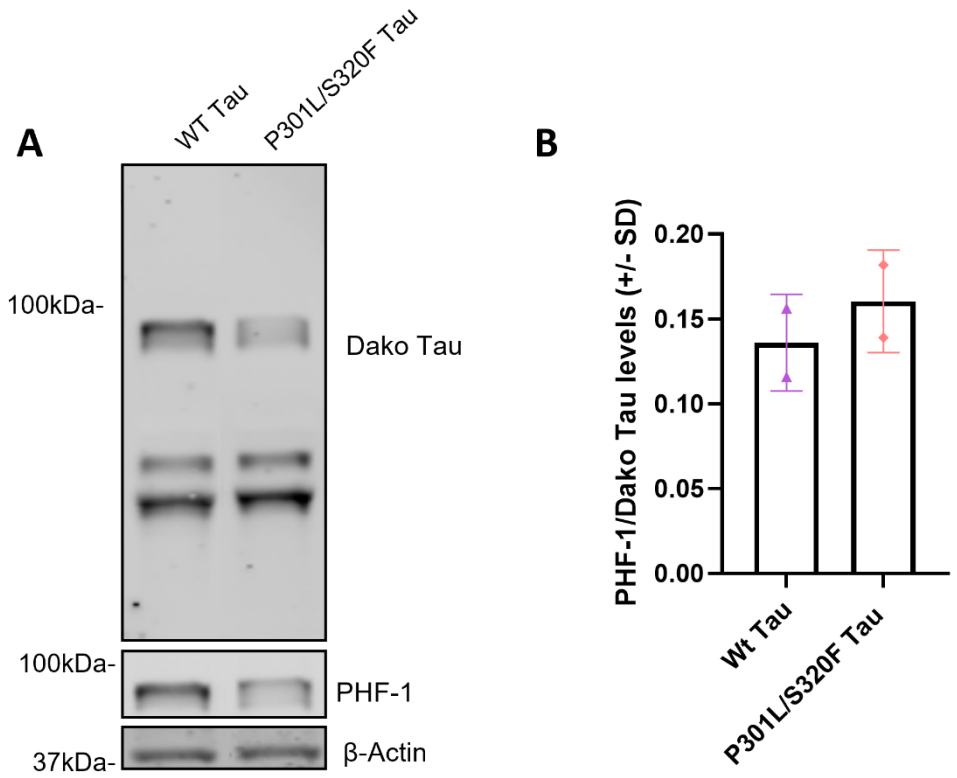

Figure 5.7: Changes in tau levels in primary mouse neurons transduced at 6 DIV with either WT tau or P30L1/S320F tau AAV at MOI=100,000 and collected at 12 DIV.

A) Representative western blot using antibodies against total tau (Dako tau), tau phosphorylated at Ser396/404 (PHF-1) and loading control β-Actin across 2 biological replicates. B) Quantification of the levels of phosphorylated tau as a proportion of total tau, graph shows mean +/- SEM across 2 biological repeats.

Next, mouse neuron cultures were treated with recombinant HSPB1 to explore whether this would have any effect on the abundance of P301L/S320F tau inclusions. Neurons were treated with 50ng/ml recombinant HSPB1 at 6, 8 and 10 DIV before being collected for immunoblotting and immunocytochemistry analysis. For immunocytochemical analysis, quantification was performed using those neuron cultures transduced with just the P30L1/S320F tau construct, with and without recombinant HSPB1 treatment, since no MC1 positive tau foci structures are observed in the WT tau AAV treated neurons. A total of at least 500 GFP-positive neurons per technical replicate were counted, as confirmed by MAP2 positive staining, and the number of neurons containing MC1 positive foci (termed, “dotty” neurons) were counted as a proportion of the total number of GFP-positive neurons (*Figure 5.8A*). It was found that there was a significant reduction in the number of these neurons containing MC1 foci in those neuron cultures transduced with the mutant tau AAV and treated with the recombinant HSPB1, compared to those control neurons transduced with the tau AAVs (*Figure 5.8B*), indicating a potentially protective effect of HSPB1 in reducing the accumulation of tau pathology.

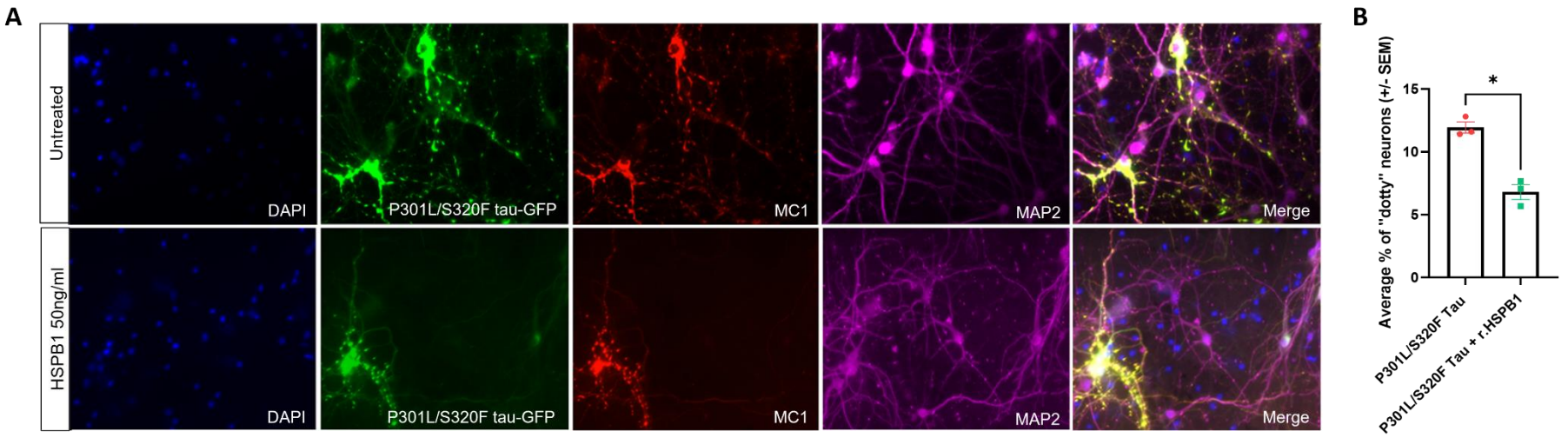

Figure 5.8: Immunofluorescent analysis of primary neurons transduced at 6 DIV with P30L1/S320F tau AAV at MOI=100,000 and treated with recombinant human HSPB1 at 50 ng/ml at 6, 8 and 10 DIV, with antibodies against tau in the conformational form (MC1) and neurons (MAP2).

A) Representative immunolabelling of 3 biological repeats, images were taken on the Zeiss AxioImager Z1 microscope, scale bar = 100µm. B) Quantification of the percentage of "dotty" neurons containing MC1 positive foci in primary neurons transduced with P30L1/S320F tau AAV, was quantified as a proportion of the total number of GFP positive neurons in untreated vs HSPB1 treated, graph shows mean +/- SEM of 3 biological replicates, paired t-test, P<0.05

Neurons transduced with both wild type and P301L/S320F tau AAVs and treated with recombinant HSPB1 were also collected at 12 DIV for western blot analysis (*Figure 5.9A*). When quantifying the levels of phosphorylated tau (PHF-1) as a proportion of total tau (Dako Tau), the data indicates a reduction in phosphorylated tau, as a proportion of total tau, in those mutant AAV tau slices also treated with the recombinant HSPB1 (*Figure 5.9B*), reflecting what was determined by immunofluorescent imaging. More replicates are required to confirm the changes seen in these pilot experiments.

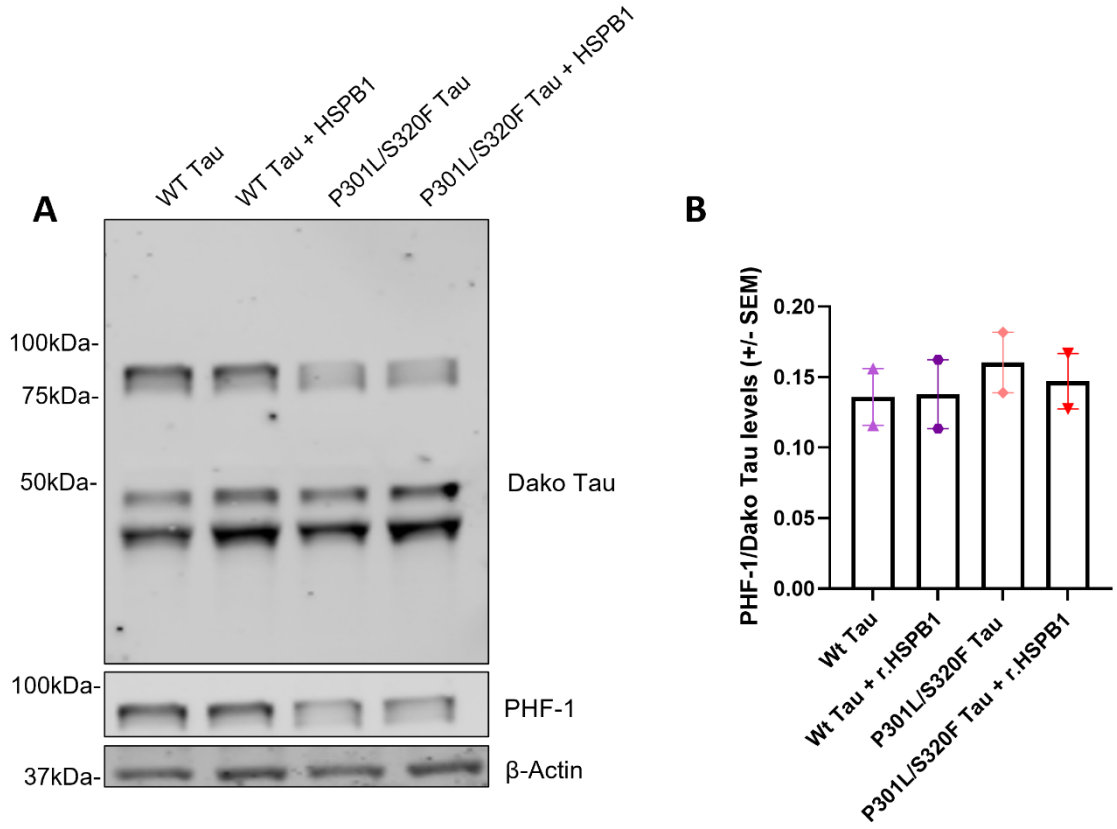

Figure 5.9: Levels of tau markers in primary mouse neurons transduced with either WT tau AAV or P301L/S320F tau AAV constructs at MOI=100,000 on 6 DIV and treated with recombinant human HSPB1 at 50ng/ml on 6, 8 and 10 DIV, neurons were collected at 12 DIV.

A) Representative western blot using antibodies against total tau (Dako tau), tau phosphorylated at Ser396/404 (PHF-1), and loading control β-Actin across 2 biological replicates. B) Quantification of the levels of phosphorylated tau as a proportion of total tau, graph shows mean +/- SEM across 2 biological repeats.

To determine whether recombinant HSPB1 reduced synaptotoxicity resulting from the accumulation of tau foci, preliminary western blot analysis was also carried out to determine whether induced tau pathology could be synaptotoxic and whether this could be rescued through treatment with extracellular HSPB1. Neuron conditioned media was collected and used to measure cell toxicity through the LDH assay. Quantification revealed no differences in cell toxicity between slices transduced either with WT tau or P301L/S320F tau AAVs but there was a slight reduction in those slices transduced with P301L/S320F tau and treated with recombinant HSPB1 compared to the untreated P301L/S320F tau AAV neurons (*Figure 5.10B*). Furthermore, preliminary experiments were performed using one biological replicate to investigate whether the levels of apoptosis changed upon recombinant HSPB1 treatment. There was no difference in apoptosis, as detected using a marker for cleaved caspase-3, in neurons transduced with WT tau AAVs compared to P301L/S320F tau but more interestingly, treating neurons transduced with P301L/S320F tau with recombinant HSPB1 was seen to reduce the levels of apoptosis, potentially caused by the aggregated tau. (*Figure 5.10C*).

Neurons were also lysed and western blots were probed using a post-synaptic marker (PSD95) and a pre-synaptic marker (Synaptophysin). Preliminary data suggests that transduction with the mutant tau AAV constructs results in lower levels of PSD95 compared to those slices transduced with the WT tau AAVs, indicating that the pro-aggregant constructs are more synaptotoxic than the WT tau AAV construct (*Figure 5.10D*). In addition, treatment with recombinant HSPB1 increased PSD95 levels in slices treated with either tau AAV construct (*Figure 5.10D*). Further preliminary western blot analysis, using one biological replicate, also found that neurons treated with recombinant HSPB1 showed a potential rescue of pre-synaptic marker synaptophysin in slices transduced with either WT or P301L/S320F tau (*Figure 5.10E*). Taken together, these results indicate a potentially protective role of HSPB1 in preventing synaptic loss. It would be necessary to repeat these experiments to

confirm the changes presented here and consequently analyse synapse health and function in more depth.

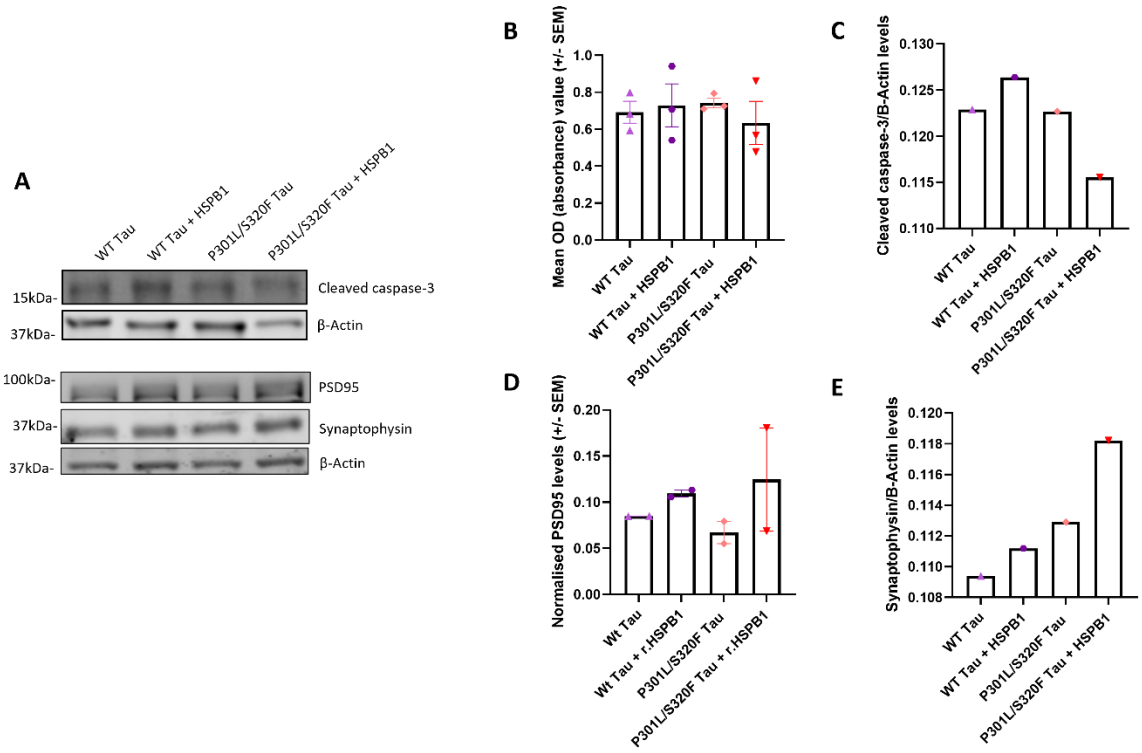

Figure 5.10: Levels of apoptotic markers (LDH and cleaved caspase-3) and synaptic markers (PSD95 and synaptophysin) in primary mouse neurons transduced with either WT tau AAV or P301L/S320F tau AAV constructs at MOI=100,000 on 6 DIV and treated with recombinant human HSPB1 at 50ng/ml on 6, 8 and 10 DIV, neurons were lysed at 12 DIV.

A) Representative western blot using antibodies against apoptosis (cleaved caspase-3), post-synaptic protein (PSD95), pre-synaptic protein (Synaptophysin), and loading control β-Actin B) Graph shows average LDH values across three biological repeats, +/- SEM, C) Quantification of levels of cleaved caspase-3 were normalised against loading control β-Actin, graph shows results taken from 1 biological repeat, D) Quantification of levels of post-synaptic maker PSD95 normalised to loading control β-Actin, graph show mean +/- SEM across 2 biological replicates. E) Quantification of the levels of synaptophysin were normalised against loading control β-Actin, graph shows 1 biological repeats

5.4.4 Recombinant HSPB1 treatment has no effect on the accumulation of P301L/S320F tau inclusions in organotypic brain slice cultures

Having established the potential role of HSPB1 in protecting neurons from the synapototoxic effects induced by tau pathology in a primary cell culture model, it was necessary to next determine whether these results are reflected in a more physiologically relevant *ex vivo* model of tau pathology. Slices were transduced with either the WT tau or P301L/S320F tau AAV constructs and then treated with 50ng/ml recombinant HSPB1 over 14 DIV. As the neuron data indicated that HSPB1 could reduce the abundance of MC1 positive foci, changes in the accumulation of insoluble tau in slices upon treatment with recombinant HSPB1 were explored. Therefore, slice cultures were harvested and sarkosyl was used to extract the hyperphosphorylated insoluble tau fractions. The total tau (low speed supernatant) and hyperphosphorylated tau fractions (sarkosyl insoluble pellet) were analysed by western blotting (*Figure 5.11A*).

Similar to what was indicated in Chapter 4, Section 4.4.3 of this thesis, levels of phosphorylated tau as a proportion of total tau levels were increased in those slices transduced with the mutant P301L/S320F tau constructs compared to those slices treated with the WT tau construct (*Figure 5.11B*). Upon treatment with the recombinant HSPB1, there was no apparent change in the levels of phosphorylated tau as a proportion of total tau in the slices treated with either of the tau AAVs.

Further quantification was performed to determine whether there was any difference in the levels of total insoluble tau between slices transduced with P301L/S320F tau and treated with recombinant HSPB1. To do this, the levels of total tau in the sarkosyl insoluble fraction was determined as a proportion of the total soluble and insoluble tau in the LSS fraction. Analysis revealed no significant differences in the levels of overall insoluble tau in slices transduced with P301L/S320F tau and

treated with recombinant HSPB1 (*Figure 5.11C*). Lastly, the relative proportion of insoluble tau phosphorylation was established by quantifying the levels of tau phosphorylated at Ser396/404 (PHF-1) in the sarkosyl insoluble fraction as a proportion of total tau found in the sarkosyl insoluble fraction. The results reflected what was seen in the previous quantification of insoluble tau as there was no significant differences in the proportion of phosphorylated insoluble tau in those slices treated with recombinant HSPB1 compared to those slices transduced with P301L/S320F tau only (*Figure 5.11D*).

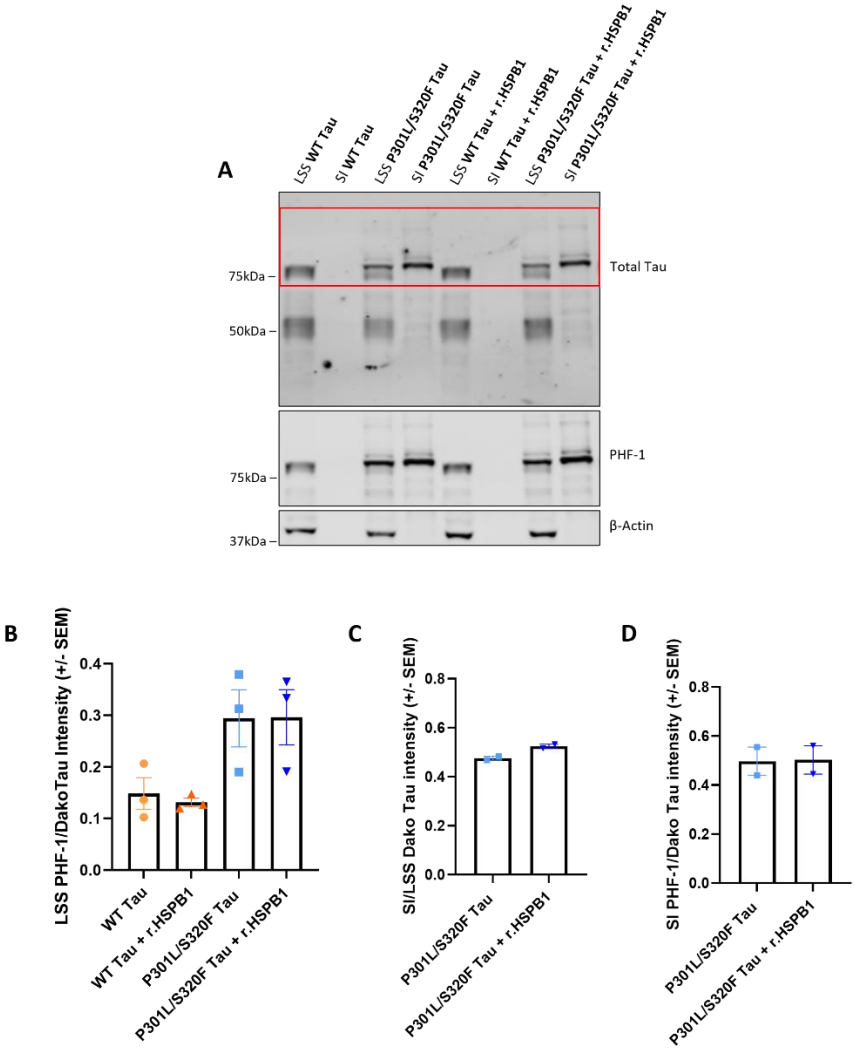

Figure 5.11: Levels of tau pathology in sarkosyl extracted tau fractions from slice cultures transduced at 0 DIV with either WT tau AAV or P301L/S320F tau AAV constructs at 1x10^11 viral genomes/ml, and treated with recombinant human HSPB1 at 50ng/ml for 14 DIV then harvested at 28 DIV

A) Representative western blot with antibodies against total tau (Dako Tau) and tau phosphorylated at Ser396/404 (PHF-1) with β-Actin used as a loading control, LSS = low speed supernatant, total fraction, SI = sarkosyl insoluble pellet, hyperphosphorylated tau fraction, the red box highlights the presence of hyperphosphorylated tau in the SI fractions B) Quantification of phosphorylated tau as a proportion of total tau in the LSS fractions, graph shows mean +/- SEM across 3 biological replicates C) Quantification of total sarkosyl insoluble tau as a proportion of total sarkosyl soluble and insoluble tau in the LSS fractions, graph shows mean +/- SEM across 2 biological replicates D) Quantification of tau phosphorylated at Ser396/404 (PHF-1) as a proportion of total tau in the sarkosyl insoluble fraction, graph shows mean +/- SEM across 2 biological repeats

5.4.5 Overexpression of astrocytic HSPB1 does not alter the levels of insoluble P301L/S320F tau in organotypic brain slice cultures

Having investigated the potential therapeutic effects of recombinant extracellular HSPB1 treatment on tau pathology in the slices, AAVs were utilised to overexpress astrocytic HSPB1 within the slice cultures to determine whether an increase in this astrocyte-derived human HSPB1 could potentially affect the neuronal tau induced by either the WT or mutant tau AAV constructs. A GFAP-HSPB1-AAV expressing HSPB1 specifically within the astrocytes under the GFAP promoter (pAAV[Exp]-GFAP(short)>hHSPB1[NM_001540.5](ns):P2A:TagBFP2:WPRE) was added directly to the slice media at 0 DIV at $2x10^{10}$ VG/well. An empty vector targeting astrocytes (pAAV[Exp]-GFAP(short)>TagBFP2:WPRE) was used under the exact same conditions as a control, referred to as GFAP-AAV.

Initial characterisation experiments were performed to determine firstly whether transduction with these AAVs were toxic to the slices. LDH assay for measuring cell toxicity showed there was no significant differences in cell death in those slices transduced with either control GFAP-AAV or GFAP-HSPB1-AAV constructs (*Figure 5.12A*).

Previous studies have shown that fusing sHSPs with various fluorescent proteins can potentially alter their chaperone function (Datskevich et al., 2012; Datskevich and Gusev, 2014). Therefore, polycistronic constructs were designed in which both HSPB1 and blue fluorescent protein (BFP) were both expressed under the GFAP promoter, in order to simultaneously express both within the same cell. As the AAVs are able to transduce any cell but are expressed only in those cells where the GFAP promoter is active, it was necessary to confirm whether the BFP and HSPB1 were expressed specifically in astrocytes. Initial immunofluorescence of the live slice cultures shows that the slices

have been transduced and that the AAVs are expressed by a set of the cells present within the slices, as indicated by the BFP seen in the images (*Figure 5.12B*). Co-localisation experiments with antibodies against astrocytes (GFAP) and human HSPB1 were performed but due to technical problems these were not completed and would need to be repeated in order to confirm the specific localisation of the AAVs. Although it was not confirmed in these experiments, previous studies have demonstrated the localisation of GFAP-AAVs to the astrocytes in the slice cultures so it can be assumed the expression shown here is also restricted to astrocytes (Croft et al., 2019; Goodwin et al., 2020).

Lastly, slices transduced with GFAP-AVV and GFAP-HSPB1-AAV were lysed and western blotting was performed to determine whether HSPB1 overexpression can be detected. Lysates were probed with an antibody against human HSPB1 which detected human HSPB1 in those slices transduced with GFAP-HSPB1-AAV and not GFAP-AAV, confirming HSPB1 overexpression by the GFAP-HSPB1-AAV construct only (*Figure 5.12C*).

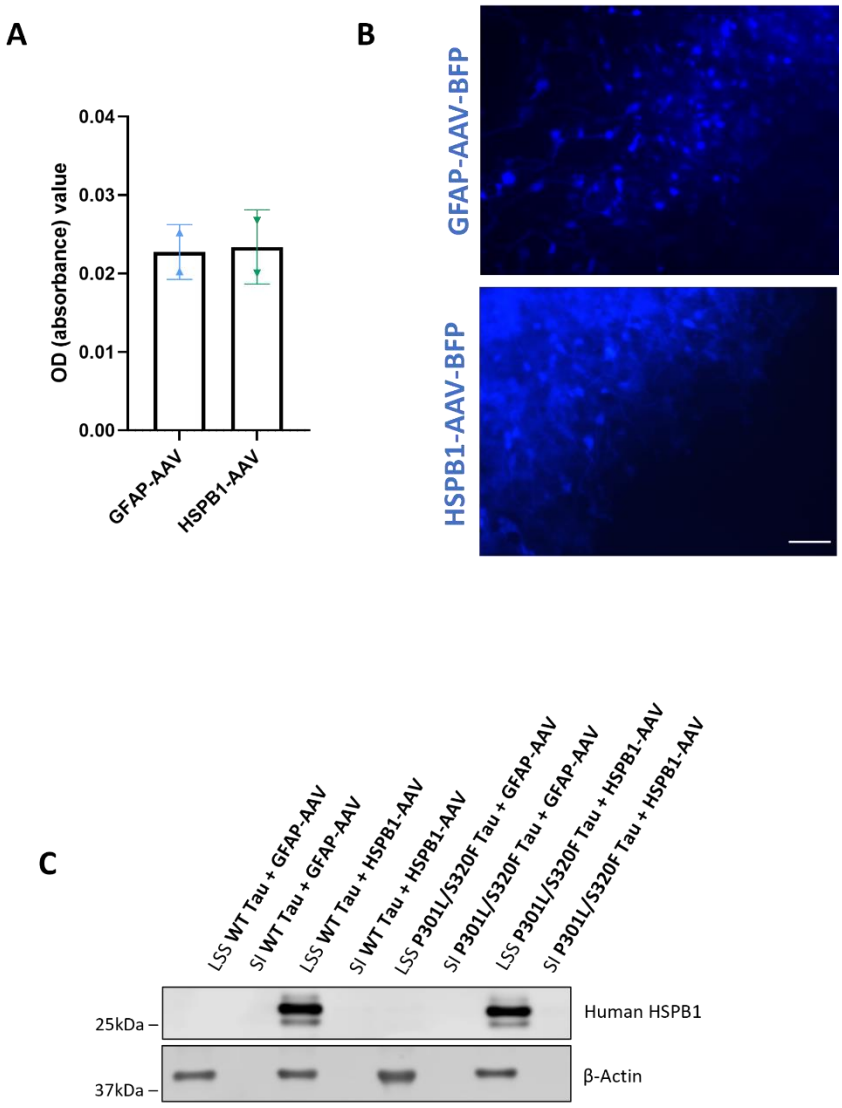

Figure 5.12: Immunoblotting and immunofluorescent characterisation experiments of CD1 WT organotypic brain slice cultures transduced with GFAP-BFP AAV and GFAP-HSPB1-BFP2 at 2x10^10 VG/ml at 0 DIV and collected at 28 DIV.

A) LDH assay was performed using slice media OD values which were normalised to OD values of slice lysates, graph shows data from two slices take from one biological repeat +/- SD. B) Representative live images of the GFAP-AAV and GFAP-HSPB1-BFP2 AAV transduced slices at 28 DIV, images were taken with Evos fluorescence microscope, scale bar = 52µ, C) Representative western blot with probes against human HSPB1, with ß-Actin used as a loading control, LSS = low speed supernatant, total tau fractions, SI = sarkosyl insoluble pellet, hyperphosphorylated tau fraction

To investigate whether overexpressing astrocytic HSPB1 can modulate AAV-tau pathology, slice cultures were transduced with both tau AAV constructs and HSPB1-AAV concurrently at 0 DIV and harvested for sarkosyl extraction of aggregated tau at 28 DIV. As before, the total tau (low speed supernatant) and hyperphosphorylated tau aggregates (sarkosyl insoluble pellet) were analysed using immunoblotting. As seen in previous tau-AAV characterisation experiments, there was an increase in the levels of phosphorylated tau normalised to total tau (PHF-1/Dako Tau) in those slices transduced with P301L/S320F tau compared to slices transduced with the WT tau AAVs (*Figure 5.13B*). The levels of phosphorylated tau/total tau in those slices transduced with GFAP-HSPB1-AAV were not significantly different to the levels seen in the GFAP-AAV transduced slices, when the slices were also transduced with either the WT tau or P301L/S320F tau AAV constructs (*Figure 5.13B*).

WB quantification was also performed to determine whether there was any difference in the levels of total insoluble tau between slices transduced with P301L/S320F tau and treated either GFAP-AAV or GFAP-HSBP1-AAV. The levels of total tau in the sarkosyl insoluble fraction were determined as a proportion of the total soluble and insoluble tau in the LSS fraction. Analysis revealed an increase in overall insoluble tau in slices transduced with GFAP-HSPB1-AAV compared to GFAP-AAV (*Figure 5.13C*). Next, the levels of tau phosphorylated at Ser396/404 (PHF-1) in the sarkosyl insoluble fraction as a proportion of total tau found in the sarkosyl insoluble fraction was quantified to assess the relative proportion of insoluble tau phosphorylation in those slices transduced with either GFAP-AAV or GFAP-HSPB1-AAV. The results reflected what was seen in the previous quantification of insoluble tau as there was an increase in the proportion of phosphorylated insoluble tau in those slices transduced with GFAP-HSPB1-AAV compared to those slices transduced with GFAP-AAV (*Figure 5.13D*). These results reveal that the increase in total insoluble tau seems to increase in a similar manner to the levels of phosphorylated insoluble tau in those slices transduced with GFAP-

HSPB1-AAV compared to those slices transduced with GFAP-AAV, and so the overall proportion of phosphorylated tau does not change (*Figure 5.13B*).

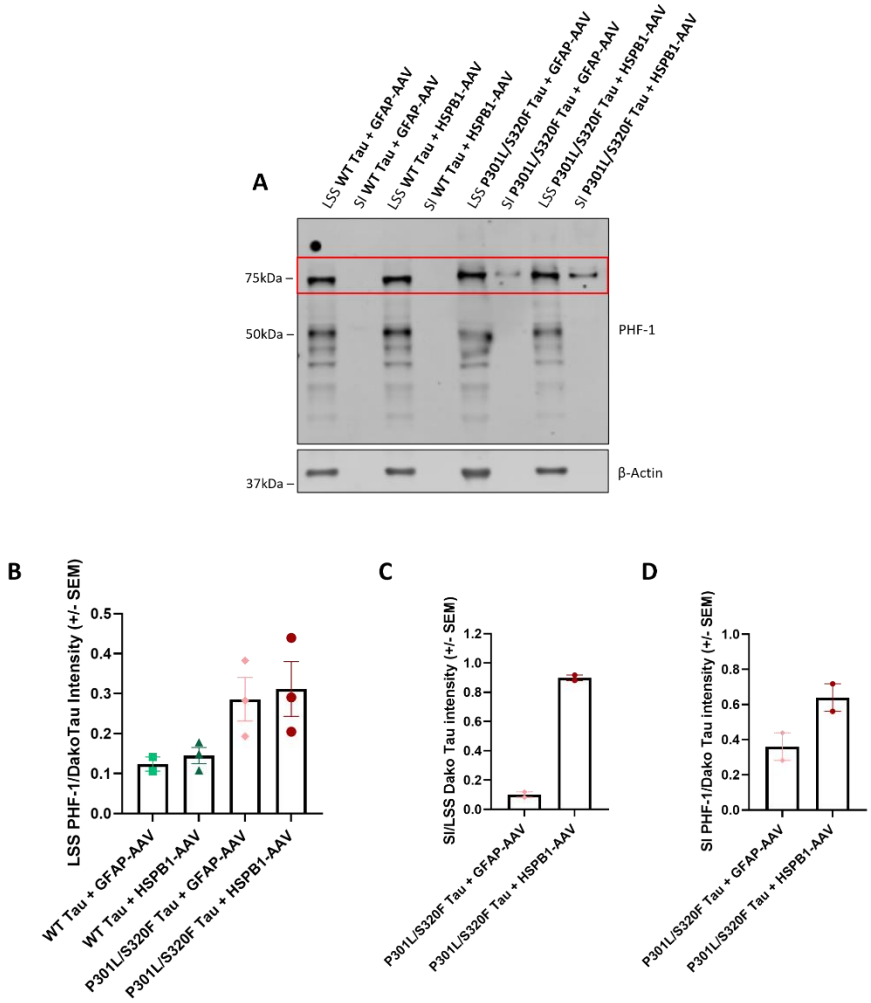

Figure 5.13: Levels of tau pathology in sarkosyl extracted tau fractions taken from slice cultures transduced at 0 DIV with either WT tau AAV or P301L/S320F tau AAV constructs at 1x10^11 viral genomes/ml, and transduced with GFAP-BFP AAV or GFAP-HSPB1-BFP2 at2x10^10 VG/ml at 0 DIV and collected at 28 DIV.

A) Representative western blot with probes against total tau (Dako Tau) and tau phosphorylated at Ser396/404 (PHF-1) and ß-Actin used as a loading control, LSS = low speed supernatant, total tau fractions, SI = sarkosyl insoluble pellet, hyperphosphorylated tau fraction, the red box highlights the presence of hyperphosphorylated tau in the SI fractions B) Quantification of phosphorylated tau as a proportion of total tau in the LSS fractions, graph shows mean +/- SEM across 3 biological replicates, C) Quantification of total sarkosyl insoluble tau as a proportion of total sarkosyl soluble and insoluble tau in the LSS fractions, graph shows mean +/- SEM across 2 biological replicates D) Quantification of tau phosphorylated at Ser396/404 (PHF-1) as a proportion of total tau in the sarkosyl insoluble fraction, graph shows mean +/- SEM across 2 biological repeats

5.5 Discussion

In order to investigate the non-cell autonomous function of astrocytic HSPB1 in AD, the organotypic brain slice culture model was initially used to replicate some of the known pathological features of neurodegeneration. Slices were treated with TNFα and IL1α, cytokines known to be released by activated microglia (Liddelow et al., 2017), which led to the induction of reactive astrocytes, as seen in human neurodegenerative disease. Next, the slices were transduced with tau-AAVs in order to induce sarkosyl insoluble tau pathology. To then investigate the potentially protective non-cell autonomous function of extracellular HSPB1, slices were firstly treated with recombinant human HSPB1. In the slices treated with TNFα and IL1α, the anti-inflammatory potential of HSPB1 was investigated by determining whether the treatment with recombinant HSPB1 was able to modulate the induction of reactive astrocytes, as confirmed by the increase in reactive astrocyte marker LCN2 (Chapter 4, Section 4.4.2). Recombinant HSPB1 treatment did not significantly reduced the levels of reactive astrocytes in the cytokine treated slices and it did not affect synaptic or neuronal health. Next, the non-cell autonomous chaperone function of HSPB1 was tested by exploring whether recombinant HSPB1 treatment could modulate the P301L/S320F tau accumulation within primary mouse neurons and the organotypic brain slice model. Treating the P301L/S320F tau transduced neurons with recombinant HSPB1 protein reduced the levels of MC1 positive foci, highlighting the potentially protective role of HSPB1 in the reduction of misfolded tau. Lastly, human HSPB1 was overexpressed in the astrocytes of those slices transduced with tau-AAVs as a second method to explore the potentially protective non-cell autonomous role of HSPB1. Overexpression of astrocytic HSPB1 had no effect on the tau pathology induced by either of the tau-AAV constructs. Further work is required to investigate the potentially protective functions of HSPB1 within the context of AD and neuronal tau accumulation.

5.5.1 Recombinant HSPB1 treatment in slices treated with cytokines TNFα and IL1α

Organotypic brain slice cultures treated with AD-relevant cytokines TNFα and IL1α were characterised in Chapter 4, Section 4.4.2 of this thesis. It was found that a 24 hour treatment with 30ng/ml TNFα and 3ng/ml IL1α lead to an increase in reactive astrocyte marker LCN2 in the slices and a trend towards an increase in HSPB1 in reactive astrocytes. However, when slices were co-treated with TNFα and IL1α, together with recombinant HSPB1 for 24 hours, there were no changes in the cytokine-induced increase in reactive astrocytes. Due to the primarily anti-inflammatory nature of the sHSPs explored in various mouse models of disease (Ousman et al., 2007; Guo et al., 2019; Teramoto et al., 2013) and the anti-inflammatory potential of extracellular HSPB1 (Kurnellas et al., 2012), it was hypothesised that treatment of slices with cytokines would reduce the pro-inflammatory response, and this would reduce the cytokine-induced increase in the reactive astrocyte marker LCN2. This may not have been the case in the studies presented here for a number of technical reasons. Firstly, the changes induced by TNFα and IL1α treatment, although increased, were not robust enough since the number of biological repeats was lower than what had been previously performed in Chapter 4. Most probably, this prevented for any potential effect upon treatment with HSPB1 to be detected. To address this, it could be advisable to treat the slices with TNFα and IL1α for longer than 24 hours to try to amplify any potential change in the cytokine treated slices in order to investigate any potential rescue with HSPB1. Preliminary data from our lab suggests that a 72 hour treatment with TNFα and IL1α does not dramatically alter any changes seen in the treated slices compared to those slices treated for 24 hours (*Figure 5.14*). A pre-treatment with recombinant HSPB1 in combination with extended treatment time may be necessary to elicit any protective change, as was demonstrated by *Nahomi et al., 2013,* when a pre-treatment with CRYAB 6 hours before, and then once a day for 4 days after insult protected from cell apoptosis in a rat model of cataract development (Nahomi et al., 2013).

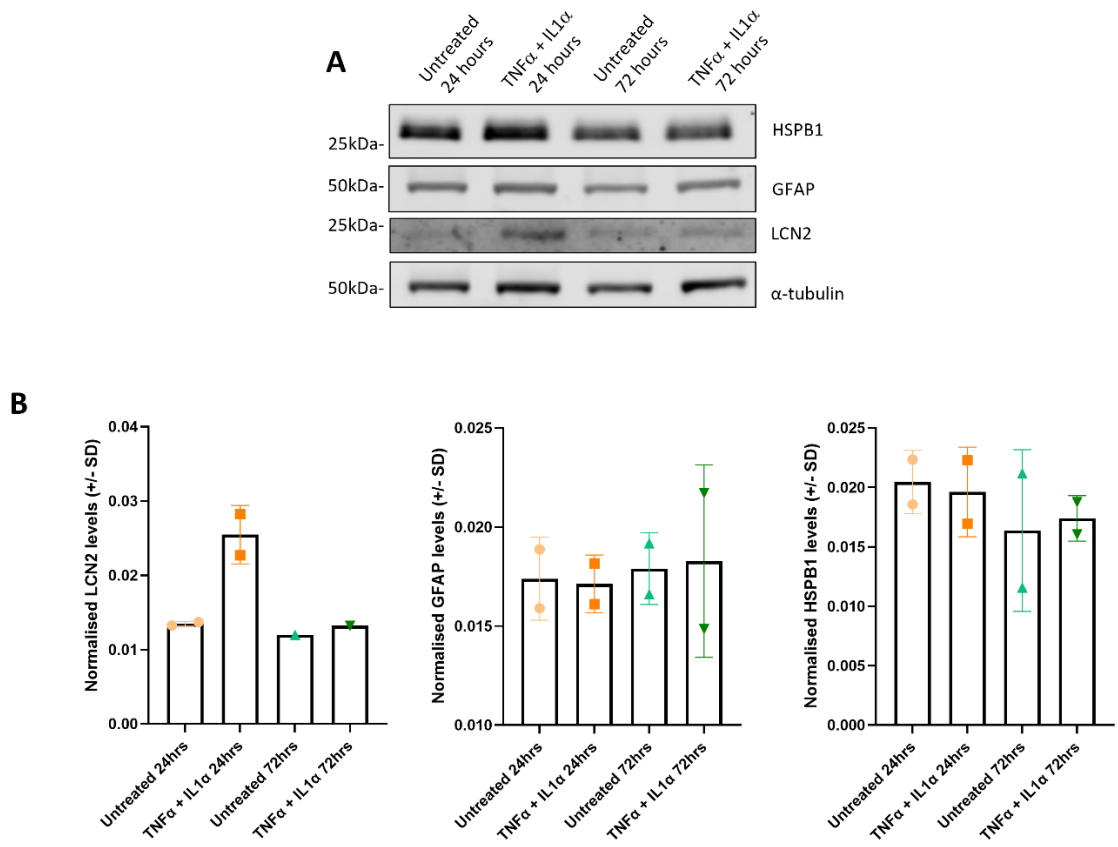

Figure 5.14: Preliminary data showing 21 DIV CD1 slices treated with cytokines TNFα and IL1α for 24 or 72 hours.

A) Representative blot with antibodies against HSPB1, reactive astrocytes (GFAP and LCN2) and loading control α-tubulin. B) The levels of LCN2, GFAP and HSPB1 were normalised against the loading control, graphs show two technical repeats taken from one mouse pup, mean +/- SD

In addition to the length of the recombinant HSPB1 treatment, further consideration must be taken in relation to the concentration of recombinant HSPB1 used in these slice culture experiments. To determine the physiologically relevant levels of recombinant HSPB1 to use, the culture media from primary astrocytes overexpressing HSPB1 was collected and analysed by western blot. Different concentrations of recombinant HSPB1 were then compared to the levels secreted by the astrocytes to determine the amount of HSPB1 that is secreted into the media. The final concentration of recombinant HSPB1 necessary to treat neurons was set to be four times the levels of protein found

in the astrocyte condition media in order to have the treatment in excess but to still remain within physiological levels (Caldwell et al., 2020). A concentration of 50ng/ml had a positive effect on neurons, however this may not be directly applicable to the organotypic brain slices cultures as they are a more complex system containing a number of different cell types acting in synergy (Croft and Noble, 2018). The data presented in this chapter showing a protective response elicited in the primary mouse neurons using 50ng/ml HSPB1 treatment but not in any of the slices treated with the same concentrations supports this idea. Therefore, further dose response experiments should be carried out to determine the optimal levels of recombinant HSPB1 required to elicit a response in the slices, while trying to remain within a physiologically relevant range of treatment.

Finally, in order to explore the potentially protective function of HSPB1 in human disease, the human recombinant HSPB1 protein and AAV expressing HSPB1 were chosen for the extracellular treatments of both the primary neuron cultures and the organotypic slice cultures. It is necessary to emphasise that both neurons and slices were cultured from mice, whilst the recombinant HSPB1 is the human form, and although the proteins have high levels of similarity, it is still possible that the human HSPB1 may not have the full physiological effect that could be seen when using a mouse recombinant HSPB1 for the treatment of mouse cells.

5.5.2 Exploring the potentially protective role of recombinant HSPB1 in reducing the accumulation of P301L/S320F tau

There are a number of studies that support the interaction of HSPB1 with tau. HSPB1 has been shown to recognise aggregation-prone regions of tau (Freilich et al., 2018) and by directly interacting with certain tau species, HSPB1 is able to reduce tau misfolding and reducing the formation of tau fibrils (Lin et al., 2020; Baughman et al., 2018; Abisambra et al., 2010). Not only this, but sHSP

including HSPB1, have been shown to contribute to the reduction in both soluble and aggregated tau deposits (Webster et al., 2020; Chiang et al., 2021). Taking the literature into account, it was hypothesized that the P301L/S320F tau accumulation seen in the transduced organotypic brain slice cultures would be somewhat diminished in those slices treated with extracellular HSPB1.

In Chapter 4 of this thesis, slices transduced either with the WT tau or pro-aggregatory P301L/S320F tau AVV constructs were characterised. It was shown that slices transduced with either of the constructs exhibited tau phosphorylated at Ser396/404, as detected by the PHF-1 antibody. More interestingly, slices transduced with the P301L/S320F tau AAV were able to accumulate sarkosyl insoluble hyperphosphorylated tau, found primarily in the somadendritic departments of neurons. In order to further characterise the use of the tau AAVs as a system to induce physiologically relevant tau aggregates, primary mouse neurons were also transduced with either the WT Tau or P301L/S320F tau AAVs. The results of primary neurons transduced with both tau-AAV constructs reflects those results seen in the organotypic brain slice cultures. Both tau constructs were able to induce changes in tau conformation, detected using the MC1 antibody. This MC1 antibody recognises a fold conformation of tau containing amino acids 2-10 and 312-342 and reacts with aggregated tau found in human paired-helical fibrils and neurofibrillary tangles (Jicha et al., 1998; Wolozin and Davies, 1987). In those neurons transduced with the P301L/S320F tau AAV, tau inclusions developed, mainly surrounding the nucleus of the neurons. Further to this, treating the neurons with extracellular recombinant HSPB1 resulted in the reduction of this abnormal tau when analysed by immunofluorescence. These results support the use of the AAVs in primary neurons as a system to study the potentially protective role of HSPB1 in relation to tau pathology.

Having established the potential chaperone function of HSPB1 in reducing tau pathology in the neurons, it could be interesting to further investigate the protective function of this extracellular

HSPB1 on neuronal health. As an association between tau and synapses has been established in AD, with tau mislocalisation from the cytoplasm to synaptic fractions being a strong correlate with AD-related dementia (Perez-Nievas, et al., 2013), whilst also representing a key hallmark in the tauopathy brain (Braak et al., 2011). Pre-synaptic release of tau can lead to further dysregulation of synapses in AD (John and Reddy, 2021), whilst the increased levels of tau at the post-synaptic sites can negatively affect memory and synaptic plasticity (Yu and Lu, 2012). Synapse loss has also been shown to strongly correlate with AD progression and cognitive decline (DeKosky and Scheff, 1990; Chen et al., 2018), and so it seems sensible to investigate synaptic health using the tau transduced neurons. The preliminary western blot analysis of AAV transduced neurons indicated a potential rescue of the reduction of both pre- and post-synaptic proteins after treatment with recombinant HSPB1. Further preliminary western blot analysis found a decrease in cleaved caspase-3, an indicator of apoptosis, but which is also involved in non-apoptotic processes such as modulation of synaptic function (D'Amelio et al., 2012). These experiments would need to be repeated but taken together, these results could imply that the addition of extracellular HSPB1 might be neuroprotective in potentially reducing the synaptotoxic effect of the mutant tau-AAVs. To confirm this, further markers of neuronal health and neuronal complexity could also be carried out through high resolution confocal microscope analysis of dendritic spine density, neurite length and the number of neuronal nodes and roots (Perez-Nievas et al., 2021).

In contrast to the primary neuron data, western blot analysis of the sarkosyl-insoluble tau fraction of lysates from slice transduced with P301L/S320F tau AAV and treated with recombinant HSPB1 revealed there was no significant changes in the levels of phosphorylated tau at Ser396/404 as a proportion of total tau in slices treated with recombinant HSPB1. Further to this, recombinant HSPB1 treatment did not alter the levels of insoluble overall tau either, as quantified by investigating the total levels of tau found in the sakosyl insoluble fractions as a proportion of the total tau levels found in the LSS fraction containing both sarkosyl soluble and insoluble tau. This is at odds with the

reduction in the MC1 positive foci found in those neurons transduced with P301L/S320F tau and treated with recombinant HSPB1.

The most plausible explanation as to why we did not see the expected chaperone functions of HSPB1 in the organotypic brain slice cultures is due to the localisation of HSPB1 and the client protein, tau. Whilst the treatment with recombinant HSPB1 investigates the role of extracellular HSPB1 (Reddy et al., 2018; den Broek et al., 2021), the tau induced in these slice cultures and in the primary cultures is found within the neurons, and so potential chaperone function would depend on internalisation of HSPB1 by the neurons. This process could be further explored using a model similar to the SH-SY5Y cells which were differentiated to create a neuron-like model and used to monitored the uptake of tau antibodies and subsequent interaction with fluorescently-tagged PHF tau within the cells (Shamir et al., 2020). An additional reason for the lack of HSPB1 chaperone function could be due to the specificity required for functional tau-HSPB1 interactions. It has been shown that different chaperones are only able to suppress the aggregation of a few specific tau variants, as well as acting at different stages of the tau fibrilization process (Mok et al., 2018). For example, both CRYAB and HSPB1 were only able to act on the tau elongation process (Mok et al., 2018), which may not be as abundant in the slice cultures as late as 28 DIV and so by this point, any potential changes elicited by HSPB1 chaperone function may already have been missed in those slices treated with recombinant HSPB1 at 14 DIV. Not only must the tau species be eligible for interaction with HSPB1, but HSPB1 must also be in the correct state in order to carry out its chaperone functions. Mechanistic studies into HSPB1 functionality have described numerous potential binding sites of HSPB1 where tau is able to bind, but it seems only tau bound to the n-terminal region of HSPB1 can lead to productive chaperone activity (Baughman et al., 2020). In addition to this, the comparison of HSPB1 and its phosphorylated variant also demonstrated the need for HSPB1 to be functionally dynamic and able to switch between the non- and phosphorylated forms to enable any interaction with the tau

protein (Abisambra et al., 2010). As organotypic brain slice cultures are a relatively large *ex vivo* model, it could be possible that the levels of tau produced by transduction with the P301L/S320F construct is so vast that the potentially protective functions of HSPB1 are not strong enough to be detected. It would perhaps be better, therefore, to investigate region specific changes in tau, such as tau co-localisation at the synapse (Perez-Nievas et al., 2013), through isolation of synaptic vesicles (Ahmed et al., 2013) within the organotypic brain slice cultures. Following on from this, as suggested by data presented on synaptic changes in the primary neuron cultures in this chapter, the levels of synaptic markers and synaptic function (Greenberg et al., 1985; Gotoh et al., 1999) could also be measured.

Finally, to further explore the protective function of HSPB1, it may also be necessary to extend the investigation into the anti-apoptotic function of this sHSP. Whilst apoptosis was briefly explored by measuring the levels of cleaved caspase-3 in immunoblotting analysis of cytokine treated slices and tau-AAV transduced neurons, the range of techniques could be extended to include a number of immunohistochemical protocols including Neutral Red or Methyl Green staining for apoptotic cells by which chromatin condensation is visualised, TUNEL (TdT-mediated dUTP-biotin nick end labelling) staining to detect DNA fragmentation which occurs during apoptosis (Lee and McKinnon, 2009) or other biochemical techniques for detecting caspase activity like the luminescent cell-based assay Caspase-Glo (Promega) (Gianinazzi et al., 2004).

It important to note that due to extra time constraints and external disruptive factors, it was only possible to achieve relatively low numbers of replicates for the slices transduced with the tau-AAVs and treated with either recombinant HSPB1 or overexpressed HSPB1. In addition to this, some experiments may have been negatively impacted by a large number of complete power outages which affected our building and therefore the conditions under which the slices were incubated

often fluctuated, potentially increasing the levels of cell stress within the cultures. For these reasons, to fully determine whether HSPB1 is able to impact the tau pathology induced in these slices, it is vital to replicate these experiments a further three times, to obtain a total number of 6 replicates necessary to achieve significant and reliable results when working with brain slice cultures, as demonstrated by characterisation of slices treated with cytokines (Chapter 4, Section 4.4.2).

Chapter 6: Discussion

The overall hypothesis for this PhD thesis was that the upregulation of HSPB1, specifically in reactive astrocytes, is neuroprotective against tau pathology in a non-cell autonomous manner. To investigate this hypothesis, it was first necessary to explore the localisation and expression of HSPB1 in the context of the human disease and so immunofluorescence analysis was carried out using post-mortem brain tissue sections from AD cases of different Braak stages. To explore the potentially non-cell autonomous role of HSPB1, a model was required which would allow us to explore the interaction between different cell types (Croft and Noble, 2018). Therefore, organotypic brain slice cultures were treated with various stimuli to replicate AD-relevant conditions in order to study the potentially non-cell autonomous role of HSPB1 in the context of disease. Finally, the brain slices were treated with either extracellular HSPB1 or HSPB1 was overexpressed in astrocytes to determine whether either modification can provide neuroprotection against tau-AAV induced pathology.

6.1 HSPB1 levels are increased in reactive astrocytes in AD brain

Previous studies have found that in the AD brain, there is high expression of HSPB1 in those reactive astrocytes residing across the neocortex and the hippocampus. Further to this, these HSPB1 positive astrocytes were also shown to be frequently found near to amyloid plaques (Renkawek et al., 1994; Wilhelmus et al., 2006), although in *Wilhelmus et al., 2006* this conclusion was made whilst the data was not shown. These aforementioned studies were performed using immunohistochemical analysis on serially stained sections to confirm the presence of HSPB1 within astrocytes, rather than dual immunofluorescence staining using the same tissue section, and therefore no formal co-localisation analysis was performed. To address this issue, immunofluorescence was performed using markers

for reactive astrocytes (GFAP), HSPB1 and amyloid-β (6E10) on sections of the temporal cortex, taken from cases ranging in severity from Braak II to Braak VI. It was found, as was previously reported, that the majority of GFAP-positive astrocytes were also HSPB1 positive and as the severity of disease increased, the number of concurrently GFAP- and HSPB1-positive cells seemed to also increase. These results are supported by recent transcriptome studies which not only found that HSPB1 is specifically upregulated in astrocytes during AD (Grubman et al., 2019; Smith et al., 2022; Lau et al., 2020), but there is also an upregulation of HSPB1 in those cases determined to have late-stage AD pathology compared to early-stage AD pathology (Mathys et al., 2019).

sHSPs have not only been seen to be upregulated in AD, but also in a number of tauopathies (López-González et al., 2014; Dabir et al., 2004). CRYAB is robustly upregulated in astrocytes found in number of tauopathies which involve significant glial contribution such as PSP and FTD17, and whilst the levels of HSPB1 are not as significantly increased in these tauopathy brains compared to CRYAB, it was found that all HSPB1 also co-localised with reactive astrocytes (López-González et al., 2014; Dabir et al., 2004).. It can be hypothesised that this upregulation of astrocytic sHSPs in tauopathy disorders occurs as a protective mechanism against this accumulation of tau.

In order to investigate the potential role of this increased HSPB1 in the reactive astrocytes found in AD, the organotypic brain slice cultures were treated with microglial cytokines TNFα and IL1α, known to induced reactive astrocytes in neurodegenerative disease (Liddelow et al., 2017). Data generated from Fangjia Yang in our laboratory has previously found that treating primary mouse astrocytes with these same cytokines led to a significant increase in the levels of the pan-reactive astrocyte markers LCN2 and Serpin3a, both known to be highly expressed in reactive astrocytes responding to injury (Zamanian et al,, 2012; Das et al., 2020). In addition to this, there was also an increase in the pro-inflammatory cytokine IL-6, the cytokine produced not only by astrocytes but

also by other glia cells and neurons (Kummer et al., 2021). In slices treated with TNFα and IL1α for 24 hours, reactive astrocytes were induced, as demonstrated by the significant increase in LCN2 levels, alongside preliminary ELISA data from Caoimhe Goldrick in our laboratory, which also found an increase in IL-6 levels in the media obtained from the TNFα and IL1α treated slices. In response to this induction of reactive astrocytes, there was also a trend towards an increase in HSPB1 in those slices treated with cytokines TNFα and IL1α, similar to what has been previously published about reactive astrocytes in human AD brain (Renkawek et al., 1994; Wilhelmus et al., 2006) and presented in Chapter 3, Section 3.4.3 of this thesis.

One potential function of this trending increase of HSPB1 in reactive astrocytes could be to fulfil an anti-inflammatory response to mediate against the induced pro-inflammatory environment. The anti-inflammatory potential of CRYAB has also been demonstrated through the use of a CRYAB knock-out mouse modelling EAE, where this mouse was shown to exhibit increasingly widespread inflammation, enhanced infiltration of activated CD4+ lymphocytes and macrophages, and higher levels of glial apoptosis compared to the corresponding wild type animals (Ousman et al., 2007; Arac et al., 2011). In addition, overexpressing HSPB1 in a cellular model of HD protected from poly(Q) aggregation and the subsequent cell death by reducing the levels of reactive oxygen species (Wyttenback et al., 2002). In contrast to this, there are some studies which highlight the potentially pro-inflammatory role of HSPB1, for example, treating macrophage cultures with recombinant HSPB1 has been shown to activate NF-κB signalling, resulting in the upregulation of anti-inflammatory factors IL-10 and GM-CSF but also the upregulation of pro-inflammatory factors IL-1β and TNFα (Salari et al., 2013). Another *in vitro* astrocyte study found that treatment with HSPB1 was seen to induce the production of IL-8 whilst reducing the expression of anti-inflammatory growth factor-β1 (TGF-β1) (Bruinsma et al., 2011). And finally, inducing neuroinflammation through ethanol-induced brain injury in the transgenic mouse overexpressing HSPB1 led to an increased expression of

pro-inflammatory cytokines TNF and IL1β, alongside an increase in astrocyte and microglia activation (Dukay et al., 2021). Intriguingly, this increase in neuroinflammation did not result in neuronal damage or apoptosis, highlighting the complex nature of HSPB1 involvement in the regulation of inflammation (Dukay et al., 2021). These studies highlight the necessity in exploring the specific cell autonomous role of HSPB1 in regards to inflammation during AD.

A previous study exploring the genes encoding nine chaperone gene families including, HSP90, HSP70, HSP60 and the sHSPs, identified a highly interconnected chaperome subnetwork which displays specific repression and induction expression patterns during normal human ageing and AD (Brehme et al., 2014). HSPB1 was among this chaperome system and was found to be consistently increased during ageing and disease together with other sHSPs, whilst other chaperone families such as HSP90 were found to be significantly repressed (Brehme et al., 2014; Mayer, M. 2013). sHSPs are predominantly expressed in glial cells during neurodegeneration, as shown in the literature (Grubman et al., 2019; Smith et al., 2022; Mathys et al., 2019, López-González et al., 2014; Dabir et al., 2004) and in the human brain data from this thesis. The mechanisms behind an increased expression of sHSPs in disease has not been explored and it could be speculated that upregulation of glial sHSPs could occur in response to the reduction of other neuronal chaperone families seen during aging and AD (Brehme et al., 2014), and it may be a compensatory mechanism to help overcome the loss of neuronal proteostasis which occurs during AD (Inhara et al., 2012).

This increase in HSPB1 expression may be induced by a number of transcription factors. The main transcription factor for chaperones, HSF1, when in cross-talk regulation with nuclear factor (erythroid-derived 2)-like 2 (NRF2), has been shown to upregulate a number of sHSPs, including HSPB1 as well as increasing antioxidant enzyme expression in AD (Ramon et al., 2016; Ramos et al., 2018). Further to this, it was also found through knockdown experiments in *C. elegans* modified to

overexpress HSPB1, that NRF2 and HSF-1 may be responsible for the life extension seen in this model (Alexander et al., 2022). In a tau-induced cell model treated with flavones, an antioxidant and anti-inflammation molecule (Kumar and Panday, 2013), it was suggested that flavone treatment may increase HSPB1 expression through NRF2 upregulation (Chiang et al., 2021). Contrary, a recent systematic review of immunohistochemical studies in post-mortem AD brain followed by bioinformatics analyses, identifed a number of functional alterations and changes in protein levels in astrocytes in AD, and these included proteostasis and HSPB1. For HSPB1, CTCF and ESR emerged as potential transcription factors responsible for these functional changes (Viejo et al., 2022). CTCF depletion in mice has been shown to lead to overexpression of inflammatory genes in the brain (McGill et al., 2018) and ESR1 and ESR2 have been seen to be overexpressed in astrocytes in AD (Lu et al., 2003). This suggests a potential link between these transcription factors and an increase in HSPB1 in AD, however further investigation is required to fully determine the master regulators of astrocytic HSPB1 in AD.

6.2 Exploring the non-cell autonomous function of HSPB1

In the human brain there is evidence of an association between HSPB1 and Aβ, with HSPB1 co-localising with Aβ in 15% of all cortical amyloid plaques (Wilhelmus et al,, 2006). This is supported by a study exploring two different mouse models of AD, the Tg2576 transgenic mouse expressing AAP with Swedish mutations (Hsiao et al., 1996) and the APPswe/PS1dE9 double transgenic mouse expressing both human and mouse APP (Jankowsky et al., 2004), in which plaques are apparent from 11-12 months of age. In these mice HSPB1 was found in the penumbral area surrounding these plaques (Ojha et al., 2011). Our data also supports these findings since it was observed that not only there were more HSPB1 positive reactive astrocytes in close proximity to the plaques compared to far from the plaques, but HSPB1-positive staining was also observed within the plaques, implying that HSPB1 is not only intracellular but it can also be released from the astrocytes. This increase in

HSPB1 into the extracellular space in close proximity to amyloid plaques has been explained as an active, rather than a passive release brought on by possible cell death (Ojha et al., 2011). It has been suggested that exposure to Aβ triggers the exosomal release of astrocytic HSPB1 and then this secreted HSPB1 goes on to interact with this extracellular Aβ (Nafar et al., 2016). HSBP1 may then act as a chaperone to mediate the sequestration of toxic Aβ oligomers into non-toxic Aβ aggregates (Ojha et al., 2011; Kudva et al., 1997) as a protective role against AD-related pathology. Taken together, these results support the notion of the non-cell autonomous role of astrocytic sHSPs and the importance of the continued study of these functions in AD.

In order to study the potentially protective non-cell autonomous role of sHSPs in the context of AD, the organotypic brain slice culture model was set-up and treated with various stimuli. The brain slice cultures contain all the relative neuronal and non-neuronal cell types usually found within the brain, in the correct physiological proportions which are all functionally and anatomically connected to form one complete integrated system (Croft and Noble, 2018; Bahr, 1995; Staal et al., 2011; del Rio, 1991). In addition to this, the slice cultures allow easy manipulation of the molecular processes which are usually inaccessible *in vivo* (Harwell and Coleman, 2016). Therefore, the slice culture model was selected for this PhD project as it allows for the study of the non-cell autonomous function of astrocytic sHSPs within an easily inducible system capable of replicating some of the relevant AD pathology.

As previously mentioned, in those slice cultures treated with cytokines TNFα and IL1α there was an increase in reactive astrocyte marker LCN2 and preliminary data from the laboratory also indicated and increase in pro-inflammatory cytokine IL-6. To investigate the hypothetical protective functions of extracellular sHSPs in response to this pro-inflammatory environment, slices were further treated with recombinant human HSPB1 protein to mimic the HSPB1 release triggered in response to

pathological changes (den Broek et al., 2021). Although sHSPs are classically known to perform intracellular functions, the extracellular presence of HSPB1 has been indirectly suggested by the increasing evidence showing that HSPB1 is detected at slightly higher levels in the CSF of AD patients compared to healthy individuals (Sathe et al., 2019; Bai et al., 2020; Bader et al., 2020). Furthermore, the presence of sHSPs has been confirmed within the exosome (Sreekumar et al., 2010; Reddy et al., 2018) and more relevantly, HSPB1 is released in exosomes from primary rat astrocytes after stimulation with Aβ (Nafar et al., 2016). On the contrary, Fangjia Yang in our group detected HSPB1 in the conditioned media of primary mouse astrocytes and found HSPB1 was not present in extracellular vesicles. Instead, HSPB1 was found in the extracellular media as a free protein. Therefore, to replicate this physiological free HSPB1, this project utilises a treatment with recombinant HSPB1 to investigate the potentially protective nature of the extracellular sHSPs.

Slice cultures were simultaneously treated with cytokines TNFα and IL1α and recombinant human HSPB1 to test the effect of extracellular HSPB1 on astrocyte reactivity. However, in these experiments, the initial cytokines treatments resulted in a weak change in the slices as reactive astrocytes were not induced compared to the untreated slices, which in turn prevented the detection of any potential effect upon treatment with recombinant HSPB1. Although we could not confirm it in this thesis, there are a number of studies which indicate that extracellular sHSPs provides protection due to their anti-inflammatory roles. Exposure to extracellular sHSPs appears to activate macrophages during inflammatory stress, stimulating the release of anti-inflammatory cytokines and chemokines (Bhat and Coleman, 1999; De et al., 2000; van Noort et al., 2010; Banerjee et al., 2011). Over the years, there have a been a number of studies testing the potentially anti-inflammatory roles of CRYAB using various animal disease models in which neuroinflammation is seen to be a key pathological event. For example, in models of EAE, administering CRYAB was able to suppress LPS-induced inflammation and markedly improved symptoms and outcome (Guo et al.,

2019). CRYAB has also been seen to elucidate a protective neuroglial response in a model of tauopathy (Hampton et al., 2020). In the P301S tauopathy mouse model, CRYAB was intracerebrally infused into 8 week old mice leading to a rescue of neuronal loss in the outer cortical layers of the brain, presenting the first experimental evidence in the support of the neuroprotective role or CRYAB in a model of tau-related neurodegeneration (Hampton et al., 2020).

There have been fewer studies exploring the anti-inflammatory properties of HSPB1, however, given the structural homology between sHSPs, it is highly likely both sHSPs share some similar anti-inflammatory functions (van Noort et al., 2012). The protective role of HSPB1 has also been mainly studied after ischemic stroke, where levels of astrocytic HSPB1 are upregulated (Bartelt-Kirbach and Golenhofen, 2014). It was found that an injection of human-derived HSPB1 into a mouse after cerebral ischemia provided neuroprotection against inflammation-related neuronal death (Teramoto et al., 2013). Further to this, it has been demonstrated that HSPB1 can also modulate the immune response in atherosclerosis through modulating NF-κB activity in macrophages (Batulan et al., 2016). All in all, this literature strongly supports a protective anti-inflammatory role for extracellular sHSPs.

In order to replicate the tau pathology seen in human AD, slice cultures were transduced with P301L/S320F tau AAV constructs (Croft et al., 2019), kindly gifted by Dr Cara Croft and Prof Todd Golde. Although this model utilises a tau construct reliant on a mutation that it is associated with the tauopathy FTD-17, but not found in AD, it is the first slice model which has recapitulated tau inclusion pathology resembling the NFT in human AD (Croft et al., 2019; Grundke-Iqbal et al., 1986; Murray et al., 2014), whilst also displaying pathology which is localised to the AD-relevant neuronal compartments (Uchihara et al., 2001). Other slice models prepared from transgenic mice lines have failed to replicate robust tau inclusions (Croft et al., 2017; Croft et al., 2017; Messing et al., 2013). In addition, the ability to induce varying degrees of tau pathology can be useful when replicating the

different stages of human AD (Croft et al., 2019). Transduction with this pro-aggregatory tau construct resulted in the formation of hyperphosphorylated tau foci which were restricted to the somatodendritic neuronal compartments, as reported by *Croft, C. et al., 2019.* To investigate the potentially protective non-cell autonomous role of HSPB1 against tau aggregation, slices were first treated with recombinant human HSPB1 to replicate the extracellular HSBP1 released by astrocytes, as mentioned above (Nafar et al., 2016). Treating the slices with recombinant HSPB1 did not change the levels of phosphorylated tau as a proportion of total tau in the sarkosyl insoluble tau fraction in the P301L/S320F tau transduced slices, however, the same recombinant HSPB1 treatment in primary neuron cultures transduced with the P301L/S320F tau AAV was shown to reduce the accumulation of misfolded tau, as detected by the MC1 antibody.

One reason as to why the recombinant HSPB1 treatment may have elicited an protective response in the primary neurons and not in the slice cultures is the fact that the organotypic brain slice cultures are a more complex system compare to primary cultures (Croft and Noble, 2018; Humpel, 2015). Although the reduction in tau foci in the primary neurons was significant after recombinant HSPB1 treatment, the overall levels of GFP-positive neurons which contained these foci was quite low, around 12% in the untreated neurons and 5% in the recombinant HSPB1 treated neurons, and these small changes could be easily lost in the slice lysates collected for western blot analysis as the slices contain other tissue and cell types, along with neurons. In relation to this, within the slice cultures, HSPB1 is available to other cell types and may not necessarily be acting on neurons alone as sHSPs have the potential to act on other glial cells involved in neuroinflammatory response (Bsibsi et al., 2013; Bsibsi et al., 2014). Finally, the concentration of 50ng/ml of recombinant HSPB1 used to treat the neuronal cultures was the same concentration used to treat three slices cultured in one well. Although this concentration may be optimal in neurons, as calculated according to the physiological levels of HSPB1 released by cultured primary mouse astrocytes, this may not be directly applicable

to the slice culture model. Further work is required to determine the mechanism behind how recombinant HSPB1 reduces the levels of P301L/S320F tau foci in the primary neurons before this same mechanism can be explored in the more complex organotypic brain slice system.

One potential means by which HSPB1 could be reducing the conformational tau in the P301L/S320F transduced neurons is through a protective chaperone response. HSPB1 is able to detect regions of tau which are vulnerable to aggregation (Freilich et al., 2018), and it has been shown that HSPB1 preferentially binds directly to pathological hyperphosphorylated tau and PHFs (Shimura et al., 2004). By binding to these tau species within the human cortical neuronal cell line HCN2A, HSPB1 facilitated its degradation and dephosphorylation by altering the conformation of tau, resulting in the rescue of hyperphosphorylated tau induced cell death via the reduction of caspase-3 initiated apoptosis (Shimura et al., 2004). Using fluorescence and nuclear magnetic resonance (NMR) spectroscope it was demonstrated that HSPB1 also inhibits tau by binding to the microtubule-binding repeat terminal of tau and delaying tau fibril formation (Baughman et al, 2018). Further to this, it was this interaction with early stage tau which facilitated tau clearance from neurons in the rTg4510 tau mouse model in which HSPB1-AAV was overexpress in the hippocampus (Abisambra et al., 2010). When a synthetic chalcone was tested in human stem cells expressing a pro-aggregatory tau deletion mutation within C-terminal repeat domain, it was shown to upregulate HSPB1 and when tested in the 3xTg-AD mouse model, this resulted in the reduction of misfolded tau and neuronal loss (Lin et al., 2020). In support of the important role of HSPB1 in facilitating this reduction of tau, treatment with another family of substrates, the flavones, also protected against tau aggregation via a similar pathway (Chiang et al., 2021).

To further explore the non-cell autonomous role of astrocytic HSPB1, slices were also transduced using AAVs to overexpress human HSPB1 specifically in the astrocytes. To overexpress astrocytic

HSPB1, slices were transduced with an AAV which simultaneously expressed HSPB1 and the BFP within the astrocytes under the GFAP promoter, as previous studies have shown that fusing sHSPs with other fluorescent proteins can alter chaperone function (Datskevich et al, 2012; Datskevich and Gusev, 2014). This approach differs from the recombinant HSPB1 treatment of the slices because it mimics increased levels of HSPB1 in astrocytes, as seen in human AD brain, rather than only increasing the extracellular HSPB1. Therefore, this approach will be able to investigate non-cell autonomous effects, which could be mediated by HSPB1 release but also by changes in the astrocyte secretome as a consequence of HSPB1 overexpression in astrocytes. There are only few studies available reporting the effects of the astrocytic overexpression of sHSPs and their non-cell autonomous impact in neurodegeneration. The non-cell autonomous role of astrocytic sHSPs has been explored by overexpressing astrocytic CRYAB in a mouse model of HD in which it was shown that this could modulate levels of mutant htt levels and inclusion body formation leading to improved motor and cognitive function (Oliveira et al., 2016). This study, however, did not provide a functional mechanism to explain the non-cell autonomous protection of astrocytic CRYAB. It was also recently demonstrated that by expressing the human heat shock protein DNAJB6, a potent suppressor of PolyQ aggregation, in the astrocytes of the *D. melanogaster* model, progressive neuronal degradation was delayed and lifespan extended (Bason et al., 2019). Overexpressing HSPB1 in the organotypic slices did not alter the levels of phosphorylated tau pathology detected in the sarkosyl insoluble tau fraction of slices transduced with P301L/S320F tau. However, preliminary data from Fangjia Yang has analysed the media from these slice overexpressing astrocytic HSPB1 and it was found that HSPB1 can be detected (*Figure 6.1)*. This suggests that human HSPB1 is being secreted in this system and could provide a valuable mode for continued investigation into HSPB1 secretion.

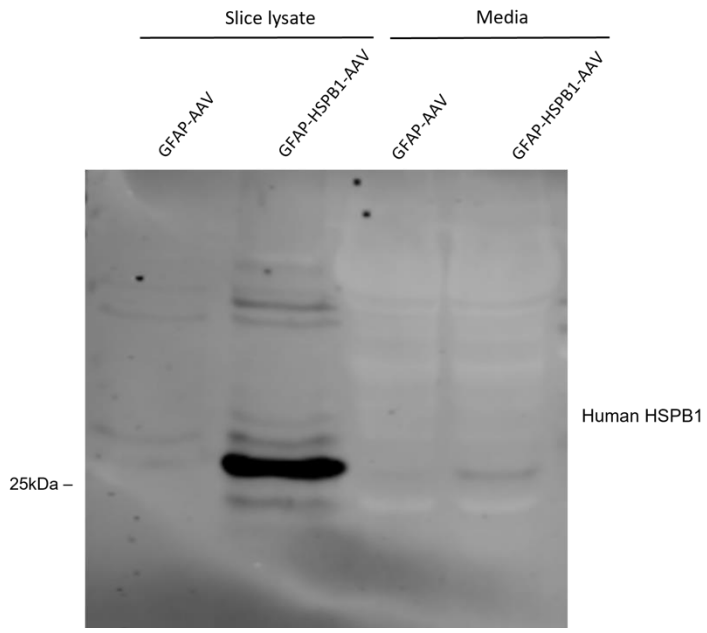

Figure 6.1: Preliminary data produced by Fangjia Yang in the laboratory showing western blot analysis of slices transduced with GFAP-BFP AAV and GFAP-HSPB1-BFP2 at 2x10^10 VG/ml at 0 DIV and corresponding slice media, using antibodies against human HSPB1 (n=1).

To explore this overexpression approach in further detail, additional protocol optimisation is required. For example, HSPB1 overexpression was confirmed by western blot analysis using a human HSPB1 antibody, and this overexpression occurred within a subset of cells in the slices, however, the specific cells in which this overexpression was present was not confirmed. As the majority of studies suggest HSPB1 is found increased specifically in astrocytes and not in other cell types (Wilhelmus et al., 2006; Mathys et al., 2019; Grubman et al., 2019; Lau et a., 2020; Smith et al., 2022; Renkawek et al., 1994), this implies that were HSPB1 to be overexpressed in other cell types then it may not perform the same functions as those exhibited by astrocytic HSPB1 and so would not provide the protective functions explored in this thesis. Using LDH assays, we excluded the possibility that overexpression of HSPB1 may be toxic to the cells, as overproduction of proteins can overload normal physiological pathways and exhaust cell resources needed to make and transport proteins (Tang and Amon, 2013; Birchler and Veitia, 2012), however these experiments need to repeated due

to the relatively low n-numbers. Further to this, overexpressing HSPB1 could modify the balance of different forms of sHSPs, such as phosphorylated and non-phosphorylated HSPB1, and therefore impact the ability of sHSPs to carry out proper function (Bakthisaran et al., 2015; Webster et al., 2019). To explore the functional outcomes of overexpressing HSPB1, it could be preferable to test this in a simpler, less diverse set-up such as primary cultures before replicating this in the slice cultures. If the decrease in tau inclusions observed in primary neurons upon recombinant HSPB1 treatment can be reproduced by co-culturing neurons with HSPB1-overexpressing astrocytes, it could help confirm whether astrocytic HSPB1 protects from tau pathology in neurons and whether this is due to HSPB1 secretion.

6.3 Limitations of the study

Although every effort was made to ensure that the experiments carried out during this PhD were well designed, planned and correctly controlled, it is important to discuss some of the limitations to this study.

6.3.1 Post-mortem human brain tissue

To explore the levels and co-localisation of the sHSPs CRYAB and HSPB1 in the human AD, brain tissue sections were analysed across different stages of disease severity. However, the brain tissue sections only represent a snapshot into the changes which are occurring in one moment in time, specifically at the end of life. As cellular interactions are more dynamic, it could be advantageous to also include a longitudinal approach when studying these sHSPs in the human disease, to track these expression changes overtime, using, for example, CSF samples taken from pathologically confirmed AD patients over a period of a few years (Lanzrein et al., 1998).

It is also important to note here that although GFAP, a marker for a major protein component of astrocyte filaments, was chosen for this thesis as an indicator of reactive astrocytes due of its prominence as the most widely used marker of reactive astrocytes (Escartin et al., 2021), it has now come to light that it should not be the sole determinant of the presence of reactive astrocytes. It has been ascertained that the upregulation of GFAP may not be a common feature of all reactive astrocytes and GFAP expression may also change in response to other normal physiological stimuli such as exercise and circadian rhythm rather than pathological stimuli only (Escartin et al., 2021; Gerics et al., 2006; Rodríguez et al., 2013). It would therefore beneficial to use other markers of reactive astrocytes alongside GFAP when determining the presence of reactive astrocytes, such as other filament markers including Synemin (Jing et al., 2007), or calcium binding proteins such as S100B which is mainly concentrated in astrocytes (Michetti et al., 2019).

6.3.2 Organotypic brain slice cultures

After slice culture preparation, slices develop a layer of reactive astrocytes in response to injury (Croft and Noble, 2018). Although the slices are left for 14 DIV before any analysis is carried out to allow for astrocyte reactivity to diminish, there is a possibility that some cells involved in this process are still present and so collected for experimental use, potentially skewing some results. Furthermore, when preparing mouse slice cultures, brain slices are collected starting from the frontal cortex and then collected sequentially to monitor the location of the slices throughout the brain. This plating of slices could induce variability within the results when compared between wells as not only does the volume of tissue differ between sections but it is also now known that there are region-specific differences in astrocytes subsets in the mouse brain (Hasel et al., 2021; Batiuk et al., 2020). In an attempt to minimise these variabilities, it was decided that it would be preferable to omit the first and last three slices when plating and keep only those slices in the middle of the brain where tissue composition and volumes where most comparable.

The original method of inducing tau pathology in the organotypic brain slice cultures was to prepare slice cultures from the pups of the htau mouse model (Andorfer et al., 2003). Slices prepared from this model would develop similar pathological changes seen in early human AD, including the development of AD-associated tau, but along an accelerated timeline compared to the *in vivo* mouse (Duff et al., 2002). However, due to prolonged problems with the breeding of the colony, followed by the laboratory shut-down due to COVID-19, it was decided a different model was required. Transducing the organotypic brain slices with tau-AAVs produced robust hyperphosphorylated tau foci, however, one of the downsides to this method is that overexpression of the tau mutants is not as directly relevant to AD as using a model which normally expresses human tau isoforms (Andorfer et al., 2003). As previously mentioned, the tau constructs used to induce tau aggregation in this study was expressing a mutation associated with FTD-Tau, as there is no evidence for mutations in tau in AD (Joel et al., 2018) and so this does not fully replicate what is seen in the human disease. In addition to this, the overexpression of tau could disrupt the functional equilibrium between the numbers of microtubules and the amount of tau that binds to them, with increasingly unbounded tau more likely to be phosphorylated, and so shifting the system towards hyperphosphorylation resulting into non-physiological pathology (Götz et al., 2018). The overexpression of tau can lead to increased levels of soluble hyperphosphorylated tau which has been suggested to be the primary cause of cell death, as opposed to tau tangle (Fox et al., 2011; Gendreau and Hall, 2013), and which is not a trait observed in human AD where there is little evidence for increased levels of overall tau protein (Pooler et al., 2014). Having said this, these problems with tau overexpression can also arise when also using the htau mouse model expressing normal human tau and so slices transduced with tau-AAVs are suitable for this PhD as it is the first slice model which has recapitulated tau inclusion pathology resembling the NFT in human AD , whilst also localising to the AD-relevant somadendritic region (Croft et al., 2019; Grundke-Iqbal et al., 1986; Murray et al., 2014).

6.3.3 Recombinant human HSPB1 treatment

To explore the role of extracellular sHSPs in response to AD-relevant stimuli, the mouse brain slices were treated with the recombinant human HSPB1 protein in order to mimic HSPB1 secretion from the astrocytes. Although the human and mouse recombinant HSPB1 proteins have high levels of similarity as confirmed using BLAST, it is possible that the full physiological effects of HSPB1 is not recapitulated when using a human protein to treat mouse cell cultures. In addition to this, the recombinant HSPB1 protein does not contain the post-translational modifications which are essential in assisting sHSPs with their functions (Webster et al., 2019). It was demonstrated using rat sensory neurons that the phosphorylated form of HSPB1 is required for neuronal survival after peripheral nerve injury and that this phosphorylated form was only found in adult and not neonatal mouse neurons (Benn et al., 2002). More relevantly, the comparison of HSPB1 and its phosphorylated variant also demonstrated the need for HSPB1 to be functionally dynamic and be able to switch between the non- and phosphorylated forms to enable any interaction with the tau protein in a mouse model of tauopathy (Abisambra et al., 2010). Using AAVs to express HSPB1 in astrocytes and to induce the secretion of posttranslational modified HSPB1 should overcome these limitations.

6.4 Future directions

To confirm whether the hyperphosphorylated tau foci produced by the transduction of the organotypic brain slice cultures with the pro-aggregatory tau construct are in fact tau aggregates, fluorescence recovery after photobleaching (FRAP) could be utilized. FRAP is a fluorescent microscopy technique where fluorescent molecules are bleached using a short burst of high-intensity laser light. Following this, the recovery of fluorescence is measured, caused by the inward diffusion of surrounding unbleached fluorophores. The rate at which the fluorescence intensity

recovers is dependent on the mobility of the surrounding molecules and mathematical modelling can be utilised to determine molecular dynamics such as diffusion and binding (Rayan et al., 2010; Loren et al., 2015). Previous studies have used this technique to allow for protein aggregation measurements in human serum (Xiong et al., 2016). Further to this, FRAP has allowed for the exploration of the dynamic nature of tau *in vitro* (Wegmann et al., 2018; Kanaan et al., 2020) and in other neurodegenerative diseases, this technique has been used to characterise α-synuclein amyloid aggregates (Roberti et al., 2011) and ataxin1 inclusions (Stenoien et al., 2002). In this project, if the tau foci found in those slices transduced with the mutant tau AAV were to be true tau aggregates, FRAP recovery would be hypothesized to be slower than FRAP recovery of the phosphorylated tau found in those slices transduced with the WT-tau construct.

One major disadvantage of using the organotypic brain slice cultures to study the potential protective function of HSPB1, as with other *ex vivo* or *in vitro* cell based models, is that it is not possible to replicate the detrimental clinical and behavioural outcomes of AD, most notably the loss of memory and cognitive decline. A model overexpressing HSBP1 has been generated by overexpressing human HSPB1 controlled by viral CMV vector resulting in expression detected in cells found in the cerebellum, hippocampus, cerebral cortex and olfactory and thalamic regions of the brain, as well as in the heart and liver (Toth et al., 2010). These transgenic mice have fewer degenerating neurons after ethanol-drinking, compared to wild-type mice, highlighting the potentially neuroprotective phenotype of HSPB1 (Toth et al., 2010). Further to this, the same overexpressing HSPB1 transgenic mouse has been crossed with an amyloid mouse model of AD, where the resulting cross seemed to display improve neuronal function and reduced build-up of amyloid, compared to the AD mouse model alone (Tóth et al., 2013). To further test whether the observed increase in HSPB1 specifically in astrocytes is neuroprotective, a model that overexpresses HSPB1 specifically in astrocytes within a mouse model of tau pathology will be needed. This is similar

to the mouse model generated by overexpressing astrocytic CRYAB under the human GFAP promoter and which was crossed with the BACHD mouse model of Huntington's disease, resulting in astrocytic CRYAB protection against mutant htt levels and improved cognitive and motor function (Oliveira et al., 2016).

To further confirm that the organotypic brain slice cultures are a good tool for studying the function of sHSPs in the context of disease, it would also be necessary to characterise the cell to cell interactions between microglia and astrocytes. As this crosstalk is pivotal during neurodegeneration, it would be important to determine whether those astrocytes induced by microglial cytokines TNFα and IL1α can in turn promote either the pro- or anti-inflammatory properties of microglia (Farina et al., 2007; Jha et al., 2019).

The major aim of this thesis was to focus primarily on the potentially protective chaperone function of HSPB1, however, it may also be necessary to further explore the anti-apoptotic functions of sHSPs as another mechanism of protection against disease progression during neurodegeneration. The protective anti-apoptotic functions of HSPB1 were explored when HSPB1 was knocked down in rat sensory neurons and these neurons were then subjected to nerve injury which resulted in increased apoptosis via the intrinsic apoptosis pathway, compared to healthy neurons, (Benn et al., 2002). Conversely, by initiating viral overexpression of endogenous HSPB1 in the neurons of the rat hippocampus, it was possible to reduce neuronal loss induced by kainic acid seizure pathology (Kalwy et al., 2003). Further to this, using a transgenic mouse model overexpressing human HSPB1, it was demonstrated that HSPB1 was able to rescue motor neuron function 5-6 months after nerve injury was evoked, demonstrated through a measured improvement in overall muscle force (Sharp et al., 2006). This same transgenic mouse model was also subjected to kainic acid to induce apoptosis and it was shown that HSPB1 overexpression reduced neuronal death in the hippocampus,

along with the attenuation of caspsase-3 induction resulting in improved seizure activity (Akbar et al., 2003). Finally, functional pathway analysis of differentially expressed genes (DEGS) identified across a number of cell specific transcriptome studies of AD found that the enrichment of astrocytic HSPB1 is linked to biological processes involved in the regulation of inclusion body assembly, regulation of protein refolding and a negative regulation of cell death (Wang and Li, 2021).

Following on from this, it would be interesting to further explore the potential role of HSPB1 in protecting from synaptic loss, a potential function eluded to by the primary neuron culture experiments transduced with tau-AAVs and treated with recombinant HSPB1. In cultured hippocampal rat neurons, phosphorylated HSPB1 was shown to co-localise with synaptic marker vGlut-1 (Schmidt et al., 2012) and in response to hyperthermia, HSPB1 was shown to localise to the synaptic membrane and synaptic junctions of Bergmann glial cells whilst also localising in the perisynaptic glial processes (Bechtold and Brown, 2000), highlighting the potential role of sHSPs contributing to synaptic repair and protection in response to injury (Los Reyes and Casas-Tinto, 2022). Recently, a study using the *Drosophila melanogaster* model highlighted the importance of the post-translational modifications of sHSPs highly involved in synaptogenesis, HSP23 and HSP26 (Santana et al., 2020). By interfering with these post-translational modifications, it reduced the ability of these sHSPs to prevent synapse loss and modulate neuronal stress (Santana et al., 2020).

Lastly, due to increasingly stringent time constraints, a full characterisation of the localisation and expression of CRYAB was not complete as part of this PhD thesis, and so this would be an interesting avenue of continued investigation. CRYAB has been detected in the reactive astrocytes within the AD brain, although the levels of CRYAB seem to vary from very low to high within the cortex, with higher levels of CRYAB found in those astrocytes within the hippocampus compared to the neocortex (Renkawek and Voorter, 1994; Shinohara et al., 1993; Iwaki et al., 1992). CRYAB has been seen to

accumulate in the astrocytes near to amyloid plaques, although this is less certain than HSPB1 and the data was not shown in the publication (Wilhelmus et al., 2006). In further contrast to HSPB1, CRYAB has also been found in neurons and has been shown to correlate with areas of severe neuronal loss (Iwaki et al., 1992; Mao et al., 2001). The most general consensus is that CRYAB is located in the oligodendrocytes found in AD (Renkawek and Voorter, 1994; Shinohara et al., 1993; Iwaki et al., 1992), an idea supported by the recently published transcriptome analysis of AD brains (Mathys et al., 2019) and most closely reflects what was seen in this thesis. However, this result presented in Chapter 3 also stated that not all CRYAB positive cells were also positive for oligodendrocyte marker CAII across the temporal cortex tissue sections of all AD cases. This indicates that CRYAB may also be localised in other cell types, a notion also supported by recent cell-specific transcriptome studies (Grubman et al., 2019; Smith et al., 2022) and which should be further explored.

6.5 Conclusions

AD progression is partly characterised by neuroinflammation and the toxic build-up of pathological proteins such as extracellular amyloid-β and intracellular tau, processes which implicate the roles of both reactive astrocytes and the chaperone-like functions of sHSPs such as HSPB1. The human data presented in this thesis highlights the association between astrocytic HSPB1 and amyloid-β plaques and emphasises the need for the continued investigation into these potentially protective interactions. The organotypic brain slice cultures have proved to be a good tool for replicating some of the pathological features of neurodegeneration, such as the induction of reactive astrocytes by cytokines and the formation of hyperphosphorylated tau pathology through the use of AAVs. Extracellular recombinant HSPB1 treatment was shown to reduce the abundance of P30L1/S320F tau inclusions in primary mouse neurons, emphasizing the potentially protective role of extracellular

HSPB1 in reducing tau accumulation, however, further work is required to fully understand this phenomenon in the slice culture model. Overall, this work aims to expand the current knowledge surrounding astrocytic response and sHSP function in AD.

7. References

Abeti, R., Abramov, A., and Duchen, M. 2011. “Beta-amyloid activates PARP causing astrocytic metabolic failure and neuronal death.” *Brain* 1658-1672.

Abisambra, J., Blair, L., Hill, S., Jones, J., Kraft, C., Rogers, J., Koren 3rd, J., Jinwal, U., Lawson, L., Johnson, A., Wilcock, D., O'Leary, J., Jansen-West, K., Muschol, M., Golde, T., Weeber, E., Banko, J., and Dickey, C. 2010. “Phosphorylation dynamics regulate Hsp27-mediated rescue of neuronal plasticity deficits in tau transgenic mice.” *The Journal of Neuroscience* 15374-15382.

Abramov, A., Canevari, L., and Duchen, M. 2004. “β-Amyloid Peptides Induce Mitochondrial Dysfunction and Oxidative Stress in Astrocytes and Death of Neurons through Activation of NADPH Oxidase.” *Journal of Neuroscience* 565-575.

Afshar, P., Ashtari, N., Jiao, X., Rahimi-Balaei, M., Zhang, X., Yaganeh, B., Del Bigio, M., Kong, J., and Marzban, H. 2017. “Overexpression of Human SOD1 Leads to Discrete Defects in the Cerebellar Architecture in the Mouse.” *Frontiers in neuroanatomy.*

Ahmed, S., Holt, M., Riedel, D., and Jahan, R. 2013. “Small-scale isolation of synaptic vesicles from mammalian brain.” *Nature protocols* 998-1009.

Ahmed, Z., Cooper, J., Murray, T., Garn, K., McNaughton, E., Clarke, H., Parhizkar, S., Ward, M., Cavallini, A., Jackson, S., Bose, S., Clavaguera, F., Tolnay, M., Lavenir, I., Goedert, M., Hutton, M., and O'Neill, M. 2014. “A novel in vivo model of tau propagation with rapid and progressive neurofibrillary tangle pathology: the pattern of spread is determined by connectivity, not proximity.” *Acta Neuropathologica* 667–683.

Akama, K., and van Eldik, L. 2000. “β-Amyloid Stimulation of Inducible Nitric-oxide Synthase in Astrocytes Is Interleukin-1β- and Tumor Necrosis Factor-α (TNFα)-dependent, and Involves a TNFα Receptor-associated Factor- and NFκB-inducing Kinase-dependent Signaling Mechanism.” *Journal of Biological Chemistry* 7918-7924.

Akbar, M.,, Lundberg, A., Liu, K., Vidyadaran, S., Wells, K., Dolatshad, H., Wynn, S., Wells, D., Latchman, D., de Belleroche, J. 2003. “The neuroprotective effects of heat shock protein 27 overexpression in transgenic animals against kainate-induced seizures and hippocampal cell death.” *The Journal of Biological Chemistry* 19956-19965.

Alafuzoff, I., Thal, D., Arzberger, T., Bogdanovic, N., Al-Sarraj, S., Bodi, I., Boluda, S., Bugiani, O., Duyckaerts, C., and Gelpi, E,. 2009. “ Assessment of beta-amyloid deposits in human brain: a study of the BrainNet Europe consortium. .” *Acta Neuropathol.* 309-320.

AlaylioĞlu, M., Dursun, E., Yilmazer, S., and Ak, D. 2020. “A Bridge Between in vitro and in vivo Studies in Neuroscience: Organotypic Brain Slice Cultures.” *Archives of Neuropsychiatry* 333-337.

Allaman, I., Gavillet, M., Belanger, M., Laroche, T., Viertl, D., Lashuel, H., and Magistretti, P. 2010. “Amyloid-B Aggregates Cause Alterations of Astrocytic Metabolic Phenotype: Impact on Neuronal Viability.” *The Journal of Neuroscience* 3326-3338.

Allen, N., and Eroglu, C. 2017. “Cell Biology of Astrocyte-Synapse Interactions.” *Neuron* 697-708.

Alonso, A., Mederlyova, A., Novak, M., Grundke-Iqbal, I., and Iqbal, K. 2004. “Promotion of Hyperphosphorylation by Frontotemporal Dementia Tau Mutations.” *Journal of Biological Chemistry* 34870-34881.

Andorfer, C., Kress, Y., Espinoza, M., de Silva, R., Tucker, K,. Barde, Y., Duff, K., and Davies, P. 2003. “Hyperphosphorylation and aggregation of tau in mice expressing normal human tau isoforms.” *Journal of Neurochemistry* 582-590.

Aquilina, J., Shrestha, S., Morris, A., and Ecroyd, H. 2013. “Structural and Functional Aspects of Hetero-oligomers Formed by the Small Heat Shock Proteins αB-Crystallin and HSP27.” *Journal of biological chemistry* 13602-13609.

Arac, A., Brownell, S., Rothbard, J., Chen, C., Ko, R., Pereira, M., Albers, G., Steinman, L. and Steinberg, G. 2011. “Systemic augmentation of αB-crystallin provides therapeutic benefit twelve hours post-stroke onset via immune modulation.” *PNAS* 13287-13292.

Arai, H., and Atomi, Y. 1997. “Chaperone Activity of αB-crystallin Suppresses Tubulin Aggregation through Complex Formation.” *Cell Structure and Function* 539-544.

Arendt, T., Stieler, J., and Holzer, M. 2016. “Tau and Taopathies.” *Brain research bulletin* 238-292.

Arrigo, A-P. 2013. “Human small heat shock proteins: Protein interactomes of homo- and hetero-oligomeric complexes: An update.” *FEBS* 1959-1969.

Asai, H., Ikezu, S., Tsunoda, S., Medalla, M., Luebke, J., Haydar, T., Wolozin, B., Butovsky, O., Kügler, S., and Ikezu, T. 2015. “Depletion of microglia and inhibition of exosome synthesis halt tau propagation.” *Nature Neuroscience* 1584-1593.

Auluck, P., Chan, H., Trojanowski, J., Lee, V., and Bonini, N. 2002. “Chaperone suppression of alpha-synuclein toxicity in a Drosophila model for Parkinson's disease.” *Science* 865-868.

Azevedo, F., Carvalho, L., Grinberg, L., Farfel, J., Ferretti, R., Leite, R., Filho, W., Lent, R., Herculano-Houzel, S. 2009. “Equal numbers of neuronal and nonneuronal cells make the human brain an isometrically scaled-up primate brain.” *the Journal of Comparative Neurology* 532-541.

Bader, J., Geyer, P., Müller, J., Strauss, M., Koch, M., Leypoldt, F.,, Koertvelyessy, P.,, Bittner, D., Schipke, C., Incesoy, E., Peters, O., Deigendesch, N., Simons, M., Jensen, M., Zetterber, H., Mann, M. 2020. “Proteome profiling in cerebrospinal fluid revealsnovel biomarkers of Alzheimer’s disease.” *Molecular Systems Biology.*

Bagheri, M., Nair, R., Singh, K., and Saini, D. 2017. “ATM-ROS-iNOS axis regulates nitric oxide mediated cellular senescence.” *Biochimica et Biophysica Acta (BBA) - Molecular Cell Research* 177-090.

Bahr, B. 1995. “Long-term hippocampal slices: a model system for investigating synaptic mechanisms and pathological processes.” *Journal Neuroscience Research* 294-305.

Bai, B., Wang, X., Li, Y., Chen, P-C., Yu, K., Dey, K., Yarbro, J., Han, X., Lutz, B., Rao, S., Jiao, Y., Sifford, J., Han, J., Wang, M., Tan, H., Shaw, T., Cho., J-H., Zhou, S., Wang, H., Niu, M., Mancieri, A., Messler, K., Sun, X., Wu, Z., Pagala, V.,. 2020. “Deep Multilayer Brain Proteomics Identifies Molecular Networks in Alzheimer's Disease Progression.” *Neuron* 975-991.

Bajetto, A., Bonavia, R., Barbero, S., Schettini, G. 2002. “Characterization of chemokines and their receptors in the central nervous system: physiopathological implications.” *Journal of Neurochemistry* 1311-1329.

Bakthisaran, R., Tangirala, R., and Rao, C. 2015. “Small heat shock proteins: Role in cellular functions and pathology.” *Biochimica et Biophysica Acta (BBA) - Proteins and Proteomics* 291-319.

Banerjee, S., Lin, C-F., Skinner, K., Schiffhauer, L., Peacock, J., Hicks, D., Redmond, E., Morrow, D., Huston, A., Shayne, M., Langstein, H., Miller-Graziano, C., Strickland, J., O'Donoghue, L., and De, A. 2011. “Heat shock protein 27 differentiates tolerogenic macrophages that may support human breast cancer progression.” *Cancer Research* 318-327.

Bartelt-Kirbach, B., and Golenhofen, N. 2014. “Reaction of small heat-shock proteins to different kinds of cellular stress in cultured rat hippocampal neurons.” *Cell stress & chaperones* 145-153.

Basha, E., O'Neill, H., and Vierling, E. 2012. “Small heat shock proteins and α-crystallins: dynamic proteins with flexible functions.” *Trends in Biochemical Sciences* 106-117.

Bason, M., Meister-Broekema, M., Alberts, N., Dijkers, P., Bergink, S., Sibon, O., and Kampinga, H.,. 2019. “Astrocytic expression of the chaperone DNAJB6 results in non-cell autonomous protection in Huntington's disease.” *Neurobiology of disease* 108-117.

Basu, S., Binder, R., Suto, R., Anderson, K. and Srivastava, P. 2000. “Necrotic but not apoptotic cell death releases heat shock proteins, which deliver a partial maturation signal to dendritic cells and activate the NF-κB pathway.” *International Immunology* 1539-1546.

Batiuk, Y., Martirosyan, A., Wahis, J., de Vin, F., Marneffe, C., Kusserow, C., Koeppen, J., Viana, J., Oliveira, J., Voet, T., Ponting, C., Belgard, T., and Holt, M. 2020. “Identification of region-specific astrocyte subtypes at single cell resolution.” *Nature Communications.*

Batulan, Z., Venu, V., Li, Y., Koumbadinga, G., Alvarez-Olmedo, D., Shi, C., and O’Brien, E. 2016. “Extracellular Release and Signaling by Heat Shock Protein 27: Role in Modifying Vascular Inflammation.” *Frontiers in Immunology.*

Baughman, H., Clouser, A., Klevit, R., and Nath, A. 2018. “HspB1 and Hsc70 chaperones engage distinct tau species and have different inhibitory effects on amyloid formation.” *Journal of Biological Chemistry* 2687-2700.

Baughman, H., Phama, T., Adams, C., Nath, A., and Klevit, R. 2020. “Release of a disordered domain enhances HspB1chaperone activity toward tau.” *PNAS* 2923-2929.

Baumann, N., and Pham-Dinh. 2001. “Biology of Oligodendrocyte and Myelin in the Mammalian Central Nervous System.” *Physioloigcal reviews* 871-927.

Bechtold, D., and Brown, I. 2000. “Heat shock proteins Hsp27 and Hsp32 localize to synaptic sites in the rat cerebellum following hyperthermia.” *Molecular Brain Research* 309-320.

Benediktsson, A., Schachtele, S., Green, S., and Dailey, M. 2005. “Ballistic labeling and dynamic imaging of astrocytes in organotypic hippocampal slice cultures.” *Journal of neuroscience methods* 41-53.

Benn, S., Perrelet, D., Kato, A., Scholz, J., Decosterd, I., Mannion, R., Bakowska, J and Woolf, C. 2002. "Hsp27 upregulation and phosphorylation is required for injured sensory and motor neuron survival." *Neuron* 45-56.

Benndorf, R., Martin, J., Pond, S., and Wertheim, J. 2014. "Neuropathy- and myopathy-associated mutations in human small heat shock proteins: Characteristics and evolutionary history of the mutation sites." *Mutation Research/Reviews in Mutation Research* 15-30.

Bennett, R., DeVos, S., Dujardin, S., Corjuc, B., Gor, R., Gonzalez, J., Roe, A., Frosch, M., Pitstick, R., Carlson, G., and Hyman, B. 2017. "Enhanced Tau Aggregation in the Presence of Amyloid β." *The American journal of pathology* 1601-1012.

Bhat, N., and Sharma, K. 1999. "Microglial activation by the small heat shock protein, alpha-crystallin." *Neuroreport* 2869-2873.

Birchler, J., and Veitia, R. 2012. "Gene balance hypothesis: connecting issues of dosage sensitivity across biological disciplines." *PNAS* 14746-14753.

Birger, A., Ben-Dor, I., Ottolenghi, M., Turetsky, T., Gil, Y., Sweetat, S., Perez, L., Belzer, V., Casden, N., Steiner, D., Izrael, M., Galun, E., Feldman, E., Behar, O., and Reubinoff, B. 2019. "Human iPSC-derived astrocytes from ALS patients with mutated C9ORF72 show increased oxidative stress and neurotoxicity." *eBioMedicine* 274-289.

Björkdahl, C., Sjögren, M., Zhou, X., Concha, H., Avila, J., Winblad, B., and Pei, J-J. 2008. "Small heat shock proteins Hsp27 or alphaB-crystallin and the protein components of neurofibrillary tangles: tau and neurofilaments." *Journal of Neuroscience Research* 1343-1352.

Bolós, M., Llorens-Martín, M., Jurado-Arjona, J., Hernández, F., Rábano, A., and Avila, J. 2016. "Direct Evidence of Internalization of Tau by Microglia In Vitro and In Vivo." *Journal of Alzheimer's disease* 77-87.

Boncoraglio, A., Minoia, M., and Carra, S. 2012. "The family of mammalian small heat shock proteins (HSPBs): implications in protein deposit diseases and motor neuropathies." *The International Journal of Biochemistry and Cell Biology* 1657-1669.

Bova, M., Mchaourab, H., Han, Y., and Fung, B. 2000. "Subunit Exchange of Small Heat Shock Proteins: ANALYSIS OF OLIGOMER FORMATION OF αA-CRYSTALLIN AND Hsp27 BY FLUORESCENCE RESONANCE ENERGY TRANSFER AND SITE-DIRECTED TRUNCATIONS." *Journal of biological chemistry* 1035-1042.

Braak, H. Braak and E. 1995. "Staging of Alzheimer's disease related neurofibrillary changes." *Neurobiology of Aging* 271-284.

Braak, H., and Braak, A.,. 1997. "Frequency of Stages of Alzheimer-Related Lesions in Different Age Categories." *Neurobiology of ageing* 351-357.

Braak, H., and Tredici, K. 2018. "Spreading of Tau Pathology in Sporadic Alzheimer's Disease Along Cortico-cortical Top-Down Connections ." *Cerebral Cortex* 3372-3384.

Braak, H., Thal, D., Ghebremedhin, E., and Tredici, K. 2011. "Stages of the pathologic process in Alzheimer disease: age categories from 1 to 100 years." *Journal of neuropathology and experimental neurology* 960-969.

Bradford J., Shin, J-Y., Roberts, M., Wang, C-E., Sheng, G., Li, S., and Li, X-J. 2010. “Mutant huntingtin in glial cells exacerbates neurological symptoms of Huntington disease mice.” *The Journal of Biological Chemistry* 10653-10661.

Bradford, J., Shin, J-Y., Roberts, M., Wang, C-E., Sheng, G., Li, S. and Li, X-J. 2010. “Mutant Huntingtin in Glial Cells Exacerbates Neurological.” *The Journal of Biological Chemistry* 10653-10661.

Braidy, N., Zarka, M., Jugder, B-E., Welch, J., Jayasena, T., Chan, D., Sachdev, P.,and Bridge, W. 2019. “The Precursor to Glutathione (GSH), γ-Glutamylcysteine (GGC), Can Ameliorate Oxidative Damage and Neuroinflammation Induced by Aβ 40 Oligomers in Human Astrocytes.” *Frontiers in aging neuroscience.*

Brehme, M., Voisine, C., Rolland, T., Vidal, M., Ge, H., and Morimoto, R. 2014. “A Chaperome Subnetwork Safeguards Proteostasis in Aging and Neurodegenerative Disease.” *Cell reports* 1135-1150.

Brinkmalm, G., Hong, W., Wang, Z., Liu, W., O’Malley, T., Sun, X., Frosch, M., Selkoe, D., Portelius, E., Zetterberg, H., Blennow, K., and Walsh, D. 2019. “Identification of neurotoxic cross-linked amyloid-β dimers in the Alzheimer’s brain.” *Brain* 1441–1457.

Bruey, J-M., Ducasse, C., Bonniaud, P., Ravagnan, L., Susin, S., Diaz-Latoud, C., Gurbuxani, S., Arrigo, A., Kroemer, G., Solary, E., and Garrido, C. 2000. “Hsp27 negatively regulates cell death by interacting with cytochrome c.” *Nature Cell Biology* 645-652.

Bruinsma, I., Bruggink, K., Kinast, K., Versleijen, A., Nolten, I., Subramaniam, V., Kuiperij, H., Boelens, W., Waal, R., and Verbeek, M. 2011. “Inhibition of α-synuclein aggregation by small heat shock proteins.” *Proteins* 2956-2967.

Bruinsma, I., de Jager, M., Carrano, A., Versleijen, A., Veerhuis, R., Boelens, W., Rozemuller, A., de Waal, R., and Verbeek, M. 2011. “Small heat shock proteins induce a cerebral inflammatory reaction.” *The Journal of Neuroscience* 11992-20000.

Bsibsi, M., Holtman, I., Gerritsen, W., Eggen, B., Boddeke, E., van der Valk, P., van Noort, J., and Amor, S. 2013. “Alpha-B-Crystallin Induces an Immune-Regulatory and Antiviral Microglial Response in Preactive Multiple Sclerosis Lesions.” *Journal of Neuropathology & Experimental Neurology* 970-979.

Bsibsi, M., Peferoen, L., Holtman, I., Nacken, P., Gerritsen, W., Witte, M., van Horssen, J., Eggen, B., van der Valk, P., Amor, S., and van Noort, J. 2014. “Demyelination during multiple sclerosis is associated with combined activation of microglia/macrophages by IFN-γ and alpha B-crystallin.” *Acta Neuropathologica* 215-229.

Busche, M. and Hyman, B. 2020. “Synergy between amyloid-β and tau in Alzheimer's disease.” *Nature Neuroscience* 1183-1193.

Busche, M., Wegmann, S., Dujardin, S., Commins, C., Schiantarelli, J., Klickstein, N., Kamath, T., Carlson, G., Nelken, I., and Hyman, B. 2019. “Tau impairs neural circuits, dominating amyloid-β effects, in Alzheimer models in vivo.” *Nautre Neuroscience* 57-64.

Caceres, A., Banker, G., Steward, O., Binder, L., and Payne, M. 1984. “MAP2 is localized to the dendrites of hippocampal neurons which develop in culture.” *Developmental Brain Research* 314-318.

Calafate, S., Buist, A., Miskiewicz, K., Vijayan, V., Daneels, G., de Strooper, B., Wit, J., Verstreken, P., and Moechars, D. 2015. “Synaptic Contacts Enhance Cell-to-Cell Tau Pathology Propagation.” *Cell Reports* 1176-1183.

Caldwell, A., Diedrich, J., Shokhirev, M., and Allen, N. 2020. “Aberrant astrocyte protein secretion contributes to altered neuronal development in diverse disorders.” *biorxiv.*

Carrero, I., Gonzalo, M., Martin, B., Sanz-Anquel, J., .Arévalo-Serrano, J., and Gonzalo-Ruiz, A. 2012. “Oligomers of beta-amyloid protein (Aβ1-42) induce the activation of cyclooxygenase-2 in astrocytes via an interaction with interleukin-1beta, tumour necrosis factor-alpha, and a nuclear factor kappa-B mechanism in the rat brain.” *Experimental Neurology* 215-227.

Carver, J., Grosas, A., Ecroyd, H., and Quinlan, R. 2017. “The functional roles of the unstructured N- and C-terminal regions in αB-crystallin and other mammalian small heat-shock proteins.” *Cell Stress and Chaperones* 627-638.

Ce, P., Erkizan, O., and Gedlizlioglu, M. 2011. “Elevated HSP27 levels during attacks in patients with multiple sclerosis.” *Acta Neurologica Scandinavica* 317-320.

Ceyzériat, K., Haim, L., Denizot, A., Pommier, D., Matos, M., Guillemaud, O., Palomares, M., Abjean, L., Petit, F., Gipchtein, P., Gaillard, M., Guillermier, M., Bernier, S., Gaudin, M., Aurégan, G., Josephine, C., Dechamps, N., Veran, J., Langlais, V.,. 2018. “Modulation of astrocyte reactivity improves functional deficits in mouse models of Alzheimer’s disease.” *Acta Neuropathologica Communications.*

Chaari, A. 2019. “Molecular chaperones biochemistry and role in neurodegenerative diseases.” *International Journal of Biological Macromolecules* 396-411.

Chaplot, K., Jarvela, T., and Lindberg, I. 2020. “Secreted Chaperones in Neurodegeneration.” *Frontiers in Aging Neuroscience.*

Charette, S., and Landry, J. 2006. “The Interaction of HSP27 with Daxx Identifies a Potential Regulatory Role of HSP27 in Fas-Induced Apoptosis.” *Annals of the New York academy of sciences* 126-131.

Chen, M-K., Mecca, A., Naganawa, M., Finnema, S., Toyonaga, T., Lin, S-F., Najafzadeh, S., Ropchan, J., Lu, Y., McDonald, J., Michalak, H., Nabulsi, N., Arnsten, A., Huang, Y., Carso, R., and van Dyck, C. 2018. “Assessing Synaptic Density in Alzheimer Disease With Synaptic Vesicle Glycoprotein 2A Positron Emission Tomographic Imaging.” *JAMA Neurology* 1215-1224.

Chiang, N-N., Lin, T-H., Teng, Y-S., Sun, Y-C., Chang, K-H., Lin, C-Y., Hsieh-Li, H., Su, M-T., Chen, C-M., and Lee-Chen, G-J. 2021. “Flavones 7,8-DHF, Quercetin, and Apigenin Against Tau Toxicity via Activation of TRKB Signaling in ΔK280 Tau RD-DsRed SH-SY5Y Cells.” *Frontiers in ageing neuroscience.*

Chiarini, A., Armato, U., Gardenal, E., Gui, L., and Dal Pra, I. 2017. “Amyloid β-exposed human astrocytes overproduce phospho-tau and overrelease it within exosomes, effects suppressed by calcilytic NPS 2143-Further implications for Alzheimer's therapy.” *Frontiers in Neuroscience .*

Christopher, K., Pedler, M., Shieh, B., Ammar, D., Petrash, J., and Mueller, N. 2014. “Alpha-crystallin-mediated protection of lens cells against heat and oxidative stress-induced cell death.” *Biochim Biophys Acta* 309-315.

Chun H., Im, H., Kang, Y., Kim, Y., Shin, J., Won, W., Lim, J., Ju, Y., Park, Y., Kim, S., Lee, S., Lee, J., Woo, J., Hwang, Y., Cho, H., Jo, S., Park, J-H., Kim, D., Kim, D., Seo, J-S, Gwah, B., Kim, S., Park, K., Kaang, B-K., Cho, H., Ryu, H and Lee, C. 2020. "Severe reactive astrocytes precipitate pathological hallmarks of Alzheimer's disease via H2O2− production." *Nature Neuroscience* 1555-1566.

Chun, H., and Lee, C. 2018. "Reactive astrocytes in Alzheimer's disease: A double-edged sword." *Neuroscience Research* 44-52.

Chung, D., Roemer, S., Petrucelli, L., & Dickson, D. 2021. "Cellular and pathological heterogeneity of primary tauopathies." *Molecular Neurodegeneration.*

Ciechanover, A., Heller, H., Elias, S., Haas, A., and Hershko, A. 1980. "ATP-dependent conjugation of reticulocyte proteins with the polypeptide required for protein degradation." *PNAS* 1365-1368.

Clavaguera, F., Bolmont, T., Crowther, R., Abramowski, D., Frank, S., Probst, A., Fraser, G., Stalder, A., Beibel, M., Staufenbiel, M., Jucker, M., Goedert, M., and Tolnay, M. 2009. "Transmission and spreading of tauopathy in transgenic mouse brain." *Nature Cell Biology* 909–913.

Clayton, A., Turkes. A., Navabi, H., Mason, M., and Tabi, Z. 2005. "Induction of heat shock proteins in B-cell exosomes." *Journal of Cell Science* 3631-3638.

Constanza, C., and Spada, A. 2019. "TFEB dysregulation as a driver of autophagy dysfunction in neurodegenerative disease: Molecular mechanisms, cellular processes, and emerging therapeutic opportunities." *Neurobiology of Disease* 83-93.

Corder E., Saunders, A., Strittmatter, W., Schmechel, D., Gaskell, P., Small, G., Roses, A., Haines, J., and Pericak-Vance, M. 1993. "Gene dose of apolipoprotein E type 4 allele and the risk of Alzheimer's disease in late onset families." *Science* 921-923.

Crain, S. 1966. "Development of "Organotypic" Bioelectric Activities in Central Nervous Tissues During Maturation in Culture." *International Review of Neurobiology* 1-43.

Croft C., Cruz, P, E., Ryu, D, H., Ceballos-Diaz, C., Strang, K. H., Woody, B, M., Lin, W-L., Deture, M., Rodríguez-Lebrón, E., Dickson, D, W., Chakrabarty, P., Levites, Y., Giasson, B, I., Golde, T, E. 2019. "rAAV-based brain slice culture models of Alzheimer's and Parkinson's disease inclusion pathologies." *Journal of Experimental Medicine* 539–555.

Croft C., Cruz, P., Ryu, D., Diaz, C., Strang, K., Woody, B., Lin, W., Deture, M., Lebrón, E., Dickson, D., Chakrabarty, P., Levites, Y., Giasson, B., Golde, T. 2019. "rAAV-based brain slice culture models of Alzheimer's and Parkinson's diease inclusion pathology." *Journal of Experimental Medicine* 539-555.

Croft, C Kurbatskaya, K., Hanger, D., and Noble, W. 2017. "Inhibition of glycogen synthase kinase-3 by BTA-EG4 reduces tau abnormalities in an organotypic brain slice culture model of Alzheimer's disease." *Scientific Reports.*

Croft, C., Moore, B., Ran, Y., Chakrabarty, P., Levites, Y., Golde, T., and Giasson, B. 2018. "Novel monoclonal antibodies targeting the microtubule-binding domain of human tau." *PLOS One.*

Croft, C.,. Wade, M., Kurbatskaya, K., Mastrandreas, P., Hughes, M., Phillips, E., Pooler, A., Perkinton, M., Hanger, D., and Noble, W. 2017. "Membrane association and release of wild-type and pathological tau from organotypic brain slice cultures." *Cell death & Disease* e2671.

Croft, C.,L., Futch, H. S., Moore, B. D., and Golde, T. E. 2019. “Organotypic brain slice cultures to model neurodegenerative proteinopathies.” *Molecular Neurodegeneration* 45.

Croft, C.L and Noble, W. 2018. “Preparation of organotypic brain slice cultures for the study of Alzheimer’s disease [version 2; peer review: 3 approved].” *F1000Research* 592.

Croft. C., and Noble, W. 2018. “Preparation of organotypic brain slice cultures for the study of Alzheimer’s disease.” *F1000 Research* 592.

Cunningham, C., Dunne, A., and Lopez-Rodriguez, A. 2019. “Astrocytes: Heterogeneous and Dynamic Phenotypes in Neurodegeneration and Innate Immunity.” *The neuroscientist* 455-474.

Dabir, D., Trojanowski, J., Richter-Landsberg, C. and Lee, V. 2004. “Expression of the Small Heat-Shock Protein αB-Crystallin in Tauopathies with Glial Pathology.” *The American Journal of Pathology* 155-166.

D'Amelio, M., Sheng, M., and Cecconi, F. 2012. “Caspase-3 in the central nervous system: beyond apoptosis.” *Trends in neuroscience* 700-709.

DaRocha-Souto, B., Coma, M., Pérez-Nievas, B., Scotton, T., Siao, M., Sánchez-Ferrer, P., Hashimoto, T., Fan, Z., Hudry, E., Barroeta, I., Serenó, L., Rodríguez, M., Sánchez, M., Hyman, B.and Gómez-Isla, T. 2012. “Activation of glycogen synthase kinase-3 beta mediates β-amyloid induced neuritic damage in Alzheimer's disease.” *Neurobiology of Disease* 425-437.

Das, S., Li, Z., Noori, A., Hyman, B., and Serrano-Pozo, A. 2020. “Meta-analysis of mouse transcriptomic studies supports a context-dependent astrocyte reaction in acute CNS injury versus neurodegeneration.” *Journal of Neuroinflammation.*

Datskevich, P., and Gusev, N. 2014. “Structure and properties of chimeric small heat shock proteins containing yellow fluorescent protein attached to their C-terminal ends.” *Cell Stress & chaperones.*

Datskevich, P., Mymrikov, E., Sluchanko, N., Shemetov, A., Sudnitsyna, M., and Gusev, N. 2012. “Expression, purification and some properties of fluorescent chimeras of human small heat shock proteins.” *Protein expression and purification* 45-54.

Datskevich, P., Nefedova, V., Sudnitsyna, M., and Gusev, N. 2012. “Mutations of small heat shock proteins and human congenital diseases.” *Biochemistry* 1500-1514.

Dawson, T., Golde, T., Lagier-Tourenne, C. 2018. “Animal models of neurodegenerative diseases.” *Nature Neuroscience* 1370-1379.

de Calignon, A., Polydoro, M., Suárez-Calvet, M., William, C., Adamowicz, D., Kopeikina, K., Pitstick, R., Sahara, N., Ashe, K., Carlson, G., Spires-Jones, T., and Hyman, B. 2012. “Propagation of Tau Pathology in a Model of Early Alzheimer's Disease.” *Neuron* 685-697.

De Maio, A., and Vazquez, D. 2013. “Extracellular heat shock proteins: a new location, a new function.” *Shock* 239-246.

De, A., Kodys, K., Yeh, B., and Miller-Graziano, C. 2000. “Exaggerated human monocyte IL-10 concomitant to minimal TNF-alpha induction by heat-shock protein 27 (Hsp27) suggests Hsp27 is primarily an antiinflammatory stimulus.” *Journal of Immunology* 3951-3958.

Deane, C., and Brown, I. 2018. “Intracellular Targeting of Heat Shock Proteins in Differentiated Human Neuronal Cells Following Proteotoxic Stress.” *Journal of Alzheimer's Disease* 1295-1308.

Deane, R., Sagare, A., Hamm, K., Parisi, M., Lane, S., Finn, M., Holtzman, D., and Zlokovic, B. 2008. “apoE isoform-specific disruption of amyloid beta peptide clearance from mouse brain.” *The Journal of Clinical Investigation* 4002-4013.

Decker, T., and Lohmann-Matthes, M. 1988. “A quick and simple method for the quantitation of lactate dehydrogenase release in measurements of cellular cytotoxicity and tumor necrosis factor (TNF) activity.” *Journal of immunological methods* 61-69.

Dehle, F., Ecroyd, H., Musgrave, I., and Carver, J. 2010. “αB-Crystallin inhibits the cell toxicity associated with amyloid fibril formation by κ-casein and the amyloid-β peptide.” *Cell Stress & Chaperones* 1013-1026.

DeKosky, S., and Scheff, S. 1990. “Synapse loss in frontal cortex biopsies in Alzheimer's disease: correlation with cognitive severity.” *Annals of neurology* 457-464.

del Rio, J., Heimrich, B., Soriano, E., Schwegler, H., and Frotscher, M. 1991. “Proliferation and differentiation of glial fibrillary acidic protein-immunoreactive glial cells in organotypic slice cultures of rat hippocampus.” *Neuroscience* 335-347.

den Broek, B., Wuyts, C., and Irobi, J. 2021. “Extracellular vesicle-associated small heat shock proteins as therapeutic agents in neurodegenerative diseases and beyond.” *Advanced Drug Delivery Reviews.*

Desagher, S., Glowinski, J., and Premont, J. 1996. “Astrocytes protect neurons from hydrogen peroxide toxicity.” *The Journal of Neuroscience* 2553-2562.

DeTure, M., and Dickson, D. 2019. “The neuropathological diagnosis of Alzheimer’s disease.” *Molecular Neurodegeneration.*

Dickey, C., Kamal, A., Lundgren, K., Klosak, N., Bailey, R., Dunmore, J., Ash, P., Shoraka, S., Zlatkovic, J., Eckman, C., Patterson, C., Dickson, D., Nahman Jr., N., Hutton, M., Burrows, F., and Petrucelli, L. 2007. “The high-affinity HSP90-CHIP complex recognizes and selectively degrades phosphorylated tau client proteins.” *The Journal of Clinical Investigation* 648-658.

Diniz, L., Tortelli, V., Matias, I., Morgado, J., Araujo, A., Melo, H., da Silva, G., Alves-Leon, S., de Souza, J., Ferreira, S., De Felice, F., and Gomes, F. 2017. “Astrocyte Transforming Growth Factor Beta 1 Protects Synapses against Aβ Oligomers in Alzheimer's Disease Model.” *Journal of Neuroscience* 6797-6809.

Dinkova-Kostova, A. 2012. “The Role of Sulfhydryl Reactivity of Small Molecules for the Activation of the KEAP1/NRF2 Pathway and the Heat Shock Response.” *Scientifica.*

DiSabato, D., Quan, N., and Godbout, J. 2016. “Neuroinflammation: the devil is in the details.” *Journal of Neurochemistry* 136-153.

Ditsworth D., Maldonado, M., McAlonis-Downes, M., Sun, S., Seelman, A., Drenner, K., Arnold, E., Ling, S-C., Pizzo, D., Ravits, J., Cleveland, D., and Da Cruz, S. 2017. “Mutant TDP-43 within motor neurons drives disease onset but not progression in amyotrophic lateral sclerosis.” *Acta Neuropathologica* 907-922.

Dou, F., Netzer, W., Tanemura, K., Li, F., Hartl, F., Takashima, A., Gouras, G., Greengard, P., and Xu. 2003. “Chaperones increase association of tau proteinwith microtubules.” *PNAS* 721-726.

Du, H., and Yan, S. 2010. “Mitochondrial permeability transition pore in Alzheimer's disease: Cyclophilin D and amyloid beta.” *Biochimica et Biophysica Acta (BBA) - Molecular Basis of Disease* 198-204.

Duff K, Knight H, Refolo LM, Sanders S, Yu X, Picciano M, Malester B, Hutton M, Adamson J, Goedert M, Burki K, Davies P. 2000. “Characterization of pathology in transgenic mice over-expressing human genomic and cDNA tau transgenes.” *Neurobiology of Disease* 87-98.

Duff, K., Noble, W., Gaynor, K., and Matsuoka, Y. 2002. “Organotypic slice cultures from transgenic mice as disease model systems.” *Journal of Molecular Neuroscience* 317-320.

Dukay, B., Walter, F., Vigh, J., Barabási, B., Hajdu, P., Balassa, T., Migh, E., Kincses, A., Hoyk, Z., Szögi, T., Borbély, E., Csoboz, B., Horváth, P., Fülöp, L., Penke, B., Vígh, L., Deli, M., Sántha, M., and Tóth, M. 2021. “Neuroinflammatory processes are augmented in mice overexpressing human heat-shock protein B1 following ethanol-induced brain injury.” *Journal of Neuroinflammation.*

Eaton, P., Fuller, W., and Shattock, M. 2002. “S-Thiolation of HSP27 Regulates Its Multimeric Aggregate Size Independently of Phosphorylation.” *Journal of biological chemistry* 1189-21196.

Ecroyd, H., Meehan, S., Horwitz, J., Aquilina, A., Benesch, J., Robinson, C., Macphee, C., and Carver, J. 2007. “Mimicking phosphorylation of αB-crystallin affects its chaperone activity.” *Biochemical Journal* 129-141.

Eidenmüller, J., Fath, T., Maas, T., Pool, M., Sontag, E., and Brandt, R. 2001. “Phosphorylation-mimicking glutamate clusters in the proline-rich region are sufficient to simulate the functional deficiencies of hyperphosphorylated tau protein.” *The Biochemical Journal* 759-767.

Eng, L. F., Vanderhaeghen, J. J., Bignami, A. and Gerstl, B. 1971. “An acidic protein isolated from fibrous astrocytes.” *Brain Research* 351-354.

Escartin, C., Galea, E., Lakatos, A., O’Callaghan, J., Petzold, G., Serrano-Pozo, A., Steinhäuser, C., Volterra, A., Carmignoto, G., Agarwal, A., Allen, N., Araque, A., Barbeito, L., Barzilai, A., Bergles, D., Bovento, G., Butt, A., and Verkhratsky, A. 2021. “Reactive astrocyte nomenclature, definitions, and future directions.” *Nautre Neuroscience* 312-325.

Evans, C., Wisen, S., and Gestwicki, J. 2006. “Heat Shock Proteins 70 and 90 Inhibit Early Stages of Amyloid β-(1–42) Aggregation in Vitro.” *Protein structure and folding* 33182-33191.

Fan, R., and Tenner, A. 2004. “Complement C1q expression induced by Abeta in rat hippocampal organotypic slice cultures.” *Experimental Neurology* 241-253.

Farina, C., Aloisi, F., and Meinl, E. 2007. “Astrocytes are active players in cerebral innate immunity.” *Trends in Immunology* 138-145.

Felsky, D., Roostaei, T., Nho, K., Risacher, S., Bradshaw, E., Petyuk, V., Schneider, J., Saykin, A., Bennett, D., and De Jager, P. 2019. “Neuropathological correlates and genetic architecture of microglial activation in elderly human brain.” *Nature Communications.*

Ferrer, I., García, M., González, I., Lucena, D., Villalonga, A., Tech, M., Llorens, F., Garcia-Esparcia, P., Martinez-Maldonado, A., Mendez, M., Escribano, B., Bech-Serra, J., Sabido, E., Gomez, C., and del Rio, J. 2018. "Aging-related tau astrogliopathy (ARTAG): not only tau phosphorylation in astrocytes." *Brain Pathology* 965-985.

Filipcik, P., Cente, M., Zilka, N., Smolek, T., Hanes, J., Kucerak, J., Opattova, A., Kovacech, B. and Novak, M. 2015. "Intraneuronal accumulation of misfolded tau protein induces overexpression of Hsp27 in activated astrocytes." *Biochimica et Biophysica Acta (BBA) - Molecular Basis of Disease* 1219-1229.

Fitzjohn, S., Doherty, A., and Collingridge, G. 2008. "The use of the hippocampal slice preparation in the study of Alzheimer's disease." *European Journal of Pharmacology* 50-59.

Fonte, V., Kapulkin, W., Taft, A., Fluet, A., Friedman, D., and Link, C. 2002. "Interaction of intracellular β amyloid peptide with chaperone proteins." *PNAS* 9439-9444.

Fox, L., William, C., Adamowicz, D., Pitstick, R., Carlson, G., Spires-Jones, T., and Hyman, B. 2011. "Soluble tau species, not neurofibrillary aggregates, disrupt neural system integration in a tau transgenic model." *Journal of neuropathology and experimental neurology* 588-595.

Franklin, T., Kruegar, A., Clarke, D., Arrigo, A-P., and Currie, R. 2005. "The role of heat shock proteins Hsp70 and Hsp27 in cellular protection of the central nervous system." *International Journal of Hyperthermia* 379-392.

Fraser, P. 2014. "Prions and Prion-like Proteins." *The Journal of Biological Chemistry* 19839-19840.

Freilich, R., Betegon, M., Tse, E., Mok, S-A., Julien, O., Agard, D., Southworth, D., Takeuchi, K., and Gestwicki, J. 2018. "Competing protein-protein interactions regulate binding of Hsp27 to its client protein tau." *Nature Communications.*

Fukada, Y., Yasui, K., Kitayama, M., Doi, K., Nakano, T., Watanabe, Y., and Nakashima, K. 2007. "Gene expression analysis of the murine model of amyotrophic lateral sclerosis: studies of the Leu126delTT mutation in SOD1." *Brain Research* 1-10.

Gahwiler, B. 1981. "Organotypic monolayer cultures of nervous tissue." *Journal Neuroscience Methods* 329-342.

Gahwiler, B., Capogna, M., Debanne, D., McKinney, R., and Thompson, S. 1997. "Organotypic slice cultures: a technique has come of age." *Trends Neuroscience* 471-477.

Gallo, V., and Armstrong, R. 1995. "Developmental and growth factor-induced regulation of nestin in oligodendrocyte lineage cells." *The Journal of Neuroscience* 394-406.

Gangalum, R., Bhat, A., Kohan, S., and Bhat, S. 2016. "Inhibition of the Expression of the Small Heat Shock Protein αB-Crystallin Inhibits Exosome Secretion in Human Retinal Pigment Epithelial Cells in Culture." *Journal of Biological Chemistry* 12930-12942.

Garrido, C., Gurbuxani, S., Ravagnan, L., and Kroemer, G. 2001. "Heat Shock Proteins: Endogenous Modulators of Apoptotic Cell Death." *Biochemical and biophysical research communications* 433-442.

Garwood, C., Pooler, A., Atherton, J., Hanger, D., and Noble, W. 2011. "Astrocytes are important mediators of Aβ-induced neurotoxicity and tau phosphorylation in primary culture." *Cell death & disease.*

Gendreau, K., and Hall, G. 2013. “Tangles, toxicity, and tau secretion in AD – new approaches to a vexing problem.” *Frontiers in Neurology.*

Gerics, B., Szalay, F., and Hajos, F. 2006. “Glial fibrillary acidic protein immunoreactivity in the rat suprachiasmatic nucleus: circadian changes and their seasonal dependence.” *Journal of Anatomy* 231-237.

Gesase, A., and Kiyama, H. 2007. “Peripheral nerve injury induced expression of mRNA for serine protease inhibitor 3 in the rat facial and hypoglossal nuclei but not in the spinal cord.” *Italian journal of anatomy and embryology* 157-168.

Ghetti, B., Oblak, A., Boeve, B., Johnson, K., Dickerson, B., and Goedert, M. 2014. “Invited review: Frontotemporal dementia caused by microtubule-associated protein tau gene (MAPT) mutations: a chameleon for neuropathology and neuroimaging.” *Neuropathology and applied neurobiology* 24-46.

Gianinazzi, C., Grandgirard, D., Simon, F., Imboden, H., Joss, P., Täuber, M., and Leib, L. 2004. “Apoptosis of Hippocampal Neurons in Organotypic Slice Culture Models: Direct Effect of Bacteria Revisited.” *Journal of Neuropathology & Experimental Neurology* 610-617.

Gibbons, G., Banks, R.., Kim, B., Changolkar, L., Riddle, D., Leight, S., Irwin, D., Trojanowski, J., and Lee, V. 2018. “Detection of Alzheimer Disease (AD)-Specific Tau Pathology in AD and NonAD Tauopathies by Immunohistochemistry With Novel Conformation-Selective Tau Antibodies.” *Journal of neuropathology and experimental neurology* 216-228.

Goedert M., Masuda-Suzukake, M., and Falcon, B. 2017. “Like prions: the propagation of aggregated tau and α-synuclein in neurodegeneration.” *Brain* 266–278.

Gogolla, N., Galimberti, I., DePaola, V., and Caroni, P. 2006. “Staining protocol for organotypic hippocampal slice cultures.” *Nature Protocols* 2452-2456.

Golenhofen, N., and Bartelt-Kirbach, B. 2016. “The Impact of Small Heat Shock Proteins (HspBs) in Alzheimer's and Other Neurological Diseases.” *Current Pharmaceutical Design* 4050-4062.

Gomes, L., Hipp, S., Upadhaya, A., Balakrishnan, K., Ospitalieri, S., Koper, M., Largo-Barrientos, P., Uytterhoeven, V., Reichwald, J., Rabe, S., Vandenberghe, R., von Arnim, C., Tousseyn, T., Feederle, R., Giudici, C., Willem, M., and Thal, D. 2019. “Aβ-induced acceleration of Alzheimer-related τ-pathology spreading and its association with prion protein.” *Acta Neuropathologica* 913-941.

Goncalves, C., Sharon, I., Schmeing, T., Ramos, C., and Young, J. 2021. “The chaperone HSPB1 prepares protein aggregates for resolubilization by HSP70.” *Scientific Reports.*

Gong, C., Lidsky, T., Wegiel, J., Zuck, L., Grundke-Iqbal, I., and Iqbal, K. 2000. “Phosphorylation of Microtubule-associated Protein Tau Is Regulated by Protein Phosphatase 2A in Mammalian Brain: IMPLICATIONS FOR NEUROFIBRILLARY DEGENERATION IN ALZHEIMER'S DISEASE.” *Journal of Biological Chemistry* 5535-5544.

González-Reyes, G., Nava-Mesa, M., Vargas-Sánchez, K., Ariza-Salamanca, D., and Mora-Muñoz, L. 2017. “Involvement of Astrocytes in Alzheimer’s Disease from a Neuroinflammatory and Oxidative Stress Perspective.” *Frontiers in Molecular Neuroscience.*

Goodwin, M., Croft, C., Futch, H., Ryu, D., Ceballos-Diaz, C., Liu, X., Paterno, G., Mejia, C., Deng, D., Menezes, K., Londono, L., Arjona, K., Parianos, M., Truong, V., Rostonics, E., Hernandez, A.,

Boye, S., Boye, S., Levites, Y., Cruz, P., & Golde T. 2020. “Utilizing minimally purified secreted rAAV for rapid and cost-effective manipulation of gene expression in the CNS.” *Molecular Neurodegeneration .*

Gorman, M., Feigl, E., and Buffington, C. 2007. “Human Plasma ATP Concentration .” *Clinical Chemistry* 318-325.

Gotoh, H., Kajikawa, M., Kato, H., and Suto, K. 1999. “Intracellular Mg2+ surge follows Ca2+ increase during depolarization in cultured neurons.” *Brain Research* 163-168.

Götz, J., Bodea, L-G., and Goedert, M. 2018. “Rodent models for Alzheimer disease.” *Nature Reviews, Neuroscience* 583-598.

Gratuze, M., Leyns, C., and Holtzman, D. 2018. “New insights into the role of TREM2 in Alzheimer's Disease.” *Molecular Neurodegeneration .*

Greenberg SG, Davies P. 1990. “A preparation of Alzheimer paired helical filaments that displays distinct tau proteins by polyacrylamide gel electrophoresis.” *Proceedings of the National Academy of Sciences* 5827-5831.

Greenberg, M., Greene, L., and Ziff, E. 1985. “Nerve growth factor and epidermal growth factor induce rapid transient changes in proto-oncogene transcription in PC12 cells.” *The Journal of Biological Chemistry* 14101-14110.

Grubman, A., Chew, G., Ouyang, J., Sun, G., Choo, X., McLean, C., Simmons, R., Buckberry, S., Vargas-Landin, D., Poppe, D., Pflueger, J., Lister, R., Rackham, O., Petretto, E., and Polo, J. 2019. “A single-cell atlas of entorhinal cortex from individuals with Alzheimer’s disease reveals cell-type-specific gene expression regulation.” *Nature Neuroscience* 2087-2097.

Grundke-Iqbal, I., Iqbal, K., Quinlan, M., Tung, Y., Zaidi, M., and Wisniewski, H. 1986. “Microtubule-associated protein tau. A component of Alzheimer paired helical filaments.” *Journal of Biological Chemistry* 6084-6089.

Gu, J., Congdon, E., and Sigurdsson, E. 2013. “Two Novel Tau Antibodies Targeting the 396/404 Region Are Primarily Taken Up by Neurons and Reduce Tau Protein Pathology.” *The Journal of Biological Chemistry* 33081-33095.

Guo, J., Narasimhan, S., Changolkar, L., He, Z., Stieber, A., Zhang, B., Gathagan, R., Iba, M., McBride, J., Trojanowski, J and Lee, V. 2016. “Unique pathological tau conformers from Alzheimer's brains transmit tau pathology in nontransgenic mice.” *The journal of experimental medicine* 2635-2654.

Guo, Y-S., Liang, P-Z., Lu, S-Z., Chen, R., Yin, Y-Q., and Zhou, J-W. 2019. “Extracellular αB-crystallin modulates the inflammatory responses.” *Biochemical and biophysical research communications`* 282-288.

Haim, L., Carrillo-de Sauvage, M., Ceyzériat, K., and Escartin, C. 2015. “Elusive roles for reactive astrocytes in neurodegenerative diseases.” *Cell Neuroscience.*

Hamos, J., Oblas, B., Pulaski-Salo, D., Welch, W., Bole, D., and Drachman, D. 1991. “Expression of heat shock proteins in Alzheimer's disease.” *Neurology* 345-350.

Hampton, D., Amor, S., Story, D., Torvell, M., Bsibsi, M., van Noort, J., and Chandran, S. 2020. “HspB5 Activates a Neuroprotective Glial Cell Response in Experimental Tauopathy.” *Frontiers in Neuroscience.*

Hanger, D., Anderton, B., and Noble, W. 2009. “Tau phosphorylation: the therapeutic challenge for neurodegenerative disease.” *Trends in Molecular Medicine* 112-119.

Hartl F. and Hayer-Hartl, M. 2002. “Molecular Chaperones in the Cytosol: from Nascent Chain to Folded Protein.” *Science* 1852-1858.

Hartl F., Bracher, A., and Hayer-Hartl, M. 2011. “Molecular chaperones in protein folding and proteostasis.” *Nature* 324-332.

Hartl, F., and Hayer-Hartl, M. 2009. “Converging concepts of protein folding in vitro and in vivo.” *Natire Structual & molecular biology* 574-581.

Hartl, F., Bracher, A., and Hayer-Hartl, M. 2011. “Molecular chaperones in protein folding and proteostasis.” *Nature* 324-332.

Harwell, C., and Coleman, M. 2016. “Synaptophysin depletion and intraneuronal Aβ in organotypic hippocampal slice cultures from huAPP transgenic mice.” *Molecular Neurodegeneration .*

Hasel, P., Rose, I., Sadick, S., Kim, R., Liddelow, S. 2021. “Neuroinflammatory astrocyte subtypes in the mouse brain.” *Nature Neuroscience* 1475-1487.

Haslbeck, M., Franzmann, T., Weinfurtner, D., and Buchner, J. 2005. “Some like it hot: the structure and function of small heat-shock proteins.” *Nature Structural & Molecular Biology* 842-846.

Haslbeck, M., Weinkauf, S., and Buchner, J. 2018. “Small heat shock proteins: Simplicity meets complexity.” *The journal of biological chemistry* 2121-2132.

Hayes, D., Napoli, V., Mazurkie, A., Stafford, W., and Graceffa, P. 2009. “Phosphorylation Dependence of Hsp27 Multimeric Size and Molecular Chaperone Function*.” *Journal of biological chemistry* 18801-18807.

He, Z., Guo, J., McBride, J., Narasimhan, S., Kim, H., Changolkar, L., Zhang, B., Gathagan, R., Yue, C., Dengler, C., Stieber, A., Nitla, M., Coulter, D., Abel, T., Brunden, K., Trojanowski, J., and Lee, V. 2017. “Amyloid-β plaques enhance Alzheimer's brain tau-seeded pathologies by facilitating neuritic plaque tau aggregation.” *Nature Medicine* 29-38.

He, Z., McBride, J., Xu, H., Changolkar, L., Kim, S-J., Zhang, B., Narasimhan, S., Gibbons, G., Guo, J., Kozak, M., Schellenberg, G., Trojanowski, J., and Lee, V. 2020. “Transmission of tauopathy strains is independent of their isoform composition.” *Nature Communications.*

Hecker, J., and McGarvey, M. 2011. “Heat shock proteins as biomarkers for the rapid detection of brain and spinal cord ischemia: a review and comparison to other methods of detection in thoracic aneurysm repair.” *Cell Stress and Chaperones* 119-131.

Hellwig, S., Masuch, A., Nestel, S., Katzmarski, N., Meyer-Luehmann, M., and Biber, K. 2015. “Forebrain microglia from wild-type but not adult 5xFAD mice prevent amyloid-β plaque formation in organotypic hippocampal slice cultures.” *Scientific Reports.*

Heneka, M., Carson, M., Khoury, E., Landreth, G., Brosseron, F., Feinstein, D., Jacobs, A., Wyss-Coray, T., Vitorica, J., Ransohoff, R., Herrup, K., Frautschy, S., Finsen, B., Brown, G., Verhratsky, A.,

Yamanaka, K., Koistinaho, J., Latz, E., and Kummer,. 2015. “Neuroinflammation in Alzheimer's disease.” *The Lancet Neurology* 388-405.

Herculano-Houzel, S. 2014. “The glia/neuron ratio: how it varies uniformly across brain structures and species and what that means for brain physiology and evolution.” *Glia* 1377-1391.

Herrmann, J., Imura, T., Song, B., Qi, J., Ao, Y., Nguyen, T., Korsak, R., Takeda, K., Akira, S., and Sofroniew, M. 2008. “STAT3 is a critical regulator of astrogliosis and scar formation after spinal cord injury.” *Journal of Neuroscience* 7231-7243.

Hochberg, G., and Benesch, J. 2014. “Dynamical structure of αB-crystallin.” *Progress in biophysics and molecular biology* 11-20.

Hong, S., Beja-Glasser, V., Nfonoyim, B., Frouin, A., Li, S., Ramakrishnan, S., Merry, K., Shi, Q., Rosenthal, A., Barres, B., Lemere, C., Selkoe, D., and Stevens, B. 2016. “Complement and microglia mediate early synapse loss in Alzheimer mouse models.” *Science* 712-716.

Hong, W., Wang, Z., Liu, W., O’Malley, T., Jin, M., Willem, M., Haass, C., Frosch, M., and Walsh, D. 2018. “Diffusible, highly bioactive oligomers represent a critical minority of soluble Aβ in Alzheimer’s disease brain.” *Acta Neuropathologica* 19-40.

Hoover, B., Reed, M., Su, J., Penrod, R., Kotilinek, L., Grant, M., Pitstick, R., Carlson, G., Lanier, L., Yuan, L., Ashe, K., and Liao, D. 2010. “Tau Mislocalization to Dendritic Spines Mediates Synaptic Dysfunction Independently of Neurodegeneration.” *Neuron* 1067-1081.

Horwitz, J. 1992. “Alpha-crystallin can function as a molecular chaperone.” *PNAS* 10449-10453.

Hoter, A., El-Sabban, M., and Naim, H. 2018. “The HSP90 Family: Structure, Regulation, Function, and Implications in Health and Disease.” *International journal of molecular science.*

Hsiao, K., Chapman, P., Nilsen, S., Eckman, C., Harigaya, Y., Younkin, S., Yang, F., and Cole, G. 1996. “Correlative Memory Deficits, Aβ Elevation, and Amyloid Plaques in Transgenic Mice.” *Science* 99-103.

Hsiao, K., Chapman, P., Nilsen, S., Eckman, C., Harigaya, Y., Younkin, S., Yang, F., Cole, G. 1996. “Correlative Memory Deficits, Aβ Elevation, and Amyloid Plaques in Transgenic Mice.” *Science* 99-103.

Hu, J., Akama, K., Krafft, G., Chromy, B., and van Eldik, L. 1998. “Amyloid-β peptide activates cultured astrocytes: morphological alterations, cytokine induction and nitric oxide release.” *Brain Research* 195-206.

Huang, C., Cheng, H., Hao, S., Zhou, H., Zhang, X., Gao, J., Sun, Q, Hu, H., and Wang, C. 2006. “Heat Shock Protein 70 Inhibits α-Synuclein Fibril Formation via Interactions with Diverse Intermediates.” *Journal of Molecular Biology* 323-336.

Hudry, E., Wu, H., Arbel-Ornath, M., Hashimoto, T., Matsouaka, R., Fan, Z., Spires-Jones, T., Betensky, R., Bacskai, B., and Hyman, B. 2012. “Inhibition of the NFAT Pathway Alleviates Amyloid Beta Neurotoxicity in a Mouse Model of Alzheimer's Disease.” *The Journal of Neuroscience* 3176-3192.

Humpel, C. 2015. “Organotypic brain slice cultures: A review.” *Neuroscience* 86-98.

Humpel, C. 2015. “Organotypic vibrosections from whole brain adult Alzheimer mice (overexpressing amyloid-precursor-protein with the Swedish-Dutch-Iowa mutations) as a model to study clearance of beta-amyloid plaques.” *Frontiers in aging neuroscience* 47.

Hutter-Schmid, B., Kniewallner, K., and Humpel, C.Organotypic brain slice cultures as a model to study angiogenesis of brain vessels. 2015. “Organotypic brain slice cultures as a model to study angiogenesis of brain vessels.” *Frontiers in cell and developmental biology.*

Hutton, M., Lendon, C., Rizzu, P., Baker, M., Froelich, S., Houlden, H., Pickering-Brown, S., Chakraverty, S., Isaacs, A., Grover, A., Hackett, J., Adamson, J., Lincoln, S., Dickson, D., Davies, P., Peter, R., Ptereson, R., Stevens. M., and Heutink, P.,. 1998. “Association of missense and 5’-splice-site mutations in tau with the inherited dementia FTDP-17.” *Nature* 702-705.

Ingelsson, M., Fukumoto, H., Newell, K. L., Growdon, J. H., Hedley-Whyte, E. T., Frosch, M. P., Albert, M. S., Hyman, B. T., and Irizarry, M. C. 2004. “Early Abeta accumulation and progressive synaptic loss, gliosis, and tangle formation in AD brain.” *Neurology* 925-931.

Ingelsson, M., Fukumoto, H., Newell, K., Growdon, J., Hedley-Whyte, E., Frosch, M., Albert, M., Hyman, B., and Irizarry, M. 2004. “Early Abeta accumulation and progressive synaptic loss, gliosis, and tangle formation in AD brain.” *Neurology* 925-931.

Inhara, Y., Morishima-Kawashima, M., and Nixon, R. 2012. “The Ubiquitin–Proteasome System and the Autophagic–Lysosomal System in Alzheimer Disease.” *Cold Spring Harb Perspect Med.*

Iram, T., Trudler, D., Kain, D., Kanner, S., Galron, R., Vassar, R., Barzilai, A., Blinder, P., Fishelson, Z., and Frenkel, D. 2016. “Astrocytes from old Alzheimer's disease mice are impaired in Aβ uptake and in neuroprotection.” *Neurobiology of disease* 84-94.

Itagaki, S., McGeer, P., Akiyama, H., and Selkoe, D. 1989. “Relationship of microglia and astrocytes to amyloid deposits of Alzheimer disease.” *Journal of Neuroimmunology* 173-182.

Ito, H., Kamei, K., Iwamoto, I., Inaguma, Y., Nohara, D., and Kato, K. 2001. “Phosphorylation-induced Change of the Oligomerization State of αB-crystallin.” *Journal of biological chemistry* 5346-5352.

Iwaki, T., Wisniewski, T., Iwaki, A., Corbin, E., Tomokane, N., Tateishi, J., and Goldman, J. 1992. “Accumulation of alpha B-crystallin in central nervous system glia and neurons in pathologic conditions.” *The American Journal of Pathology* 345-356.

Jakob, U., Gaestel, M., Engel, K., and Buchner, J. 1993. “Small heat shock proteins are molecular chaperones.” *The Journal of biological chemistry* 1517-1520.

Jana, A., and Pahan, K. 2010. “Fibrillar Amyloid-β-Activated Human Astroglia Kill Primary Human Neurons via Neutral Sphingomyelinase: Implications for Alzheimer's Disease.” *Journal of Neuroscience* 12676-12689.

Jankowsky, J., Fadale, D., Anderson, J., Xu, G., Gonzales, V., Jenkins, N., Copeland, N., Lee, M., Younkin, L., Wagner, S., Younkin, S., and Borchelt, D. 2004. “Mutant presenilins specifically elevate the levels of the 42 residue beta-amyloid peptide in vivo: evidence for augmentation of a 42-specific gamma secretase.” *Human Molecular Genetics* 159-170.

Jaya, N., and Vierling, E. 2009. “Substrate binding site flexibility of the small heat shock protein molecular chaperones.” *PNAS* 15604-15609.

Jehle, S., Vollmar, B., Bardiaux, B., Dove, K., Rajagopal, P., Gonen, T., Oschkinat, H., and Klevit, R. 2011. “N-terminal domain of αB-crystallin provides a conformational switch for multimerization and structural heterogeneity.” *PNAS* 6409-6414.

Jha, M., Jo, M., Kim, J., and Suk, K. 2019. “Microglia-Astrocyte Crosstalk: An Intimate Molecular Conversation.” *The Neuroscientist* 227-240.

Jicha, G., Bowser, R., Kazam, I., and Davies, P. 1998. “Alz-50 and MC-1, a new monoclonal antibody raised to paired helical filaments, recognize conformational epitopes on recombinant tau.” *Journal of Neurosciecne Research* 128-132.

Jin, C., Cleveland, J., Ao, L., Li, J., Zeng, Q., Fullerton, D., and Meng, X. 2014. “Human Myocardium Releases Heat Shock Protein 27 (HSP27) after Global Ischemia: The Proinflammatory Effect of Extracellular HSP27 through Toll-like Receptor (TLR)-2 and TLR4.” *Molecular Medicine* 280-289.

Jing L., Cheng, S., Pan, Y., Liu, Q,. Yang, W., Li, S., and Li, X-J. 2021. “Accumulation of Endogenous Mutant Huntingtin in Astrocytes Exacerbates Neuropathology of Huntington Disease in Mice.” *Molecularu Neurobiology* 5112-5126.

Jing, R., Wilhelmsson, U., Goodwill, W., Li, L., Pan, Y., Pekny, M., and Skalli, O. 2007. “Synemin is expressed in reactive astrocytes in neurotrauma and interacts differentially with vimentin and GFAP intermediate filament networks.” *Journal of Cell Science* 1267-1277.

Jiwaji, Z., Tiwari, S., Avilés-Reyes, R., Hooley, M., Hampton, D., Torvell, M., Johnson, D., McQueen, J., Baxter, P., Sabari-Sankar, K., Qiu, J., He, X., Fowler, J., Febery, J., Gregory, J., Rose, J., Tulloch, J., Loan, J., Story, D., McDade, K., Smith, A. 2022. “Reactive astrocytes acquire neuroprotective as well as deleterious signatures in response to Tau and Aß pathology.” *Nature Communications.*

Joel, Z., Izquierdo, P., Salih, D., Richardson, J., Cummings, D., and Edwards, F. 2018. “Improving Mouse Models for Dementia. Are All the Effects in Tau Mouse Models Due to Overexpression?” *CSH Symposia on quantitative biology* 151-161.

John, A., and Reddy, P. 2021. “Synaptic basis of Alzheimer’s disease: Focus on synaptic amyloid beta, P-tau and mitochondria.” *Ageing Research Reviews.*

Jurga, A., Paleczna, M., and Kuter, K. 2020. “Overview of General and Discriminating Markers of Differential Microglia Phenotypes.” *Frontiers in cellular neuroscience.*

Kahlson, M., and Colodner, K. 2015. “Glial Tau Pathology in Tauopathies: Functional Consequences.” *Journal of Experimental Neuroscience* 43-50.

Kalwy, S., Akbarb, M., Coffin, R., de Belleroche, J., and Latchman, D.,. 2003. “Heat shock protein 27 delivered via a herpes simplex virus vector can protect neurons of the hippocampus against kainic-acid-induced cell loss.” *Molecular Brain Research* 91-103.

Kamboh, M. 2018. “A Brief Synopsis on the Genetics of Alzheimer's Disease.” *Current genetic medicine reports* 133-135.

Kamphuis, W., Kooijman, L., Orre, M., Stassen, O., Pekny, M., and Hol, E. 2015. “GFAP and vimentin deficiency alters gene expression in astrocytes and microglia in wild-type mice and changes the transcriptional response of reactive glia in mouse model for Alzheimer's disease.” *Glia* 1036-1056.

Kampinga H. and Craig, E. 2010. “The HSP70 chaperone machinery: J proteins as drivers of functional specificity.” *Nature reviews: Molecular cell biology* 579-592.

Kampinga, H., Hageman, J., Vos, M., Kubota, H., Tanguay, R., Bruford, E., Cheetham, M., Chen, B., and Hightower, L.,. 2009. “Guidelines for the nomenclature of the human heat shock proteins.” *Cell Stress & Chaperones* 105-111.

Kamradt, M., Chen, F., Sam, S., and Cryns, V. 2002. “The small heat shock protein alpha B-crystallin negatively regulates apoptosis during myogenic differentiation by inhibiting caspase-3 activation.” *The Journal of Biological Chemistry* 38731-38736.

Kanaan, N., Hamel, C., Grabinski, T., and Combs, B. 2020. “Liquid-liquid phase separation induces pathogenic tau conformations in vitro.” *Nature Communications .*

Karagöz, G., Duarte, A., Akoury, E., Boelens, R., and Madl, T. 2014. “Hsp90-Tau Complex Reveals Molecular Basis for Specificity in Chaperone Action.” *Cell* 963-974.

Kato, S., Hirano, A., Umahara, T., Kato, M., Herz, F. and Ohama, E. 1992. “Comparative immunohistochemical study on the expression of αB crystallin, ubiquitin and stress-response protein 27 in ballooned neurons in various disorders.” *Neuropathology and Applied Neurobiology* 335-340.

Kim, K., Kim, R., and Kim, S. 1998. “Crystal structure of a small heat-shock protein.” *Nature* 595-599.

Klaips, C., Jayaraj, G., and Hartl, U. 2017. “Pathways of cellular proteostasis in aging and disease .” *Journal of Cell Biology* 51-63.

Kleizen, B., and Braakman, I. 2004. “Protein folding and quality control in the endoplasmic reticulum.” *Current opinion in cell biology* 343-349.

Klopstein, A., Santos-Nogueira, E., Francos-Quijorna, I., Redensek, A., David, S., Navarro, X., and López-Vales, R. 2012. “Beneficial effects of αB-crystallin in spinal cord contusion injury.” *Journal of Neuroscience* 14478-14488.

Kobayashi, E., Suzuki, T., Funayama, R., Nagashima, T., Hayashi, M., Sekine, H., Tanaka, N., Moriguchi, T., Motohashi, H., Nakayama, K., and Yamamoto, M.,. 2016. “Nrf2 suppresses macrophage inflammatory response by blocking proinflammatory cytokine transcription.” *Nature Communications.*

Koffie, R., Meyer-Luehmann, M., Hashimoto, T., Adams, K., Mielke, M., Garcia-Alloza, M., Micheva, K., Smith, S., Kim, M., Lee, V. Hyman, B., and Spires-Jones, T. 2009. “Oligomeric amyloid β associates with postsynaptic densities and correlates with excitatory synapse loss near senile plaques.” *PNAS* 4012-4017.

Koistinaho, M., Lin, S., Wu, X., Esterman, M., Koger, D., Hanson, J., Higgs, R., Liu, F., Malkani, S., Bales, K., and Paul, S. 2004. “Apolipoprotein E promotes astrocyte colocalization and degradation of deposited amyloid-beta peptides.” *Nautre Medicine* 719-726.

Kore, R., and Abraham, E. 2016. “Phosphorylation negatively regulates exosome mediated secretion of cryAB in glioma cells.” *Biochimica et biophysica Acta* 368-377.

Kovacs, G. 2020. “Astroglia and Tau: New Perspectives.” *Frontiers in Aging Neuroscience.*

Kovacs, G. 2016. “Molecular Pathological Classification of Neurodegenerative Diseases: Turning towards Precision Medicine.” *International Journal of Molecular Sciences.*

Kraft, A., Hu, X., Yoon, H., Yan, P., Xiao, Q., Wang, Y., Gil, S., Brown, J., Wilhelmsson, U., Restivo, J., Cirrito, J., Holtzman, D., Kim, J., Pekny, M., and Lee, J-M. 2013. “Attenuating astrocyte activation accelerates plaque pathogenesis in APP/PS1 mice.” *FASEB Journal1* 187-198.

Kummer, K., Zeidler, M., Kalpachidou, T., and Kress, M. 2021. “Role of IL-6 in the regulation of neuronal development, survival and function.” *Cytokine* 155582.

Kurnellas, M. Brownell, S., Su, L., Malkovskiy, A., Rajadas, J., Dolganov, G., Chopra, S., Schoolnik, G., Sobel, R., Webster, J., Ousman, S., Becker, R., Steinman, L., and Rothbard, J. 2012. “Chaperone Activity of Small Heat Shock Proteins Underlies Therapeutic Efficacy in Experimental Autoimmune Encephalomyelitis.” *Journal of Biological Chemistry.*

Lanzrein, A., Johnston, C., Perry, V., Jobst, K., King, E., Smith, A. 1998. “Longitudinal study of inflammatory factors in serum, cerebrospinal fluid, and brain tissue in Alzheimer disease: interleukin-1beta, interleukin-6, interleukin-1 receptor antagonist, tumor necrosis factor-alpha, the soluble tumor necrosis factor receptors .” *Alzheimer's disease and assoicated disorders* 215-227.

LaRocca, T., Cavalier, A., Roberts, C., Lemieux, M., Ramesh, P., Garcia, M., and Link, C. 2021. “Amyloid beta acts synergistically as a pro-inflammatory cytokine.” *Neurobiology of Disease.*

Laskowska, E., Matuszewska, E., and Kuczynska-Wisnik, D. 2010. “Small Heat Shock Proteins and Protein-Misfolding Diseases.” *Current Pharmaceutical Biotenchology* 1389-2010.

Lau, S-F., Cao, H., Fu, A., and Ip, N. 2020. “Single-nucleus transcriptome analysis reveals dysregulation of angiogenic endothelial cells and neuroprotective glia in Alzheimer’s disease.” *PNAS* 2500-25809.

Lee, Y., and McKinnon, P. 2009. “Detection of Apoptosis in the Central Nervous System.” *Methods in molecular biology.*

Lee, Y-J., Lee, H-J., Choi, S-H., Jin, Y., An, H., Kang, J-H., Yoon, S., and Lee, Y-S. 2012. “Soluble HSPB1 regulates VEGF-mediated angiogenesis through their direct interaction.” *Angiogenesis* 229-242.

Leissring, M. 2016. “Aβ-Degrading Proteases: Therapeutic Potential in Alzheimer Disease.” *CNS Drugs* 667-675.

Leng, F., and Edison, P. 2021. “Neuroinflammation and microglial activation in Alzheimer disease: where do we go from here?” *Nature Reviews Neurology* 157-172.

Lewis, J., McGowan, E., Rockwood, J., Melrose, H., Nacharaju, P., Van Slegtenhorst, M., Gwinn-Hardy, K., Murphy, M., Baker, M., Yu, X., Duff, K., Hardy, J., Corral, A., Lin, W., Yen, S., Dickson, D., Davies, P., and Hutton, M. 2000. “Neurofibrillary tangles, amyotrophy and progressive motor disturbance in mice expressing mutant (P301L) tau protein.” *Nautre Genetics* 402-405.

Leyns, C., Ulrich, J., Finn, M., Stewart, F., Koscal, L., Serrano, J., Robinson, G., Anderson, E., Colonna, M., and Holtzman, D. 2017. “TREM2 deficiency attenuates neuroinflammation and protects against neurodegeneration in a mouse model of tauopathy.” *PNAS.*

Li J., Kanekiyo, T., Shinohara, M., Zhang, Y., LaDu, M., Xu, H., and Bu, G. 2012. “Differential regulation of amyloid-β endocytic trafficking and lysosomal degradation by apolipoprotein E isoforms.” *The Journal of Biological Chemistry* 44593-445601.

Li, A., Ceballos-Diaz, DiNunno, N., Levites, Y., Cruz, P., Lewis, J., Golde, T., and Chakrabarty, P. 2015. “IFN-gpromotestphosphorylation without affectingmature tangles.” *The FASEB journal* 438-4398.

Li, J., and Yuan, J. 2008. “Caspases in apoptosis and beyond.” *Oncogene* 6194-6206.

Liddelow, S., Guttenplan, K., Clarke, L., Bennett, F., Bohlen, C., Schirmer, L., Bennett, M., Münch, A., Chung, W-S., Peterson, T., Wilton, D., Frouin, A., Napier, B., Panicke, N., Kumar, M., Buckwalter, M., Rowitch, D., Dawson, V., Dawson, T., Stevens, B. 2017. “Neurotoxic reactive astrocytes are induced by activated microglia.” *Nature* 481-487.

Liebl, M., Windschmitt, J., Besemer, A., Schäfer, A-K., Reber, H., Behl, C., and Clement, C. 2015. “Low-frequency magnetic fields do not aggravate disease in mouse models of Alzheimer's disease and amyotrophic lateral sclerosis.” *Scientific Reports.*

Lin, T-H., Chiu, Y-J., Lin, C-h., Lin, C-Y., Chao, C-Y., Chen, Y-C., Yang, S-M., Lin, W., Hsieh-Li, H., Wu, Y-R., Chang, K-H., Lee-Chen, G-J., and Chen, C-M. 2020. “Exploration of multi-target effects of 3-benzoyl-5-hydroxychromen-2-one in Alzheimer's disease cell and mouse models.” *Aging Cell* e13169.

Liu F., Iqbal, K., Grundke-Iqbal, I., Rossie, S., and Gong, C. 2005. “Dephosphorylation of Tau by Protein Phosphatase 5: IMPAIRMENT IN ALZHEIMER'S DISEASE.” *The Journal of Biological Chemistry* 1790-1796.

Liu, F. Li, B., Tung, E., Grundke-Iqbal, I., Iqbal, K., and Gong, C. 2007. “Site-specific effects of tau phosphorylation on its microtubule assembly activity and self-aggregation.” *The European Journal of Neuroscience.*

Liu, F., Grundke-Iqbal, I., Iqbal, K., and Gong, C. 2005. “Contributions of protein phosphatases PP1, PP2A, PP2B and PP5 to the regulation of tau phosphorylation.” *European Journal of Neuroscience* 1942-1950.

Liu, L., Drouet, V., Wu, J., Witter, M., Small, S., Clelland, C., and Duff, K. 2012. “Trans-Synaptic Spread of Tau Pathology In Vivo.” *PLOS One.*

Long, J., and Holtzman, D. 2019. “Alzheimer Disease: An update on pathobiology and treatment strategies.” *Cell* 312 - 339.

López-González, I., Carmona, M., Arregui, L., Kovacs, G. and Ferrer, I. 2014. “αB-crystallin and HSP27 in glial cellsin tauopathies.” *Neuropathology* 517-526.

Lopez-Rodriguez, A., Hennessy, E., Murray, C., Nazmi, A., Delaney, H., Healy, D., Fagan, S., Rooney, M., Stewart, E., Lewis, A., de Barra, N., Scarry, P., Riggs-Miller, L., Boche, D., Cunningham, M., and Cunningham, C. 2021. “Acute systemic inflammation exacerbates neuroinflammation in Alzheimer's disease: IL-1β drives amplified responses in primed astrocytes and neuronal network dysfunction.” *Alzheimer's & Dementia* 1735-1755.

Loren, N., Hagman, J., Jonasson, J., Deschout, H., Bernin, D., Cella-Zanacchi, F., Diasprom A., McNally, J., Ameloot, M., Smisdom, N., Nyden, M., Hermansson, A-M., Rudemo, M., and Braeckmans,

K. 2015. “Fluorescence recovery after photobleaching in material and life sciences: putting theory into practice.” *Quarterly Reviews of Biophysics* 323-387.

Los Reyes, T., and Casas-Tinto, S. 2022. “Neural functions of small heat shock proteins.” *Neural regeneration research* 512-515.

Lu, M., and Kosik, K. 2001. “Competition for Microtubule-binding with Dual Expression of Tau Missense and Splice Isoforms.” *Molecular Biology of the Cell* 171-184.

Luo, W., Rodina, A., Chip, S., Kim, J., Zhao, Q., Moulick, K., Aguirre, J., Wu, N., Greengard, P., and Chiosis, G. 2007. “Roles of heat-shock protein 90 in maintaining and facilitating the neurodegenerative phenotype in tauopathies.” *PNAS* 9511-9516.

Mackenzie, I., Neumann, M., Bigio, E., Cairns, N., Alafuzoff, I., Kril, J., Kovacs, G., Ghetti, B., Halliday, G., Holm, I., Ince, P., Kamphorst, W., Revesz, T., Rozemuller, A., Kumar-Singh, S., Akiyama, H., Baborie, A., Spina, S., and Mann, D.,. 2010. “Nomenclature and nosology for neuropathologic subtypes of frontotemporal lobar degeneration: an update.” *Acta Neuropathologica* 1-4.

Magrané, J., Smith, R., Walsh, K., and Querfurth, H. 2004. “Heat Shock Protein 70 Participates in the Neuroprotective Response to Intracellularly Expressed β-Amyloid in Neurons.” *Journal of Neuroscience* 1700-1706.

Maia, L., Kaeser, S., Reichwald, J., Hruscha, M., Martus, P., Staufenbiel, M., and Jucker, M. 2013. “Changes in amyloid-β and Tau in the cerebrospinal fluid of transgenic mice overexpressing amyloid precursor protein.” *Science translational medicine .*

Mambula, S., Stevenson, M., Ogawa, K., and Calderwood, S. 2007. “Mechanisms for Hsp70 secretion: Crossing membranes without a leader.” *Methods* 168-175.

Mandelkow, E., von Bergen, M., Biernat, J., and Mandelkow, E. 2007. “Structural Principles of Tau and the Paired Helical Filaments of Alzheimer’s Disease.” *Brain Pathology.*

Mannini, B., Cascella, R., Zampagni, M., van Waarde-Verhagen, M., Meehan, S., Roodveldt, C., Campioni, S., Boninsegna, M., Penco, A., Relini, A., Kampinga, H., Dobson, C., Wilson, M., Cecchi, C., and Chiti, F. 2012. “Molecular mechanisms used by chaperones to reduce the toxicity of aberrant protein oligomers.” *PNAS* 12479-12484.

Mao, J., Katayama, S., Watanabe, C., Harada, Y., Noda, K., Yamamura, Y. and Nakamura, S. 2001. “The relationship between αB-crystallin and neurofibrillary tangles in Alzheimer's disease.” *Neuropathology and Applie Neurobiology* 180-188.

Mao, Y-W., Liu, J-P., and Li, D. 2004. “Human αA- and αB-crystallins bind to Bax and Bcl-XS to sequester their translocation during staurosporine-induced apoptosis.” *Cell death and differentiation* 512-526.

Martin, L., Latypova, X., and Terro, F. 2011. “Post-translational modifications of tau protein: Implications for Alzheimer's disease.” *Neurochemistry International* 458-471.

Martini-Stoica, H., Cole, A., Swartzlander, D., Chen, F., Wan, Y-W., Bajaj, L., Bader, D., Lee, V., Trojanowski, J., Liu, Z., Sardiello, M., and Zheng, H. 2018. “TFEB enhances astroglial uptake of extracellular tau species and reduces tau spreading.” *Journal of Experimental Medicine* 2355-2377.

Masilamonia, J., Vignesha, S., Kirubagaranb, R., Jesudasona, E., and Jayakumara, R. 2005. “The neuroprotective efficacy of α-crystallin against acute inflammation in mice.” *Brain Research Bulletin* 235-241.

Mathys, H., Davila-Velderrain, J., Peng, Z., Gao, F., Mohammadi, S., Young, J., Menon, M., He, L., Abdurrob, F., Jiang, X., Martorell, A., Ransohoff, R., Hafler, B., Bennett, D., Kellis, M., and Tsai, L-H. 2019. “Single-cell transcriptomic analysis of Alzheimer’s disease.” *Nature* 332-337.

Matsumoto, S., Motoi, Y., Ishiguro, K., Tabira, T., Kametani, F., Hasegawa, M., and Hattori, N. 2015. “The twenty-four KDa C-terminal tau fragment increases with aging in tauopathy mice: implications of prion-like properties.” *Human Molecular Genetics* 6403–6416.

Mayer, M. 2013. “Hsp70 chaperone dynamics and molecular mechanism.” *Trends in Biochemical Sciences* 507-514.

Mayer, M., and Bukau, B. 2005. “Hsp70 chaperones: Cellular functions and molecular mechanism.” *Cellular and molecular life science* .

McClellan, A., Xia, Y., Deutschbauer, A., Davis, R., Gerstein, M., and Frydman, J. 2007. “Diverse Cellular Functions of the Hsp90 Molecular Chaperone Uncovered Using Systems Approaches.” *Cell* 121-135.

McDonald, J., O'Malley, T., Liu, W., Mable, A., Brinkmalm, G., Portelius, E., Wittbold, W., Frosch, M., and Walsh, D. 2015. “The aqueous phase of Alzheimer's disease brain contains assemblies built from ~4 and~7kDa A-beta species.” *Alzheimer's & Dementia* 1286-1305.

McGreal, R., Kantorow, W., Chauss, D., Wei, J., Brennan, L., and Kantorow, M. 2012. “αB-crystallin/sHSP protects cytochrome c and mitochondrial function against oxidative stress in lens and retinal cells.” *Biochimica et Biophysica Acta (BBA) - General Subjects* 921-930.

Messing, L., Decker, J., Joseph, M., Mandelkow, E., and Mandelkow, E-M. 2013. “Cascade of tau toxicity in inducible hippocampal brain slices and prevention by aggregation inhibitors.” *Neurobiology of Ageing* 1343-1354.

Micheau, O., and Tschopp, J. 2003. “Induction of TNF receptor I-mediated apoptosis via two sequential signaling complexes.” *Cell* 181-190.

Michetti, F., D'Ambrosi, N., Toesca, A., Puglisi, M., Serrano, A., Marchese, E., Corvino, V., and Geloso, M. 2019. “The S100B story: from biomarker to active factor in neural injury.” *Journal of neurochemistry* 168-187.

Mishra, A., Kim, H., Shin, A., and Thayer, S. 2012. “Synapse Loss Induced by Interleukin-1β Requires Pre- and Post-Synaptic Mechanisms.” *Journal of neuroimmune pharmacology* 571-578.

Mok, S-A., Condello, C., Freilich, R,. Gillies, A., Arhar, T., Oroz, J., Kadavath, H., Julien, O., Assimon, V., Rauch, J., Dunyak, B., Lee, J., Tsai, F., Wilson, M., Zweckstetter, M., Dickey, C., and Gestwicki, J. 2018. “Mapping interactions with the chaperone network reveals factors that protect against tau aggregation.” *Nature Structural & Molecular Biology* 384-393.

Montine, T,J., Monsell, S., Beach, T., Bigio, E., Bu, Y., Cairns, N., Frosch, M., Henriksen, J., Kofler, J., and Kukull, W. 2016. “Multisite assessment of NIA-AA guidelines for the neuropathologic evaluation of Alzheimer's disease. .” *Alzheimers Dement.* 164-169.

Moreno, H., Morfinib, G., Buitrago, L.,Ujlaki, G., Choi, S., Yu, E., Moreir, J., Avil, J., Brady, S., Pant, H., Sugimori, M., and Llinás, R. 2016. “Tau pathology-mediated presynaptic dysfunction.” *Neuroscience* 30-38.

Morsh, R., Simon, W., and Coleman, P. 1999. “Neurons may live for decades with neurofibrillary tangles.” *Journal of neuropathology and experimental neurology* 188-197.

Muñoz, Y., Paula-Lima, A., and Núñez, M. 2018. “Reactive oxygen species released from astrocytes treated with amyloid beta oligomers elicit neuronal calcium signals that decrease phospho-Ser727-STAT3 nuclear content.” *Free Radical Biology and Medicine* 132-144.

Murray, M., Kouri, N., Lin, W-L., Jack Jr, C., Dickson, D., Vemuri, P. 2014. “Clinicopathologic assessment and imaging of tauopathies in neurodegenerative dementias.” *Alzheimer's Research & Therapy.*

Mymeikov, E., Daake, M., Richter, B., Haslbeck, M., and Buchner, J. 2017. “The Chaperone Activity and Substrate Spectrum of Human Small Heat Shock Proteins.” *Jorunal of Biological Chemistry* 672-684.

Nafar, F., Williams, B., and Mearow, K. 2016. “Astrocytes release HSPB1 in response to amyloid beta exposure in vitro.” *Journal of Alzheimer's Disease* 251-263.

Nagaraj, R., Oya-Ito, T., Padayatti, P., Kumar, R., Mehta, S., West, K., Levison, B., Sun, J., Crabb, J., and Padival, A. 2003. “Enhancement of Chaperone Function of α-Crystallin by Methylglyoxal Modification.” *Biochemistry* 10746-10755.

Nahomi, R., DiMauro, M., Wang, B., and Nagaraj, R. 2015. “Identification of peptides in human Hsp20 and Hsp27 that possess molecular chaperone and anti-apoptotic activities.” *Biochemical Journal* 115-125.

Nahomi, R., Wang, B., Raghavan, C., Voss, O., Doseff, A., Santhoshkumar, P., and Nagaraj, R. 2013. “Chaperone peptides of α-crystallin inhibit epithelial cell apoptosis, protein insolubilization, and opacification in experimental cataracts.” *The Journal of Biological Chemistry* 13022-13035.

Narayan, P., Holmström, K., Kim, D-H., Whitcomb, D., Wilson, M., George-Hyslop, P., Wood, N., Dobson, C., Cho, K., Abramov, A., and Klenerman, D. 2014. “Rare Individual Amyloid-β Oligomers Act on Astrocytes to Initiate Neuronal Damage.” *Biochemistry* 2442-2453.

Nasrabady, S., Rizvi, B., Goldman, J., and Brickman, A. 2018. “White matter changes in Alzheimer’s disease: a focus on myelin and oligodendrocytes.” *Acta Neuropathologica Communications.*

Nicholl, I., and Quinlan, R. 1994. “Chaperone activity of alpha-crystallins modulates intermediate filament assembly.” *The EMBO Journal* 945-953.

Oddo, S., Caccamo, A., Shepherd, J., Murphy, M., Golde, T., Kayed, R., Metherate, R., Mattson, M., Akbari, Y., and LaFerla, F. 2003. “Triple-transgenic model of Alzheimer's disease with plaques and tangles: intracellular Abeta and synaptic dysfunction.” *Neuron* 409-421.

Ojha, J., Karmegam, R., Masilamoni, J., Terry Jr., A., and Cashikar, A. 2011. “Behavioral Defects in Chaperone-Deficient Alzheimer's Disease Model Mice.” *PLOS One.*

Ojha, J., Masilamoni, G., Dunlap, D., Udoff, R., and Cashikar, A. 2011. “Sequestration of Toxic Oligomers by HspB1 as a Cytoprotective Mechanism.” 3146-3157.

Oliveira, A., Osmand, A., Outeiro, T., Muchowski, P., and Finkbeiner, S. 2016. “αB-Crystallin overexpression in astrocytes modulates the phenotype of the BACHD mouse model of Huntington's disease.” *Human Molecular Genetics* 1677-1689.

Orre, M., Kamphuis, W., Osborn, L., Jansen, A., Kooijman, L., Bossers, K., Hol, E. 2014. “Isolation of glia from Alzheimer's mice reveals inflammation and dysfunction.” *Neurobiology of Ageing* 2746-2760.

Ospina, S., Blazier, D., Criado-Marrero, M., Gould, L., Gebru, N., Beaulieu-Abdelahad, D., Wang, X., Remily-Wood, E., Chaput, D., Stevens, S., Uversky, V., Bickford, P., Dickey, C., and Blair, L. 2022. “Small Heat Shock Protein 22 Improves Cognition and Learning in the Tauopathic Brain.” *International journal of molecular sciences.*

Ousman, S., and Kubes, P. 2012. “Immune surveillance in the central nervous system.” *Nature Neuroscience* 1096-1101.

Ousman, S., Tomooka, B., van Noort, J., Wawrousek, E., O’Conner, K., Hafler, D., Sobel, R., Robinson, W., and Steinman, L. 2007. “Protective and therapeutic role for αB-crystallin in autoimmune demyelination.” *Nature* 474-479.

Owens, T., Khorooshi, R., Wlodarczyk, A., and Asgari, N. 2014. “Interferons in the central nervous system: a few instruments play many tunes.” *Glia* 339-355.

Paolicelli, R., Bolasco, G., Pagani, F., Maggi, L., Scianni, M., Panzanelli, P., Giustetto, M., Ferreira, T., Guiducci, E., Dumas, L., Ragozzino, D., and Gross, C. 2011. “Synaptic pruning by microglia is necessary for normal brain development.” *Science* 1456-1458.

Papuć, E., Krupski, W., Kurys-Denis, E., and Rejdak, K. 2016. “Antibodies against small heat-shock proteins in Alzheimer’s disease as a part of natural human immune repertoire or activation of humoral response?” *Journal of Neural Transmission* 455-461.

Papuć, E., Kurys-Denis, E., Krupski, W., and Rejdak, K. 2015. “Humoral Response against Small Heat Shock Proteins in Parkinson’s Disease.” *PLOS One.*

Parhizkar, S., Arzberger, T., Brendel, M., Kleinberger, G., Deussing, M., Focke, C., Nuscher, B., Xiong, M., Ghasemigharagoz, A., Katzmarski, N., Krasemann, S., Lichtenthaler, S., Müller, S., Colombo, A., Monasor, L., Tahirovic, S., Herms, J., Willem, M.,. 2019. “Loss of TREM2 function increases amyloid seeding but reduces plaque-associated ApoE.” *Nature Neuroscience* 191-204.

Patel, Y., Smith, M., Belleroche, J., and Latchman, D. 2005. “Hsp27 and Hsp70 administered in combination have a potent protective effect against FALS-associated SOD1-mutant-induced cell death in mammalian neuronal cells.” *Molecular Brain Research* 256-274.

Patterson, C. 2018. “World Alzheimer's Report 2018.” *Alzheimer's disease international .*

Pearl, L., and Prodromou, C. 2006. “Structure and Mechanism of the Hsp90 Molecular Chaperone Machinery.” *Annuals Review of Biochemistry.*

Pelvig, D., Pakkenberg, H., Stark, A., and Pakkenberg, B. 2008. “Neocortical glial cell numbers in human brains.” *Neurobiology of Ageing* 1754-1762.

Perea, J., Lopez, E., Diez-Ballesteros, J., Avila, J., Hernandez, F., and Bolos, M. 2019. “Extracellular monomeric tau is internalized by astrocytes.” *Frontiers in Neuroscience.*

Perez, N., Sugar, J., Charya, S., Johnson, G., Merril, C., Bierer, L., Pearl, D., Haroutunian, V., and Wallace, W. 1991. “Increased synthesis and accumulation of heat shock 70 proteins in Alzheimer's disease.” *Molecular Brain Research* 249-254.

Perez-Nievas B., Stein, T., Tai, H-C., Dols-Icardo, O., Scotton, T., Barroeta-Espar, I., Fernandez-Carballo, L., Munain, E., Perez, J., Marquie, M., Serrano-Pozo, A., Frosch M., Lowe, V., Parisi, J., Petersen, R., Ikonomovic, M., López, O., Klunk, W.,. 2013. “Dissecting phenotypic traits linked to human resilience to Alzheimer's pathology.” *Brain* 2510-2526.

Perez-Nievas, B., Johnson, L., Beltran-Lobo, P., Hughes, M.,Gammallieri, L., Tarsitano, F., Myszczynska, M., Vazquez-Villasenor, I., Jimenez-Sanchez, M., Troakes, C., Wharton, S., Ferraiuolo, L., and Noble, W. 2021. “Astrocytic C–X–C motif chemokine ligand-1 mediates β-amyloid-induced synaptotoxicity.” *Journal of Neuroinflammation.*

Perez-Nievas, B., Stein, T., Tai, H-C., Dols-Icardo, O., Scotton, T., Barroeta-Espar, I., Fernandez-Carballo, L., Munain, E., Perez, J., Marquie, M., Serrano-Pozo, A., Frosch M., Lowe, V., Parisi, J., Petersen, R., Ikonomovic, M., López, O., Klunk, W.,. 2013. “Dissecting phenotypic traits linked to human resilience to Alzheimer's pathology.” *Brain* 2510-2526.

Perez-Nievas, B.G., and Serrano-Pozo, A. 2018. “Deciphering the astrocyte reaction in Alzheimer’s disease.” *Frontiers in Aging Neuroscience.*

Perng, M., Cairns, L., van den IJssel, P., Prescott, A., Hutcheson, A., and Quinlan, R. 1999. “Intermediate filament interactions can be altered by HSP27 and alphaB-crystallin .” *Journal of Cell Science* 2099-2112.

Perng, M., Muchowski, P., IJssel, P., Wu, G., Hutcheson, A., Clark, J., and Quinlan, R. 1999. “The Cardiomyopathy and Lens Cataract Mutation in αB-crystallin Alters Its Protein Structure, Chaperone Activity, and Interaction with Intermediate Filaments in Vitro .” *Journal of Biological Chemistry* 33235-33243.

Peschek, J., Braun, N., Franzmann, T., Georgalis, Y., Haslbeck, M., Weinkauf, S., and Buchner, J. 2009. “The eye lens chaperone α-crystallin forms defined globular assemblies.” *PNAS* 13272-13277.

Phillips, E., Croft, C., Kurbatskaya, K., O'Neill, M., Hutton, M., Hanger, D., Garwood, C., and Noble, W. 2014. “Astrocytes and neuroinflammation in Alzheimer's disease.” *Biochemical Society Transactions* 1321-1325.

Piacentini, R., Puma, D., Mainardi, M., Lazzarino, G., Tavazzi, B., Arancio, O., and Grassi, C. 2017. “Reduced gliotransmitter release from astrocytes mediates tau-induced synaptic dysfunction in cultured hippocampal neurons.” *Glia* 1302-1316.

Picard, D. 2002. “Heat-shock protein 90, a chaperone for folding and regulation.” *Cellular and Molecular Life Sciences CMLS* 1640-1648.

Pirttilä, T., Kim, K., Mehta, P., Frey, H., and Wisniewski, H. 1994. “Soluble amyloid beta-protein in the cerebrospinal fluid from patients with Alzheimer's disease, vascular dementia and controls.” *Journal of the neurological sciences* 90-95.

Pivovarova, A., Chebotareva, N., Chernik, I., Gusev, N., and Levitsky, D. 2007. “Small heat shock protein Hsp27 prevents heat-induced aggregation of F-actin by forming soluble complexes with denatured actin.” *The FEBS Journal* 5937-5948.

Pooler, A., Noble, W., and Hanger, D. 2014. “A role for tau at the synapse in Alzheimer's disease pathogenesis.” *Neuropharmacology.*

Poorkaj, P., Bird, T., Wijsman, E., Nemens, E., Garruto, R., Anderson, L., Andreadis, A., Wiederholt, W., Raskind, M., and Schellenberg, G. 1998. “Tau is a candidate gene for chromosome 17 frontotemporal dementia.” *Annals of Neurology* 815-825.

Prudovsky, I., Mandinova, A., Soldi, R., Bagala, C., Graziani, I., Landriscina, M., Tarantini, F., Duarte, M., Bellum, S., Doherty, H., and Maciag, T. 2003. “The non-classical export routes: FGF1 and IL-1alpha point the way.” *Journal of Cell Science* 4871-4881.

Quraishe, S., Asuni, A., Boelens, W. C., O’Connor, V., and Wyttenbach, A. 2008. “Expression of the small heat shock protein family in the mouse CNS: differential anatomical and biochemical compartmentalization.” *Neuroscience* 483-491.

Ramos, E., Romero, A., Marco-Contelles, J., and Pino, J. 2016. “Upregulation of Antioxidant Enzymes by ASS234, a Multitarget Directed Propargylamine for Alzheimer's Disease Therapy.” *CNS Neuroscience and Therapeutics* 799-802.

Ramos, E., Romero, A., Marco-Contelles, J., Lopez-Munoz, F., and Pino, J. 2018. “Modulation of Heat Shock Response Proteins by ASS234, Targeted for Neurodegenerative Disease Therapy.” *Chemical Research in Toxicology* 839-842.

Rayan, G., Guet, J-E., Taulier, N., Pincet, F., and Urbach, W. 2010. “Recent Applications of Fluorescence Recovery after Photobleaching (FRAP) to Membrane Bio-Macromolecules.” *Sensors* 5927-5948.

Rayner, K., Sun, J., Chen, Y-X., McNulty, M., Simard, T., Zhao, X., Wells, D., de Belleroche, J., and O'Brien, E. 2009. “Heat Shock Protein 27 Protects Against Atherogenesis via an Estrogen-Dependent Mechanism.” *Arteriosclerosis, Thrombosis, and Vascular Biology* 1751-1756.

Reddy, V., Madala, S., Trinath, J., and Reddy, G. 2018. “Extracellular small heat shock proteins: exosomal biogenesis and function.” *Cell stress & chaperones* 441-454.

Reed-Geaghan, E., Savage, J., Hise, A., and Landreth, G. 2009. “CD14 and Toll-Like Receptors 2 and 4 Are Required for Fibrillar Aβ-Stimulated Microglial Activation.” *The Journal of Neuroscience* 11982-11992.

Reichenbach, N., Delekate, A., Plescher, M., Schmitt, F., Krauss, S., Blank, N., Halle, A., and Petzold, G. 2019. “Inhibition of Stat3-mediated astrogliosis ameliorates pathology in an Alzheimer's disease model.” *EMBO molecular medicien.*

Reinbold, R. 1954. “Organotypic differentiation of the eye of the chick embryo in vitro.” *C R Seances Soc Biol Fil* 1493-1495.

Ren, Y., and Sahara, N. 2013. “Characteristics of tau oligomers.” *Frontiers in Neurology.*

Renkawek, K., Bosman, G. and de Jong, W. 1994. “Expression of small heat-shock protein hsp 27 in reactive gliosis in Alzheimer's disease and other types of dementia.” *Acta Neuropathol* 511-519.

Renkawek., K and Voorter, C. E. M. 1994. “Expression of aB-crystallin in Alzheimer's disease .” *Acta Neuropathol* 155-160.

Richer, K., and Buchner, J. 2006. “hsp90: Twist and Fold.” *Cell* 251-253.

Richetin, K., Steullet, P. Pachoud, M., Perbet, R., Parietti, E., Maheswaran, M., Eddarkaoui, S., Bégard, S., Pythoud, C., Rey, M., Caillierez, R., Do, K., Halliez, S., Bezzi, P., Buée, L., Leuba G., Colin, M., Toni, N., and Déglon, N. 2020. “Tau accumulation in astrocytes of the dentate gyrus induces neuronal dysfunction and memory deficits in Alzheimer’s disease.” *Nature Neuroscience* 1567-1579.

Ries, M., and Sastre, M. 2016. “Mechanisms of Aβ Clearance and Degradation by Glial Cells.” *Front. Aging Neuroscience.*

Ritossa, F. 1962. “A new puffing pattern induced by temperature shock and DNP in drosophila.” *Experientia* 571-573.

Robert, A., Scholl, M., and Vogels, T. 2021. “Tau Seeding Mouse Models with Patient Brain-Derived Aggregates.” *International Journal of Molecular Science.*

Roberti, M., Jovin, T., and Jares-Erijman, E. 2011. “Confocal Fluorescence Anisotropy and FRAP Imaging of α-Synuclein Amyloid Aggregates in Living Cells.” *PLoS One* 23338.

Rodríguez, J., Terzieva, S., Olabarria, M., Lanza, R., and Verkhratsky, A. 2013. “Enriched environment and physical activity reverse astrogliodegeneration in the hippocampus of AD transgenic mice.” *Cell Death & Disease* e678.

Rohn, T. 2013. “The triggering receptor expressed on myeloid cells 2: "TREM-ming" the inflammatory component associated with Alzheimer's disease.” *Oxidative medicine and cellular longevity .*

Rosso, S., van Herpen, E., Deelen, W., Kamphorst, W., Severijnen, L-A., Willemsen, R., Ravid, R., Niermeijer, M., Dooijes, D., Smith, M., Goedert, M., Heutink, P., and van Swieten, J. 2002. “A novel tau mutation, S320F, causes a tauopathy with inclusions similar to those in Pick's disease.” *Annals of Neurology* 373-376.

Rothbard, J., Kurnellas, M., Brownell, S., Adams, C., Su, L., Axtell, R., Chen, R., Fathman, C., Robinson, W., and Steinman, L. 2012. “Therapeutic effects of systemic administration of chaperone αB-crystallin associated with binding proinflammatory plasma proteins.” *The Journal of Biological Chemistry* 9708-9721.

Rudiger, S., Buchberger, A., and Bukau, B. 1997. “Interaction of Hsp70 chaperones with substrates.” *Nature Structural Biology* 342-349.

Ryan, N., Nicholas, J., Weston, P., Liang, Y., Lashley, T., Guerreiro, R., Adamson, G., Kenny, J., Beck, J., Chavez-Gutierrez, L., de Strooper, B., Revesz, T., Holton, J., Mead, S., Rossor, M., and Fox, N. 2016. “Clinical phenotype and genetic associations in autosomal dominant familial Alzheimer's disease: a case series.” *The Lancet, Neurology* 1326-1335.

Sacconi, S., Féasson, L., Antoine, J., Pécheux, C., Bernard, R., Cobo, A., Casarin, A., Salviati, L., Desnuelle, C., and Urtizberea, A. 2012. “A novel CRYAB mutation resulting in multisystemic disease.” *Neuromuscular disorders* 66-72.

Saito, K., Dai, Y. and Ohtsuka, K. 2005. “Enhanced expression of heat shock proteins in gradually dying cells and their release from necrotically dead cells.” *Experimental Cell Research* 229-236.

Salari, S., Seibert, T., Chen, Y-X., Hu, T., Shi, C., Zhao, X., Cuerrier, C., Raizman, J., and O'Brien, E. 2013. "Extracellular HSP27 acts as a signaling molecule to activate NF-κB in macrophages." *Cell Stress and Chaperones* 53-63.

Salter, M., and Stevens, B. 2017. "Microglia emerge as central players in brain disease." *Nature Medicine* 1018-1027.

Santana, E., Reyes, T., and Casas-Tinto, S. 2020. "Small heat shock proteins determine synapse number and neuronal activity during development." *PLOS One.*

Santhanagopalan, I., Degiacomi, M., Shepard, D., Hochberg, G., Benesch, J., and Vierling, E. 2018. "It takes a dimer to tango: Oligomeric small heat shock proteins dissociate to capture substrate." *Journal of Biological Chemistry* 19511-19521.

Sardiello, M., Palmieri, M., di Ronza, A., Medina, D., Valenza, M., Gennarino, V., Di Malta, C., Donaudy, F., Embrione, V., Polishchuk, R., Banfi, S., Parenti, G., Cattaneo, E., and Ballabio, A.,. 2009. "A gene network regulating lysosomal biogenesis and function." *Science* 473-477.

Sathe, G., Na, C., Renuse, S., Madugundu, A., Albert, M., Moghekar, A., and Pandey, A. 2019. "Quantitative Proteomic Profiling of Cerebrospinal Fluid to Identify Candidate Biomarkers for Alzheimer's Disease." *Proteomics: Clincal Applications* .

Saunders, A., Strittmatter, W., Schmechel, D., St. George-Hyslop, P., Pericak-Vance, M., Joo, S., Rosi, B., Gusella, J., Crapper-MacLachlan, D., Alberts, M., Hulette, C., Crain, B., Goldgaber, D., and Roses, A. 1993. "Association of apolipoprotein E allele ϵ4 with late-onset familial and sporadic Alzheimer's disease." *Neurology.*

Sayed, F., Telpoukhovskaia, M., Kodama, L., Li, Y., Zhou, Y., Le, D., Hauduc, A., Ludwig, C., Gao, F., Clelland, C., Zhan, L., Cooper, Y., Davalos, D., Akassoglou, K., Coppola, G., and Gan, L. 2018. "Differential effects of partial and complete loss of TREM2 on microglial injury response and tauopathy." *PNAS.*

Schelle, J., Häsler, L., Göpfert, J., Joos, T., Vanderstichele, H., Stoops, E., Mandelkow, E-M., Neumann, U., Shimshek, D., Staufenbiel, M., Jucker, M., and Kaeser, S. 2017. "Prevention of tau increase in cerebrospinal fluid of APP transgenic mice suggests downstream effect of BACE1 inhibition." *Alzheimer's & Dementia* 701-709.

Schmidt, T., Bartelt-Kirbach, B., and Golenhofen, N. 2012. "Phosphorylation-dependent subcellular localization of the small heat shock proteins HspB1/Hsp25 and HspB5/αB-crystallin in cultured hippocampal neurons." *Histochemistry and cell biology* 407-418.

Scimemi, A., Meabon, J., Woltjer, R., Sullivan, J., Diamond, J., and Cook, D. 2013. "Amyloid-β1–42 Slows Clearance of Synaptically Released Glutamate by Mislocalizing Astrocytic GLT-1." *The Journal of Neuroscience* 5312-5318.

Sehlin, D., Englund, H., Simu, B., Karlsson, M., Ingelsson, M., Nikolajeff, F., Lannfelt, L., and Pettersson, F. 2012. "Large Aggregates Are the Major Soluble Aβ Species in AD Brain Fractionated with Density Gradient Ultracentrifugation." *PLOS One.*

Seltman, R., and Matthews, B. 2012. "Frontotemporal lobar degeneration: epidemiology, pathology, diagnosis and management." *CNS drugs* 841-870.

Serrano-Pozo A., Das, S., and Hyman, B. 2021. "APOE and Alzheimer's disease: advances in genetics, pathophysiology, and therapeutic approaches." *Lancet Neurology* 68-80.

Serrano-Pozo A., William, C., Ferrer, I., Uro-Coste, E., Delisle, M-B., Maurage, C-A., Hock, C., Nitsch, R., Masliah, E., Growdon, J., Frosch, M., and Hyman, B. 2010. “Beneficial effect of human anti-amyloid-β active immunization on neurite morphology and tau pathology.” *Brain* 1312-1327.

Serrano-Pozo, A., Betensky, R., Frosch, M., and Hyman, B. 2016. “Plaque-Associated Local Toxicity Increases over the Clinical Course of Alzheimer Disease.” *The American Journal of Pathology* 375-384.

Serrano-Pozo, A., Frosch, M., Masliah, E., and Hyman, B. 2011. “Neuropathological alterations in Alzheimer disease.” *CSH Perspectives in Medicine .*

Serrano-Pozo, A., Gómez-Isla, T., Growdon, J. H., Frosch, M. P. and Hyman, B. 2013. “The American Journal of Pathology.” *A phenotypic change but not proliferation underlies glial responses in Alzheimer disease* 2332-2344.

Serrano-Pozo, A., Mielke, M., Gómez-Isla, T., Betensky, R., Growdon, J., Frosch, M., and Hyman, B. 2011. “Reactive Glia not only Associates with Plaques but also Parallels Tangles in Alzheimer's Disease.” *The American Journal of Pathology* 1373-1384.

Shakeri, R., Kheirollahi, A., and Davoodi, J. 2017. “Apaf-1: Regulation and function in cell death.” *Biochimie* 111-125.

Shamir, D., Deng, Y., Wu, Q., Modak, S., Congdon, E., and Sigurdsson, E. 2020. “Dynamics of Internalization and Intracellular Interaction of Tau Antibodies and Human Pathological Tau Protein in a Human Neuron-Like Model.” *Frontiers in neurology.*

Shammas, S., Waudby, C., Wang, S., Buell, A., Knowles, T., Ecroyd, H., Welland, M., Carver, J., Dobson, C., and Meehan, S. 2011. “Binding of the molecular chaperone αB-crystallin to Aβ amyloid fibrils inhibits fibril elongation.” *Biophysical Journal* 1681-1689.

Shan, R., Liu, N., Yan, Y., and Lin, B. 2021. “Apoptosis, autophagy and atherosclerosis: Relationships and the role of Hsp27.” *Pharmalogical research.*

Shankar, G., Li, S., Mehta, T., Garcia-Munoz, A., Shepardson, N., Smith, I., Brett, F., Farrell, M., Rowan, M., Lemere, C., Regan, C., Walsh, D., Sabatini, B., and Selkoe, D. 2008. “Amyloid-β protein dimers isolated directly from Alzheimer's brains impair synaptic plasticity and memory.” *Nature Medicine* 837–842 .

Sharma, K., Kaur, H., and Kester, K. 1997. “Functional Elements in Molecular Chaperone α-Crystallin: Identification of Binding Sites in αB-Crystallin.” *Biochemical and Biophysical Research Communications* 217-222.

Sharoar, M., Palko, S., Ge, Y., Saido, T., and Yan, R. 2021. “Accumulation of saposin in dystrophic neurites is linked to impaired lysosomal functions in Alzheimer’s disease brains.” *Molecular Neurodegeneration volume .*

Sharp, P., Krishnan, M., Pullar, O., Navarrete, R., Wells, D and de Belleroche, J. 2006. “Heat shock protein 27 rescues motor neurons following nerve injury and preserves muscle function.” *Experimental Neurology* 511-518.

Shemetov, A., Seit-Nebi, A., and Gusev, N. 2011. “Phosphorylation of human small heat shock protein HspB8 (Hsp22) by ERK1 protein kinase.” *Molecular and Cellular Biochemistry* 47-55.

Shi, Y., and Holtzman, D. 2018. “Interplay between innate immunity and Alzheimer disease: APOE and TREM2 in the spotlight.” *Nature Reviews Immunology* 759-772.

Shiau, A., Harris, S., Southworth, D., and Agard, D. 2006. “Structural Analysis of E. coli hsp90 reveals dramatic nucleotide-dependent conformational.” *Cell* 329-340.

Shimura, H., Miura-Shimura, Y. and Kosik, K. 2004. “Binding of Tau to Heat Shock Protein 27 Leads to Decreased Concentration of Hyperphosphorylated Tau and Enhanced Cell Survival.” *Journal of Biological Chemistry* 17957-17962.

Shinohara, H., Inaguma, Y., Goto, S., Inagaki and Kato, K. 1993. “αB crystallin and HSP28 are enhanced in the cerebral cortex of patients with Alzheimer's disease.” *Journal of the Neurological Sciences* 203-208.

Singh, B., Rao, S., Ramakrishna, T., Rangaraj, N., and Rao, C. 2007. “Association of αB-Crystallin, a Small Heat Shock Protein, with Actin: Role in Modulating Actin Filament Dynamics in Vivo.” *Journal of Moleculuar Biology* 756-767.

Singh, R., Letai, A., and Sarosiek, K. 2019. “Regulation of apoptosis in health and disease: the balancing act of BCL-2 family proteins.” *Nature Reviews Molecular Cell Biology* 175-193.

Smethurst, P., Risse, E., Tyzack, G., Mitchell, J., Taha, D., Chen, Y-R., Newcombe, J., Collinge, J., Sidle, K., and Patani, R. 2020. “Distinct responses of neurons and astrocytes to TDP-43 proteinopathy in amyotrophic lateral sclerosis.” *Brain* 430-440.

Smith, A., Davey, K., Tsartsalis, S., Khozoie, C., Fancy, N., Tang, S., Liaptsi, E., Weinert, M., McGarry, A., Muirhead, R., Gentleman, S., Owen, D., and Matthews, P. 2022. “Diverse human astrocyte and microglial transcriptional responses to Alzheimer's pathology.” *Acta Neuropathologica* 75-91.

Sofroniew, M., and Vinters, H. 2010. “Astrocytes: biology and pathology`.” *Acta Neuropathologica* 7-35.

Sokolow, S., Henkins, K., Bilousova, T., Gonzalez,B., Vinters, H., Miller, C., Cornwell, L., Poon, W., and Gylys, K. 2014. “Pre-synaptic C-terminal truncated tau is released from cortical synapses in Alzheimer's disease.” *The Journal of Neurochemistry .*

Solé-Domènech, S., Cruz, D., Capetillo-Zarate, E., and Maxfield, F. 2016. “The endocytic pathway in microglia during health, aging and Alzheimer's disease.” *Ageing Research Reviews* 89-103.

Song, J-X., Malampati, S., Zeng, Y., Durairajan, S., Yang, C-B., Tong, B., Iyaswamy, A., Shang, W-B., Sreenivasmurthy, S., Zhu, Z., Cheung, K-H., Lu, J-H., Tang, C., Xu, N., and Li, M. 2020. “A small molecule transcription factor EB activator ameliorates beta-amyloid precursor protein and Tau pathology in Alzheimer's disease models.” *Ageing Cell* e13069.

Spangenberg, E., Severson, P., Hohsfield, L., Crapser, J., Zhang, J., Burton, E., Zhang, Y., Spevak, W., Lin, J., Phan, N., Habets, G., Rymar, A., Tsang, G., Walters, J., Nespi, M., Singh, P., Broome, S., Ibrahim, P., Zhang, C., Bollag, G., West, B.,. 2019. “Sustained microglial depletion with CSF1R inhibitor impairs parenchymal plaque development in an Alzheimer’s disease model.” *Nature Communications.*

Spires-Jones, T., Stoothoff, W., de Calignon, A., Jones, P., and Hyman, B. 2009. “Tau pathophysiology in neurodegeneration: a tangled issue.” *Trends in Neuroscience* 150-159.

Sreekumar, P., Kannan, R., Kitamura, M., Spee, C., Barron, E., Ryan, S., and Hinton, D. 2010. “αB crystallin is apically secreted within exosomes by polarized human retinal pigment epithelium and provides neuroprotection to adjacent cells.” *PLoS One* 12578.

Staal, J., Alexander, S., Liu, Y., Dickson, S., and Vickers, J. 2011. “Characterization of Cortical Neuronal and Glial Alterations during Culture of Organotypic Whole Brain Slices from Neonatal and Mature Mice.” *PLOS One.*

Stenoien, D., Mielke, M., and Mancini, M. 2002. “Intranuclear ataxin1 inclusions contain both fast- and slow-exchanging components.” *Nature Cell Biology* 806-810.

Stetler, R., Gao, Y., Zhang, L., Weng, Z., Zhang, F., Hu, X., Wang, S., Vosler, P., Cao, G., Sun, D., Graham, S., and Chen, J. 2012. “Phosphorylation of HSP27 by Protein Kinase D Is Essential for Mediating Neuroprotection against Ischemic Neuronal Injury.” *Journal of Neuroscience* 2667-2682.

Stevens, B., Allen, N., Vazquez, L. Smith, S., John, S., and Barres, B. 2007. “The Classical Complement Cascade Mediates CNS Synapse Elimination.” *Cell* 1164-1178.

Stoppini, L., Buchs, P., and Muller, D. 1991. “A simple method for organotypic cultures of nervous tissue.” *Journal Neuroscience Methods* 173-182.

Strang, K., Croft, C., Sorrentino, Z., Chakrabarty, P., Golde, T., and Giasoon B. 2018. “Distinct differences in prion-like seeding and aggregation between Tau protein variants provide mechanistic insights into tauopathies.” *Journal of biological chemistry* 2408-2421.

Strittmatter, W., Saunders, A., Schmechel, D., Pericak-Vance, M., Enghild, J., Salvesen, G., and Roses, A. 1993. “Apolipoprotein E: high-avidity binding to beta-amyloid and increased frequency of type 4 allele in late-onset familial Alzheimer disease.” *PNAS* 1977-1981.

Stromer, T., Fischer, E., Richter, K., Haslbeck, M., Buchner, J. 2004. “Analysis of the Regulation of the Molecular Chaperone Hsp26 by Temperature-induced Dissociation.” *Journal of Biochemistry* 11222-11228.

Sullivan, K., and Cleveland, D. 1986. “Identification of conserved isotype-defining variable region sequences for four vertebrate beta tubulin polypeptide classes.” *PNAS* 4327-4331.

Sun, X., Fontaine, J-M., Rest, J., Shelden, E., and Welsh, M. 2004. “Interaction of Human HSP22 (HSPB8) with Other Small Heat Shock Proteins.” *Journal of biological chemistry* 2394-2402.

Tanemura, K., Murayama, M., Akagi, T., Hashikawa, T., Tominaga, T., Ichikawa, M., Yamaguchi, H., and Takashima, A. 2002. “Neurodegeneration with tau accumulation in a transgenic mouse expressing V337M human tau.” *Journal of Neuroscience* 133-141.

Tang, Y-C., and Amon, A. 2013. “Gene copy-number alterations: a cost-benefit analysis.” *Cell* 394-405.

Tatsuta, T., Model, K., and Langer, T. 2004. “Formation of Membrane-bound Ring Complexes by Prohibitins in Mitochondria.” *Molecular biology of the cell.*

Tebay, L., Robertson, H., Durant, S., Vitale, S., Penning, T., Dinkova-Kostova, A., and Hayes, J. 2015. “Mechanisms of activation of the transcription factor Nrf2 by redox stressors, nutrient cues, and energy status and the pathways through which it attenuates degenerative disease.” *Free radical biology & medicine .*

Tejera, D., and Heneka, M. 2016. “Microglia in Alzheimer's disease: the good, the bad and the ugly.” *Current Alzheimer's Research* 370-380.

Teramoto, S., Shimura, H., Tanaka,R., Shimada, Y., Miyamoto, N., Arai, H., Urabe, T., and Hattori, N. 2013. “Human-Derived Physiological Heat Shock Protein 27 Complex Protects Brain after Focal Cerebral Ischemia in Mice.” *PLOS One.*

Thal, D., Capetillo-Zarate, E., Tredici, K., and Braak, H. 2006. “The development of amyloid beta protein deposits in the aged brain. .” *Sci Aging Knowledge Environ.*

Thal, D., Rub, U., Orantes, M., and Braak, H. 2022. “Phases of A beta-deposition in the human brain and its relevance for the development of AD.” *Neurology* 1791-1800.

Thuringer, D., Jego, G., Wettstein, G., Terrier, O., Cronier, L., Yousfi, N., Hébrard, S., Bouchot, A., Hazoumé, A., Joly, A-L., Gleave, M., Rosa-Calatrava, M., Solary, E., and Garrido, C. 2013. “Extracellular HSP27 mediates angiogenesis through Toll-like receptor 3.” *The FASEB Journal* 4169-4183.

Tian, X., Zhao, L., Song, X., Yan, Y., Liu, N., Li, T., Yan, B., and Liu, B. 2016. “HSP27 Inhibits Homocysteine-Induced Endothelial Apoptosis by Modulation of ROS Production and Mitochondrial Caspase-Dependent Apoptotic Pathway.” *BioMed Research International.*

Tong J., Huang, C., Bi, F., Wu, Q., Huang, B., Liu, X., Li, F., Zhou, H. and Xia, X-G. 2013. “Expression of ALS-linked TDP-43 mutant in astrocytes causes non-cell-autonomous motor neuron death in rats.” *The EMBO Journal* 1917-1926.

Tong, J., Huang, C., Bi, F., Wu, Q., Huang, B., L:iu, X., Li, Fang, Zhouo, H., and Xia, X-G. 2013. “Expression of ALS-linked TDP-43 mutant in astrocytes causes non-cell-autonomous motor neuron death in rats.” *The EMBO Journal* 1917-1926.

Toth, M., Gonda, S., Vigh, L., and Santha, M. 2010. “Neuroprotective effect of small heat shock protein, Hsp27, after acute and chronic alcohol administration.” *Cell Stress and Chaperones* 807-817.

Tóth, M., Szegedi, V., Varga, E., Juhász, G., Horváth, J., Borbély, E., Csibrány, B., Alföldi, R., Lénárt, N., Penke, B., and Sántha, M. 2013. “Overexpression of Hsp27 ameliorates symptoms of Alzheimer's disease in APP/PS1 mice.” *Cell stress & chaperones* 759-771.

Tucker, K., Meyer, M. & Barde, YA. 2001. “Neurotrophins are required for nerve growth during development.” *Nature Neuroscience* 29–37.

Tyzack, G., Sitnikov, S., Barson, D., Adams-Carr, K., Lau, N., Kwok, J., Zhao, C., Franklin, R., Karadottir, R., Fawcett, J., and Lakatos, A. 2014. “Astrocyte response to motor neuron injury promotes structural synaptic plasticity via STAT3-regulated TSP-1 expression.” *Nature communications.*

Uchihara, T., Nakamura, A., Yamazaki, M., and Mori, O. 2001. “Evolution from pretangle neurons to neurofibrillary tangles monitored by thiazin red combined with Gallyas method and double immunofluorescence.” *Acta Neuropathologica* 535-539.

van den Ijssel, P., Overkamp, P., Bloemendal, H., de Jong, W. 1998. “Phosphorylation of αB-Crystallin and HSP27 Is Induced by Similar Stressors in HeLa Cells.” *Biochemical and Biophysical Research Communications* 518-523.

van Noort, J., Bsibsi, M., Gerritsen, W., van der Valk, P., Bajramovic, J., Steinman, L., and Amor, S. 2010. “Alphab-crystallin is a target for adaptive immune responses and a trigger of innate responses in preactive multiple sclerosis lesions.” *Journal of Neuropathology and experimental neurology* 694-703.

van Noort, J., Bsibsi, M., Nacken, P., Gerritsen, W. and Amor, S. 2012. “The link between small heat shock proteins and the immune system.” *The International Journal of Biochemistry & Cell Biology* 1670-1679.

van Noort, J., Bsibsi, M., Nacken, P., Gerritsen, W., and Amor, S. 2012. “The link between small heat shock proteins and the immune system.” *The international journal of biochemistry and cell biology* 1670-1679.

Verkhratsky, A., Nedergaard, M., and Hertz, L. 2015. “Why are astrocytes important?” *Neurochemical Research* 389-401.

Vicart, P., Caron, A., Guicheney, P., Li, Z., Prévost, M., Faure, A., Chateau, D., Chapon, F Tomé, F., Dupret, J., Paulin, D., and Fardeau, M. 1998. “A missense mutation in the alphaB-crystallin chaperone gene causes a desmin-related myopathy.” *Nature Genetics* 92-95.

Voisine, C., Pedersen, S., and Morimoto, R. 2010. “Chaperone networks: Tipping the balance in protein folding diseases.” *Neurobiology of disease* 12-20.

von Bergen, M., Friedhoff, P., Biernat, J., Heberle, J., Mandelkow, E., and Mandelkow, E. 2000. “Assembly of τ protein into Alzheimer paired helical filaments depends on a local sequence motif (306VQIVYK311) forming β structure.” *PNAS.*

Voss, O., Batra, S., Kolattukudy, S., Gonzalez-Mejia, M., Smith, J., and Doseff, A. 2007. “Binding of Caspase-3 Prodomain to Heat Shock Protein 27 Regulates Monocyte Apoptosis by Inhibiting Caspase-3 Proteolytic Activation.” *Journal of Biological Chemistry* 25088-25099.

Walsh, D., and Selkoe, D. 2020. “Amyloid β-protein and beyond: the path forward in Alzheimer’s disease.” *Current Opinion in Neurobiology* 116-124.

Wang C, . Xiong M., Gratuze M., Bao X., Shi Y., Andhey P., Manis M., Schroeder C., Yin Z., Madore C., Butovsky O., Artyomov M., Ulrich J., and Holtzman D. 2021. “Selective removal of astrocytic APOE4 strongly protects against tau-mediated neurodegeneration and decreases synaptic phagocytosis by microglia.” *Neuron* 1657-1674.

Wang, W., Hou, T-T., Jia, L-F., Wu, Q-Q., Quan, M-N, Jia, J-P. 2019. “Toxic amyloid-β oligomers induced self-replication in astrocytes triggering neuronal injury.” *eBioMedicine* 174-187.

Wang, X-L., and Li. 2021. “Cell type-specific potential pathogenic genes and functional pathways in Alzheimer’s Disease.” *BMC Neurology.*

Webster, J., Darling, A., Sanders, T., Blazier, D., Vidal-Aguiar, Y., Beaulieu-Abdelahad, D., Plemmons, D., Hill, S., Uversky, V., Bickford, P., Dickey, C., and Blair, L. 2020. “Hsp22 with an N-Terminal Domain Truncation Mediates a Reduction in Tau Protein Levels.” *Internation journal of molecular science .*

Webster, J., Darling, A., Uversky, V., and Blair, L. 2019. “Small Heat Shock Proteins, Big Impact on Protein Aggregation in Neurodegenerative Disease.” *Frontiers in Pharmacology.*

Wegmann, S., Eftekharzadeh, B., Tepper, K., Zoltowska, K., Bennet, R., Dujardin, S., Laskowski, P., MacKenzie, D., Kamath, T., Commins, C., Vanderburg, C., Roe, A., Fan, Z., Molliex, A., Hernandez-Vega, A., Muller, D., Hyman, A., Mandelkow, E., Taylor, J. 2018. "Tau protein liquid-liquid phase separation can initiate tau aggregation." *The EMBO Journal* 98049.

Wettstein, G., Bellaye, P., Micheau, O., and Bonniaud, P. 2012. "Small heat shock proteins and the cytoskeleton: an essential interplay for cell integrity?" *The international journal of biochemistry and cell biology* 1680-1686.

White, J., Manelli, A., Holmberg, K., Van Eldik, L., and LaDu, M. 2005. "Differential effects of oligomeric and fibrillar amyloid-β1–42 on astrocyte-mediated inflammation." *Neurobiology of disease* 459-465.

Wilhelmus, M., Otte-Holler, I., Wesseling, P., De Waal, R., Boelens, W. and Verbeek, M. 2006. "Specific association of small heat shock proteins with the pathological hallmarks of Alzheimer's disease brains." *Neuropathology and Applied Neurobiology* 119-130.

Williams, D. 2006. "Tauopathies: classification and clinical update on neurodegenerative diseases associated with microtubule-associated protein tau." *Internal Medicine Journal* 652-660.

Wisniewski, H., and Wegiel, J. 1991. "Spatial relationships between astrocytes and classical plaque components." *Neurobiology of Ageing* 593-600.

Wolf, M. 1970. "Anatomy of cultured mouse cerebellum. II. Organotypic migration of granule cells demonstrated by silver impregnation of normal and mutant cultures." *The Journal of Comparative Neurology* 281-297.

Wolozin, B., and Davies, P. 1987. "Alzheimer-related neuronal protein A68: specificity and distribution." *Annals of Neurology* 521-526.

Wu, H., Hudry, E., Hashimoto, T., Kuchibhotla, K., Rozkalne, A., Fan, Z., Spires-Jones, T., Xie, H., Arbel-Ornath, M., Grosskreutz, C., Bacskai, B., and Hyman, B. 2010. "Amyloid beta induces the morphological neurodegenerative triad of spine loss, dendritic simplification, and neuritic dystrophies through calcineurin activation." *The Journal of Neuroscience* 2636-2649.

Wu. H., Hudry, E., Hashimoto, T., Uemura, K., Fan, Z., Berezovska, O., Grosskreutz, C., Bacskai, B., and Hyman, B. 2012. "Distinct Dendritic Spine and Nuclear Phases of Calcineurin Activation after Exposure to Amyloid-β Revealed by a Novel Fluorescence Resonance Energy Transfer Assay." *The Journal of Neuroscience* 5298-5309.

Wyatt, A., Yerbury, J., Ecroyd, H., and Wilson, M. 2013. "Extracellular chaperones and proteostasis." *Annual review of biochemistry* 295-322.

Wyttenback, A., Sauvageot, O., Carmichael, J., Diaz-Latoud, C., Arrigo, A., and Rubinsztein, D. 2002. "Heat shock protein 27 prevents cellular polyglutamine toxicity and suppresses the increase of reactive oxygen species caused by huntingtin." *Human Molecular Genetics* 1137-1151.

Xiao, Q., Yan, P., Ma, X., Liu, H., Perez, R., Zhu, A., Gonzales, E., Burchett, J., Schuler, D., Cirrito, J., Diwan, A., Lee, J-M. 2014. "Enhancing astrocytic lysosome biogenesis facilitates Aβ clearance and attenuates amyloid plaque pathogenesis." *The Journal of Neuroscience* 9607-9620.

Xiong, R., Vandenbroucke, R., Broos, K., Brans, T., Wonterghem, E., Libert, C., Demeester, J., Smedt, S., and Braeckmans, K. 2016. "Sizing nanomaterials in bio-fluids by cFRAP enables protein

aggregation measurements and diagnosis of bio-barrier permeability." *Nature Communications* 12982.

Xu, H. 2018. "Cochaperones enable Hsp70 to use ATP energy to stabilize native proteins out of the folding equilibrium." *Scientific Reports.*

Xu, K., Malouf, A., Messing, A., and Silver, J. 1999. "Glial fibrillary acidic protein is necessary for mature astrocytes to react to beta-amyloid." *Glia* 390-403.

Yang, L., Zhenmeiyu, L., Liu, Guoping, L., Li, X., and Yang, Z. 2022. "Developmental Origins of Human Cortical Oligodendrocytes and Astrocytes." *Neuroscience Bulletin* 47-68.

Yang., T., Li, S., Xu, H., Walsh, D., and Selkoe D. 2017. "Large soluble oligomers of amyloid β-protein from alzheimer brain are far less neuroactive than the smaller oligomers to which they dissociate." *The Journal of Neuroscience* 152-163.

Ye, B., Shen, H., Zhang, J., Zhu, Y-G., Ransom, B., Chen, X-C., and Ye, Z-C. 2015. "Dual pathways mediate β-amyloid stimulated glutathione release from astrocytes." *Glia* 2208-2219.

Yerbury, J., Stewart, E., Wyatt, A., and Wilson, M. 2005. "Quality control of protein folding in extracellular space." *EMBO Reports* 1131-1136.

Yu, W., and Lu, B. 2012. "Synapses and Dendritic Spines as Pathogenic Targets in Alzheimer's Disease." *Neural Plasticity .*

Yusuf, N., Nasti, T., Huang, C-M., Huber, B., Jaleel, T., Lin, H-Y., Xu, H,. and Elmets, C. 2009. "Heat shock proteins HSP27 and HSP70 are present in the skin and are important mediators of allergic contact hypersensitivity." *Journal of Immunology* 675-683.

Zamanian, J., Xu, L., Foo, L., Nouri, N., Zhou, L., Giffard, R., and Barres, B. 2012. "Genomic Analysis of Reactive Astrogliosis." *Journal of Neuroscience* 6391-6410.

Zhang, H-L., Jia, K-Y., Sun, D., and Yang, M. 2017. "Protective effect of HSP27 in atherosclerosis and coronary heart disease by inhibiting reactive oxygen species." *Journal of cellular biochemistry* 2859-2868.

Zhang, Y., Chen, K., Sloan, S., Bennett, M., Scholze, A., O'Keeffe, S., Phatnani, H., Guarnieri, P., Caneda, C., Ruderisch, N., Deng, S., Liddelow, S., Zhang, C., Daneman, R., Maniatis, T., Barres, B., and Wu, J. 2014. "An RNA-Sequencing Transcriptome and Splicing Database of Glia, Neurons, and Vascular Cells of the Cerebral Cortex." *The Journal of Neuroscience* 11929-11947.

Zhu, X., Zhao, Z., Burkholder, W., Gragerov, A., Ogata, C., Gottesman, M., and Hendrickson, W. 1996. "Structural Analysis of Substrate Binding by the Molecular Chaperone DnaK." *Science* 1606-1614.